Supporting Information

OGlcNAcylation and Phosphorylation Have Opposing Structural Effects in tau: Phosphothreonine Induces Particular Conformational Order

Michael A. Brister‡, Anil K. Pandey‡, Agata A. Bielska, and Neal J. Zondlo*
Department of Chemistry and Biochemistry
University of Delaware
Newark, DE 19716

‡ These authors contributed equally to this work.

Contents

S3. Materials
S3. Peptide synthesis
S4. Serine/threonine phosphorylation and diethylphosphorylation
S5. Synthesis of Fmoc-Thr(O-GlcNAc)-OH and Fmoc-Ser(O-GlcNAc)-OH
S6. Glycopeptide synthesis
S7. Characterization data for tau peptides
S8. Characterization data for model peptides
S12. Circular dichroism (CD) spectroscopy
S12. NMR spectroscopy
S13. ^{31}P NMR spectroscopy
S14. CD spectra of $tau_{174–183}$(T175E, T181E) and $tau_{174–183}$(T175Tle, T181Tle)
S15. CD spectra of $tau_{211–238}$ and $tau_{211–238}(OPO_3^{2–})$
S16-S19. CD spectra of $tau_{234–251}$, $tau_{234–251}$(pS235), and $tau_{234–251}$(pS235/pS237)
S20-S21. Summary of CD data for tau peptides
S22-S23. CD spectra of model peptides Ac-K*Tx*PP-NH_2
S24-S25. CD spectra of model peptides Ac-K*Sx*PP-NH_2
S27-S28. Summary of CD data for model peptides Ac-K*Tx*PP-NH_2 and Ac-K*Sx*PP-NH_2
S29-S32. CD spectra of model peptides Ac-GPK*Tx*PPGY-NH_2
S33. CD spectra of model peptides Ac-GPP*Tx*PPGY-NH_2
S35. Summary of CD data for model peptides Ac-GPK*Tx*PPGY-NH_2 and Ac-GPP*Tx*PPGY-NH_2
S36-S148. ^{1}H NMR spectra of all peptides (amide region and full spectra)
S40. Summary of ^{1}H NMR data for peptides derived from $tau_{174–183}$
S41-S45. ^{1}H-^{15}N HSQC spectra of peptides derived from $tau_{174–183}$
S45. Summary of ^{1}H-^{15}N HSQC data for peptides derived from $tau_{174–183}$
S46-S48. ^{1}H-^{13}C HSQC spectra of peptides $tau_{174–183}$ and $tau_{174–183}(OPO_3^{2–})$
S49. NOESY spectrum of peptide $tau_{174–183}(OPO_3^{2–})$ at pH 8.0 (298 K)
S50. ^{1}H-^{13}C HMBC spectra of peptides $tau_{174–183}$ at pH 4.0 and $tau_{174–183}(OPO_3^{2–})$ at pH 8.0 in D_2O (298 K)
S52. Summary of ^{1}H-^{13}C HSQC data for peptides $tau_{174–183}$ and $tau_{174–183}(OPO_3^{2–})$
S56-S57. Summary of ^{1}H NMR data for peptides derived from $tau_{196–209}$
S61. Summary of ^{1}H NMR data for peptides derived from $tau_{211–219}$
S62-S65. ^{1}H-^{15}N HSQC spectra of peptides derived from $tau_{211–219}$

S66. Summary of ^{1}H-^{15}N HSQC data for $tau_{211–219}$ and $ptau_{211–219}$
S67-S69. ^{1}H-^{13}C HSQC spectra of peptides $tau_{211–219}$ and $tau_{211–219}(OPO_3^{2–})$
S70. Summary of ^{1}H-^{13}C HSQC data for $tau_{211–219}$ and $ptau_{211–219}$
S74. Summary of ^{1}H NMR data for peptides derived from $tau_{229–238}$
S75-S78. ^{1}H-^{15}N HSQC spectra of peptides derived from $tau_{229–238}$
S79. Summary of ^{1}H-^{15}N HSQC data for $tau_{229–238}$ and $ptau_{229–238}$
S80-S82. ^{1}H-^{13}C HSQC spectra of peptides $tau_{229–238}$ and $tau_{229–238}(OPO_3^{2–})$
S83. Summary of ^{1}H-^{13}C HSQC data for $tau_{229–238}$ and $ptau_{229–238}$
S86. TOCSY spectrum (amide region) of peptides derived from $tau_{211–238}$ at 298 K
S87. Summary of ^{1}H NMR data for peptides derived from $tau_{211–238}$
S90. Summary of ^{1}H NMR data for peptides derived from $tau_{234–251}$
S91-S94. ^{1}H-^{13}C HSQC spectra of peptides $tau_{234–251}$, $tau_{234–251}$(pS235), and $tau_{234–251}$(pS235/pS237)
S95-S96. Summary of ^{1}H-^{13}C HSQC data for $tau_{234–251}$, $tau_{234–251}$(pS235), and $tau_{234–251}$(pS235/pS237)
S98. pH-dependent ^{1}H NMR spectra of peptide Ac-KpTPP-NH_2
S102. ^{1}H NMR spectra of peptide Ac-KT($OPO_3^{2–}$)PP-NH_2, salt dependence
S103. Temperature dependent ^{1}H NMR spectra of peptide Ac-KT($OPO_3^{2–}$)PP-NH_2
S106-S108. Summary of ^{1}H NMR data for peptides Ac-K*Tx*PP-NH_2
S108. ROESY spectrum of peptide Ac-KT($OPO_3^{2–}$)PP-NH_2 at pH 8.0 (298 K)
S109-S112. ^{1}H-^{15}N HSQC spectra of peptides Ac-K*Tx*PP-NH_2
S112. Summary of ^{1}H-^{15}N HSQC data for peptides Ac-KTPP-NH_2 and KpTPP-NH_2at 298 K
S113. ^{1}H-^{13}C HSQC spectrum of peptide Ac-KTPP-NH_2 at pH 8.0 in D_2O (298 K)
S114. ^{1}H-^{13}C HSQC spectrum of peptide Ac-KT($OPO_3^{2–}$)PP-NH_2 at pH 8.0 in D_2O (298 K)
S115. ^{1}H-^{13}C HSQC spectra of peptides Ac-KT($OPO_3^{2–}$)PP-NH_2 and Ac-KTPP-NH_2 at pH 8.0 in D_2O (298 K)
S116. ^{1}H-^{13}C HMBC spectra of peptides Ac-KTPP-NH_2 and Ac-KT($OPO_3^{2–}$)PP-NH_2 at pH 8.0 in D_2O (298 K)
S117. Summary of ^{1}H-^{13}C HSQC and ^{1}H-^{13}C HMBC data for peptides Ac-KTPP-NH_2 and Ac-KT($OPO_3^{2–}$)PP-NH_2 at 298 K
S118. Summary of ^{1}H-^{13}C HSQC data for peptides Ac-KTPP-NH_2 and Ac-KT($OPO_3^{2–}$)PP-NH_2 at 278 K
S119. ^{31}P NMR spectra of peptides Ac-KT($OPO_3H^{–}$)PP-NH_2 and Ac-KT($OPO_3^{2–}$)PP-NH_2
S120. Summary of ^{31}P NMR data for peptide Ac-KT($OPO_3^{–/2–}$)PP-NH_2
S121. pH-dependent ^{1}H NMR spectra of peptide Ac-KpSPP-NH_2
S124. Summary of ^{1}H NMR data for peptides Ac-K*Sx*PP-NH_2
S125-S127. ^{1}H-^{13}C HSQC spectra of peptides Ac-KSPP-NH_2 and Ac-KS($OPO_3^{2–}$)PP-NH_2
S128. Summary of ^{1}H-^{13}C HSQC data for peptides Ac-KSPP-NH_2 and Ac-KpSPP-NH_2 at 298 K
S132-S135. ^{1}H-^{15}N HSQC spectra of peptides Ac-GPP*Tx*PPGY-NH_2
S136. Summary of ^{1}H NMR data for peptides Ac-GPP*Tx*PPGY-NH_2
S136. Summary of ^{1}H-^{15}N HSQC data for peptides Ac-GPP*Tx*PPGY-NH_2 at 298 K
S141. Summary of ^{1}H NMR data for peptides Ac-GPK*Tx*PPGY-NH_2
S142. Analysis of steric versus stereoelectronic effects of ROH, $ROPO_3H^{–}$, $ROPO_3^{2–}$, and $ROPO_3Et_2$ functional groups in Ac-TAXN-NH_2 and Ac-TYXN-NH_2 peptides (X = 4*R*- and 4*S*-substituted hydroxyprolines)
S143. pH-dependent ^{1}H NMR spectra (amide region) of peptide Ac-TAP(4*R*-$OPO_3^{–/2–}$)N-NH_2
S144. pH-dependent ^{1}H NMR spectra (aliphatic region) of peptide Ac-TAP(4*R*-$OPO_3^{–/2–}$)N-NH_2
S145. pH-dependent ^{1}H NMR spectra (amide region) of peptide Ac-TAP(4*S*-$OPO_3^{–/2–}$)N-NH_2
S146. pH-dependent ^{1}H NMR spectra (aliphatic region) of peptide Ac-TAP(4*S*-$OPO_3^{–/2–}$)N-NH_2

S147. Summary of pH-dependent ^{1}H NMR data of peptides Ac-TAP(4*S*-$OPO_3^{-/2-}$)N-NH_2 and Ac-TAP(4*R*-$OPO_3^{-/2-}$)N-NH_2
S148-S149. Summary of H^N, Hα, Hβ, ^{15}N, and ^{13}C NMR chemical shift data by side chain modification for serine and threonine residues for all peptides
S149. References

Materials

Fmoc-L-amino acids were purchased from Novabiochem (San Diego, CA), Bachem (San Carlos, CA), or Chem-Impex (Wood Dale, IL). O-(1H-benzotriazol-1-yl)-1,1,3,3-tetramethyluronium hexafluorophosphate (HBTU) was purchased from Senn Chemicals (San Diego, CA). Rink amide MBHA resin and diisopropylethylamine (DIPEA) were purchased from Chem-Impex. Ethanedithiol (EDT), acetic anhydride (Ac_2O), chloroform-D ($CDCl_3$), phenol, 3% tetrazole in acetonitrile, thioanisole, triethylsilane (TES), and trifluoroacetic acid (TFA) were purchased from Acros. Boron trifluoride diethyl etherate (BF_3•Et_2O), *N,N'*-diisopropylcarbodiimide (DIC), and piperidine were purchased from Aldrich or Acros. Acetonitrile (MeCN), methylene chloride (CH_2Cl_2), methanol (MeOH), chloroform ($CHCl_3$), tetrahydrofuran (THF), dimethylformamide (DMF), pyridine, ether, sodium chloride, hydrogen peroxide, and acetic acid were purchased from Fisher. *O,O'*-dibenzyl-*N,N*-diisopropylphosphoramidite, and *O,O'*-diethyl-*N,N*-diisopropylphosphoramidite were purchased from Toronto Research Chemicals (North York, Ontario). β-D-glucosamine pentaacetate (Ac_4-GlcNAc) was purchased from Alfa-Aesar. Silica gel was purchased from SiliCycle (Québec City, Québec). Deionized water was purified by a Millipore Synergy 185 water purification system with a Simpak2 cartridge. Solid-phase phosphorylation and diethylphosphorylation reactions were performed in capped disposable fritted tubes (Image Molding) with gentle mixing on a Barnstead-Thermoline Labquake rotary shaker. CH_2Cl_2 and MeCN were dried via a column-based solvent purification system (Innovative Technologies, Inc.) and stored over activated molecular sieves (4 Å). All other compounds were used as purchased with no additional purification.

Peptide synthesis

Peptides (0.1 or 0.25 mmol) were synthesized on Rink amide resin via standard Fmoc solid phase peptide synthesis using a Rainin PS3 peptide synthesizer. Prior to the start of peptide synthesis, the resin was swelled in DMF (2 × 15 minutes). Standard amino acid couplings were achieved in 1 h using 4 equivalents of HBTU and 4 equivalents of Fmoc amino acid. Couplings of glycosylated amino acid derivatives were achieved using 1.5 equivalents of glycosylated Fmoc amino acid and 1.5 equivalents HBTU or HATU. Glycosylated amino acid couplings were allowed to react for 3-4 hours. Each cycle of peptide synthesis employed the following four steps: (1) removal of the Fmoc protecting group in 20% piperidine in DMF, 3 × 5 minutes; (2) resin wash in DMF, 5 × 1 minute; (3) amino acid coupling (Fmoc amino acid, HBTU, and 0.05 M DIPEA in DMF; 1 h or 4 h); (4) resin wash with DMF, 3 × 1 minute. After addition of the final residue, the peptide N-terminus was deprotected (20% piperidine in DMF, 3 × 5 minutes) and subsequently acetylated (10% acetic anhydride in pyridine, 5 minutes). To avoid β-elimination of the sugar moiety upon pyridine treatment, glycosylated peptides were acetylated using alternative conditions (0.5 M 1:1 DIC:acetic acid in THF, 1 h). Finally, the resin was washed with DMF (6×) and CH_2Cl_2 (3×).

The synthesis of peptides Ac-TA*Prox*N-NH_2 and Ac-TY*Prox*N-NH_2 were accomplished using the previously described automated solid phase peptide synthesis strategy termed proline editing.[1] These peptides were synthesized and purified as desribed.[2]

All peptides were subjected to TFA cleavage/deprotection reactions (2-4 hours in 84% TFA/4% each of H_2O/phenol/thioanisole/EDT, 92.5% TFA/5% TES/2.5% H_2O, or 92% TFA/4% TES/4% H_2O for non-glycosylated peptides; OGlcNAcylated peptides are described later), the TFA removed by evaporation, the peptides precipitated with ether, and the precipitates dried. Peptides were dissolved in water or phosphate buffer, filtered, and purified by reverse phase HPLC on a Vydac C18 semi-preparative column (250 x 10 mm, 5-10 μm particle, 300 Å pore) or on a Varian Microsorb MV C18 analytical column (250 x 4.6 mm, 3-5 μm particle, 100 Å pore) using linear gradients of buffer B (20% water, 80% MeCN, 0.05% TFA) in buffer A (98% water, 2% MeCN, 0.06% TFA). Peptides were purified to homogeneity and their purity verified by analytical HPLC reinjection. Peptide identity was characterized by ESI-MS (positive ion mode, unless stated otherwise) on an LCQ Advantage (Finnigan) mass spectrometer.

The concentrations of peptides containing tyrosine were determined by UV-vis spectroscopy based on tyrosine absorbance (ε_{280} = 1280 M^{-1} cm^{-1} in water). The $tau_{174-183}$ peptides, were quantified using the equation: (μg/mL) = (A_{215} – A_{225}) x 144.[3] The peptides Ac-K*Tx*PP-NH_2, Ac-K*Sx*PP-NH_2, $tau_{211-238}$, $ptau_{211–238}$, $tau_{234–251}$, $tau_{234–251}(OPO_3^{2–})$(pS235), and $tau_{234–251}(OPO_3^{2–})$(pS235/pS237) were quantified via ^{1}H NMR by adding an aqueous solution of maleic acid (500 μM final concentration) as an internal standard to the sample after the CD experiment was performed.

Serine/Threonine Phosphorylation and Diethylphosphorylation

Trityl-protected serine and threonine residues were incorporated at intended sites of chemical phosphorylation and diethylphosphorylation to allow for selective modification of the peptides on resin. To accomplish phosphorylation and diethylphosphorylation, the trityl groups were first deprotected in 2% TFA, 5% TES, and 93% CH_2Cl_2 (3 × 1 minutes, or until the flow-through solution was colorless). For chemical phosphorylation, phosphitylation was accomplished under nitrogen by the addition of tetrazole (1.35 mmol; 3 mL of 3% tetrazole solution in MeCN) and *O,O'*-dibenzyl-*N,N*-diisopropylphosphoramidite (500 μL, 1.52 mmol) and allowed to react for 6 hours with mixing (**Scheme S1**).

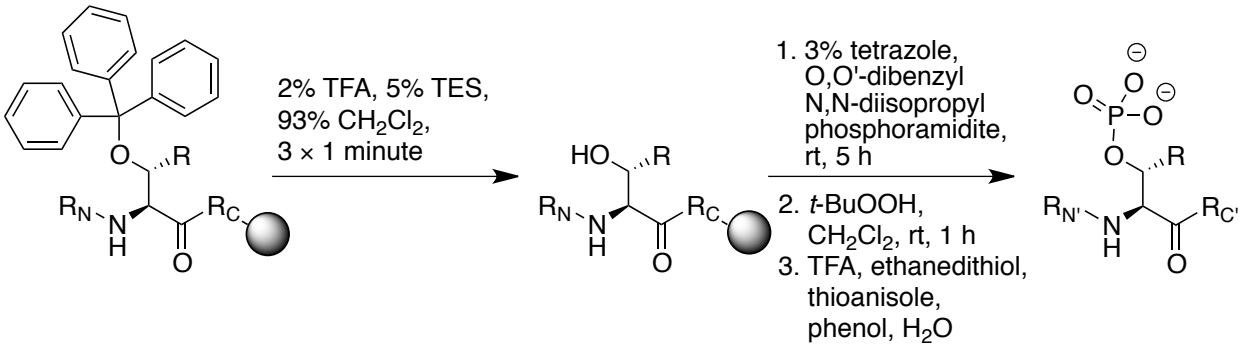

Scheme S1. Scheme for chemical phosphorylation of peptides on resin. R = CH_3 (Thr) or R = H (Ser).

The necessary phosphitylation step to achieve chemical diethylphosphorylation was analogous, with the sole difference being the substitution of *O,O'*-diethyl-*N,N*-diisopropylphosphoramidite (323 μL, 1.52 mmol) for *O,O'*-dibenzyl-*N,N*-diisopropylphosphoramidite (**Scheme S2**).

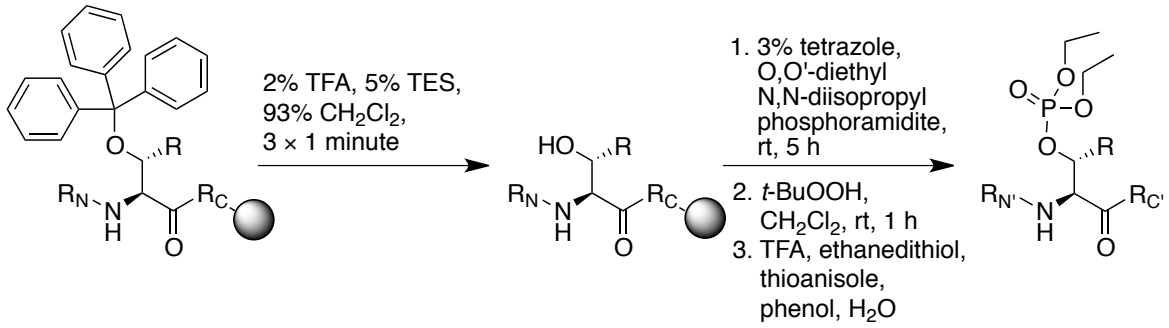

Scheme S2. Scheme for chemical diethylphosphorylation of peptides on resin. R = CH_3 (Thr) or R = H (Ser).

After phosphitylation, the reaction solution was removed and the resin washed with DMF (3×) and CH_2Cl_2 (3×). Oxidation was achieved in 1 h with mixing with *tert*-butyl hydroperoxide (4 mL of a 3 M solution in CH_2Cl_2). Following oxidation, the solution was removed and the resin washed with DMF (3×), MeOH (3×), and CH_2Cl_2 (3×). Peptides were then subjected to cleavage/deprotection and purification as described above.

Synthesis of Fmoc-Thr(O-GlcNAc)-OH (3) and Fmoc-Ser(O-GlcNAc)-OH (4)

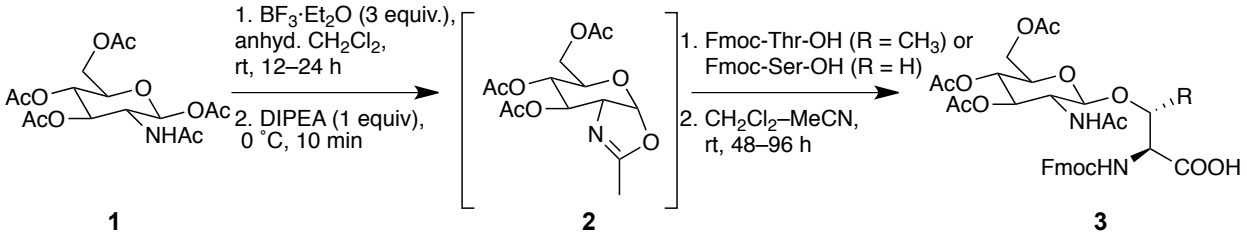

Scheme S3. Synthesis of peracetylated 2-acetamido-2-deoxy-β-D-glycosides of Fmoc-Thr-OH and Fmoc-Ser-OH.

The protected Fmoc-Thr(Ac_3-β-D-GlcNAc)-OH and Fmoc-Ser(Ac_3-β-D-GlcNAc)-OH were synthesized via a modification of the methodology of Arsequell *et al*. (**Scheme S3**).[4] After synthesis and purification, Fmoc-Thr(Ac_3-β-D-GlcNAc)-OH and Fmoc-Ser(Ac_3-β-D-GlcNAc)-OH were used as amino acid building blocks in Fmoc solid-phase glycopeptide synthesis. The peracetylated GlcNAc (960 mg, 2.5 mmol) (**1**) was vacuum dried and placed under argon in a flask containing 4 Å molecular sieves. The compound was dissolved in 16 mL of anhydrous CH_2Cl_2. At 0° C, 800 μL (7.64 mmol) of BF_3•Et_2O was added dropwise over 1 minute to the suspension and allowed to react for 12–24 h at room temperature. The reaction was monitored by TLC (10% MeOH in $CHCl_3$) and visualized using Hanessian's stain (cerium molybdate). When the formation of the oxazoline (**2**) was complete, the mixture was cooled to 0° C and 400 μL (2.29 mmol) of DIPEA was added. After 10 minutes of stirring at room temperature, Fmoc-Thr-

OH (867 mg, 2.54 mmol) or Fmoc-Ser-OH (831 mg, 2.54 mmol) was dissolved in a 9 mL solution of 2:1 CH_2Cl_2:MeCN and added to the reaction flask. The reaction mixture was gently stirred then left to stand at room temperature and allowed to react for 48–96 hours. Reaction progress was periodically monitored by TLC (10% MeOH in $CHCl_3$). A second batch of oxazoline (960 mg, 2.46 mmol), prepared as described above, was added after 24 h to increase yield. The crude reaction mixture was diluted with CH_2Cl_2 (40 mL) and filtered through Celite. The crude solution was neutralized by washing with 100 mL saturated bicarbonate solution and further washed with saturated brine solution (100 mL). The combined aqueous washes were kept for extraction of the product (**3** or **4**) with 300 mL ethyl acetate because some product was present in the aqueous fractions. The crude product was concentrated and purified via column chromatography (2–10% MeOH in $CHCl_3$). Product **3** was obtained as a white solid in 23% yield (753 mg) and product **4** was obtained as a white solid in 25% yield (811 mg). The ^{1}H NMR spectra of products **3** and **4** corresponded to literature values.[4]

Glycopeptide Synthesis

Glycosylated Fmoc amino acid couplings were performed for 4 hours. Following solid-phase peptide synthesis, the N-terminal residue was deprotected (20% piperidine in DMF, 3 × 5 minutes) and the N-terminus acetylated (0.5 M 1:1 DIC:acetic acid in THF, 60 min). The protected O-GlcNAcylated peptides were subjected to a 90 minute cleavage/deprotection reaction in 92.5% TFA/5% TES/2.5% H_2O; an abridged reaction time was used to suppress β-elimination of the sugars. TFA was partially removed by evaporation, peptide precipiated with ether, and peptides dissolved in water and purified by HPLC. After HPLC purification, the O-acetyl-protected O-GlcNAcylated peptides were lyophilized to remove solvent. The acetyl-protected OGlcNAc hydroxyls were then subjected to deesterification via NaOMe/MeOH (12 mM, 1.5 mL) for 1 h to generate free hydroxyl groups on the carbohydrate alcohols (**Scheme S4**). Following 1 h of deprotection, the reaction solution was neutralized with 60 μL of 1 M acetic acid and lyophilized. Dried and deprotected glycopeptides were dissolved in water, filtered, and purified to homogeneity by reverse phase HPLC as previously described.

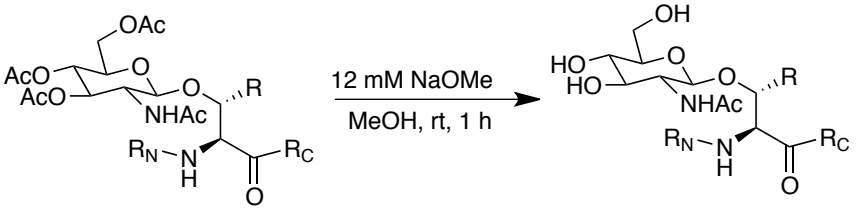

Scheme S4. Solution phase O-acetyl deprotection reaction to yield a final O-GlcNAcylated peptide product. R = CH_3 (Thr) or R = H (Ser).

Characterization data of tau peptides

	peptide	Sequence	Expected mass	Observed mass
5	$tau_{174\text{-}183}$	Ac-KTPPAPKTPP-NH_2	1073.6	1096.9 $(M+Na)^+$
6	$tau_{174\text{-}183}$	Ac-KpTPPAPKpTPP-NH_2	1232.6	1256.5 $(M+Na)^+$
7(7')	$tau_{174\text{-}183}$	Ac-KgTPPAPKgTPP-NH_2	1481.8	741.0 $(M+2H)^{2+}$
8	$tau_{174\text{-}183}$	Ac-KeTPPAPKeTPP-NH_2	1347.6	674.4 $(M+2H)^{2+}$
9	$tau_{174–183(T175E, T181E)}$	Ac-KEPPAPKEPP-NH_2	1129.6	566.0 $(M+2H)^{2+}$
10	$tau_{174–183(T175Tle, T181Tle)}$	Ac-KTlePPAPKTlePP-NH_2	1097.9	1098.7 $(M+H)^+$
11	$tau_{196\text{-}209}$	Ac-GYSSPGSPGTPGSR-NH_2	1346.6	1346.9 $(M+H)^+$
12	$tau_{196\text{-}209}$	Ac-GYSpSPGpSPGpTPGSR-NH_2	1746.7	872.5 $(M–2H)^{2–}$
13(13')	$tau_{196\text{-}209}$	Ac-GYSgSPGgSPGgTPGSR-NH_2	1956.2	979.0 $(M+2H)^{2+}$
14	$tau_{196\text{-}209}$	Ac-GYSeSPGeSPGeTPGSR-NH_2	1754.6	878.5 $(M+2H)^{2+}$
15	$tau_{211\text{-}219}$	Ac-YRTPSLPTPP-NH_2	1168.6	1169.8 $(M+H)^+$
16	$tau_{211\text{-}219}$	Ac-YRpTPpSLPpTPP-NH_2	1408.6	705.6 $(M+2H)^{2+}$
17(17')	$tau_{211\text{-}219}$	Ac-YRgTPgSLPgTPP-NH_2	1778.2	890.2 $(M+2H)^{2+}$
18	$tau_{211\text{-}219}$	Ac-YReTPeSLPeTPP-NH_2	1576.6	1577.3 $(M+H)^+$
19	$tau_{229\text{-}238}$	Ac-YVRTPPKSPSS-NH_2	1258.7	1259.7 $(M+H)^+$
20	$tau_{229\text{-}238}$	Ac-YVRpTPPKpSPpSS-NH_2	1498.7	750.7 $(M+2H)^{2+}$
21(21')	$tau_{229\text{-}238}$	Ac-YVRgTPPKgSPgSS-NH_2	1868.3	935.0 $(M+2H)^{2+}$
22	$tau_{229\text{-}238}$	Ac-YVReTPPKeSPeSS-NH_2	1666.7	834.7 $(M+2H)^{2+}$
23	$tau_{211\text{-}238}$	Ac-RTPSLPTPPTREPKKVAVVRTPPKSPSS-NH_2	3052.5	1527.2 $(M+2H)^{2+}$
24	$tau_{211\text{-}238}$	Ac-RpTPpSLPpTPPTREPKKVAVVRpTPPKpSPpSS-NH_2	3532.2	1178.2 $(M+3H)^{3+}$
25	$tau_{234\text{-}251}$	Ac-KSPSSAKSRLQTAPVPMP-NH_2	1923.2	962.3 $(M+2H)^{2+}$
26	$tau_{234–251}$(pS235)	Ac-KpSPSSAKSRLQTAPVPMP-NH_2	2002.0	1002.2 $(M+H)^{2+}$
27	$tau_{234–251}$(pS235/pS237)	Ac-KpSPpSSAKSRLQTAPVPMP-NH_2	2082.0	1042.2 $(M+H)^{2+}$

Table S1. Tau peptides examined in this study. pS or pT indicates a phosphorylated serine or threonine residue. eS or eT indicates a diethylphosphorylated (OPO_3Et_2) serine or threonine residue. gS or gT indicates an OGlcNAcylated serine or threonine residue. Residue numbers are based on the largest isoform of tau (441 amino acids). The peptides **8'**, **13'**, **17'**, and **21'** refer to peptides which are O-acetylated on the sugars prior to deacetylation.

Characterization data of model peptides

	peptide	Expected mass	Observed mass
28	Ac-KTPP-NH_2	482.2	505.3 $(M+Na)^+$
29	Ac-KpTPP-NH_2	562.2	608.2 $(M+2Na)^+$
30	Ac-KgTPP-NH_2	685.3	708.2 $(M+Na)^+$
31	Ac-KeTPP-NH_2	618.3	641.3 $(M+Na)^+$
32	Ac-KSPP-NH_2	468.2	469.3 $(M+H)^+$
33	Ac-KpSPP-NH_2	548.2	571.2 $(M+Na)^+$
34	Ac-KgSPP-NH_2	671.3	694.2 $(M+Na)^+$
35	Ac-KeSPP-NH_2	604.3	627.2 $(M+Na)^+$
36	Ac-GPKTPPGY-NH_2	856.4	879.2 $(M+Na)^+$
37	Ac-GPKpTPPGY-NH_2	936.4	959.2 $(M+Na)^+$
38	Ac-GPKgTPPGY-NH_2	1059.5	551.2 $(M+2Na)^{2+}$
39	Ac-GPKeTPPGY-NH_2	992.4	1015.0 $(M+Na)^+$
40	Ac-GPPTPPGY-NH_2	825.4	848.2 $(M+Na)^+$
41	Ac-GPPpTPPGY-NH_2	905.3	928.3 $(M+Na)^+$
42	Ac-GPPgTPPGY-NH_2	1028.4	1051.2 $(M+Na)^+$
43	Ac-GPPeTPPGY-NH_2	961.2	984.4 $(M+Na)^+$

Table S2. Model peptides examined in this study. pS or pT indicates a phosphorylated serine or threonine residue. eS or eT indicates a diethylphosphorylated (OPO_3Et_2) serine or threonine residue. gS or gT indicates an OGlcNAcylated serine or threonine residue.

Unmodified $tau_{174\text{-}183}$ (5)

Peptide **5** was purified and characterized as previously described.[5]

Phosphorylated $tau_{174\text{-}183}$ (6)

Peptide **6** was purified and characterized as previously described.[5]

O-GlcNAcylated $tau_{174\text{-}183}$ (7', 7)

O-Acetyl-protected peptide **7'** was purified via semi-preparative HPLC using a linear gradient of 0–45% buffer B in buffer A over 60 minutes: t_R = 33.4 min, exp. 1733.8, obs. 867.1 (M^{2+}). The deacetylated peptide **7** was purified via analytical HPLC using a linear gradient of 0–35% buffer B in buffer A over 60 minutes: t_R = 36.1 min, exp 1481.8, obs. 741.0 $(M+2H)^{2+}$.

Diethylphosphorylated $tau_{174\text{-}183}$ (8)

Peptide **8** was purified via analytical HPLC using a linear gradient of 0–50% buffer B in buffer A over 60 minutes: t_R = 37.7 min, exp. 1347.6, obs. 674.4 $(M+2H)^{2+}$.

tau$_{174–183}$(T175E, T181E) (9)

Peptide **9** was purified via analytical HPLC using a linear gradient of 0–35% buffer B in buffer A over 60 minutes: t_R = 29.8 min, exp. 1129.6, obs. 566.0 $(M+2H)^{2+}$.

tau$_{174-183}$(T175Tle, T181Tle) (10)

Peptide **10** was purified and characterized as previously described.[5]

Unmodified tau$_{196-209}$ (11)

Peptide **11** was purified and characterized as previously described.[5]

Phosphorylated tau$_{196-209}$ (12)

Peptide **12** was purified via analytical HPLC using a linear gradient of 0–20% buffer B in buffer A over 60 minutes: t_R = 30.8 min, exp. 1746.7, obs. 872.5 $(M–2H)^{2–}$ (negative ion mode).

O-GlcNAcylated tau$_{196-209}$ (13', 13)

O-Acetyl-protected peptide **13'** was purified via analytical HPLC using a linear gradient of 0–40% buffer B in buffer A over 60 minutes: t_R = 56.8 min, exp. 2336.9, obs. 1168.3 $(M)^{2+}$. The deacetylated peptide **13** was purified via analytical HPLC using a linear gradient of 0–30% buffer B in buffer A over 60 minutes: t_R = 33.6 min, exp 1956.2, obs. 979.0 $(M+2H)^{2+}$.

Diethylphosphorylated tau$_{196-209}$ (14)

Peptide **14** was purified via semi-preparative HPLC using a linear gradient of 0–35% buffer B in buffer A over 60 minutes: t_R = 51.8 min, exp. 1754.6, obs. 878.5 $(M+2H)^{2+}$.

Unmodified tau$_{211-219}$ (15)

Peptide **15** was purified and characterized as previously described.[5]

Phosphorylated tau$_{211-219}$ (16)

Peptide **16** was purified and characterized as previously described.[5]

O-GlcNAcylated tau$_{211-219}$ (17', 17)

O-Acetyl-protected peptide **17'** was purified via analytical HPLC using a linear gradient of 0–50% buffer B in buffer A over 60 minutes: t_R = 53.2 min, exp. 2156.5, obs. 1079.1 $(M+2H)^{2+}$. The deacetylated peptide **17** was purified via analytical HPLC using a linear gradient of 0–45% buffer B in buffer A over 60 minutes: t_R = 39.6 min, exp 1778.2, obs. 890.2 $(M+2H)^{2+}$.

Diethylphosphorylated tau$_{211-219}$ (18)

Peptide **18** was purified via analytical HPLC using a linear gradient of 0–60% buffer B in buffer A over 60 minutes: t_R = 46.9 min, exp. 1576.6, obs. 1577.3 $(M+H)^{+}$.

Unmodified tau$_{229-238}$ (19)

Peptide **19** was purified and characterized as previously described.[5]

Phosphorylated tau$_{229-238}$ (20)

Peptide **20** was purified and characterized as previously described.[5]

O-GlcNAcylated tau$_{229-238}$ (21', 21)

O-Acetyl-protected peptide **21'** was purified via analytical HPLC using a linear gradient of 0–45% buffer B in buffer A over 60 minutes: t_R = 49.3 min, exp. 2246.6, obs. 1124.2 $(M+2H)^{2+}$. The deacetylated peptide **21** was purified via analytical HPLC using a linear gradient of 0–30% buffer B in buffer A over 60 minutes: t_R = 36.7 min, exp 1868.3, obs. 935.0 $(M+2H)^{2+}$.

Diethylphosphorylated tau$_{229-238}$ (22)

Peptide **22** was purified via semipreparative HPLC using a linear gradient of 0–40% buffer B in buffer A over 60 minutes: t_R = 46.3 min, exp. 1666.7, obs. 834.7 $(M+2H)^{2+}$.

Unmodified tau$_{211-238}$ (23)

Peptide **23** was purified via semipreparative HPLC using a linear gradient of 0–30% buffer B in buffer A over 60 minutes: t_R = 44.6 min, exp. 3052.5, obs. 1527.2 $(M+2H)^{2+}$.

Phosphorylated tau$_{211-238}$ (24)

Peptide **24** was purified via analytical HPLC using a linear gradient of 0–30% buffer B in buffer A over 60 minutes: t_R = 49.3 min, exp. 3532.2, obs. 1178.2 $(M+3H)^{3+}$.

Unmodified tau$_{234-251}$ (25)

Peptide **25** was purified via semipreparative HPLC using a linear gradient of 0–30% buffer B in buffer A over 60 minutes: t_R = 57.9 min, exp. 1923.2, obs. 962.3 $(M+2H)^{2+}$.

Monophosphorylated tau$_{234-251}$(pS235) (26)

Phosphorylation of the peptide tau$_{234-251}$ was performed as described in the general procedure on page S3, with a modification to the oxidation step to obtain peptide **26**. In order to suppress methionine sulfoxide formation, oxidation was performed for 30 minutes instead of 60 minutes. Peptide **26** was purified via semipreparative HPLC using a linear gradient of 0–20% buffer B in buffer A over 60 minutes: t_R = 60 min, exp. 2002.2, obs. 1002.2 $(M+2H)^{2+}$.

Diphosphorylated tau$_{234-251}$(pS235/pS237) (27)

Phosphorylation of the peptide tau$_{234-251}$ was performed as described in the general procedure on page S3, with a modification to the oxidation step to obtain peptide **27**. In order to suppress methionine sulfoxide formation oxidation was performed for 30 minutes instead of 60 minutes. Peptide **27** was purified via semipreparative HPLC using a linear gradient of 0–20% buffer B in buffer A over 60 minutes: t_R = 58.8 min, exp. 2082.2, obs. 1042.2 $(M+2H)^{2+}$.

Ac-KTPP-NH$_2$ (28)

Peptide **28** was purified via analytical HPLC using a linear gradient of 0–30% buffer B in buffer A over 60 minutes: t_R = 18.6 min, exp. 482.2, obs. 505.3 $(M+Na)^{+}$.

Ac-KpTPP-NH$_2$ (29)

Peptide **29** was purified via analytical HPLC using a linear gradient of 0–20% buffer B in buffer A over 60 minutes: t_R = 13.1 min, exp. 562.2, obs. 608.2 $(M+2Na)^{+}$.

Ac-KT(OGlcNAc)PP-NH_2 (30) (deacetylated)

Peptide **25** was purified via analytical HPLC using a linear gradient of 0–30% buffer B in buffer A over 60 minutes: t_R = 47.3 min, exp. 685.3, obs. 708.2 $(M+Na)^+$.

Ac-KT(OPO_3Et_2)PP-NH_2 (31)

Peptide **31** was purified via analytical HPLC using a linear gradient of 0–50% buffer B in buffer A over 60 minutes: t_R = 47.3 min, exp. 618.3, obs. 641.3 $(M+Na)^+$.

Ac-KSPP-NH_2 (32)

Peptide **32** was purified via analytical HPLC using a linear gradient of 0–20% buffer B in buffer A over 60 minutes: t_R = 14.9 min, exp. 468.2, obs. 469.3 $(M+H)^+$.

Ac-KpSPP-NH_2 (33)

Peptide **33** was purified via analytical HPLC using a linear gradient of 0–20% buffer B in buffer A over 60 minutes: t_R = 17.8 min, exp. 548.2, obs. 571.2 $(M+Na)^+$.

Ac-KS(OGlcNAc)PP-NH_2 (34) (deacetylated)

Peptide **34** was purified via analytical HPLC using a linear gradient of 0–15% buffer B in buffer A over 60 minutes: t_R = 17.7 min, exp. 671.3, obs. 694.2 $(M+Na)^+$.

Ac-KS(OPO_3Et_2)PP-NH_2 (35)

Peptide **35** was purified via analytical HPLC using a linear gradient of 0–20% buffer B in buffer A over 60 minutes: t_R = 36.6 min, exp. 604.3, obs. 627.2 $(M+Na)^+$.

Ac-GPKTPPGY-NH_2 (36)

Peptide **36** was purified via analytical HPLC using a linear gradient of 0–30% buffer B in buffer A over 60 minutes: t_R = 36.0 min, exp. 856.4, obs. 879.2 $(M+Na)^+$.

Ac-GPKpTPPGY-NH_2 (37)

Peptide **37** was purified via analytical HPLC using 20 min isocratic 100% buffer A, followed by a linear gradient of 0–30% buffer B in buffer A over 60 minutes: t_R = 47.1 min, exp. 936.4, obs. 959.2 $(M+Na)^+$.

Ac-GPKT(OGlcNAc)PPGY-NH_2 (38) (deacetylated)

Peptide **38** was purified via analytical HPLC using a linear gradient of 0–30% buffer B in buffer A over 60 minutes: t_R = 35.5 min, exp. 1059.5, obs. 551.2 $(M+2Na)^{2+}$.

Ac-GPKT(OPO_3Et_2)PPGY-NH_2 (39)

Peptide **39** was purified via analytical HPLC using a linear gradient of 0–30% buffer B in buffer A over 60 minutes: t_R = 50.9 min, exp. 992.4, obs. 1015.0 $(M+Na)^+$.

Ac-GPPTPPGY-NH_2 (40)

Peptide **40** was purified via analytical HPLC using a linear gradient of 0–30% buffer B in buffer A over 60 minutes: t_R = 43.2 min, exp. 825.4, obs. 848.2 $(M+Na)^+$.

Ac-GPPpTPPGY-NH$_2$ (41)

Peptide **41** was purified via analytical HPLC using a linear gradient of 0–30% buffer B in buffer A over 60 minutes: t_R = 38.2 min, exp. 905.3, obs. 928.3 $(M+Na)^+$.

Ac-GPPT(OGlcNAc)PPGY-NH$_2$ (42) (deacetylated)

Peptide **42** was purified via analytical HPLC using a linear gradient of 0–30% buffer B in buffer A over 60 minutes: t_R = 41.1 min, exp. 1028.4, obs. 1051.2 $(M+Na)^+$.

Ac-GPPT(OPO$_3$Et$_2$)PPGY-NH$_2$ (43)

Peptide **43** was purified via analytical HPLC using a linear gradient of 0–30% buffer B in buffer A over 60 minutes: t_R = 56.6 min, exp. 961.2, obs. 984.4 $(M+Na)^+$.

Circular dichroism spectroscopy

CD spectra were collected on a Jasco J-810 Spectropolarimeter in a 1 mm cell at 25 ˚C unless otherwise indicated. Peptide concentrations were 15–450 μM. Solutions contained 25 mM KF in 5 mM phosphate buffer buffer (pH 8.0 or as indicated). Individual scans were made at 1 nm intervals with a 1 nm bandwidth and an averaging time of 4 s. Data represent the average of at least three independent trials. Data were background corrected but were not smoothed. Error bars are shown and indicate standard error.

NMR spectroscopy

NMR spectra of peptides were collected at 298 K or as indicated on a Brüker AVC 600 MHz NMR spectrometer equipped with a triple resonance cryoprobe or a TXI probe. Peptides were dissolved in buffer containing 5 mM phosphate buffer (pH 4.0, 6.5, 7.2, or 8.0) and were internally referenced with TSP. Solutions contained 25 mM NaCl, 100 μM TSP, and 90% H_2O/10% D_2O. Peptide NMR solution concentrations were 100 μM–1.0 mM. 1–D spectra were collected with a watergate pulse sequence and a relaxation delay of 2-3 s. Watergate TOCSY spectra were recorded for all peptides for resonance assignment. $^3J_{\alpha N}$ was determined directly from the 1-D spectra. Errors in $^3J_{\alpha N}$ are estimated to be ≤ 0.2 Hz. The calculation of ϕ was based on the parametrized Karplus equation, $^3J_{\alpha N} = 6.51 \cos^2(\phi - 60) - 1.76 \cos(\phi - 60) + 1.6$.[6] The calculation of χ_1 for threonine was based on the parametrized Karplus equation, $^3J_{H\alpha H\beta} = 4.37 - 1.86 \cos(\chi_1 - 120) + 3.81 \cos^2(\chi_1 - 120) - 0.37 \sin(\chi_1 - 120)$.[7] The calculation of χ_2 (χ_2 = C–H/O–P torsion angle + 120°) was based on the parametrized Karplus equation, $^3J_{PH} = 15.3 \cos^2(\chi_2 - 120) - 6.1 \cos(\chi_2 - 120) + 1.6$.[8]

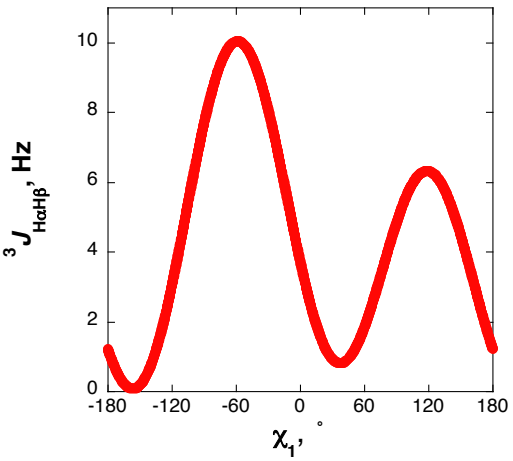

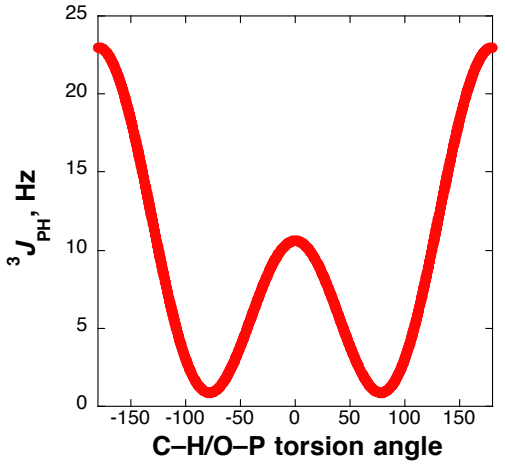

^{1}H–^{13}C HSQC (heteronuclear single quantum coherence) spectra were recorded for both the nonphosphorylated and the phosphorylated variants of the peptides $tau_{174–183}$, $tau_{211-219}$, $tau_{229–238}$, Ac-KTPP-NH_2, Ac-KSPP-NH_2, and $tau_{234–251}$. The peptides were dissolved in 100% D_2O containing 5 mM potassium phosphate (pH 8.0), 25 mM NaCl, and 100 μM TSP. Peptide concentrations were 500 μM–5 mM. NMR spectra were acquired on samples with natural abundance ^{13}C, using sweep widths of 20833 and 5388 Hz in t_1 and t_2, respectively, 400 × 2048 complex data points, 24 scans per t_1 increment and a relaxation delay of 2.0 s. Watergate TOCSY spectra were recorded to confirm resonance assignments. Spectra were recorded with ^{1}H-decoupling using spectral widths of 9 ppm and 130 ppm for peptide $tau_{174–183}$ and 9 ppm and 80-200 ppm for Ac-K*Tx*PP-NH_2 peptides. Spectral widths of 12 ppm and 80 ppm were used for the ^{1}H-decoupled spectra of Ac-K*Sx*PP-NH_2 peptides. ^{1}H–^{13}C HMBC spectra were recorded using a modified HSQC experiment with pulse sequence delays based on $J_{C–H}$ = 20 Hz instead of standard HSQC delays based on $^{1}J_{C–H}$ = 145 Hz. $^{1}J_{H\alpha C\alpha}$ coupling constants were measured directly from the HSQC spectra recorded without decoupling and were confirmed by comparison with the differences in chemical shift for the resonance recorded with decoupling. Errors in $^{1}J_{H\alpha C\alpha}$ are estimated to be ± 0.5 Hz. The value of ψ was calculated on basis of the measured $^{1}J_{H\alpha C\alpha}$, with the values of ϕ determined directly from $^{3}J_{\alpha N}$ and the parametrized Karplus equation, $^{1}J_{H\alpha C\alpha} = 140.3 + 1.4 \sin(\psi+138) – 4.1 \cos(2(\psi + 138)) + 2.0 \cos(2(\phi+ 30))$.[6]

^{1}H–^{15}N HSQC (heteronuclear single quantum coherence) spectra were recorded on samples with natural abundance ^{15}N for both the nonphosphorylated and the phosphorylated variants of the peptides $tau_{174–183}$, $tau_{211–219}$, $tau_{229–238}$, Ac-GPPTPPGY-NH_2 and Ac-KTPP-NH_2. ^{1}H–^{15}N HSQC spectra were also recorded for the OGlcNAcylated variants of $tau_{174-183}$ and Ac-KTPP-NH_2. ^{1}H–^{15}N HSQC spectra were acquired with sweep widths of 6614 Hz in t_1 and 1825 Hz in t_2, respectively, 64 × 2048 complex data points, 16 scans per t_1 increment, and a relaxation delay of 2.0 s. A Watergate pulse sequence was used for water suppression. The peptides were dissolved in 90% H_2O/10% D_2O containing 5 mM potassium phosphate (pH 8.0), 25 mM NaCl, and 100 μM TSP. Peptide concentrations were 1–2 mM. NMR spectra were recorded at 298 K.

NOESY spectra were acquired with sweep widths of 7183 Hz in t_1 and t_2, 600 × 4096 complex data points, respectively, 16 scans per t_1 increment, a relaxation delay of 2.0 s, and a NOESY mixing time of 200 ms.

Fmoc-Thr(Ac_3-β-D-GlcNAc)-OH and Fmoc-Ser(Ac_3-β-D-GlcNAc)-OH were dissolved in $CDCl_3$ at concentrations of 500 μM–2.0 mM and ^{1}H NMR spectra were collected at 296 K on a Brüker DRX 400 MHz NMR spectrometer equipped with a QNP probe.

^{31}P NMR spectroscopy

^{31}P NMR spectra were recorded on a Brüker DRX 400 MHz NMR spectrometer equipped with a BBO probe. The peptides were dissolved in buffer containing 5 mM potassium phosphate (pH 8.0) and 25 mM NaCl in 100% D_2O. To conduct NMR at pH 3.0, the peptide was dissolved in acetate buffer containing 5 mM sodium acetate (pH 3.0) in 100% D_2O. ^{31}P spectra were collected with 65536 data points and a relaxation delay of 5 seconds. The proton-coupled NMR spectra were recorded at 277, 298, 310, 323, and 338 K at pH 8.0 and at 298 K at pH 3.0. The NMR spectra were internally referenced with 85% H_3PO_4 (0.00 ppm) using a capillary filled with H_3PO_4 that was placed in the NMR tube containing the sample.

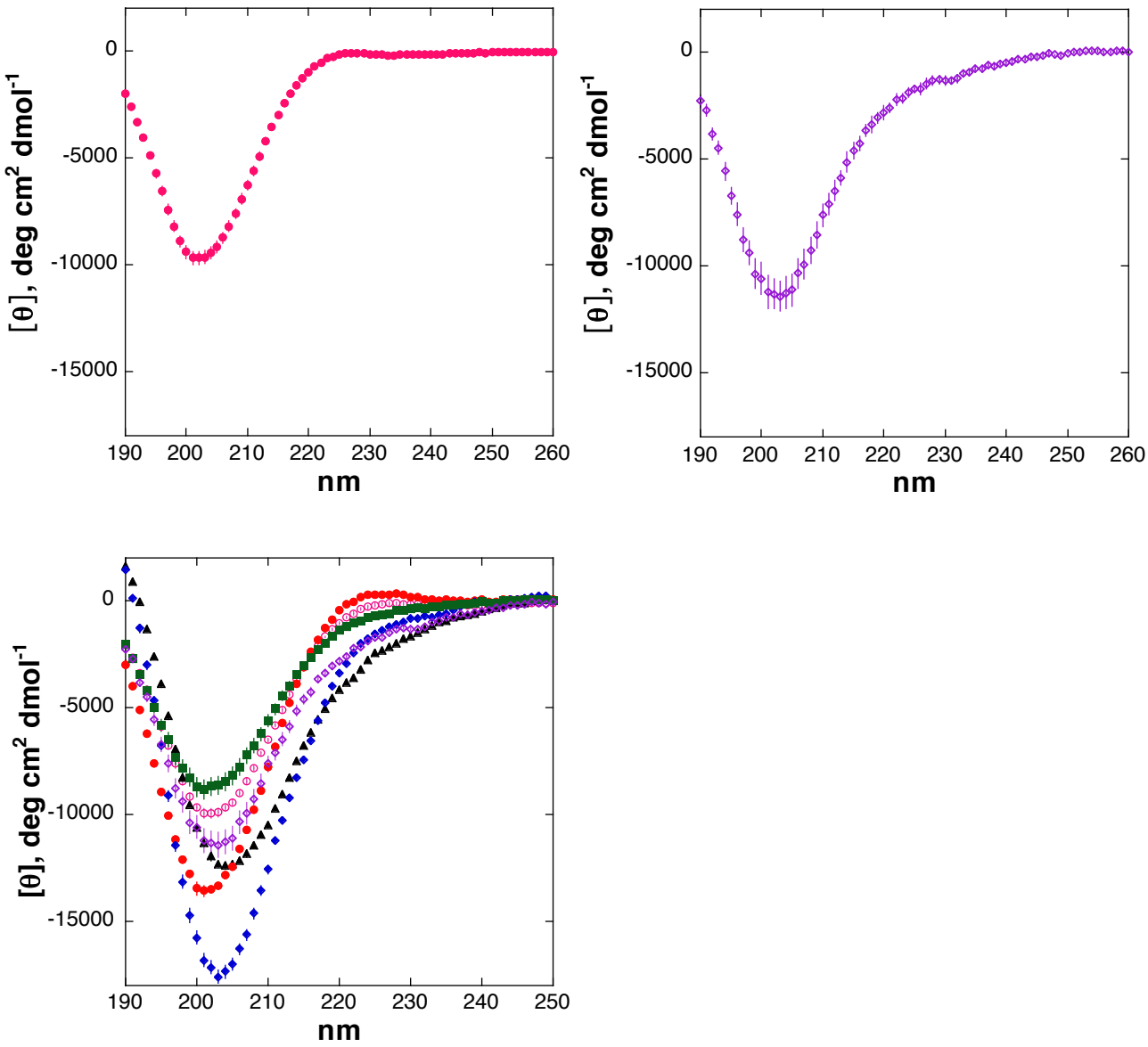

Figure S1. Top left: CD spectrum of $tau_{174–183}$(T175E, T181E) (Ac-KEPPAPKEPP-NH_2) (**9**) at pH 8.0, 25 ºC; top right: CD spectrum of $tau_{174–183}$(T175E, T181E) (Ac-KTlePPAPKTlePP-NH_2) (**10**) at pH 8.0, 25 ºC; bottom: CD spectra of $tau_{174–183}$ peptides in 5 mM phosphate buffer, 25 mM KF, pH 7.5. Thr: green squares; phosphothreonine: red circles; ThrOGlcNAc: blue diamonds; Thr diethylphosphate: black triangles; Glu: pink open circles; *tert*-leucine: purple open diamonds. Error bars indicate standard error.

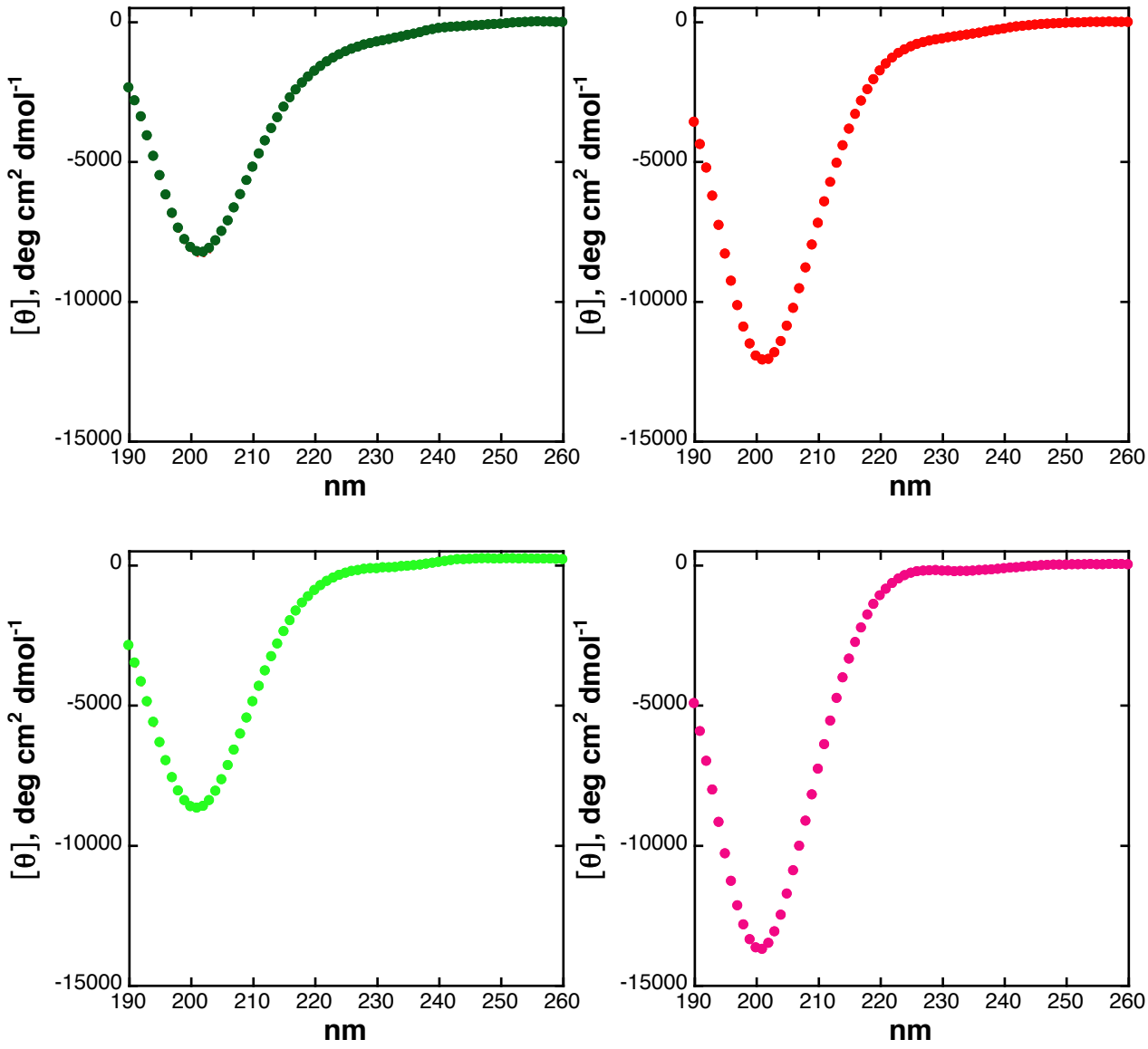

Figure S2. Top left: CD spectrum of $tau_{211–238}$ (Ac-RTPSLPTPPREPKKVAVVRTPPKSPSS-NH_2) (**23**) at pH 8.0, 25 ºC; top right: CD spectrum of $tau_{211–238}(OPO_3^{2–})$ (Ac-RpTPpSLPpTPPREPKKVAVVRpTPPKpSPpSS-NH_2) (**24**) at pH 8.0, 25 ºC; bottom left: CD spectrum of $tau_{211–238}$ (Ac-RTPSLPTPPREPKKVAVVRTPPKSPSS-NH_2) (**23**) at pH 8.0, 0.5 ºC; bottom right: CD spectrum of $tau_{211–238}(OPO_3^{2–})$ (Ac-RpTPpSLPpTPPREPKKVAVVRpTPPKpSPpSS-NH_2) (**24**) at pH 8.0, 0.5 ºC. The solutions contained 5 mM phosphate buffer and 25 mM KF. Error bars indicate standard errors.

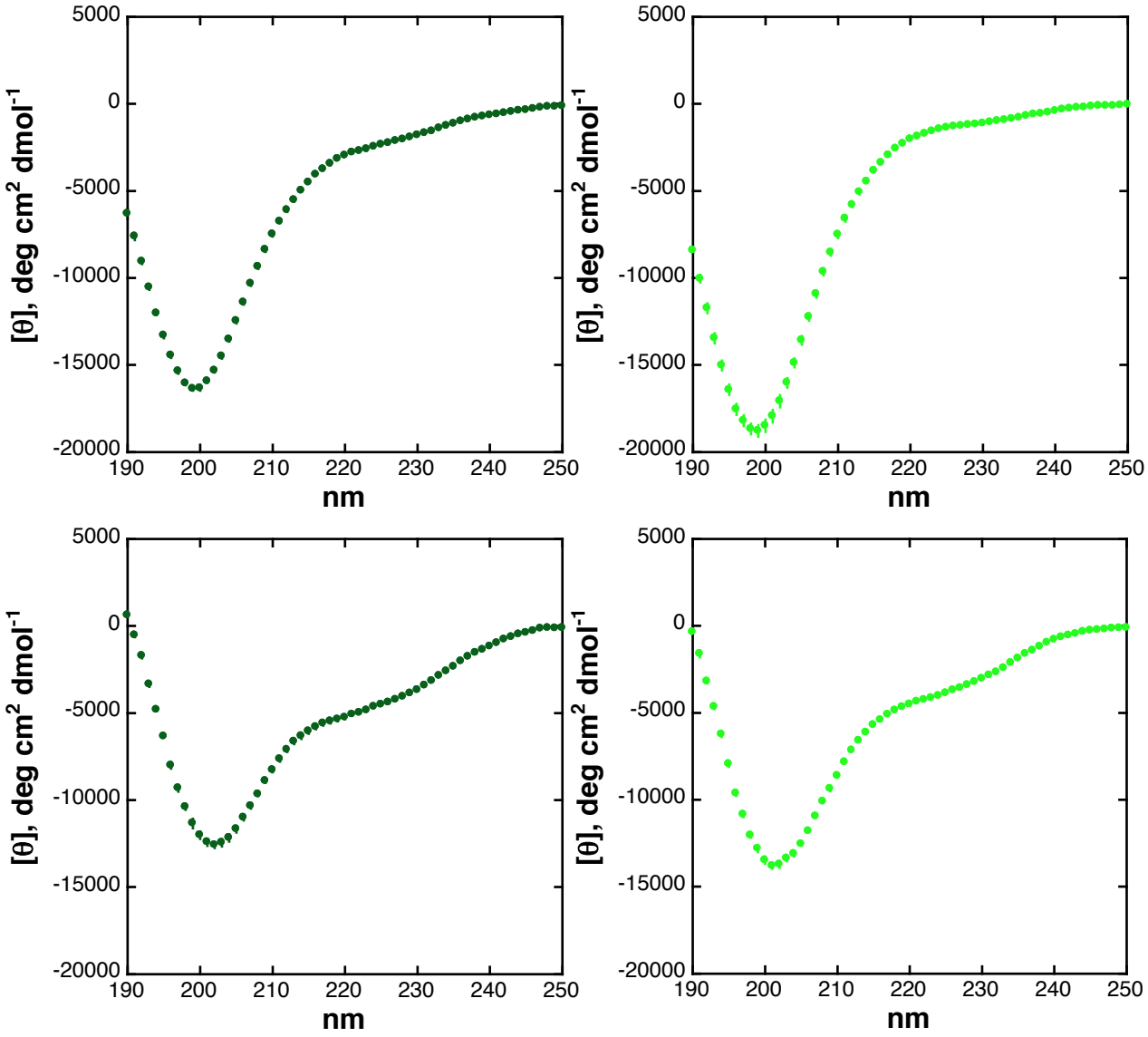

Figure S3. Top left: CD spectrum of $tau_{234–251}$ (Ac-KSPSSAKSRLQTAPVPMP-NH_2) (**25**) at pH 8.0, 25 ºC; top right: CD spectrum of $tau_{234–251}$ (Ac-KSPSSAKSRLQTAPVPMP-NH_2) (**25**) at pH 8.0, 0.5 ºC; bottom left: CD spectrum of $tau_{234–251}$ (Ac-KSPSSAKSRLQTAPVPMP-NH_2) (**25**) at pH 8.0, 0.5 ºC, in 30% TFE; bottom right: CD spectrum of $tau_{234–251}$ (Ac-KSPSSAKSRLQTAPVPMP-NH_2) (**25**) at pH 8.0, 0.5 ºC, in 30% TFE. The solutions contained 5 mM phosphate buffer and 25 mM KF. Error bars indicate standard errors.

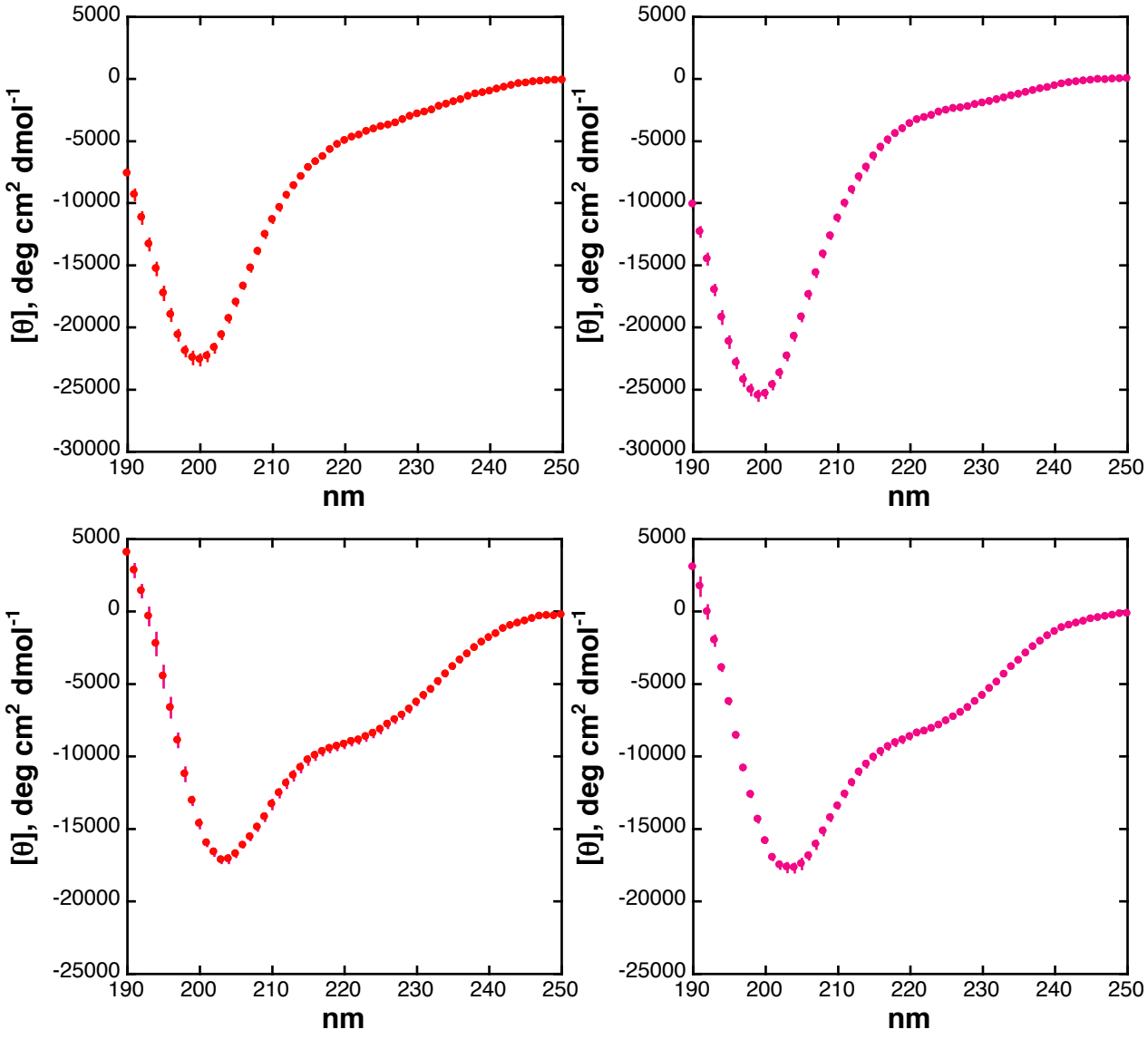

Figure S4. Top left: CD spectrum of $tau_{234–251}$(pS235) (Ac-KpSPSSAKSRLQTAPVPMP-NH_2) (**26**) at pH 8.0, 25 ºC; top right: CD spectrum of $tau_{234–251}$(pS235) (Ac-KpSPSSAKSRLQTAPVPMP-NH_2) (**26**) at pH 8.0, 0.5 ºC; bottom left: CD spectrum of $tau_{234–251}$(pS235) (Ac-KpSPSSAKSRLQTAPVPMP-NH_2) (**26**) at pH 8.0, 0.5 ºC, containing 30% TFE; bottom right: CD spectrum of $tau_{234–251}$(pS235) (Ac-KpSPSSAKSRLQTAPVPMP-NH_2) (**26**) at pH 8.0, 0.5 ºC, in 30% TFE. The solutions contained 5 mM phosphate buffer and 25 mM KF. Error bars indicate standard errors.

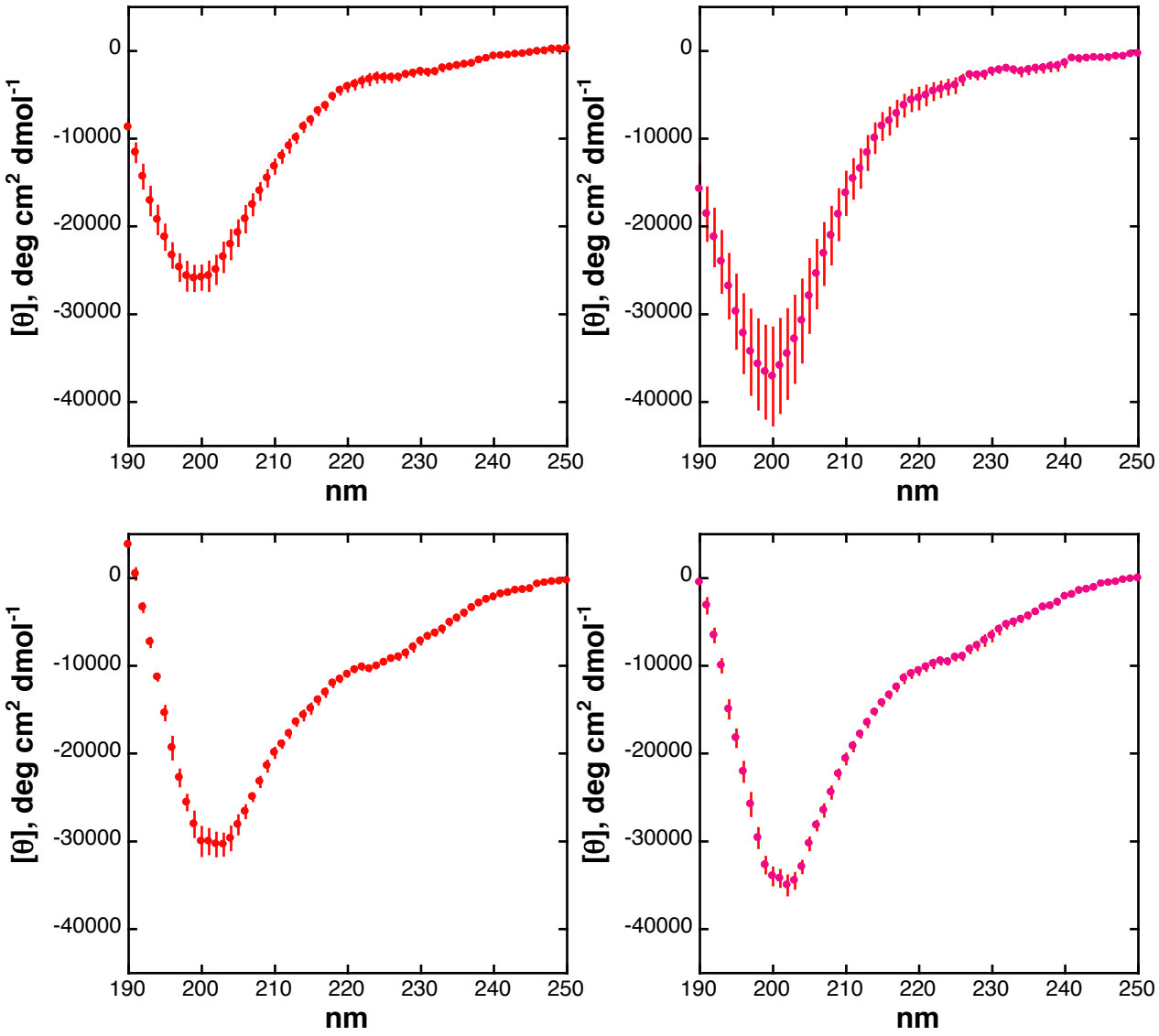

Figure S5. Top left: CD spectrum of $tau_{234–251}$(pS235/pS237) (Ac-KpSPpSSAKSRLQTAPVPMP-NH_2) (**27**) at pH 8.0, 25 ºC; top right: CD spectrum of $tau_{234–251}$(pS235/pS237) (Ac-KpSPpSSAKSRLQTAPVPMP-NH_2) (**27**) at pH 8.0, 0.5 ºC; bottom left: CD spectrum of $tau_{234–251}$(pS235/pS237) (Ac-KpSPpSSAKSRLQTAPVPMP-NH_2) (**27**) at pH 8.0, 0.5 ºC, containing 30% TFE; bottom right: CD spectrum of $tau_{234–251}$(pS235/pS237) (Ac-KpSPpSSAKSRLQTAPVPMP-NH_2) (**27**) at pH 8.0, 0.5 ºC, containing 30% TFE. The solutions contained 5 mM phosphate buffer and 25 mM KF. Error bars indicate standard errors.

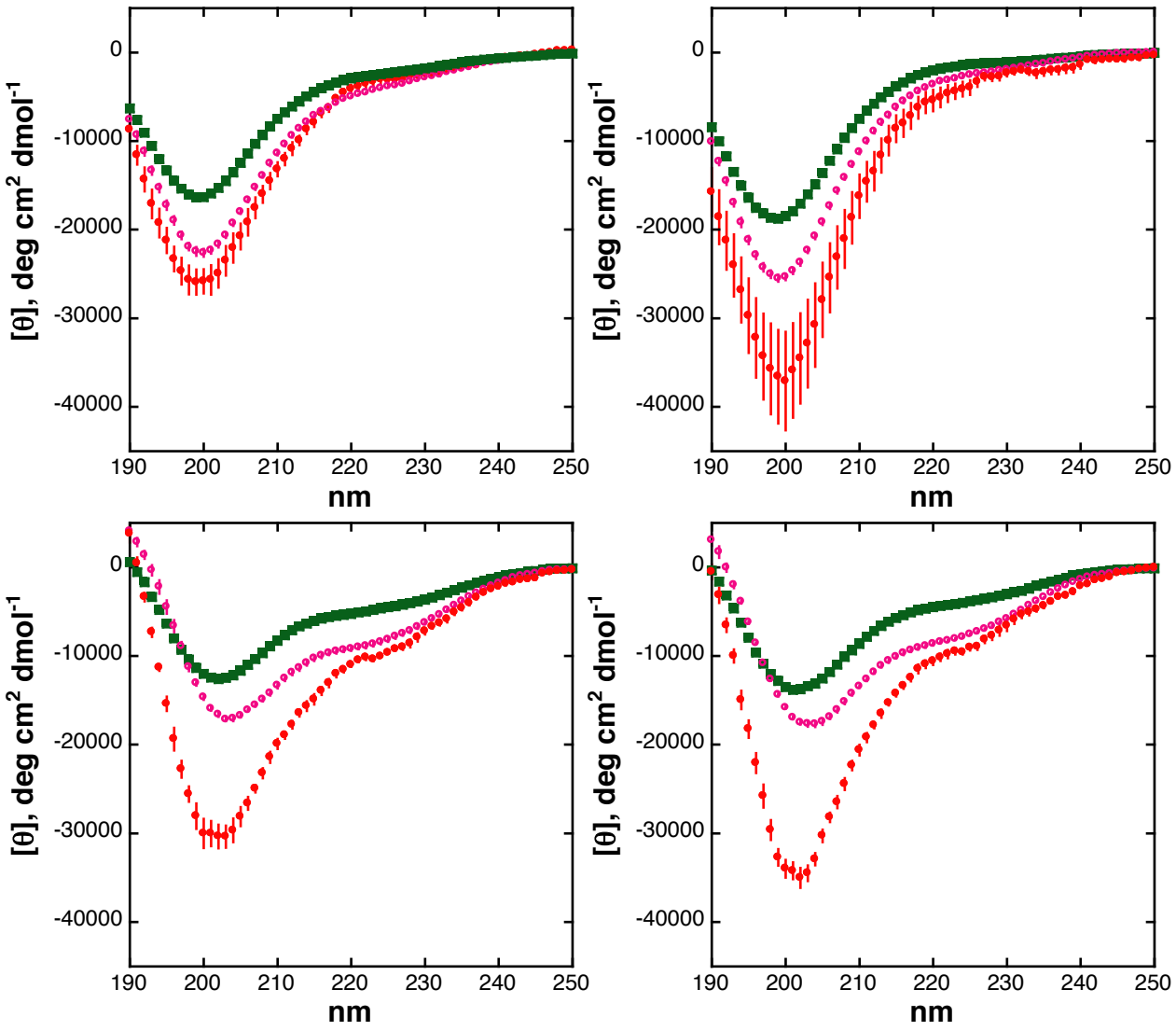

Figure S6. Top left: CD spectra of $tau_{234–251}$ (Ac-KSPSSAKSRLQTAPVPMP-NH_2) (**25**) (green squares), $tau_{234–251}$(pS235) (Ac-KpSPSSAKSRLQTAPVPMP-NH_2) (**26**) (magenta open circles), and $tau_{234–251}$(pS235/pS237) (Ac-KpSPpSSAKSRLQTAPVPMP-NH_2) (**27**) (red circles), at pH 8.0, 25 ºC; top right: CD spectra of $tau_{234–251}$ (Ac-KSPSSAKSRLQTAPVPMP-NH_2) (**25**) (green squares), $tau_{234–251}$(pS235) (Ac-KpSPSSAKSRLQTAPVPMP-NH_2) (**26**) (magenta open circles), and $tau_{234–251}$(pS235/pS237) (Ac-KpSPpSSAKSRLQTAPVPMP-NH_2) (**27**) (red circles), at pH 8.0, 0.5 ºC; bottom left: CD spectra of $tau_{234–251}$ (Ac-KSPSSAKSRLQTAPVPMP-NH_2) (**25**) (green squares), $tau_{234–251}$(pS235) (Ac-KpSPSSAKSRLQTAPVPMP-NH_2) (**26**) (magenta open circles), and $tau_{234–251}$(pS235/pS237) (Ac-KpSPpSSAKSRLQTAPVPMP-NH_2) (**27**) (red circles), at pH 8.0, 25 ºC containing 30% TFE; bottom right: CD spectra of $tau_{234–251}$ (Ac-KSPSSAKSRLQTAPVPMP-NH_2) (**25**) (green squares), $tau_{234–251}$(pS235) (Ac-KpSPSSAKSRLQTAPVPMP-NH_2) (**26**) (magenta open circles), and $tau_{234–251}$(pS235/pS237) (Ac-KpSPpSSAKSRLQTAPVPMP-NH_2) (**27**) (red circles), at pH 8.0, 0.5 ºC containing 30% TFE. Error bars indicate standard error.

Summary of CD data for tau peptides

peptide	$[\theta]_{228}$, deg cm^2 dmol^{-1}	λ at local $[\theta]_{max}$, nm	local $[\theta]_{max}$, deg cm^2 dmol^{-1}	λ at $[\theta]_{min}$, nm	$[\theta]_{min}$, deg cm^2 dmol^{-1}	$[\theta]_{190}$, deg cm^2 dmol^{-1}
Ac-KTPPAPKTPP-NH_2	–452	n.a.[a]	n.a.	201	–8843	–2040
Ac-KpTPPAPKpTPP-NH_2	339	228	339	201	–13576	–2986
Ac-KgTPPAPKgTPP-NH_2	–1121	n.a.	n.a.	203	–17583	1426
Ac-KeTPPAPKeTPP-NH_2	–1991	n.a.	n.a.	204	–12390	1589
Ac-KEPPAPKEPP-NH_2	2	228	2	202	–9949	–2058
Ac-KTlePPAPKTlePP-NH_2	–1620	n.a.	n.a.	203	–11300	–2280
Ac-GYSSPGSPGTPGSR-NH_2	–2468	n.a.	n.a.	194	–10550	–8154
Ac-GYSpSPGpSPGpTPGSR-NH_2	–2323	n.a.	n.a.	197	–14440	–5508
Ac-GYSgSPGgSPGgTPGSR-NH_2	–1370	n.a.	n.a.	200	–7462	–1384
Ac-GYSeSPGeSPGeTPGSR-NH_2	–3075	n.a.	n.a.	206	–6554	87
Ac-YRTPSLPTPP-NH_2	–732	n.a.	n.a.	201	–17256	–7865
Ac-YRpTPpSLPpTPP-NH_2	287	227	354	202	–18151	–4368
Ac-YRgTPgSLPgTPP-NH_2	–1011	n.a.	n.a.	204	–15442	4533
Ac-YReTPeSLPeTPP-NH_2	–2661	n.a.	n.a.	205	–10877	129
Ac-YVRTPPKSPSS-NH_2	–1145	n.a.	n.a.	200	–21699	–5949
Ac-YVRpTPPKpSPpSS-NH_2	904	228	904	199	–28500	–9694
Ac-YVRgTPPKgSPgSS-NH_2	–1036	n.a.	n.a.	204	–15882	1446
Ac-YVReTPPKeSPSeS-NH_2	–2556	n.a.	n.a.	203	–15532	2081
Ac-RTPSLPTPPREPKKVAVVRTPPKSPSS-NH_2	–837	n.a.	n.a.	202	–8247	–2370
Ac-RpTPpSLPpTPPREPKKVAVVRpTPPKpSPpSS-NH_2	–694	n.a.	n.a.	201	–12097	–3596

Table S3. Summary of CD data for tau peptides. CD data were collected at 0.5 or 25 ºC with 15–200 μM peptide in 5 mM phosphate buffer (pH 8.0) with 25 mM KF. [a] No local maximum was observed. pS or pT indicates a phosphorylated serine or threonine residue. eS or eT indicates a diethylphosphorylated (OPO_3Et_2) serine or threonine residue. gS or gT indicates an OGlcNAcylated serine or threonine residue. Tle indicates *tert*-leucine.

peptide	$[\theta]_{222}$, deg cm^2 dmol^{-1}	$[\theta]_{208}$, deg cm^2 dmol^{-1}	λ at $[\theta]_{min}$, nm	$[\theta]_{min}$, deg cm^2 dmol^{-1}	temp, °C	% TFE
Ac-KSPSSAKSRLQTAPVPMP-NH_2	–2710	–9352	199	–16370	25	0
Ac-KpSPSSAKSRLQTAPVPMP-NH_2	–4539	–13907	200	–22614	25	0
Ac-KpSPpSSAKSRLQTAPVPMP-NH_2	–3544	–16015	199	–25921	25	0
Ac-KSPSSAKSRLQTAPVPMP-NH_2	–1709	–9640	199	–18781	0.5	0
Ac-KpSPSSAKSRLQTAPVPMP-NH_2	–2251	–14134	199	–25495	0.5	0
Ac-KpSPpSSAKSRLQTAPVPMP-NH_2	–2818	–21062	200	–37108	0.5	0
Ac-KSPSSAKSRLQTAPVPMP-NH_2	–4987	–9668	202	–12585	25	30
Ac-KpSPSSAKSRLQTAPVPMP-NH_2	–8894	–14901	203	–17163	25	30
Ac-KpSPpSSAKSRLQTAPVPMP-NH_2	–10182	–23219	203	–30371	25	30
Ac-KSPSSAKSRLQTAPVPMP-NH_2	–4259	–10103	201	–13820	0.5	30
Ac-KpSPSSAKSRLQTAPVPMP-NH_2	–8292	–15166	204	–17710	0.5	30
Ac-KpSPpSSAKSRLQTAPVPMP-NH_2	–9786	–24430	202	–35030	0.5	30

Table S4. Summary of CD data for $tau_{234\text{-}251}$ peptides. CD data were collected at 0.5 or 25 ºC with 15–45 μM peptide in 5 mM phosphate buffer (pH 8.0) with 25 mM KF. pS indicates a phosphorylated serine residue.

CD spectra of model peptides Ac-K*Tx*PP-NH_2

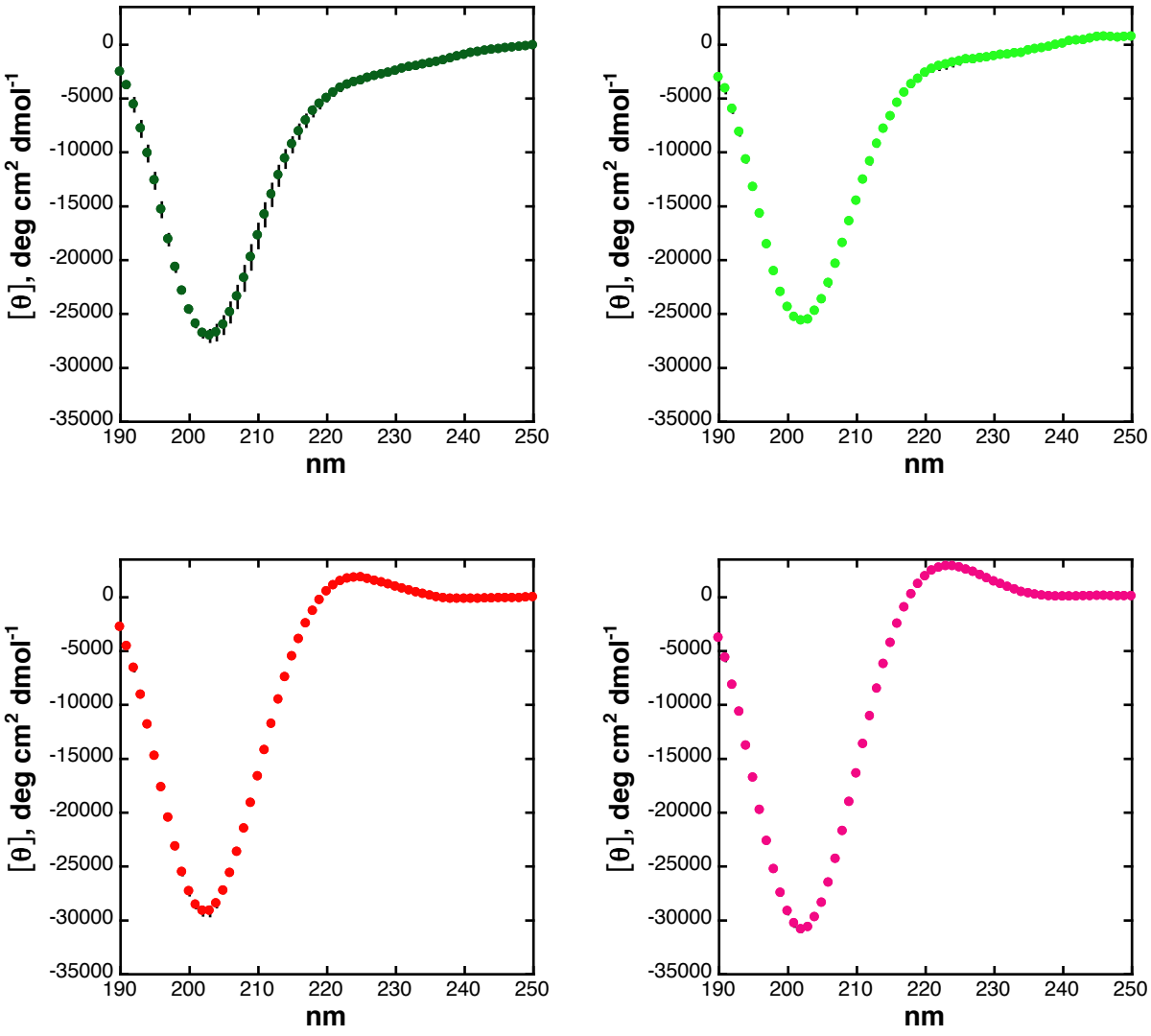

Figure S7. Top left: CD spectrum of Ac-KTPP-NH_2 (**28**) at pH 8.0, 25 ºC; top right: CD spectrum of Ac-KTPP-NH_2 (**28**) at pH 8.0, 2 ºC; bottom left: CD spectrum of Ac-KT(OPO_3^{2-})PP-NH_2 (**29**) at pH 8.0, 25 ºC; and bottom right: CD spectrum of Ac-KT(OPO_3^{2-})PP-NH_2 (**29**) at pH 8.0, 2 ºC. Error bars indicate standard errors.

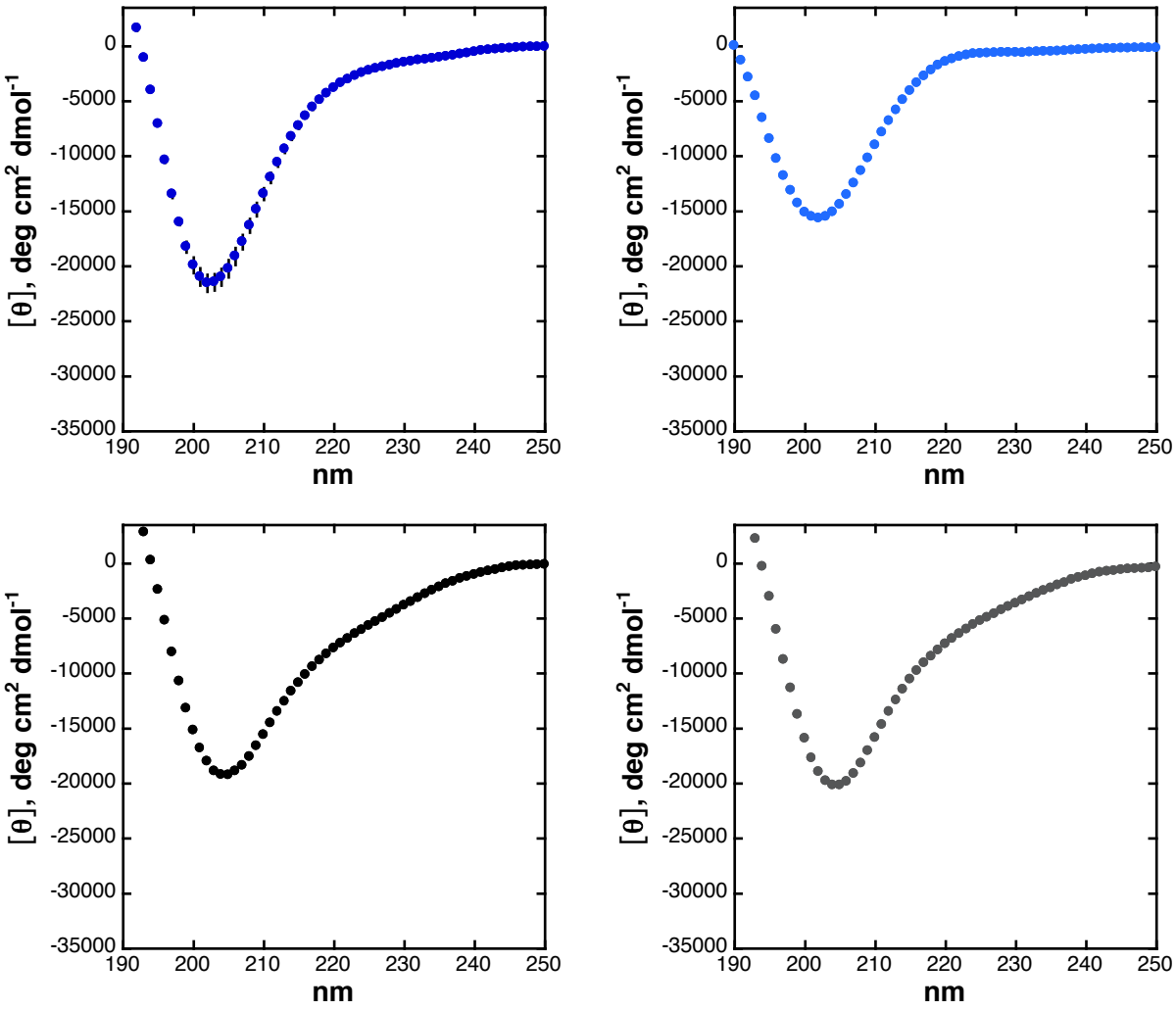

Figure S8. Top left: CD spectrum of Ac-KT(OGlcNAc)PP-NH_2 (**30**) at pH 8.0, 25 ºC; top right: CD spectrum of Ac-KT(OGlcNAc)PP-NH_2 (**30**) at pH 8.0, 2 ºC; bottom left: CD spectrum of Ac-KT(OPO_3Et_2)PP-NH_2 (**31**) at pH 8.0, 2 ºC; and bottom right: CD spectrum of Ac-KT(OPO_3Et_2)PP-NH_2 (**31**) at pH 8.0, 2 ºC. Error bars indicate standard errors.

CD spectra of model peptides Ac-K*Sx*PP-NH_2

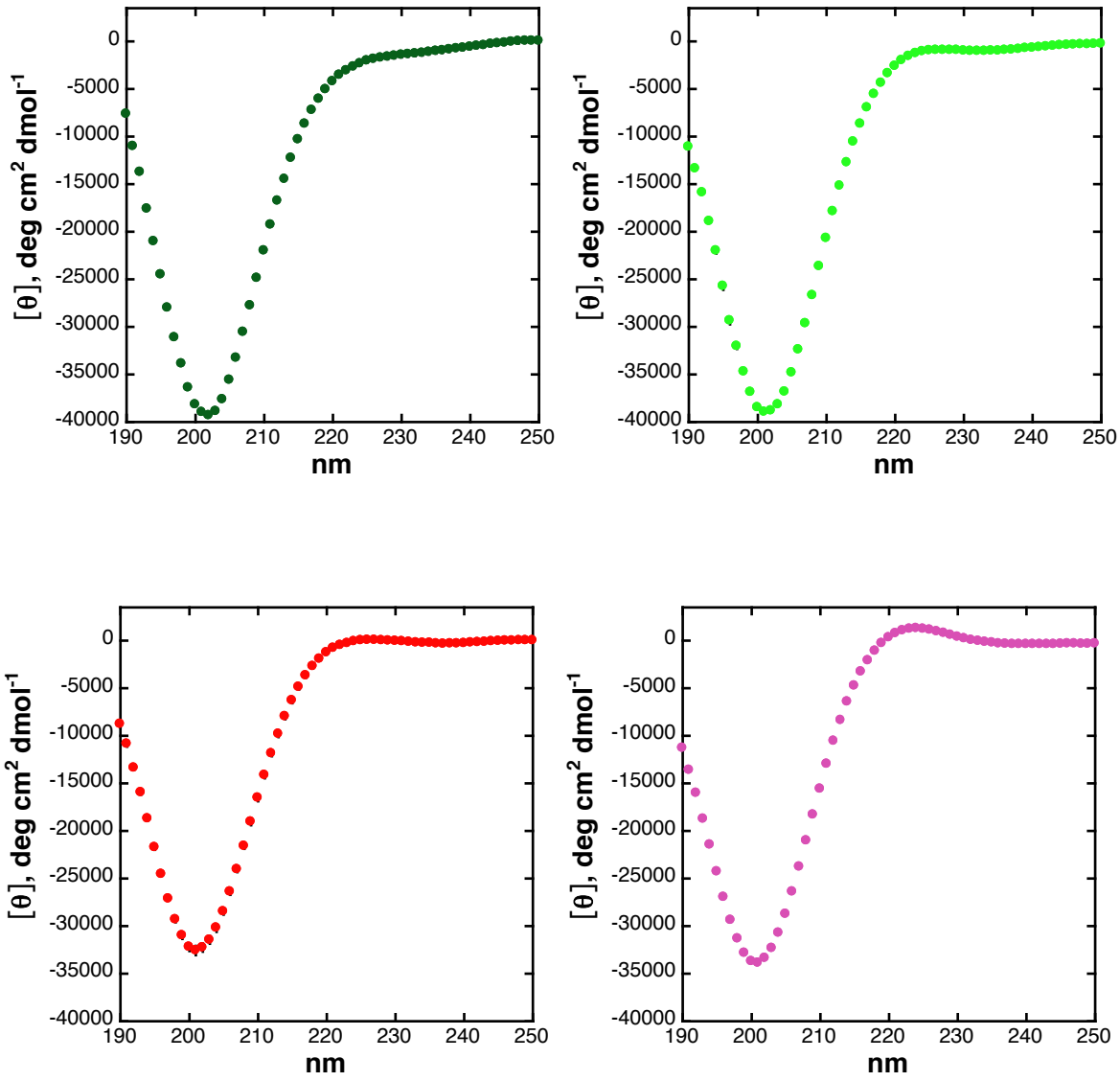

Figure S9. Top left: CD spectrum of Ac-KSPP-NH_2 (**32**) at pH 8.0, 25 ºC; top right: CD spectrum of Ac-KSPP-NH_2 (**32**) at pH 8.0, 2 ºC; bottom left: CD spectrum of Ac-KS(OPO_3^{2-})PP-NH_2 (**33**) at pH 8.0, 25 ºC; and bottom right: CD spectrum of Ac-KS(OPO_3^{2-})PP-NH_2 (**33**) at pH 8.0, 2 ºC. Error bars indicate standard errors.

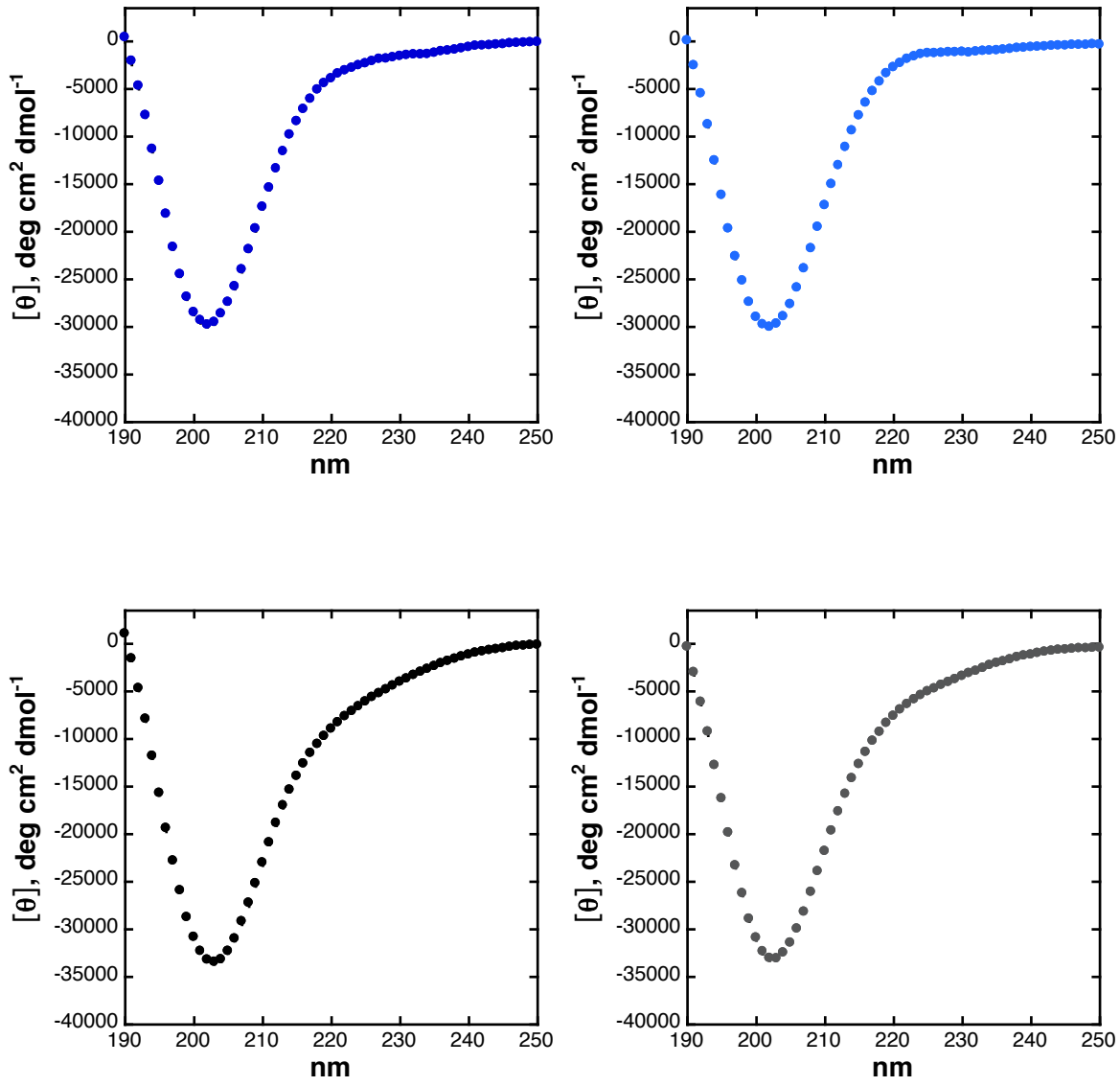

Figure S10. Top left: CD spectrum of Ac-KS(OGlcNAc)PP-NH_2 (**34**) at pH 8.0, 25 ºC; top right: CD spectrum of Ac-KS(OGlcNAc)PP-NH_2 (**34**) at pH 8.0, 2 ºC; bottom left: CD spectrum of Ac-KS(OPO_3Et_2)PP-NH_2 (**35**) at pH 8.0, 2 ºC and bottom right: CD spectrum of Ac-KT(OPO_3Et_2)PP-NH_2 (**35**) at pH 8.0, 2 ºC. Error bars indicate standard errors.

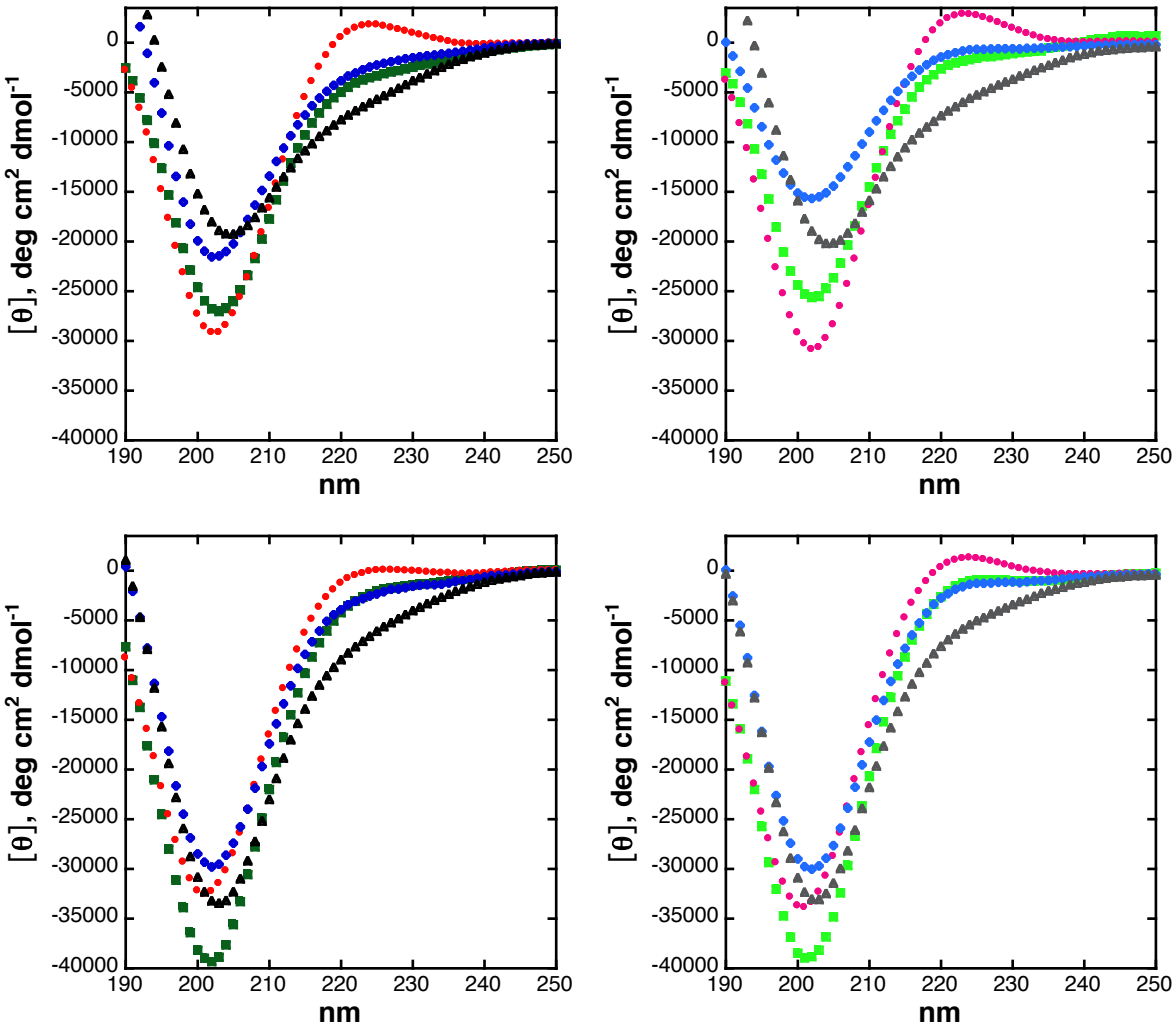

Figure S11. Top left; CD spectra of Ac-K*Tx*PP-NH_2 peptides at 25 ºC; Thr: green squares; phosphothreonine: red circles; ThrOGlcNAc: blue diamonds; Thr diethylphosphate: black triangles; top right; CD spectra of Ac-K*Tx*PP-NH_2 peptides at 2 ºC; Thr: light green squares; phosphothreonine: magenta circles; ThrOGlcNAc: light blue diamonds; Thr diethylphosphate: grey triangles; bottom left; CD spectra of Ac-K*Sx*PP-NH_2 peptides at 25 ºC; Ser: green squares; phosphoserine: red circles; SerOGlcNAc: blue diamonds; Ser diethylphosphate: black triangles; bottom right; CD spectra of Ac-K*Sx*PP-NH_2 peptides at 2 ºC; Ser: light green squares; phosphoserine: magenta circles; SerOGlcNAc: light blue diamonds; Ser diethylphosphate: grey triangles. Data were collected in 5 mM phosphate buffer buffer containing 25 mM KF.

peptide	$[\theta]_{228}$, deg cm^2 dmol^{-1}	λ at local $[\theta]_{max}$, nm	local $[\theta]_{max}$, deg cm^2 dmol^{-1}	λ at $[\theta]_{min}$, nm	$[\theta]_{min}$, deg cm^2 dmol^{-1}	Temp, °C
Ac-KTPP-NH_2	–2801	n.a.[a]	n.a.	203	–27045	25
Ac-KT(OPO_3^{2-})PP-NH_2	1321	225	1790	202	–29165	25
Ac-KT(OGlcNAc)PP-NH_2	–1761	n.a.	n.a.	202	–21545	25
Ac-KT(OPO_3Et_2)PP-NH_2	–4587	n.a.	n.a.	205	–19258	25
Ac-KTPP-NH_2	–1295	n.a.	n.a.	202	–25637	2
Ac-KT(OPO_3^{2-})PP-NH_2	2016	223	2852	202	–30878	2
Ac-KT(OGlcNAc)PP-NH_2	–602	n.a.	n.a.	202	–15672	2
Ac-KT(OPO_3Et_2)PP-NH_2	–4263	n.a.	n.a.	204	–20187	2
Ac-KSPP-NH_2	–1638	n.a.	n.a.	202	–39320	25
Ac-KS(OPO_3^{2-})PP-NH_2	8	226	49	201	–32565	25
Ac-KS(OGlcNAc)PP-NH_2	–1823	n.a.	n.a.	202	–29790	25
Ac-KS(OPO_3Et_2)PP-NH_2	–4814	n.a.	n.a.	203	–33453	25
Ac-KSPP-NH_2	–920	n.a.	n.a.	201	–38960	2
Ac-KS(OPO_3^{2-})PP-NH_2	774	224	1278	201	–33904	2
Ac-KS(OGlcNAc)PP-NH_2	–1154	n.a.	n.a.	202	–30043	2
Ac-KS(OPO_3Et_2)PP-NH_2	–4043	n.a.	n.a.	203	–33087	2

Table S5. Summary of CD data for Ac-K*Tx*PP-NH_2 and Ac-K*Sx*PP-NH_2 peptides. CD data were collected with 100–450 μM peptide in 5 mM phosphate buffer (pH 8.0) containing 25 mM KF at 2 °C and 25 °C. [a] No local maximum was observed.

peptide	$[\theta]_{224}$, deg cm^2 $dmol^{-1}$	$[\theta]_{202}$, deg cm^2 $dmol^{-1}$	$[\theta]_{190}$, deg cm^2 $dmol^{-1}$	Temp, °C
Ac-KTPP-NH_2	–3522	–26794	–2553	25
Ac-KT(OPO_3^{2-})PP-NH_2	1786	–29165	–2783	25
Ac-KT(OGlcNAc)PP-NH_2	–2449	–21545	5917	25
Ac-KT(OPO_3Et_2)PP-NH_2	–6061	–18016	7999	25
Ac-KTPP-NH_2	–1700	–25637	–3063	2
Ac-KT(OPO_3^{2-})PP-NH_2	2830	–30878	–3801	2
Ac-KT(OGlcNAc)PP-NH_2	–716	–15672	33	2
Ac-KT(OPO_3Et_2)PP-NH_2	–5603	–18954	7770	2
Ac-KSPP-NH_2	–2329	–39320	–7630	25
Ac-KS(OPO_3^{2-})PP-NH_2	–94	–32269	–8803	25
Ac-KS(OGlcNAc)PP-NH_2	–2543	–29790	414	25
Ac-KS(OPO_3Et_2)PP-NH_2	–6596	–33212	1030	25
Ac-KSPP-NH_2	–1052	–38838	–11106	2
Ac-KS(OPO_3^{2-})PP-NH_2	1278	–33389	–11286	2
Ac-KS(OGlcNAc)PP-NH_2	–1373	–30043	63	2
Ac-KS(OPO_3Et_2)PP-NH_2	–5433	–33053	–340	2

Table S6. Summary of CD data for Ac-K*Tx*PP-NH_2 and Ac-K*Sx*PP-NH_2 peptides. CD data were collected with 100–450 μM peptide in 5 mM phosphate buffer (pH 8.0) containing 25 mM KF at 2 °C and 25 °C. [a] No local maximum was observed.

CD spectra of Ac-GPK*Tx*PPGY-NH_2 peptides

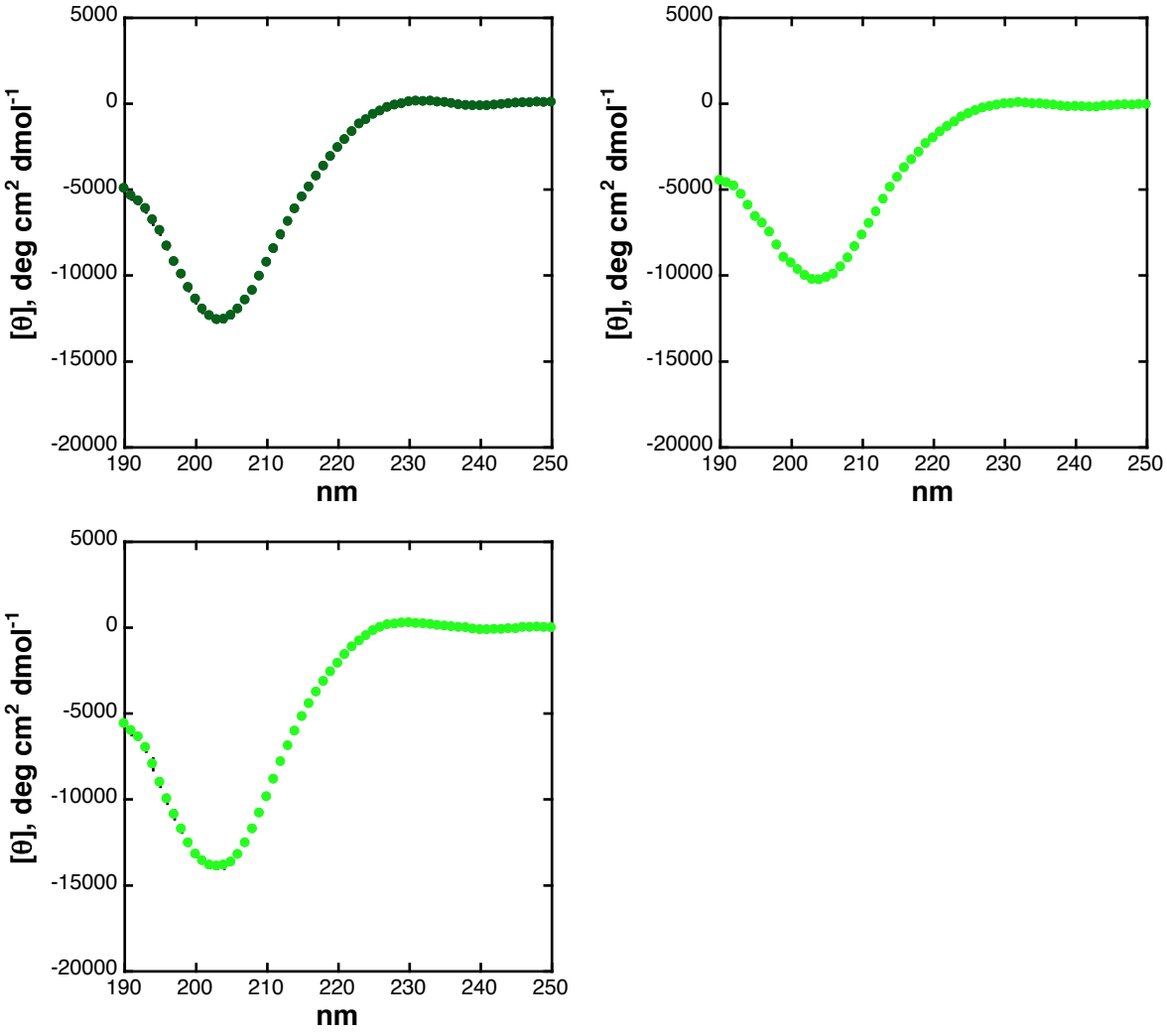

Figure S12. Top left: CD spectrum of Ac-GPKTPPGY-NH_2 (**36**) at pH 6.5, 25 ºC; top right: CD spectrum of Ac-GPKTPPGY-NH_2 (**36**) at pH 8.0, 25 ºC; and bottom: CD spectrum of Ac-GPKTPPGY-NH_2 (**36**) at pH 8.0, 2 ºC. Error bars indicate standard errors.

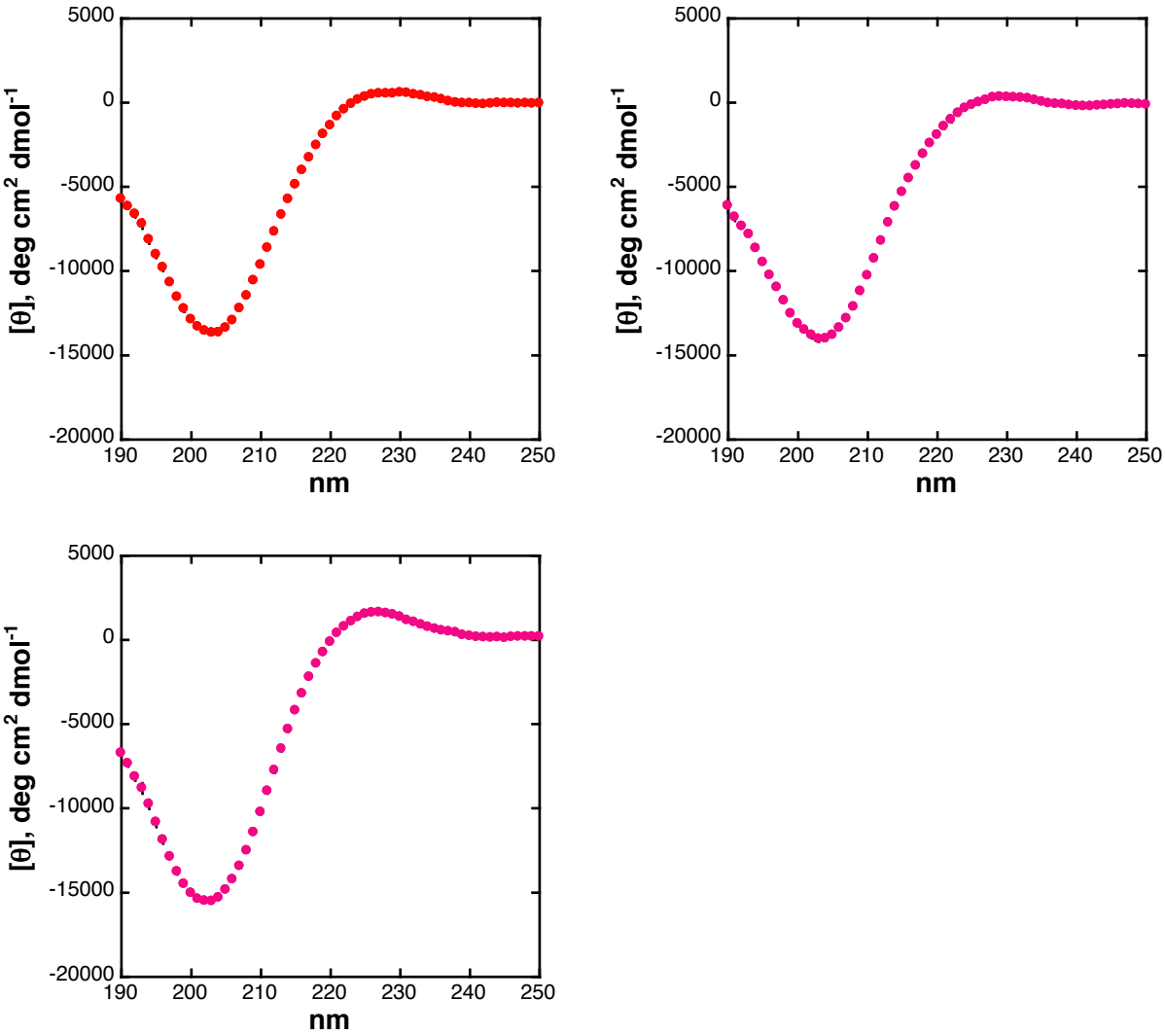

Figure S13. Top left: CD spectrum of Ac-GPKT($OPO_3^{-/2-}$)PPGY-NH_2 (**37**) at pH 6.5, 25 ºC; top right: CD spectrum of Ac-GPKT(OPO_3^{2-})PPGY-NH_2 (**37**) at pH 8.0, 25 ºC; bottom: CD spectrum of Ac-GPKT(OPO_3^{2-})PPGY-NH_2 (**37**) at pH 8.0, 2 ºC. Error bars indicate standard errors.

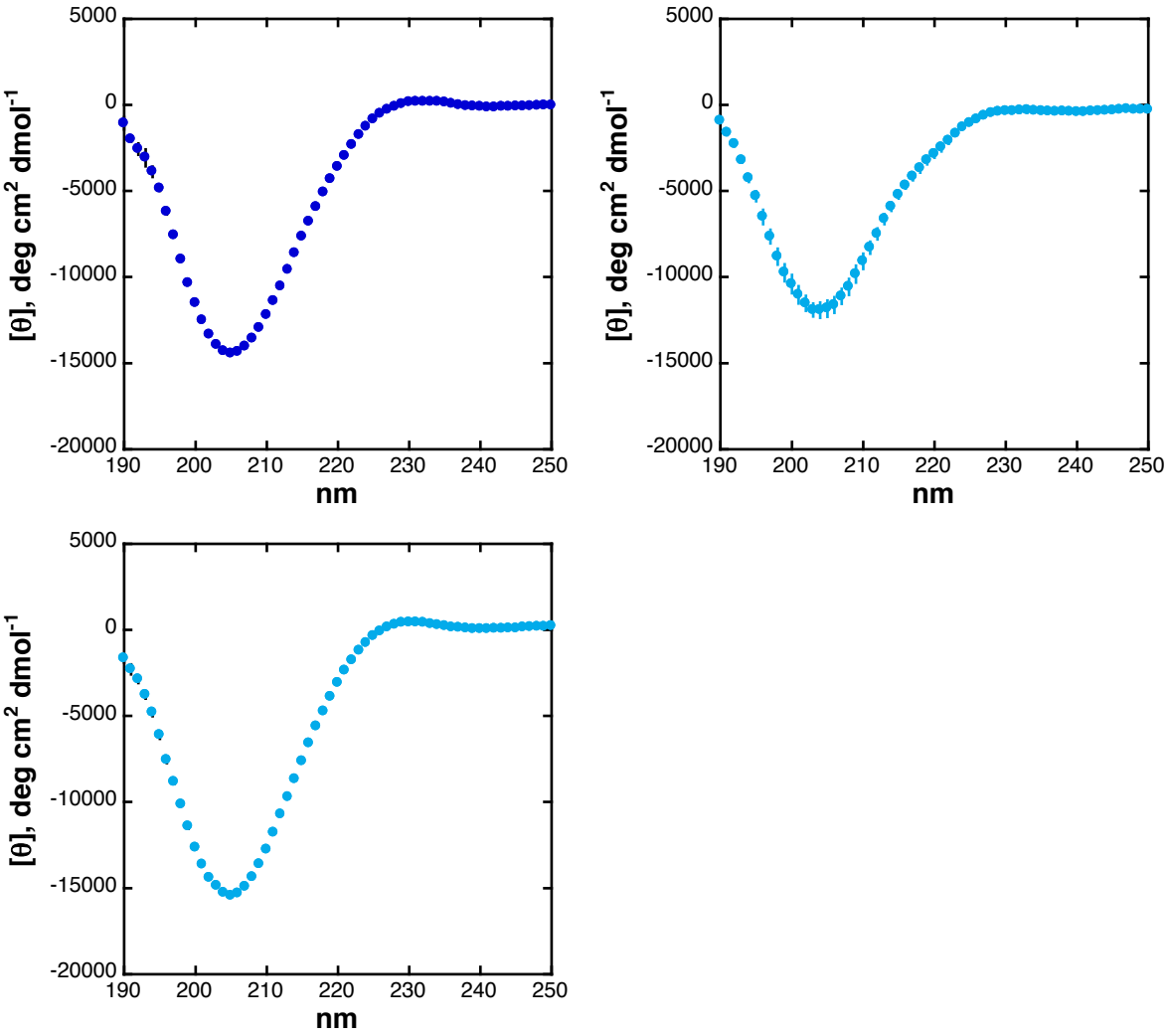

Figure S14. Top left: CD spectrum of Ac-GPKT(OGlcNAc)PPGY-NH_2 (**38**) at pH 6.5, 25 ºC; top right: CD spectrum of Ac-GPKT(OGlcNAc)PPGY-NH_2 (**38**) at pH 8.0, 25 ºC; bottom: CD spectrum of Ac-GPKT(OGlcNAc)PPGY-NH_2 (**38**) at pH 8.0, 2 ºC. Error bars indicate standard errors.

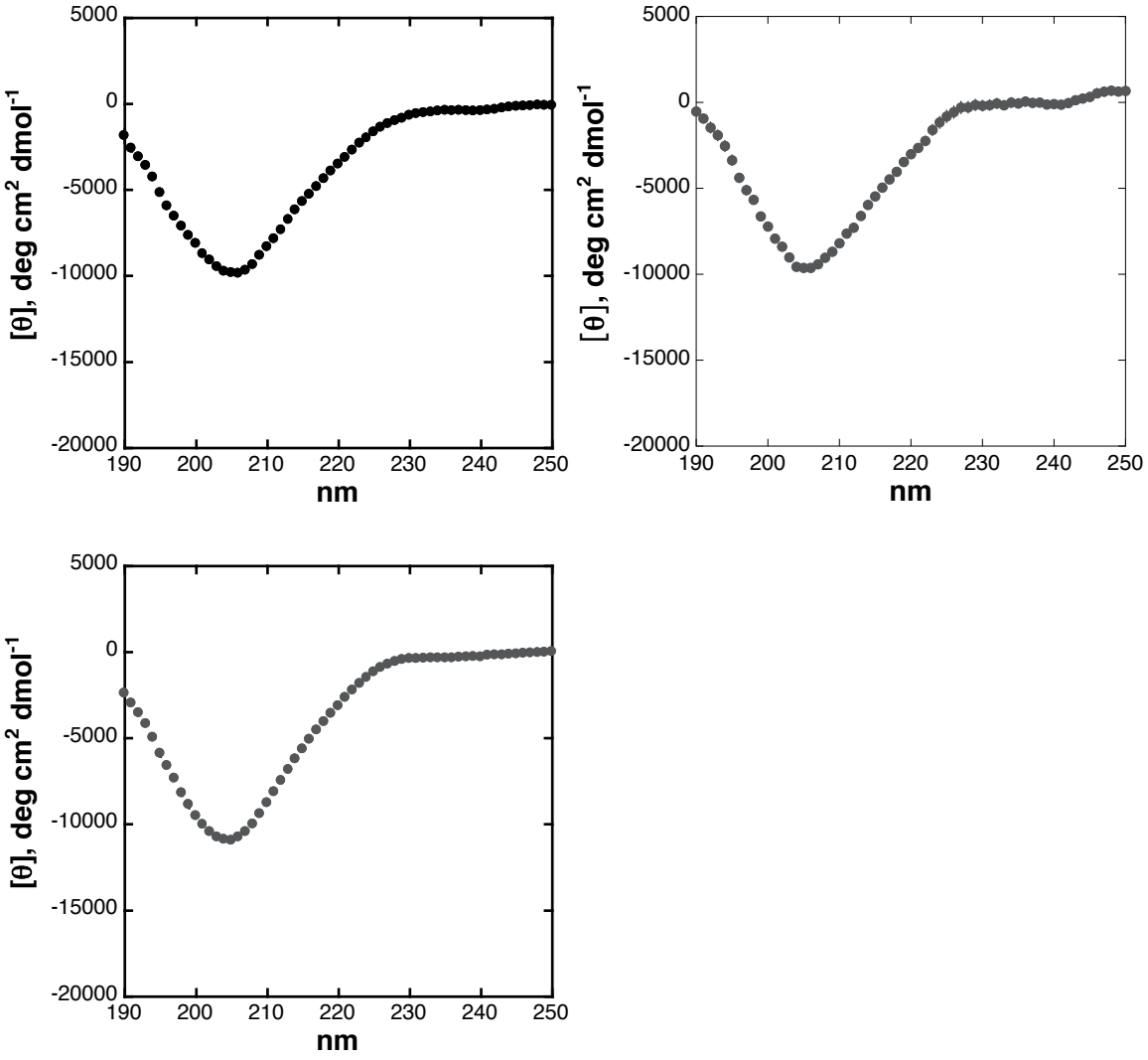

Figure S15. Top left: CD spectrum of Ac-GPKT(OPO_3Et_2)PPGY-NH_2 (**39**) at pH 6.5, 25 ºC; top right: CD spectrum of Ac-GPKT(OPO_3Et_2)PPGY-NH_2 (**39**) at pH 8.0, 25 ºC; bottom: CD spectrum of Ac-GPKT(OPO_3Et_2)PPGY-NH_2 (**39**) at pH 8.0, 2 ºC. Error bars indicate standard error.

CD spectra of peptides Ac-GPP*Tx*PPGY-NH_2

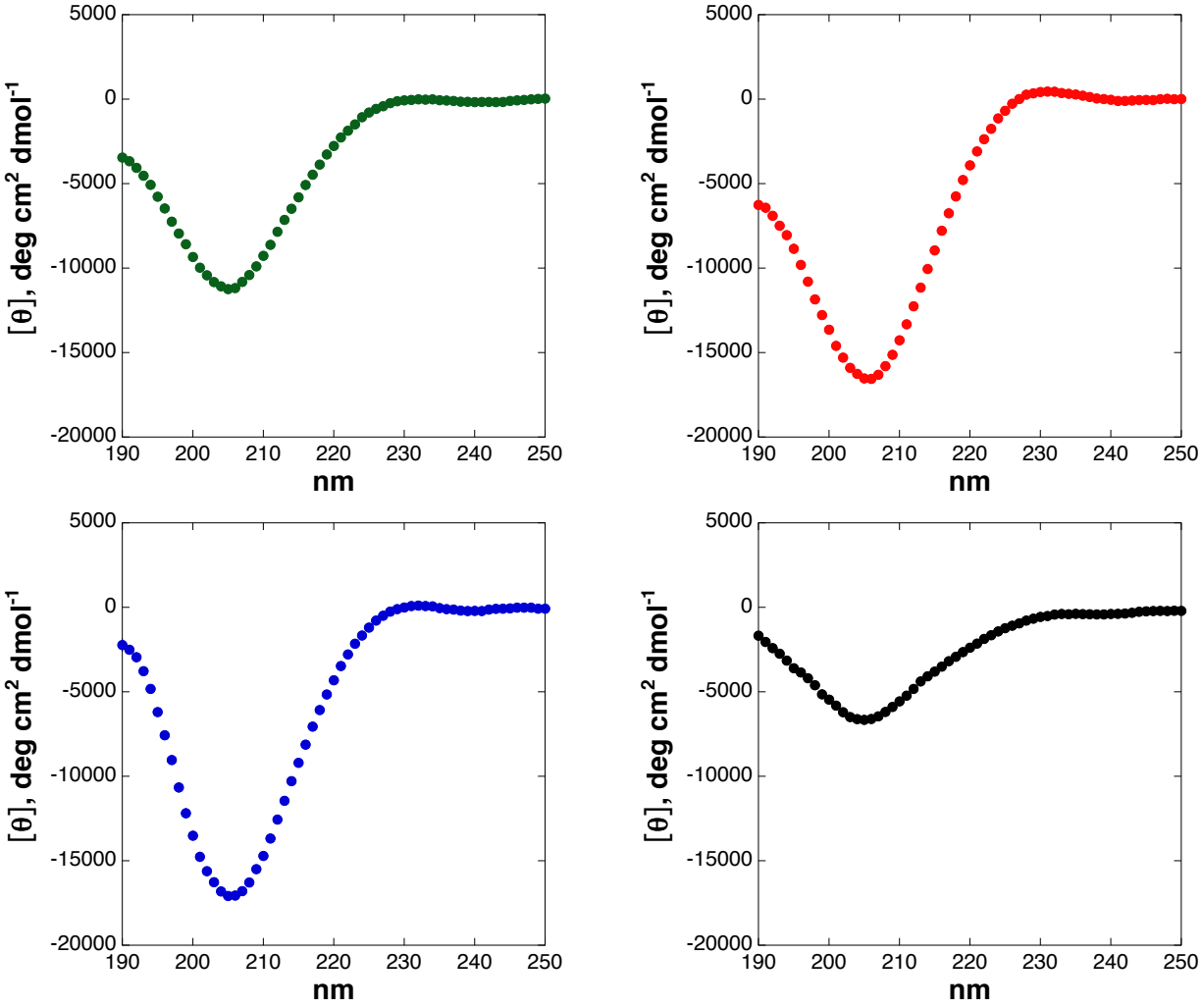

Figure S16. Top left: CD spectrum of Ac-GPPTPPGY-NH_2 (**40**) at pH 8.0, 25 ºC; top right: CD spectrum of Ac-GPPT(OPO_3^{2-})PPGY-NH_2 (**41**) at pH 8.0, 25 ºC; bottom left: CD spectrum of Ac-GPPT(OGlcNAc)PPGY-NH_2 (**42**) at pH 8.0, 25 ºC and bottom right: CD spectrum of Ac-GPPT(OPO_3Et_2)PPGY-NH_2 (**43**) at pH 8.0, 25 ºC. Error bars indicate standard error.

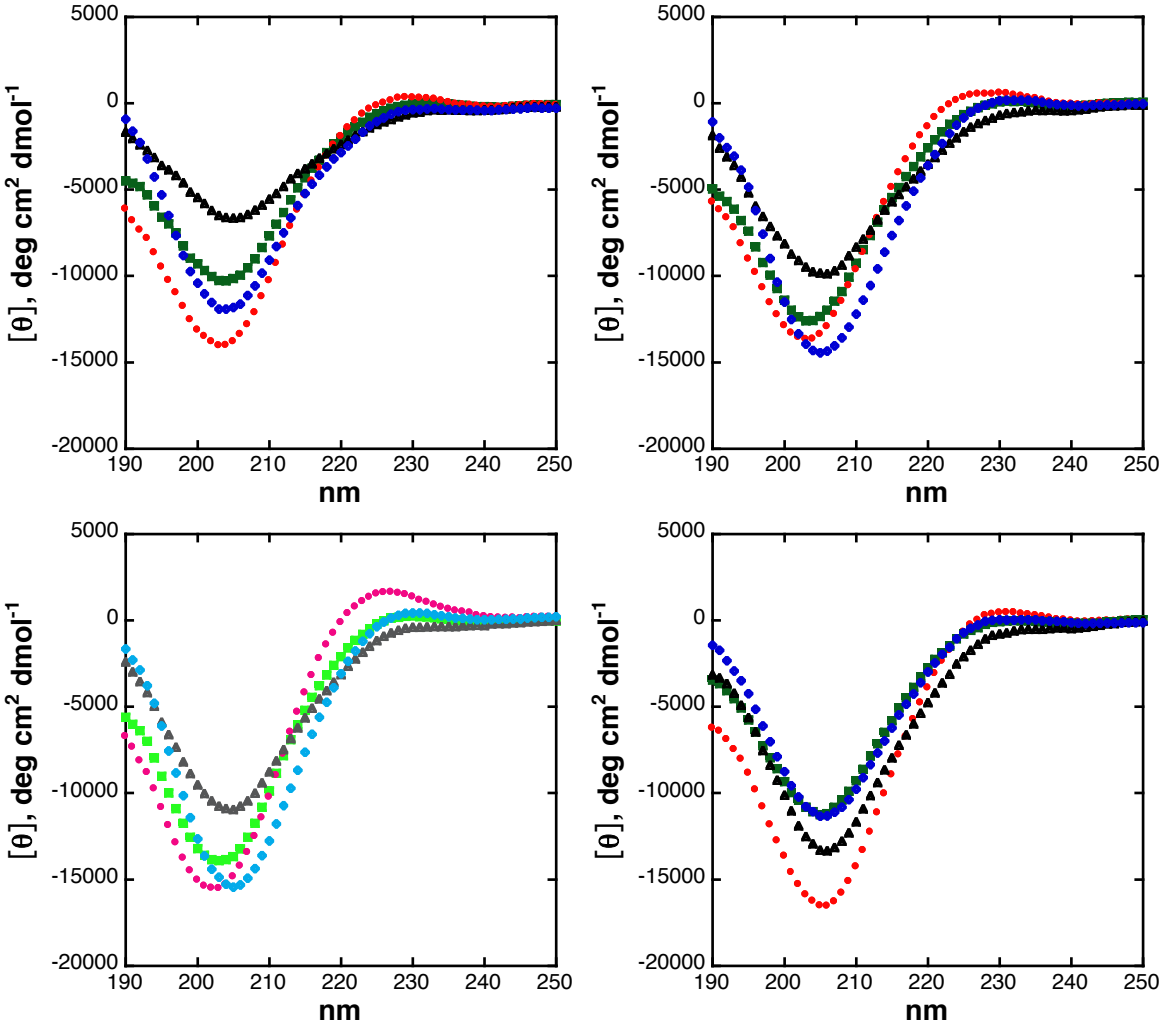

Figure S17. Top left; CD spectra of Ac-GPK*Tx*PPGY-NH_2 peptides at pH 6.5 at 25 ºC; Thr: green squares; phosphothreonine: red circles; ThrOGlcNAc: blue diamonds; Thr diethylphosphate: black triangles; top right; CD spectra of Ac-GPK*Tx*PPGY-NH_2 peptides at pH 8.0 at 25 ºC; Thr: green squares; phosphothreonine: red circles; ThrOGlcNAc: blue diamonds; Thr diethylphosphate: black triangles; bottom left; CD spectra of Ac-GPK*Tx*PPGY-NH_2 peptides at 2 ºC; Thr: light green squares; phosphothreonine: magenta circles; ThrOGlcNAc: light blue diamonds; Thr diethylphosphate: grey triangles; bottom right; CD spectra of Ac-GPP*Tx*PPGY-NH_2 peptides at pH 8.0 at 25 ºC; Thr: green squares; phosphothreonine: red circles; ThrOGlcNAc: blue diamonds; Thr diethylphosphate: black triangles. Data were collected in 5 mM phosphate buffer buffer containing 25 mM KF.

peptide	$[\theta]_{228}$, deg cm^2 dmol^{-1}	λ at local $[\theta]_{max}$, nm	local $[\theta]_{max}$, deg cm^2 dmol^{-1}	λ at $[\theta]_{min}$, nm	$[\theta]_{min}$, deg cm^2 dmol^{-1}	$[\theta]_{190}$, deg cm^2 dmol^{-1}	Temp, °C	pH
Ac-GPPTPPGY-NH_2	–230	n.a.[a]	n.a.	205	–11243	–3448	25	8
Ac-GPPT(OPO_3^{2-})PPGY-NH_2	272	231	449	206	–16553	–6253	25	8
Ac-GPPT(OGlcNAc)PPGY-NH_2	–252	232	112	205	–17077	–2234	25	8
Ac-GPPT(OPO_3Et_2)PPGY-NH_2	–1070	n.a.	n.a.	206	–13342	–3158	25	8
Ac-GPKTPPGY-NH_2	–184	232	50	204	–10285	–4483	25	8
Ac-GPKT(OPO_3^{2-})PPGY-NH_2	285	229	326	203	–14041	–6134	25	8
Ac-GPKT($OPO_3^{-/2-}$)PPGY-NH_2	516	230	581	203	–13675	–5736	25	6.5
Ac-GPKT(OGlcNAc)PPGY-NH_2	–473	n.a.	n.a.	203	–11912	–926	25	8
Ac-GPKT(OPO_3Et_2)PPGY-NH_2	–781	n.a.	n.a.	205	–6652	–1674	25	8
Ac-GPKTPPGY-NH_2	183	230	253	203	–13896	–5608	2	8
Ac-GPKT(OPO_3^{2-})PPGY-NH_2	1560	227	1620	203	–15526	–6728	2	8
Ac-GPKT(OGlcNAc)PPGY-NH_2	296	231	432	205	–15436	–1656	2	8
Ac-GPKT(OPO_3Et_2)PPGY-NH_2	–569	n.a.	n.a.	205	–10956	–2406	2	8

Table S7. Summary of CD data for model peptides. CD data were collected with 100–200 μM peptide in 5 mM phosphate buffer (pH 8.0 or 6.5) containing 25 mM KF. [a] No local maximum was observed.

^{1}H NMR spectra of all peptides: amide region (stacked spectra) and full spectra of individual peptides.

Analysis of peptides derived from tau$_{174–183}$

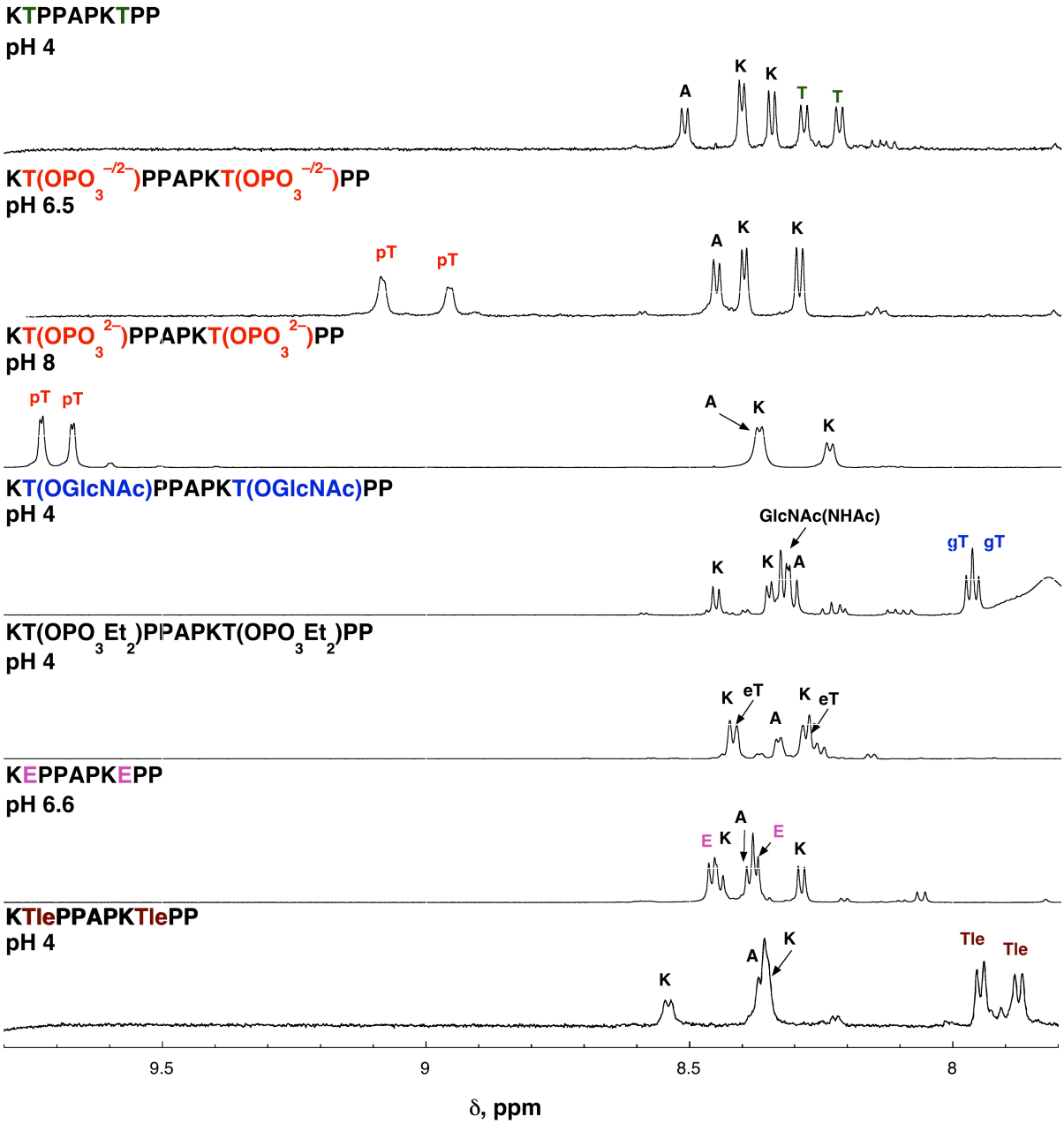

Figure S18. ^{1}H NMR spectra (amide region) of peptides derived from tau$_{174–183}$. Minor peaks in the NMR spectra are due to the presence of cis amide bonds. pT indicates a phosphorylated threonine residue. eT indicates a diethylphosphorylated (OPO_3Et_2) threonine residue. gT indicates an OGlcNAcylated threonine residue. Tle indicates *tert*-leucine. Peptides were dissolved in 5 mM phosphate buffer (pH 4.0, 6.5, or 8.0) at 298 K and were internally referenced with TSP. Solutions contained 25 mM NaCl, 100 μM TSP, and 90% H_2O/10% D_2O.

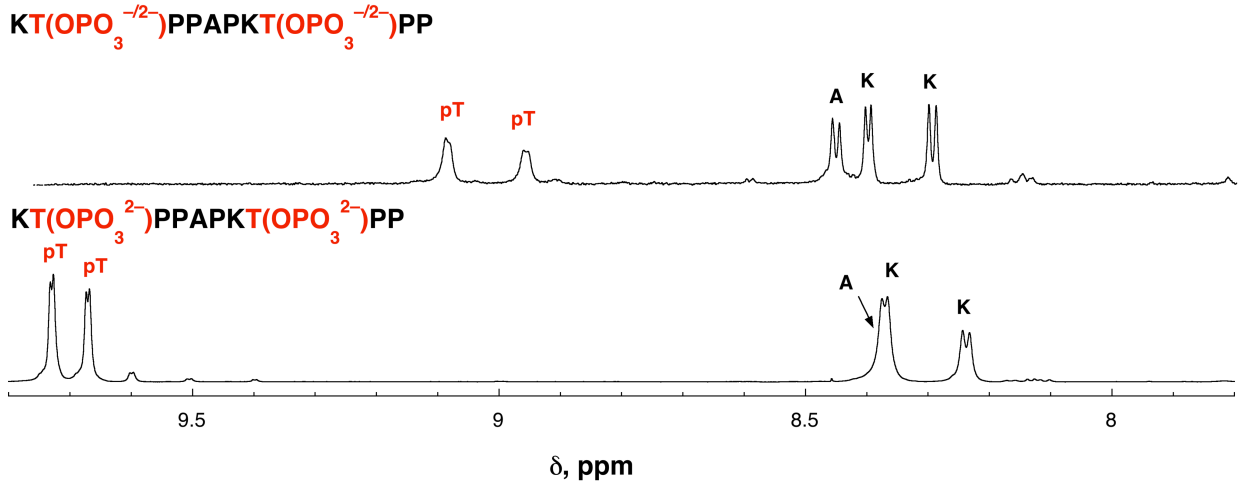

Figure S19. ^{1}H NMR spectra (amide region) of phosphorylated peptide tau$_{174–183}$ at pH 6.5 (top) and 8 (bottom) at 298 K. Minor peaks in the NMR spectra are due to the presence of cis amide bonds. pT indicates a phosphorylated threonine residue.

The phosphorylated peptide tau$_{174–183}$ showed unusually slow amide exchange at pH 8.0. All five amide protons corresponding to Thr, Ala, and Lys were observed at pH 8.0.

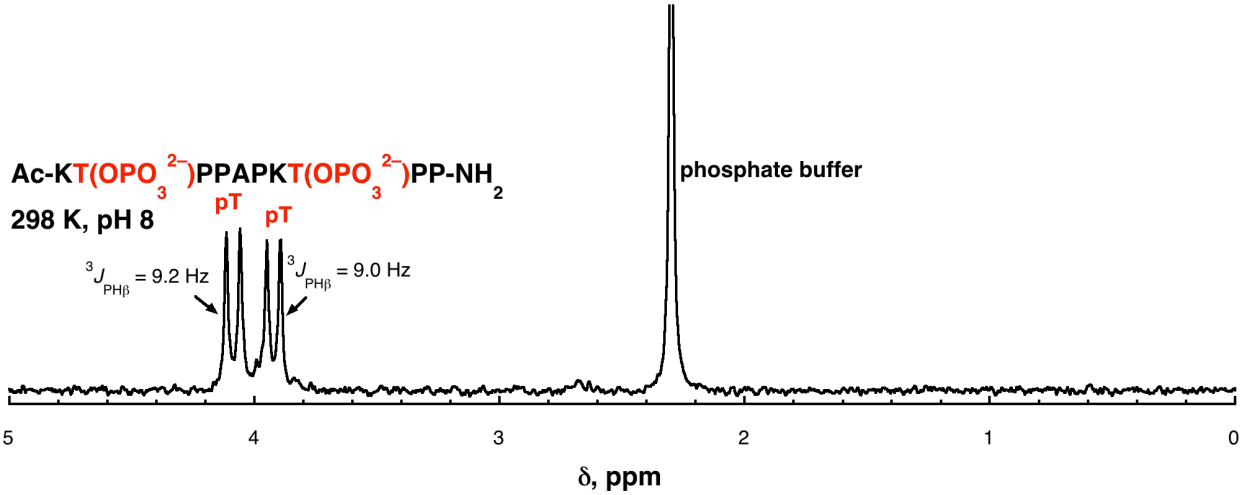

Figure S20. ^{31}P NMR spectrum of phosphorylated peptide tau$_{174–183}$($OPO_3^{2–}$) at pH 8.0 at 298 K in 5 mM phosphate buffer containing 25 mM NaCl. The NMR spectrum was internally referenced with 85% H_3PO_4 (0 ppm) using a capillary filled with H_3PO_4 located in the NMR tube containing the sample.

Full ^{1}H NMR spectra of peptides derived from tau$_{174–183}$

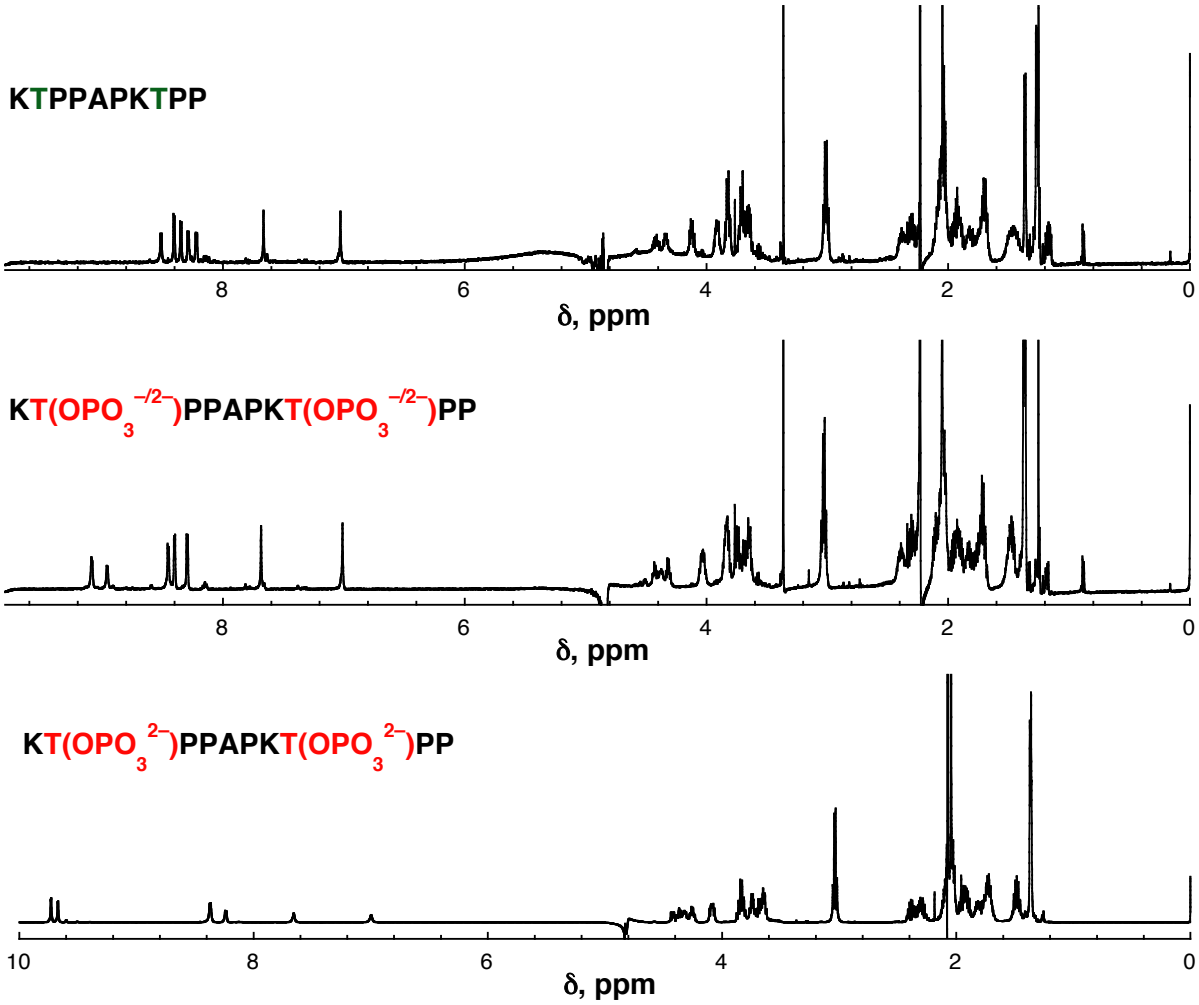

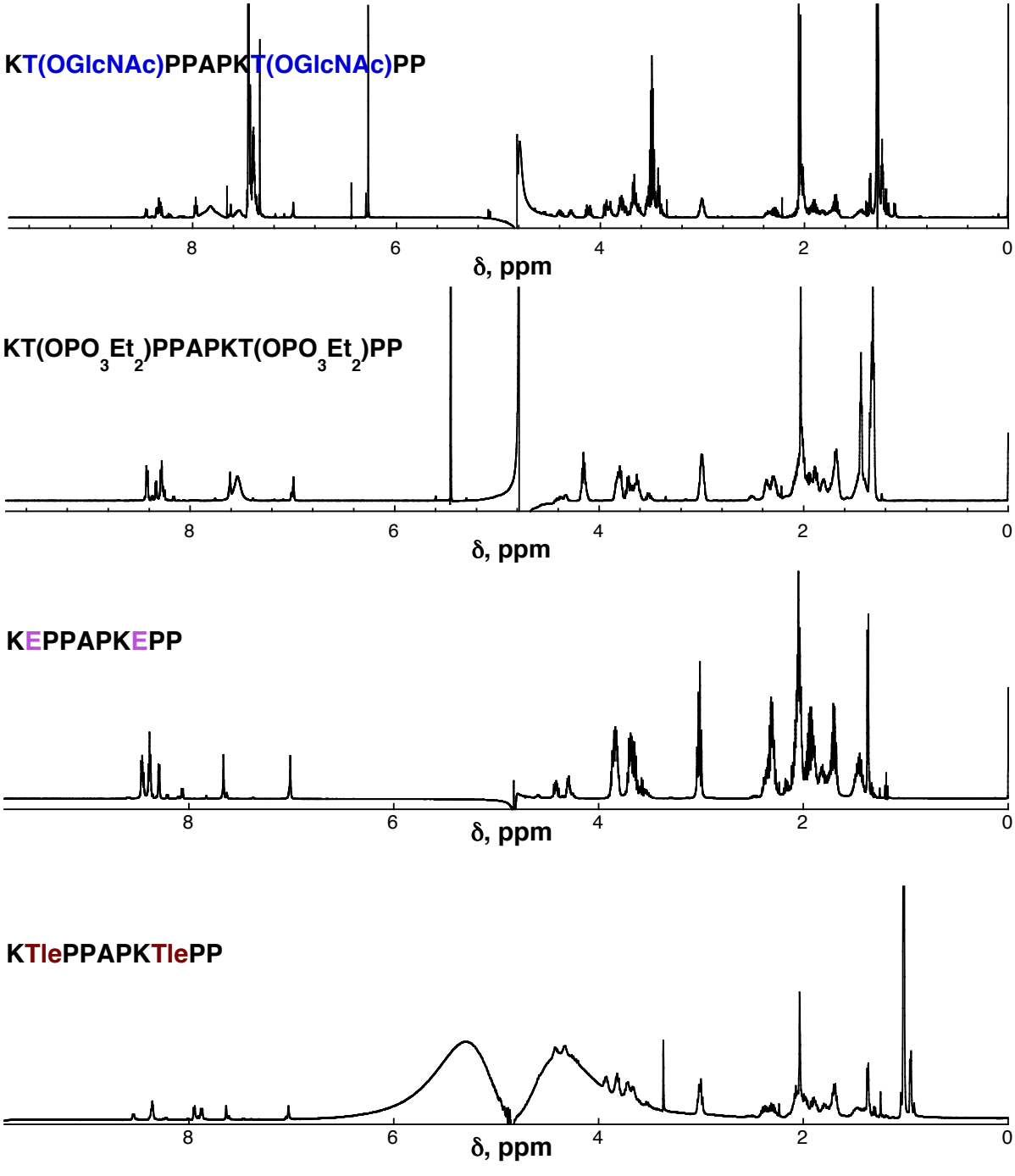
KT(OGlcNAc)PPAPKT(OGlcNAc)PP
8
6
4
2
0
δ, ppm
KT(OPO3Et2)PPAPKT(OPO3Et2)PP
8
6
4
2
0
δ, ppm
KEPPAPKEPP
8
6
4
2
0
δ, ppm
KTlePPAPKTlePP
8
6
4
2
0
δ, ppm

peptide	δ, H^N	$^3J\alpha N$	δ, Hα	δ, Hβ	$^3JH\alpha H\beta$
$tau_{174–183}$ (pH 4.0)					
T	8.22	7.3	4.58	4.11	8.1
T	8.29	7.3	4.59	4.13	n.d.[a]
K	8.35	6.9	4.33	1.84, 1.77	n.d.
K	8.40	5.5	4.34	1.83, 1.73	n.d.
A	8.51	6.8	4.59	1.37	n.d.
$tau_{174–183}(OPO_3H^-)$ (pH 3.5)					
pT	8.38	6.7	4.66	4.47	n.d.
pT	8.45	6.3	4.64	4.47	n.d.
K	8.32	7.0	4.31	1.83, 1.74	n.d.
K	8.49	6.7	4.29	1.84, 1.78	n.d.
A	8.40	5.5	4.57	1.37	n.d.
$tau_{174–183}(OPO_3^{-/2-})$ (pH 6.5)					
pT	8.96	4.3	4.51	4.37	n.d.
pT	9.08	4.2	4.55	4.38	7.6
K	8.29	7.0	4.32	1.83, 1.75	n.d.
K	8.40	5.5	4.32	1.84, 1.78	n.d.
A	8.45	6.8	4.59	1.37	n.d.
$tau_{174–183}(OPO_3^{2-})$ (pH 8.0)					
pT	9.68	3.8	4.39	4.26	n.d.
pT	9.73	3.5	4.37	4.26	n.d.
K	8.23	6.7	4.31	1.81, 1.74	n.d.
K	8.37	n.d.	4.33	1.83, 1.76	n.d.
A	8.37	n.d.	4.58	1.37	n.d.
$tau_{174–183}$(OGlcNAc) (pH 4.0)					
gT	7.96	7.5	4.58	4.13	7.4
gT	7.97	7.5	4.58	4.10	n.d.
K	8.33	n.a.	4.28	1.83, 1.75	n.d.
K	8.45	7.0	4.30	1.82, 1.71	n.d.
A	8.35	5.5	4.57	1.36	n.d.
$tau_{174–183}(OPO_3Et_2)$ (pH 4.0)					
eT	8.28	n.d.	4.87	4.66	n.d.
eT	8.42	n.d.	4.87	4.66	7.1
K	8.28	n.d.	4.33	1.81, 1.71	n.d.
K	8.42	n.d.	4.32	1.82, 1.75	n.d.
A	8.33	5.2	4.57	1.36	n.d.
$tau_{174–183}$(T175E, T181E) (pH 6.5)					
E	8.37	5.8	4.60	2.30, 2.04	n.d.
E	8.46	6.6	4.59	2.31, 2.04	n.d.
K	8.29	7.1	4.30	1.81, 1.72	n.d.
K	8.44	7.0	4.29	1.82, 1.76	n.d.
A	8.38	7.0	4.59	1.37	n.d.
$tau_{174–183}$(T175Tle, T181Tle) (pH 4.0)					
Tle	7.88	7.9	4.58	n.a.[b]	n.d.
Tle	7.95	8.8	4.57	n.a.	n.d.
K	8.35	n.d.	4.32	1.79, 1.70	n.d.
K	8.54	7.4	4.32	n.d.	n.d.
A	8.37	n.d.	4.58	1.36	n.d.

Table S8. Summary of ^{1}H NMR data for peptides derived from $tau_{174–183}$. Data were collected with 100–200 μM peptide in 5 mM phosphate buffer (pH 3.5, 4.0, 6.5 or 8) with 25 mM NaCl. pT indicates a phosphorylated threonine residue. eT indicates a diethylphosphorylated (OPO_3Et_2) threonine residue. gT indicates an OGlcNAcylated threonine residue. Tle indicates *tert*-leucine. [a] n.d. = not determined due to spectral overlap. [b] n.a. = not applicable.

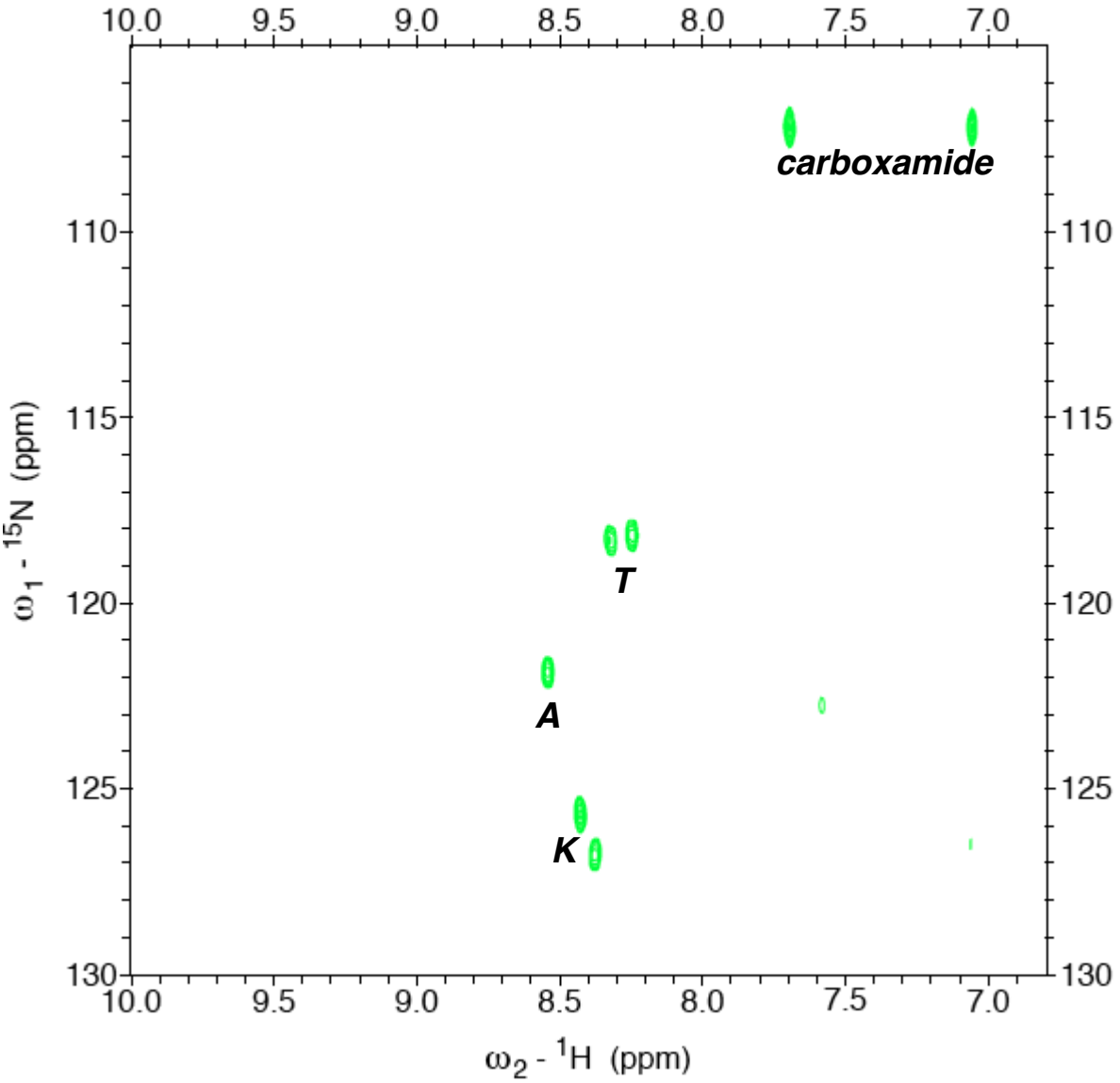

Figure S21. ^{1}H-^{15}N HSQC spectrum of peptide tau$_{174–183}$ at pH 4.0 in 5 mM phosphate buffer containing 25 mM NaCl at 298 K.

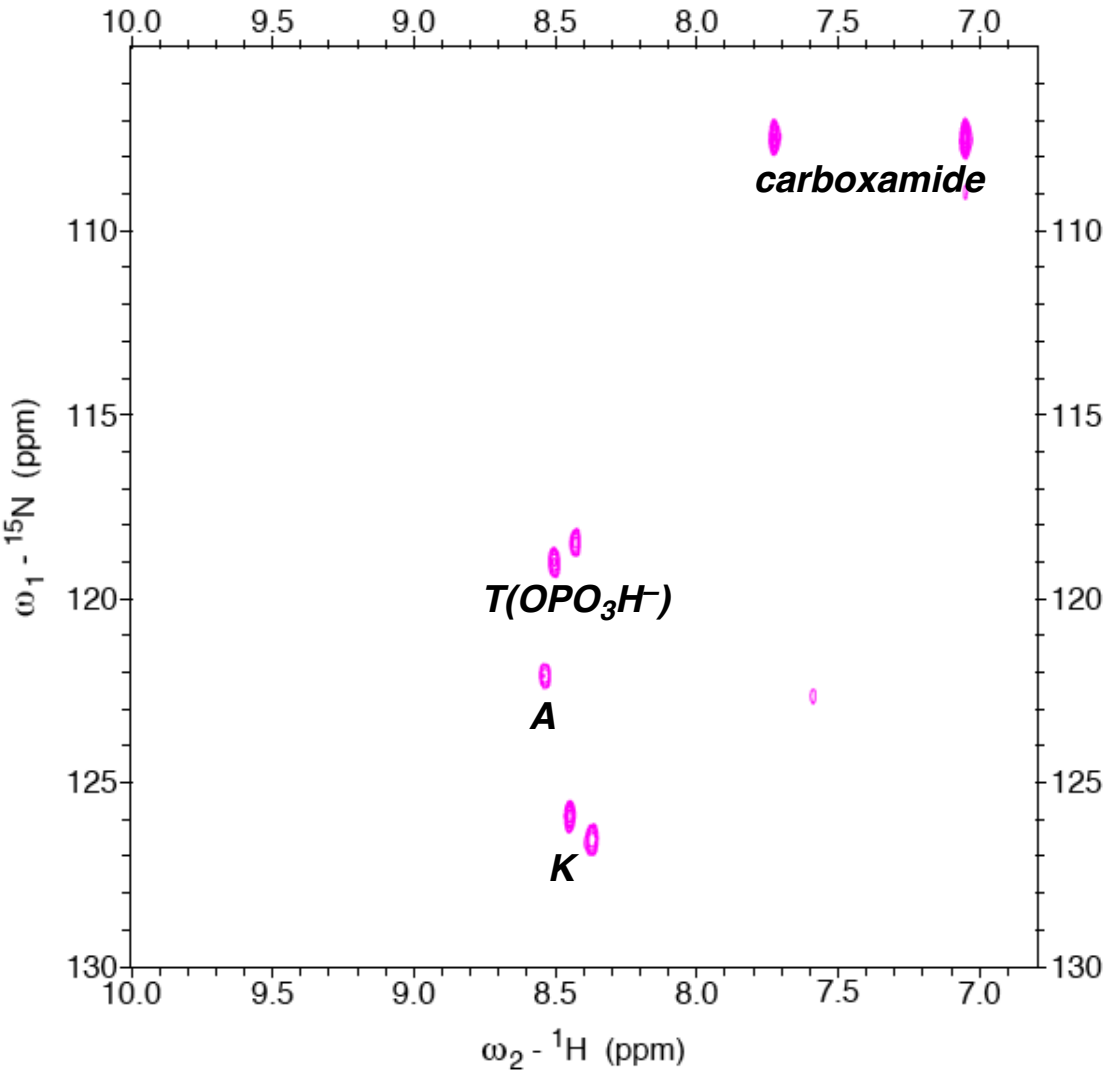

Figure S22. ^{1}H-^{15}N HSQC spectrum of peptide tau$_{174–183}$(OPO_3H^-) at pH 4.0 in 5 mM phosphate buffer containing 25 mM NaCl at 298 K.

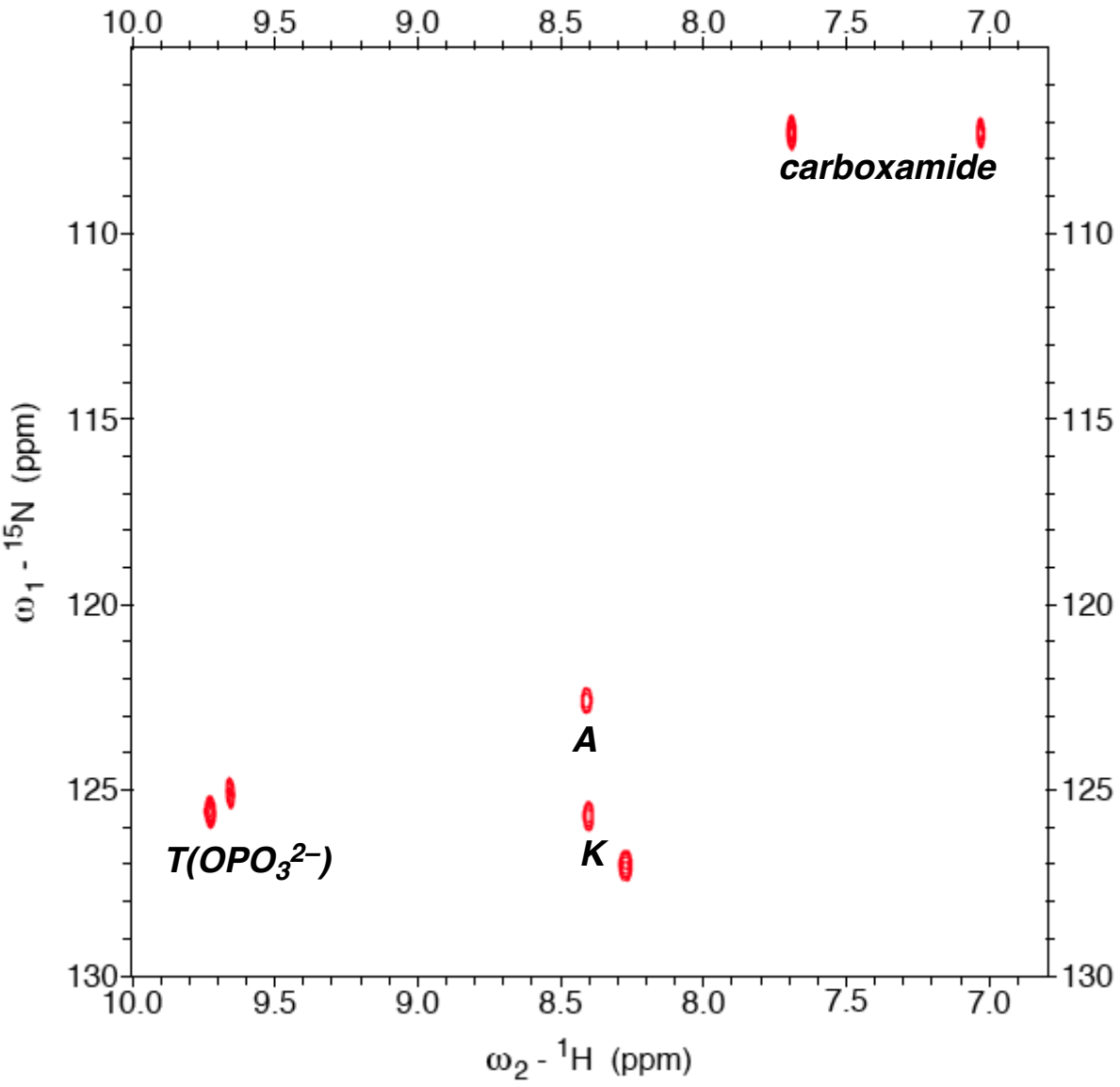

Figure S23. ^{1}H-^{15}N HSQC spectrum of peptide tau$_{174–183}$($OPO_3^{2–}$) at pH 7.5 in 5 mM phosphate buffer containing 25 mM NaCl at 298 K.

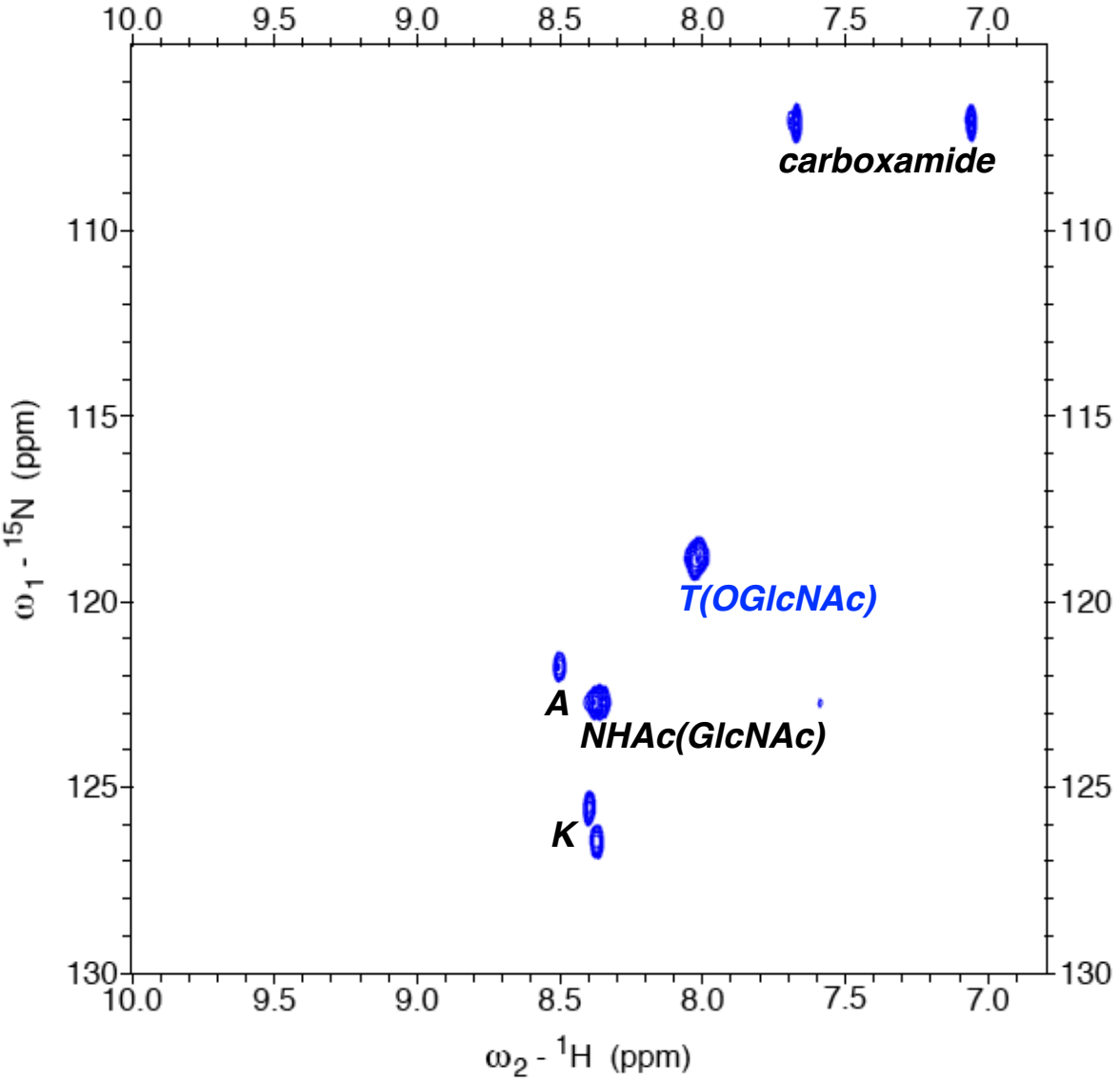

Figure S24. ^{1}H-^{15}N HSQC spectrum of peptide tau$_{174–183}$(OGlcNAc) at pH 4.0 in 5 mM phosphate buffer containing 25 mM NaCl at 298 K.

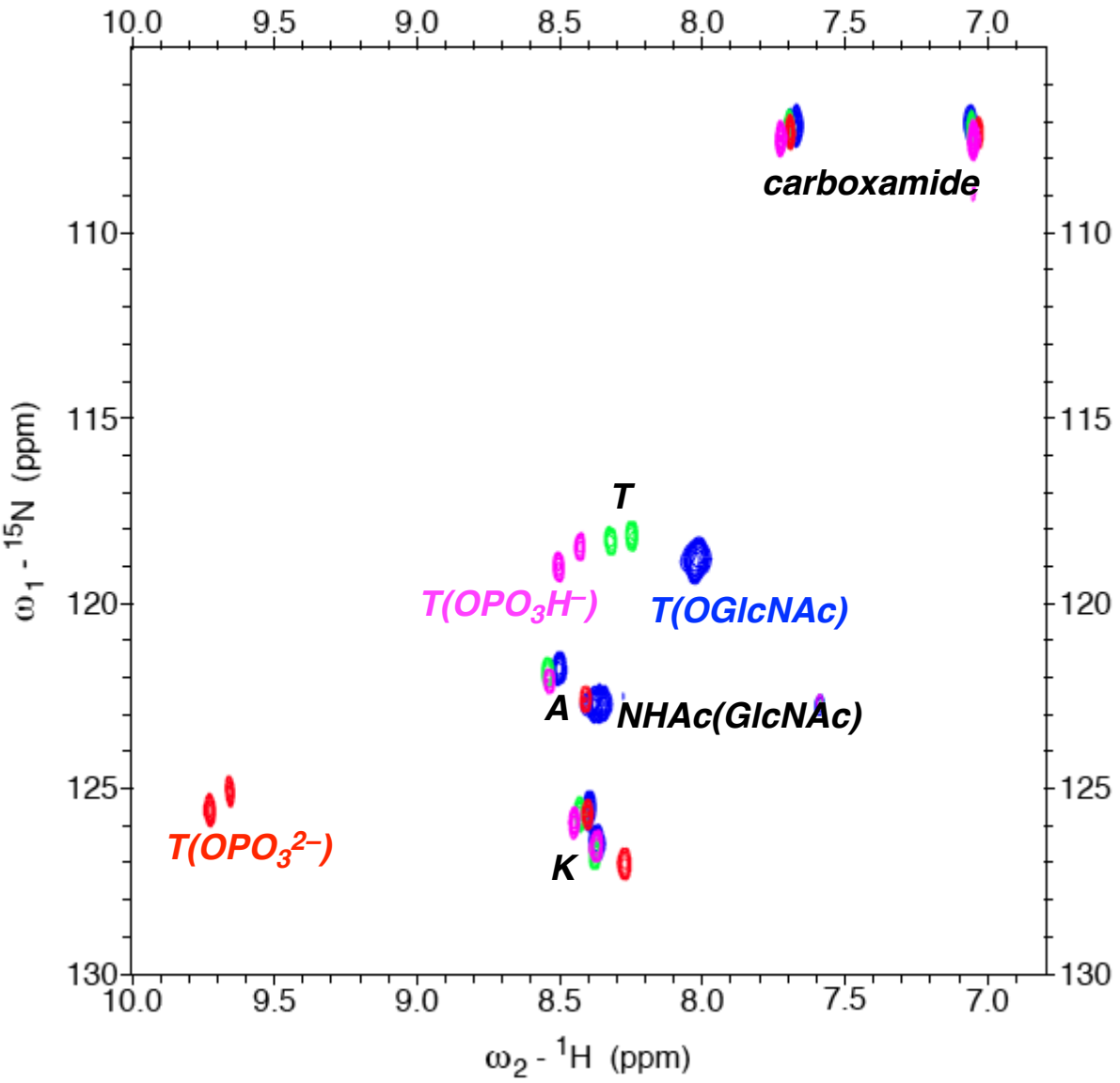

Figure S25. ^{1}H-^{15}N HSQC spectra of peptides tau$_{174–183}$ at pH 4.0 (green), tau$_{174–183}$(OPO_3^{2-}) (red), tau$_{174–183}$(OPO_3H^-) (magenta), and tau$_{174–183}$(OGlcNAc) (blue) at 298 K. Data were collected with 2–3 mM peptide in 5 mM phosphate buffer (pH 4.0 or 7.5) with 25 mM NaCl.

peptide	Thr$_N$, ppm	Lys$_N$, ppm	carboxamide	pH, Temp
Ac-KTPPAPKTPP-NH_2	118.2, 118.3	125.7, 126.8	107.2	4.0, 298 K
Ac-KT(OPO_3^{2-})PPAPKT(OPO_3^{2-})PP-NH_2	125.6, 125.1	125.8, 127.0	107.3	7.5, 298 K
Ac-KT(OPO_3H^-)PPAPKT(OPO_3H^-)PP-NH_2	119.0, 118.5	125.9, 126.6	107.5	4.0, 298 K
Ac-KT(OGlcNAc)PPAPKT(OGlcNAc)PP-NH_2	118.8, 118.8	125.5, 126.5	107.1	4.0, 298 K

Table S9. Summary of ^{1}H-^{15}N HSQC NMR data for peptides derived from tau$_{174–183}$. Data were collected with 2–3 mM peptide in 5 mM phosphate buffer (pH 4.0 or 7.5) with 25 mM NaCl.

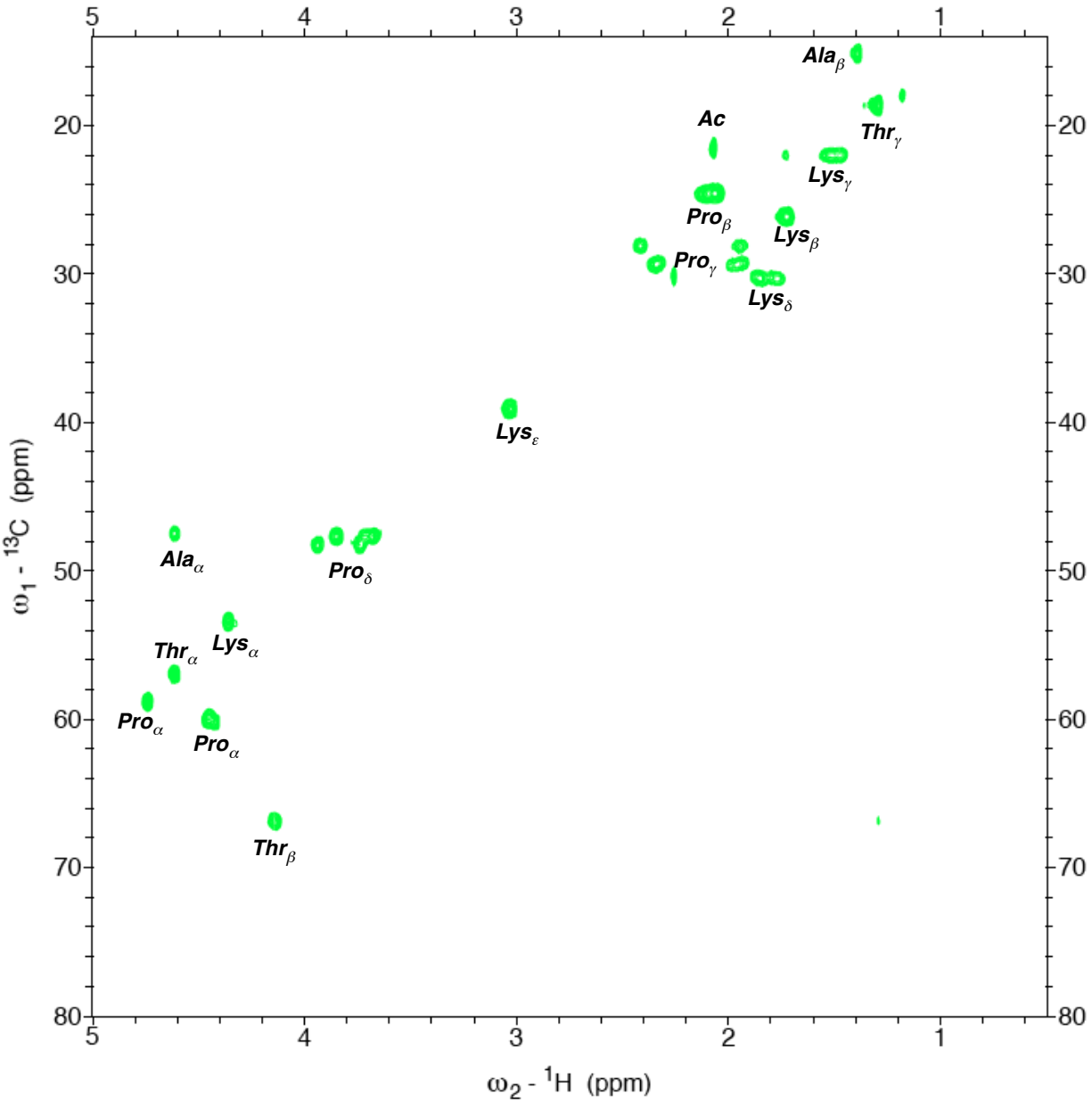

Figure S26. ^{1}H-^{13}C HSQC spectrum of peptides tau$_{174–183}$ at pH 4.0 in 5 mM phosphate buffer with 25 mM NaCl in 100% D_2O at 298 K.

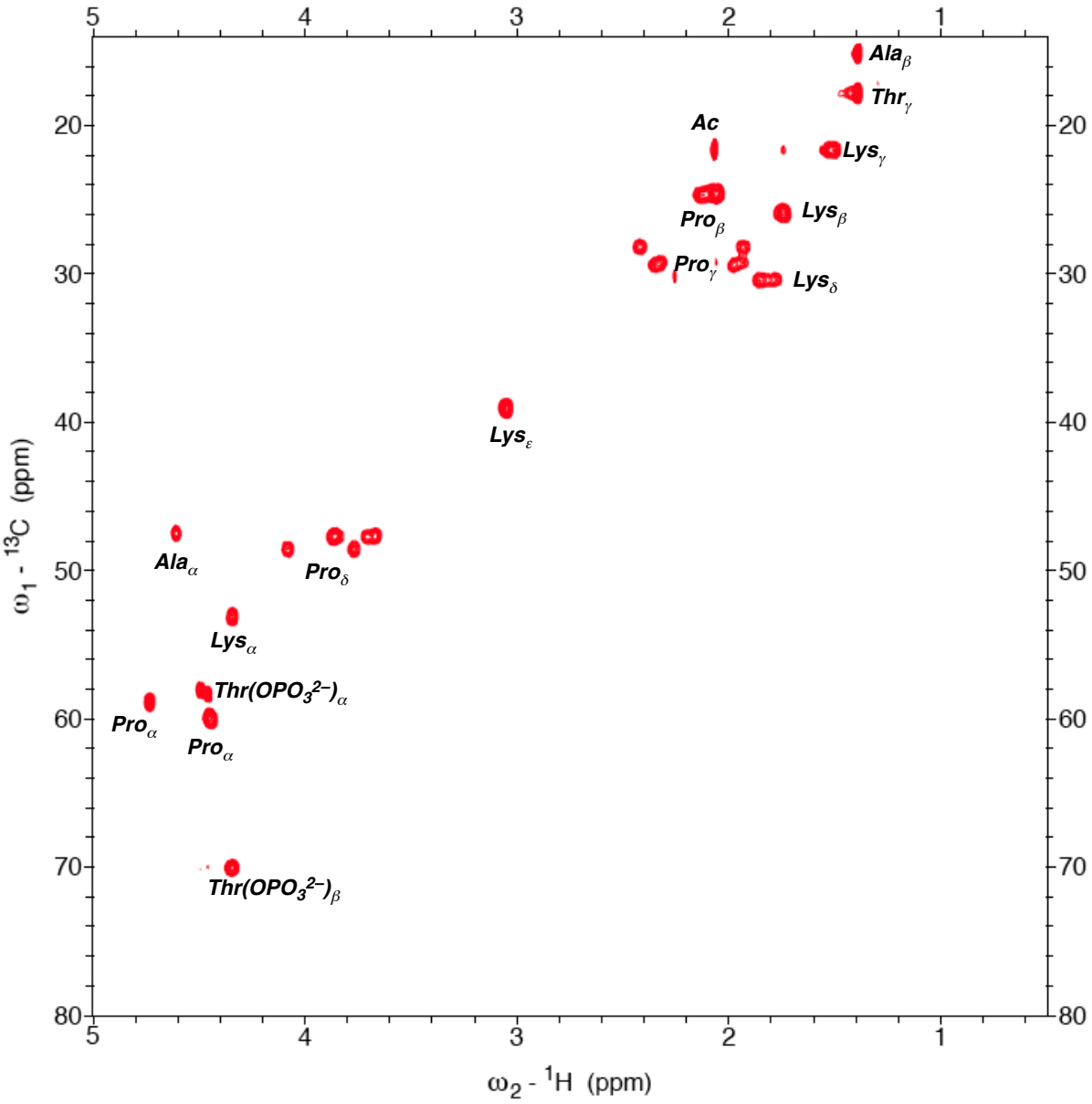

Figure S27. ^{1}H-^{13}C HSQC spectrum of peptides tau$_{174–183}$(OPO$_3^{2-}$) at pH 8.0 in 5 mM phosphate buffer with 25 mM NaCl in 100% D_2O at 298 K.

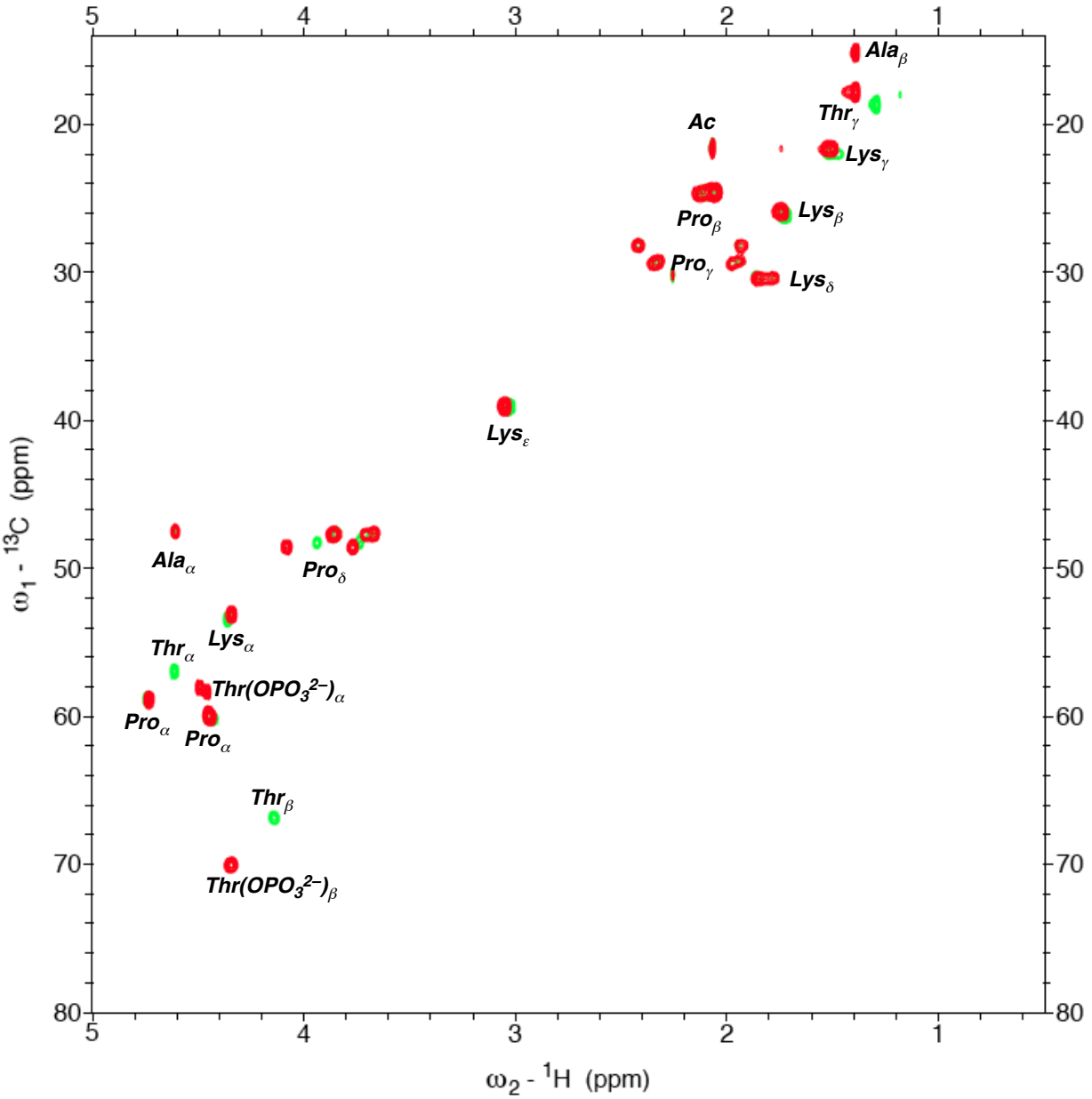

Figure S28. ^{1}H-^{13}C HSQC spectra of peptides tau$_{174–183}$ at pH 4.0 (green) and tau$_{174–183}$(OPO$_3^{2–}$) (red) at pH 8.0 in 5 mM phosphate buffer with 25 mM NaCl in 100% D_2O at 298 K.

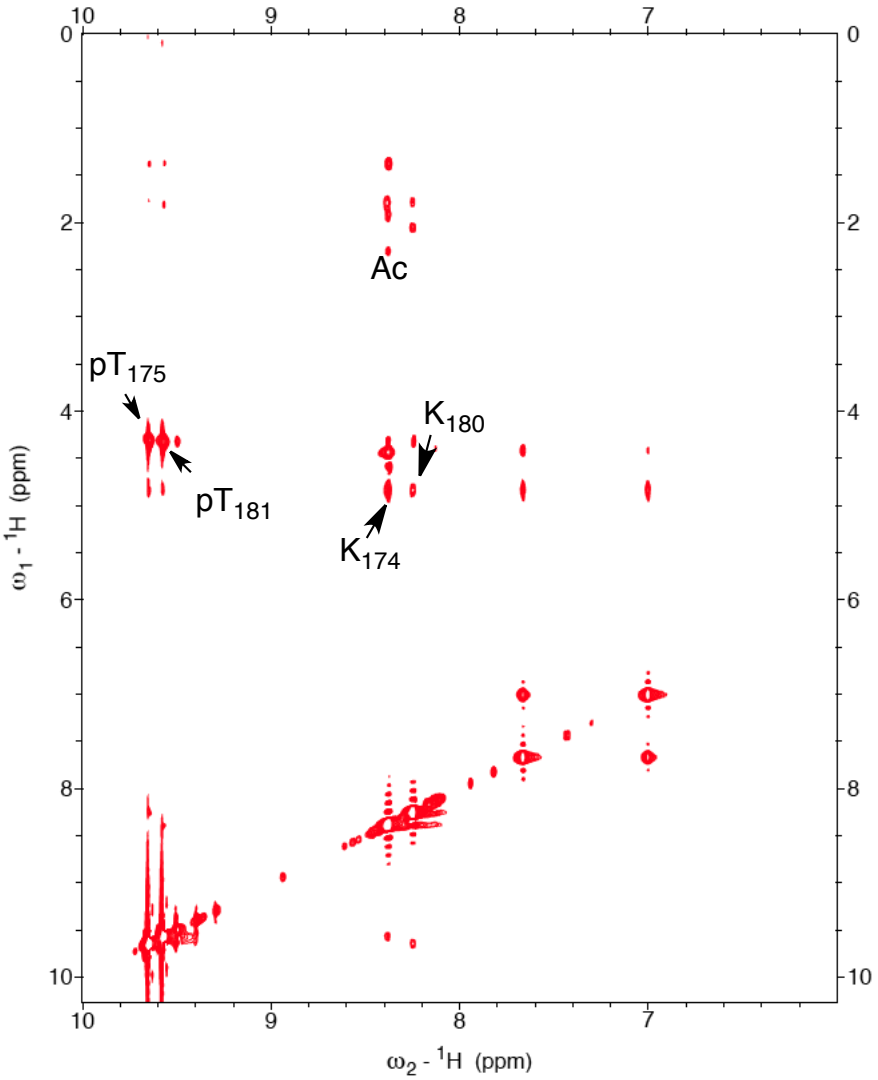

Figure S29. Partial NOESY spectrum of peptide $tau_{174–183}(OPO_3^{2–})$ at pH 8.0 in 5 mM phosphate buffer containing 25 mM NaCl at 298 K.

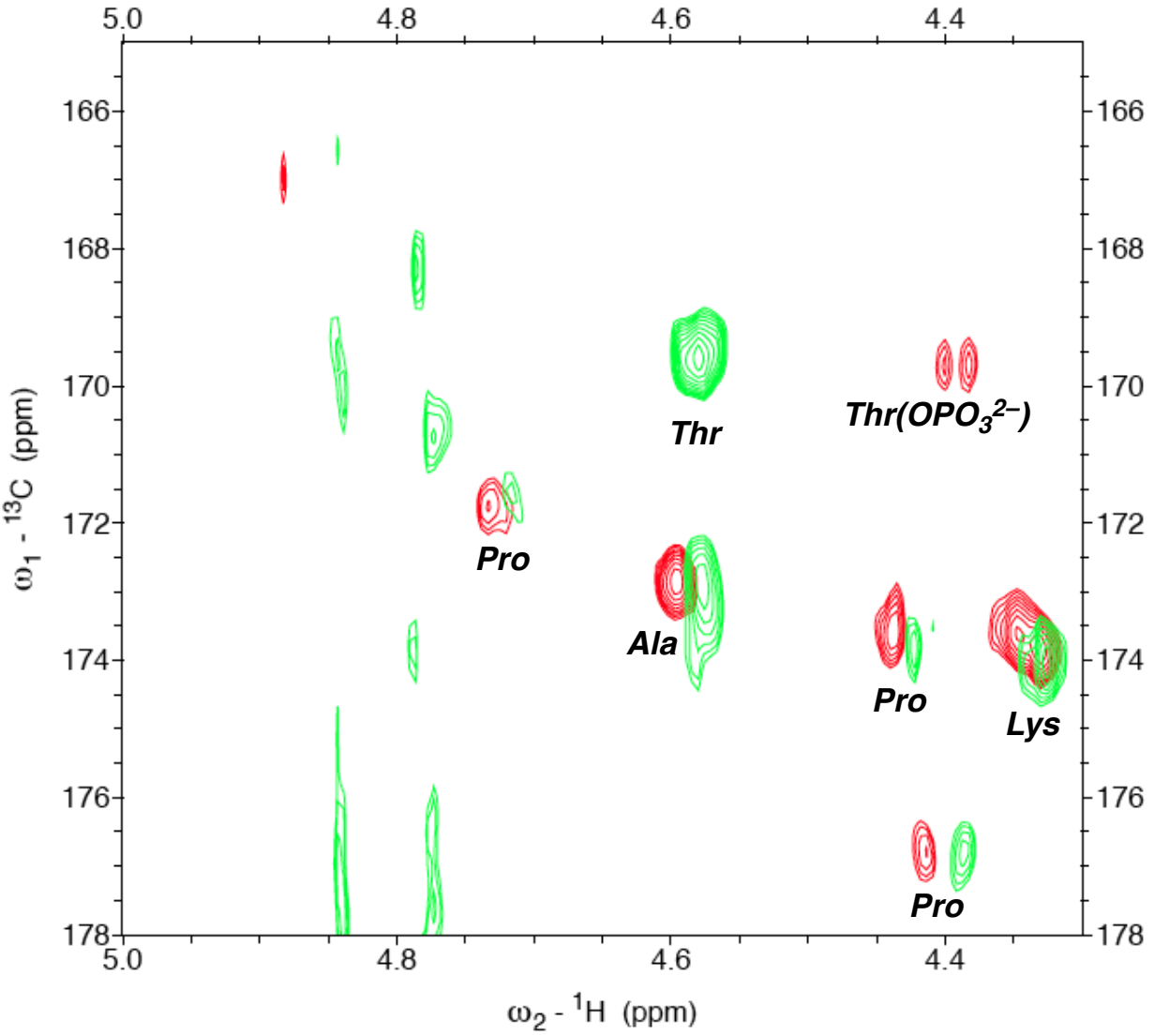

Figure S30. ^{1}H-^{13}C HMBC spectra (alpha proton region) of peptides $tau_{174–183}$ at pH 4.0 (green) and $tau_{174–183}(OPO_3^{2–})$ (red) at pH 8.0 in 5 mM phosphate buffer with 25 mM NaCl in 100% D_2O at 298 K.

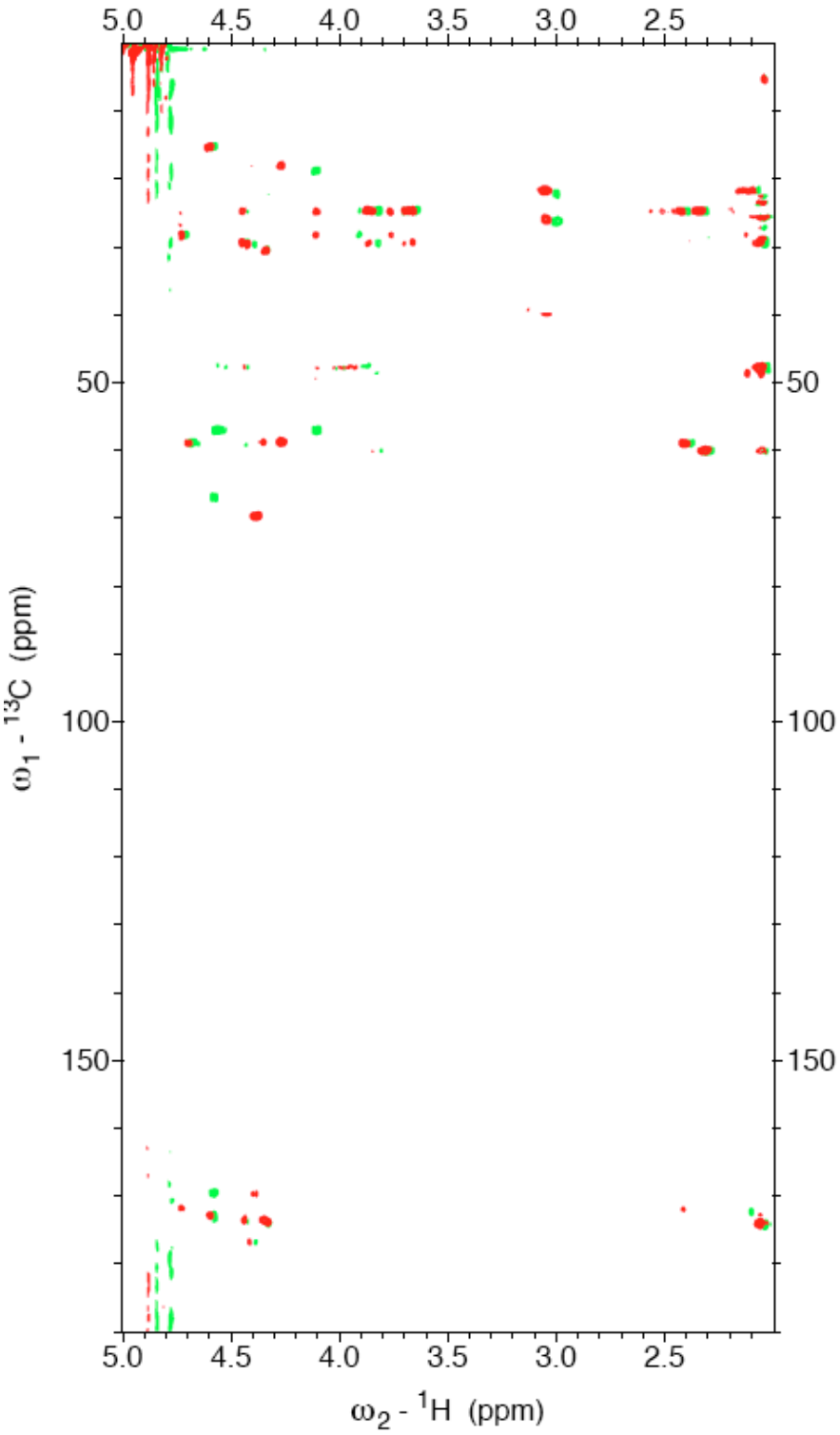

Figure S31. ^{1}H-^{13}C HMBC spectra (full spectra) of peptides $tau_{174–183}$ at pH 4.0 (green) and $tau_{174–183}(OPO_3^{2–})$ (red) at pH 8.0 in 5 mM phosphate buffer with 25 mM NaCl in 100% D_2O at 298 K.

Ac-KTPPAPKTPP-NH_2 residue	^{13}C δ, ppm	Ac-KpTPPAPKpTPP-NH_2 residue	^{13}C δ, ppm
Lys, α	53.4, 53.4	Lys, α	53.1, 53.1
Thr, α	57.0, 57.0	pThr, α	58.1, 58.4
Pro, α	58.9, 60.1	Pro, α	58.9, 60.0
Ala, α	47.5	Ala, α	47.5
Thr, β	66.9, 66.9	pThr, β	70.0, 70.0
Pro, δ	47.7, 48.3	Pro, δ	47.7, 48.6
Lys, ε	39.1, 39.1	Lys, ε	39.1, 39.1
Pro, γ	28.1, 28.1	Pro, γ	28.2, 28.2
Lys, β	30.4, 30.4	Lys, β	30.5, 30.5
Pro, β	29.4, 29.4	Pro, β	29.3, 29.3
Lys, γ	26.2. 26.2	Lys, γ	25.9, 25.9
Lys, δ	22.1, 22.1	Lys, δ	21.7, 21.7
Ala, β	15.2	Ala, β	15.2
Thr, γ	18.7, 18.7	pThr, γ	17.8, 17.8
Lys, CO	174.1, 174.1	Lys, CO	173.6, 173.9
Thr, CO	169.6, 169.6	pThr, CO	169.7, 169.7
Pro, CO	176.9, 173.8, n.d.[a]	Pro, CO	176.8, 173.6, 171.8
Ala, CO	172.9	Ala, CO	172.9
Ac, CO	174.2	Ac, CO	174.0

Table S10. Summary of ^{1}H-^{13}C HSQC NMR data for peptides $tau_{174–183}$ at pH 4.0 and $tau_{174–183}(OPO_3^{2–})$ at pH 8.0, 298 K. Data were collected with 2–3 mM peptide in 5 mM phosphate buffer with 25 mM NaCl. pThr indicates a phosphorylated threonine residue. [a] n.d. indicates not determined because peak is in the H_2O peak.

Analysis of peptides derived from tau$_{196–209}$

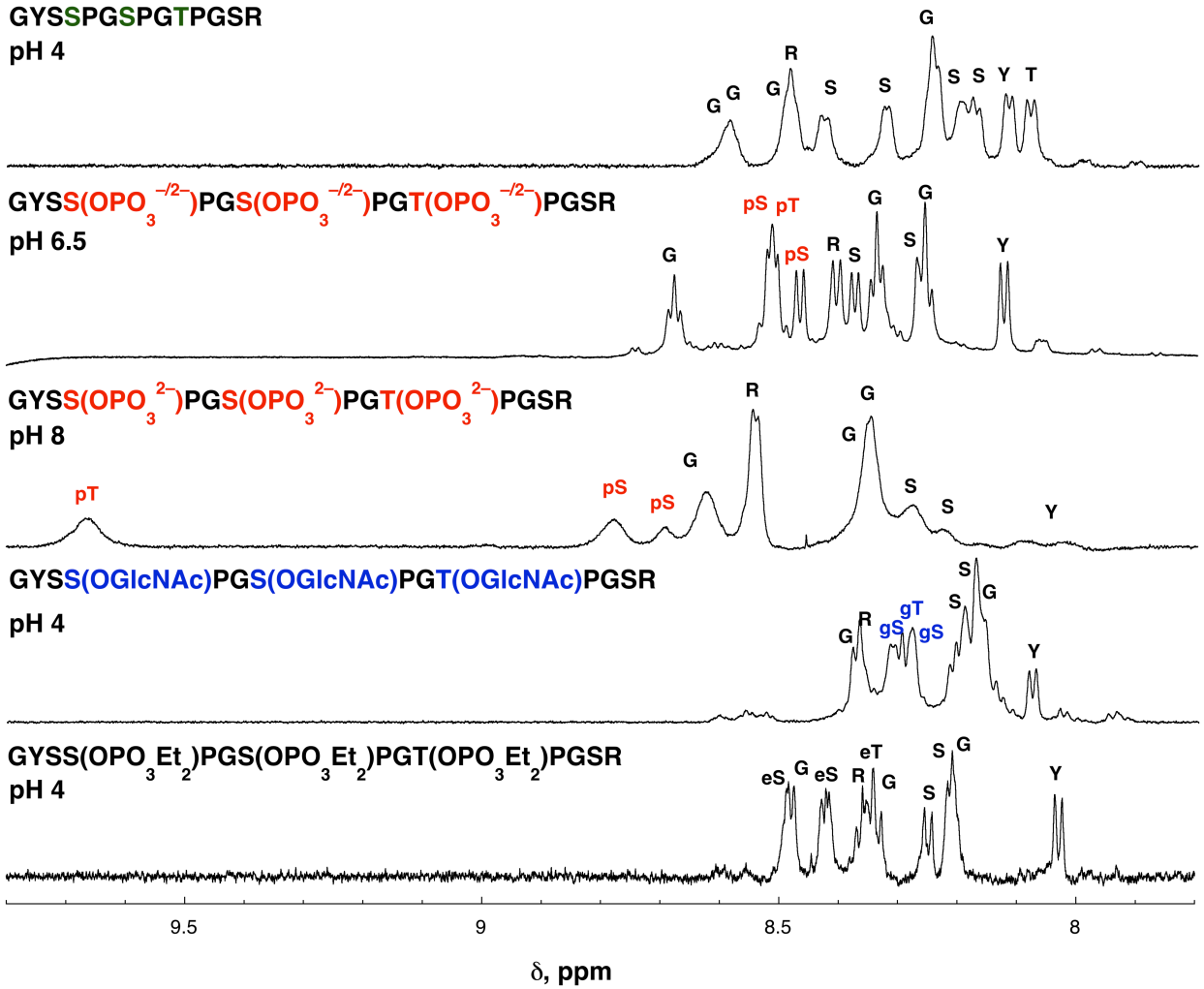

Figure S32. ^{1}H NMR spectra (amide region) of peptides derived from tau$_{196–209}$. Minor peaks in the NMR spectra are due to the presence of cis amide bonds. Peptides were dissolved in 5 mM phosphate buffer (pH 4.0, 6.5, or 8.0) and were internally referenced with TSP. Solutions contained 25 mM NaCl, 100 μM TSP, and 90% H_2O/10% D_2O. pS or pT indicates a phosphorylated serine or threonine residue. eS or eT indicates a diethylphosphorylated (OPO_3Et_2) serine or threonine residue. gS or gT indicates an OGlcNAcylated serine or threonine residue.

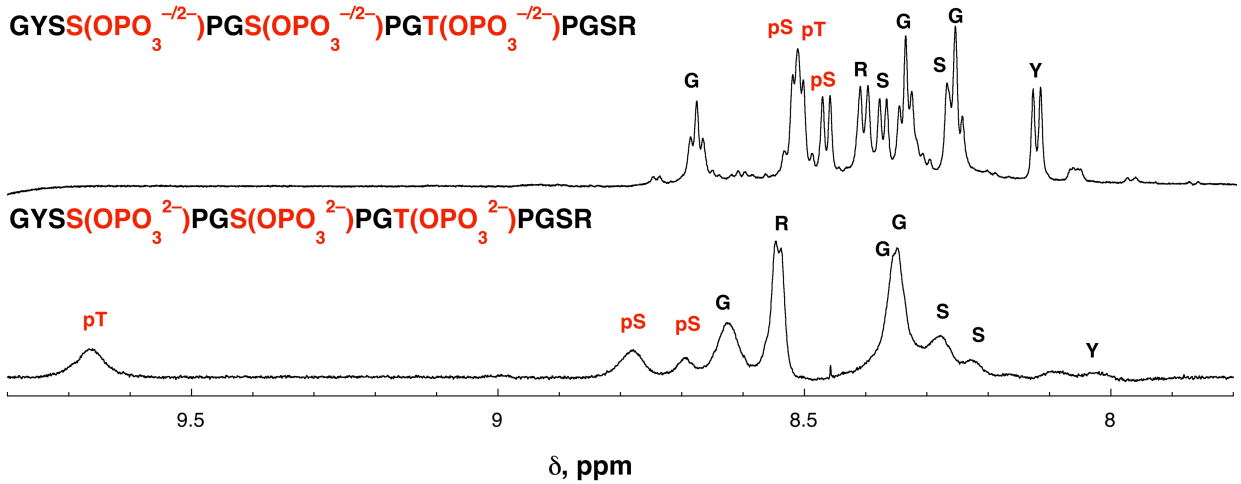

Figure S33. ^{1}H NMR spectra (amide region) of phosphorylated peptide tau$_{196–209}$ at pH 6.5 (top) and pH 8.0 (bottom). Peptides were dissolved in 5 mM phosphate buffer and were internally referenced with TSP. Solutions contained 25 mM NaCl, 100 μM TSP, and 90% H_2O/10% D_2O. Minor peaks in the NMR spectra are due to the presence of cis amide bonds. pS or pT indicates a phosphorylated serine or threonine residue.

The phosphorylated peptide tau$_{196–209}$ showed broad amide peaks indicative of faster amide proton exchange rates at pH 8.0 compared to pH 6.5. This observation is in contrast to other phosphorylated tau peptide, which showed more resolved amide protons at pH 8.0 and than at pH 6.5, suggesting less ordered structure seen in these glycine-rich peptides, which did not exhibit PPII structure, than in the other tau peptides investigated. Nonetheless, the amide protons were still observed at higher pH for phosphorylated peptide tau$_{196–209}$.

Full ^{1}H NMR spectra of peptides derived from tau$_{196–209}$

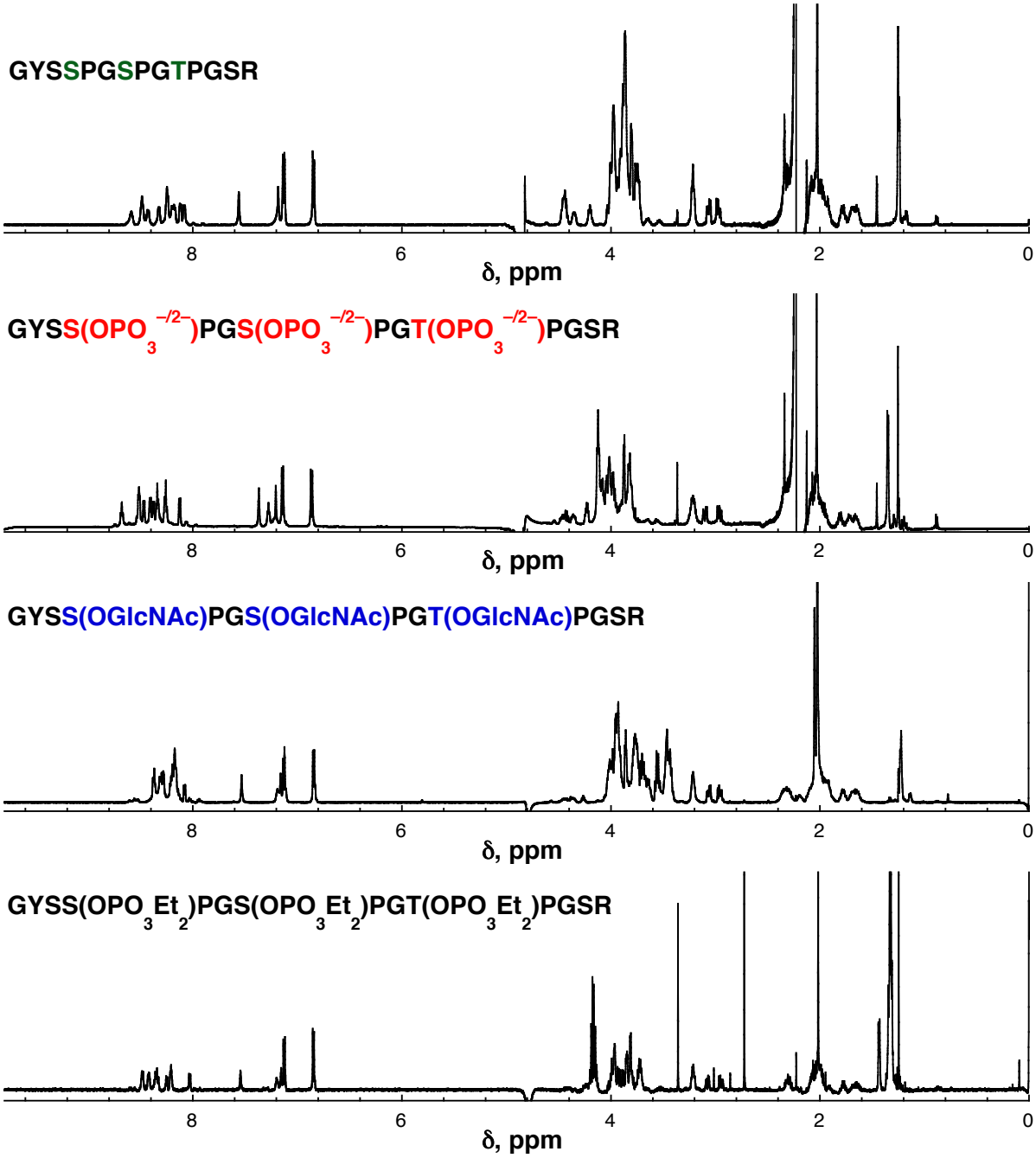

peptide	δ, H^N	$^3J_{\alpha N}$	δ, H_α	δ, H_β
$tau_{196–209}$ (pH 4.0)				
G	8.47	n.d.[b]	3.96	n.a.[a]
G	8.47	n.d.	3.96	n.a.
G	8.57	n.d.	3.98	n.a.
G	8.57	n.d.	3.98	n.a.
Y	8.11	6.3	4.60	3.06, 2.97
S	8.18	5.8	4.43	3.88, 3.87
S	8.18	5.8	4.43	3.88, 3.87
S	8.23	5.8	4.45	3.85, 3.79
S	8.23	5.8	4.45	3.85, 3.79
T	8.07	7.2	4.63	4.19
R	8.41	5.9	4.34	1.90, 1.77
$tau_{196–209}(OPO_3^{-/2-})$ (pH 6.5)				
G	8.24	n.d.	3.86	n.a.
G	8.32	n.d.	3.99	n.a.
G	8.32	n.d.	3.99	n.a.
G	8.66	n.d.	4.00	n.a.
Y	8.11	7.3	4.62	3.09, 2.95
S	8.25	n.d.	4.68	n.d.
S	8.36	6.5	4.92	4.11
pS	8.45	7.3	4.69	4.22, 4.10
pS	8.49	5.5	4.90	4.22, 4.11
pT	8.50	4.4	4.53	n.d.
R	8.39	7.7	4.34	1.96, 1.80
$tau_{196–209}(OPO_3^{2-})$ (pH 8.0)				
G	8.29	n.d.		
G	8.35	n.d.		
G	8.35	n.d.		
G	8.63	n.d.		
Y	8.06	n.d.		
S	8.23	n.d.		
S	8.28	n.d.		
pS	8.69	n.d.		
pS	8.78	n.d.		
pT	9.67	n.d.		
R	8.54	n.d.		
$tau_{196–209}$(OGlcNAc) (pH 4.0)				
G	8.21	n.d.	3.86	n.a.
G	8.28	n.d.	3.95	n.a.
G	8.37	n.d.	4.00	n.a.
G	8.61	n.d.	3.96	n.a.
Y	8.08	7.0	4.61	3.06, 2.97

S	8.16	n.d.	4.57	3.69, 3.56
S	8.19	n.d.	4.69	
gS	8.18	n.d.	4.59	3.72, 3.57
gS	8.28	n.d.	4.57	3.64, 3.55
gT	8.19	n.d.	4.70	4.27
R	8.37	6.8	8.31	1.93, 1.78
$tau_{196–209}(OPO_3Et_2)$ (pH 4.0)				
G	8.21	n.d.	3.85	n.a.
G	8.34	n.d.	3.99	n.a.
G	8.42	n.d.	3.98	n.a.
G	8.47	n.d.	3.96	n.a.
Y	8.03	7.3	4.63	3.08, 2.96
S	8.22	n.d.	4.45	3.85
S	8.25	7.6	4.49	3.82
eT	8.43	n.d.	4.91	n.d.
eS	8.48	n.d.	4.99	4.39, 4.26
eS	8.36	n.d.	5.04	4.40, 4.24
R	8.42	n.d.	4.35	1.93, 1.79

Table S11. Summary of ^{1}H NMR data for peptides derived from $tau_{196–209}$. Data were collected with 100–200 μM peptide in 5 mM phosphate buffer with 25 mM NaCl. pS or pT indicates a phosphorylated serine or threonine residue. eS or eT indicates a diethylphosphorylated (OPO_3Et_2) serine or threonine residue. gS or gT indicates an OGlcNAcylated serine or threonine residue. [a] n.a. = not applicable. [b] n.d. = not determined due to spectral overlap or exchange broadening.

Analysis of peptides derived from tau$_{211–219}$

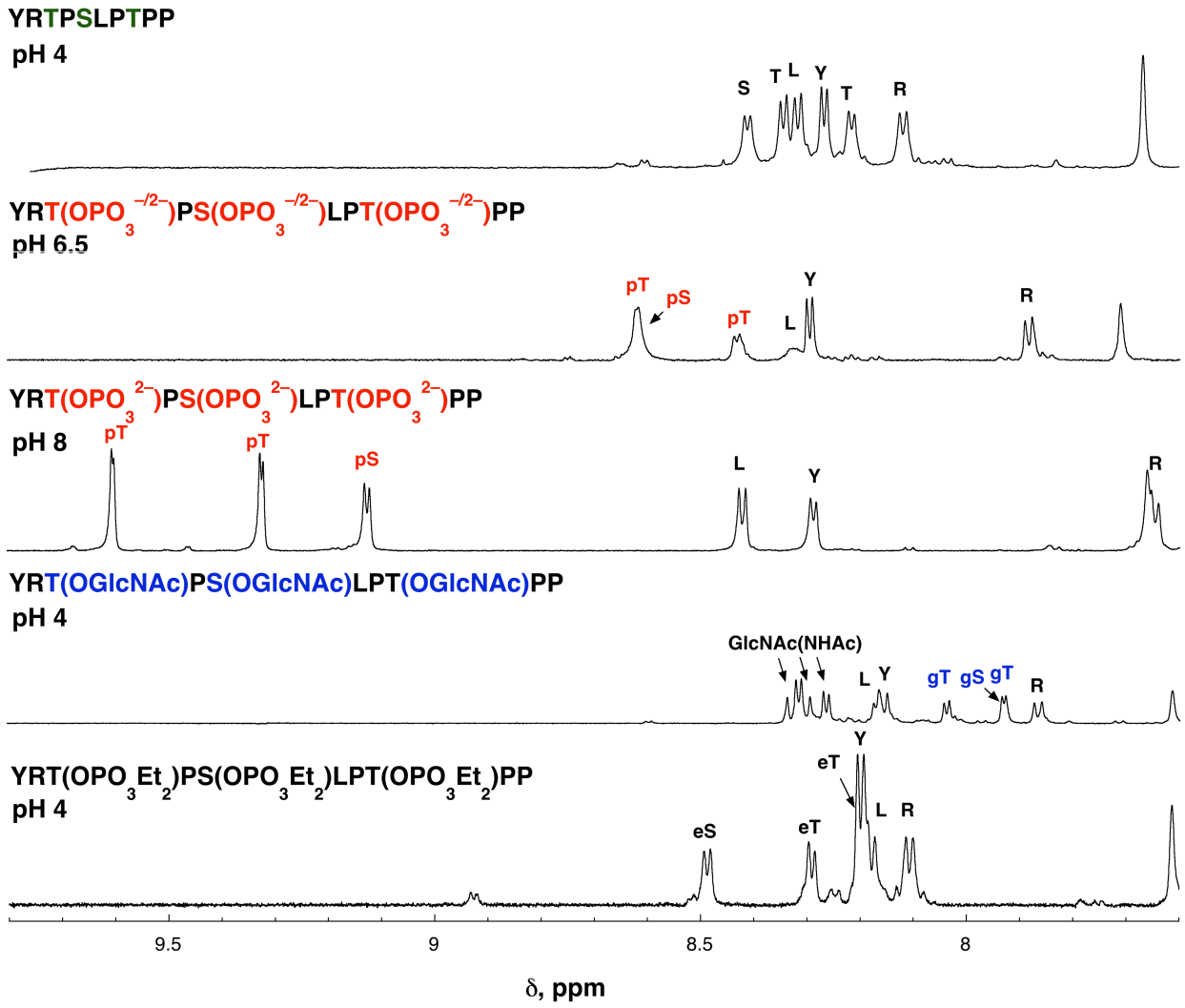

Figure S34. ^{1}H NMR spectra (amide region) of peptides derived from tau$_{211–219}$. Minor peaks in the NMR spectra are due to the presence of cis amide bonds. Peptides were dissolved in 5 mM phosphate buffer (pH 4.0, 6.5, or 8.0) and were internally referenced with TSP. Solutions contained 25 mM NaCl, 100 μM TSP, and 90% H_2O/10% D_2O. pS or pT indicates a phosphorylated serine or threonine residue. eS or eT indicates a diethylphosphorylated (OPO_3Et_2) serine or threonine residue. gS or gT indicates an OGlcNAcylated serine or threonine residue.

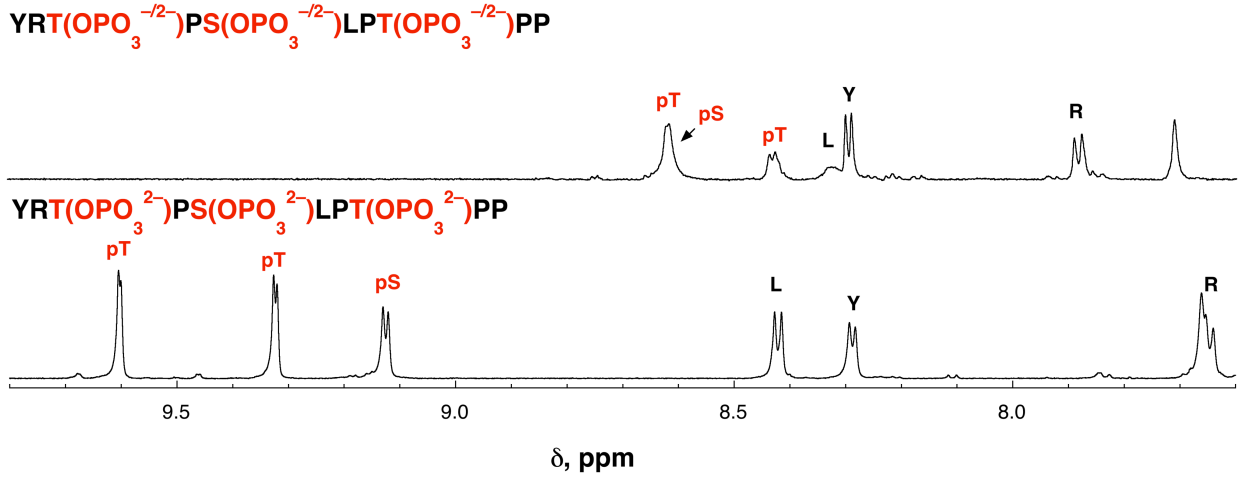

Figure S35. ^{1}H NMR spectra (amide region) of phosphorylated peptide tau$_{211–219}$ at pH 6.5 (top) and 8 (bottom). Minor peaks in the NMR spectra are due to the presence of cis amide bonds. Peptides were dissolved in 5 mM phosphate buffer and were internally referenced with TSP. Solutions contained 25 mM NaCl, 100 μM TSP, and 90% H_2O/10% D_2O. pS or pT indicates a phosphorylated serine or threonine residue.

As observed previously for phosphorylated peptide tau$_{174-183}$, the amide protons were observed to be in slow exchange and were more resolved at pH 8.0 compared to pH 6.5.

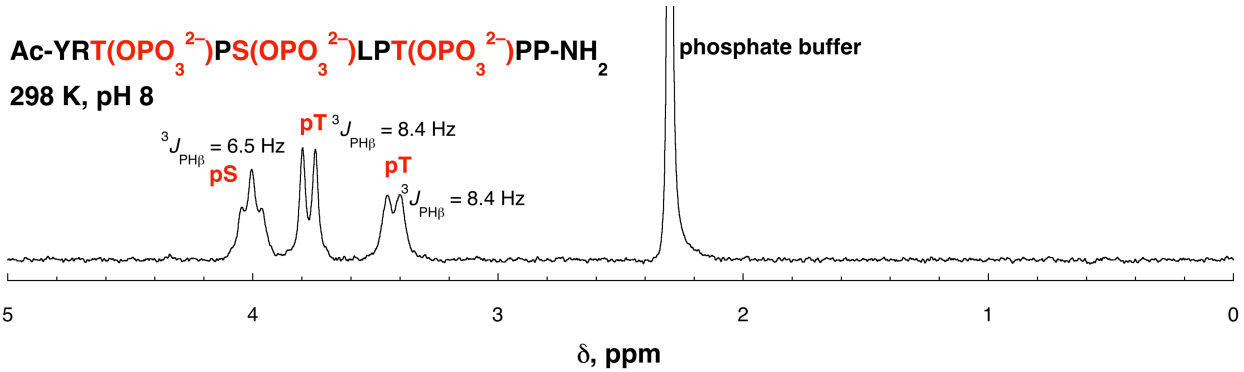

Figure S36. ^{31}P NMR spectrum of phosphorylated peptide tau$_{211–219}$ at pH 8.0, 298 K in 5 mM phosphate buffer containing 25 mM NaCl. The NMR spectrum was internally referenced with 85% H_3PO_4 (0 ppm) using a capillary filled with H_3PO_4 located in the NMR tube containing the sample.

Full ^{1}H NMR spectra of peptides derived from tau$_{211–219}$

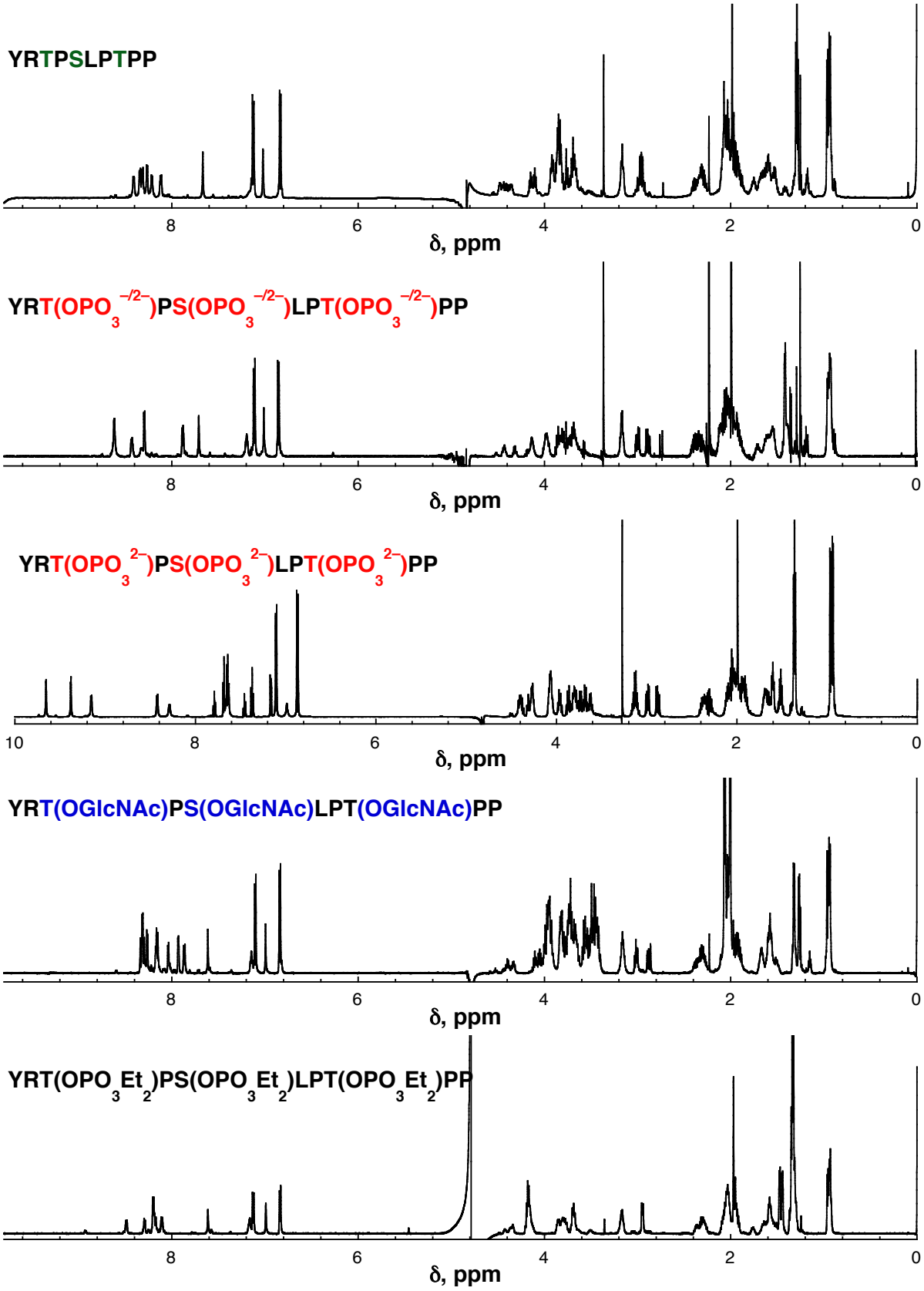

peptide	δ, H^N	$^3J\alpha N$	δ, Hα	δ, Hβ	$^3JH\alpha H\beta$
$tau_{211–219}$ (pH 4.0)					
Y	8.26	6.3	4.48	2.96, 2.96	
R	8.12	7.7	4.37	1.75, 1.66	
T	8.21	6.4	4.48	4.15	
S	8.41	6.5	4.44	3.85, 3.85	
L	8.32	7.1	4.68	1.69	
T	8.34	7.0	4.55	4.11	7.0
$tau_{211–219}(OPO_3H^-)$ (pH 4.0)					
Y	8.27	6.4	4.42	2.99, 2.88	
R	7.87	8.0	4.30	1.70, 1.61	
pT	8.39	6.6	4.65	4.49	n.d.
pS	8.57	4.5	4.49	4.11, 4.11	n.d.
L	8.31	7.4	4.69	1.67, 1.58	
pT	8.58	6.7	4.54	4.11	n.d.
$tau_{211–219}(OPO_3^{-/2-})$ (pH 6.5)					
Y	8.29	6.3	4.44	3.00, 2.89	
R	7.88	8.0	4.32	1.72, 1.63	
pT	8.42	5.9	4.68	4.53	n.d.
pS	8.62	n.d.[a]	4.53	4.14, 4.14	
L	8.32	n.d.	n.d.	n.d.	
pT	8.62	2.9	4.53	4.53	n.d.
$tau_{211–219}(OPO_3^{2-})$ (pH 8.0)					
Y	8.29	6.1	4.44	2.99, 2.89	
R	7.65	n.d.	4.27	1.68, 1.52	
pT	9.39	3.7	4.41	4.28	n.d.
pS	9.17	5.5	4.42	4.09, 3.97	n.d.
L	8.44	7.5	4.70	1.70, 1.61	
pT	9.66	3.1	4.30	4.30	n.d.
$tau_{211–219}$(OGlcNAc) (pH 4.0)					
Y	8.26	6.1	4.32	2.91, 2.77	
R	7.86	8.3	4.26		
gT	7.93	4.2	4.34	4.06	n.d.
gS	8.15	7.8	4.54	3.54, 3.43	n.d.
L	8.17	5.3	4.69	n.d.	
gT	8.03	5.7	4.53	4.11	6.6
$tau_{211–219}(OPO_3Et_2)$ (pH 4.0)					
Y	8.19	7.0	4.49	2.96, 2.96	
R	8.10	7.7	4.37		
eT	8.19	7.0	4.82	4.47	8.0
eS	8.48	7.3	4.62	4.35, 4.35	n.d.
L	8.18	7.7	4.71	n.d.	
eT	8.29	6.8	4.74	4.70	n.d.

Table S12. Summary of ^{1}H NMR data for peptides derived from $tau_{211–219}$. Data were collected with 100–200 μM peptide in 5 mM phosphate buffer with 25 mM NaCl. pS or pT indicates a phosphorylated serine or threonine residue. eS or eT indicates a diethylphosphorylated (OPO_3Et_2) serine or threonine residue. gS or gT indicates an OGlcNAcylated serine or threonine residue. [a] n.d. = not determined due to spectral overlap.

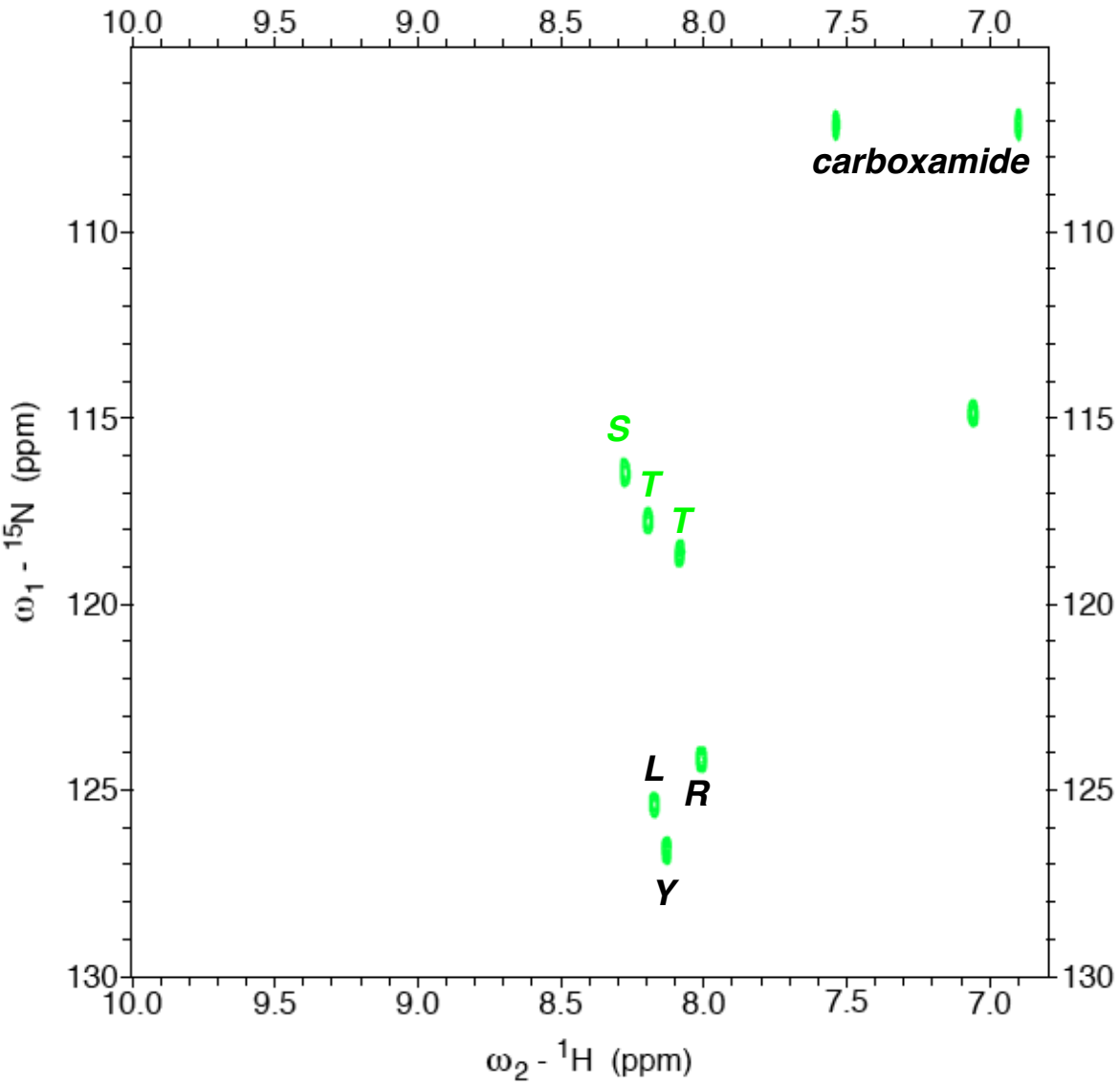

Figure S37. ^{1}H-^{15}N HSQC spectrum of peptide tau$_{211–219}$ at pH 4.0 at 298 K in 5 mM phosphate buffer containing 25 mM NaCl.

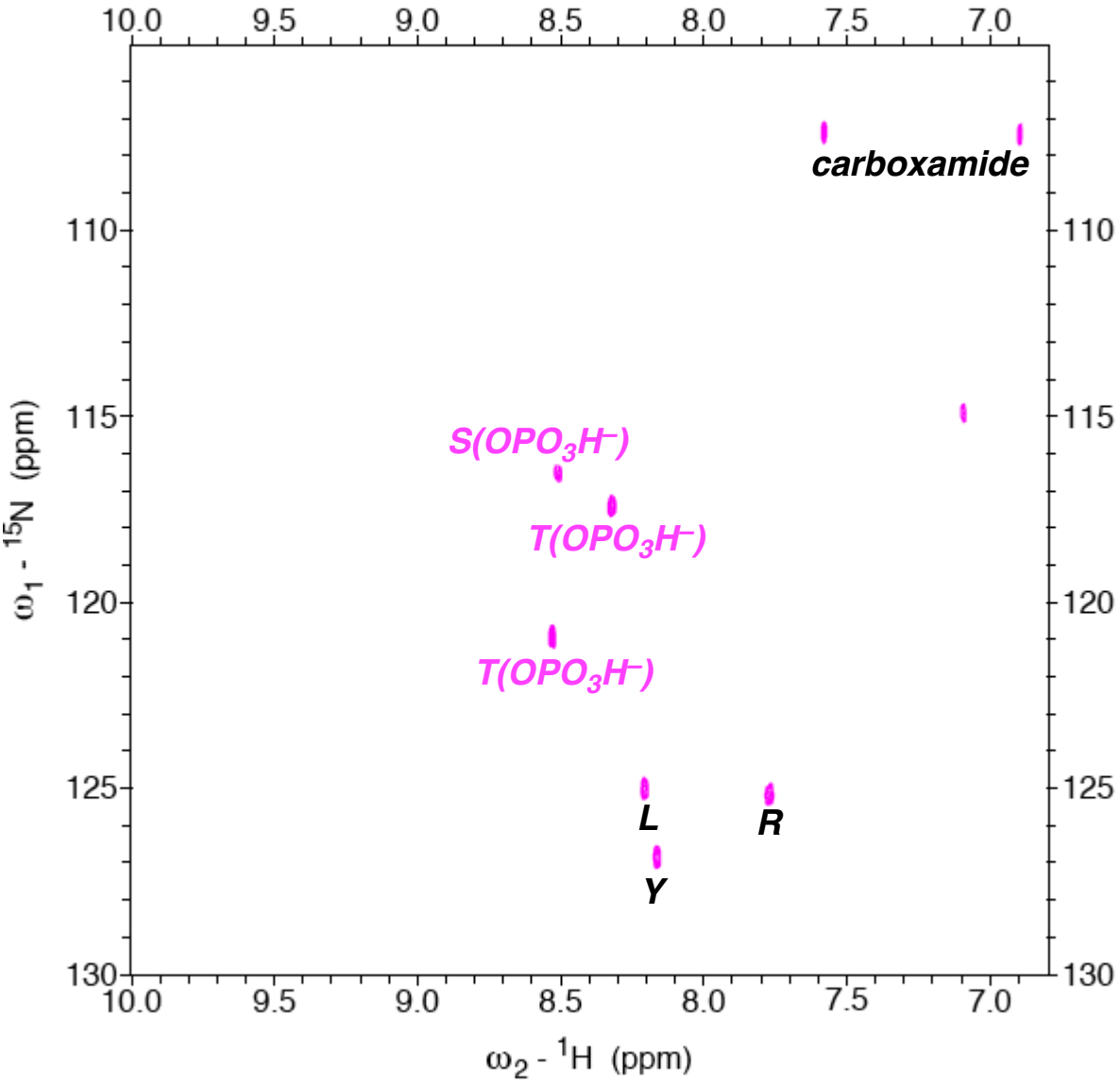

Figure S38. ^{1}H-^{15}N HSQC spectrum of peptide $tau_{211-219}(OPO_3H^-)$ at pH 4.0 at 298 K in 5 mM phosphate buffer containing 25 mM NaCl.

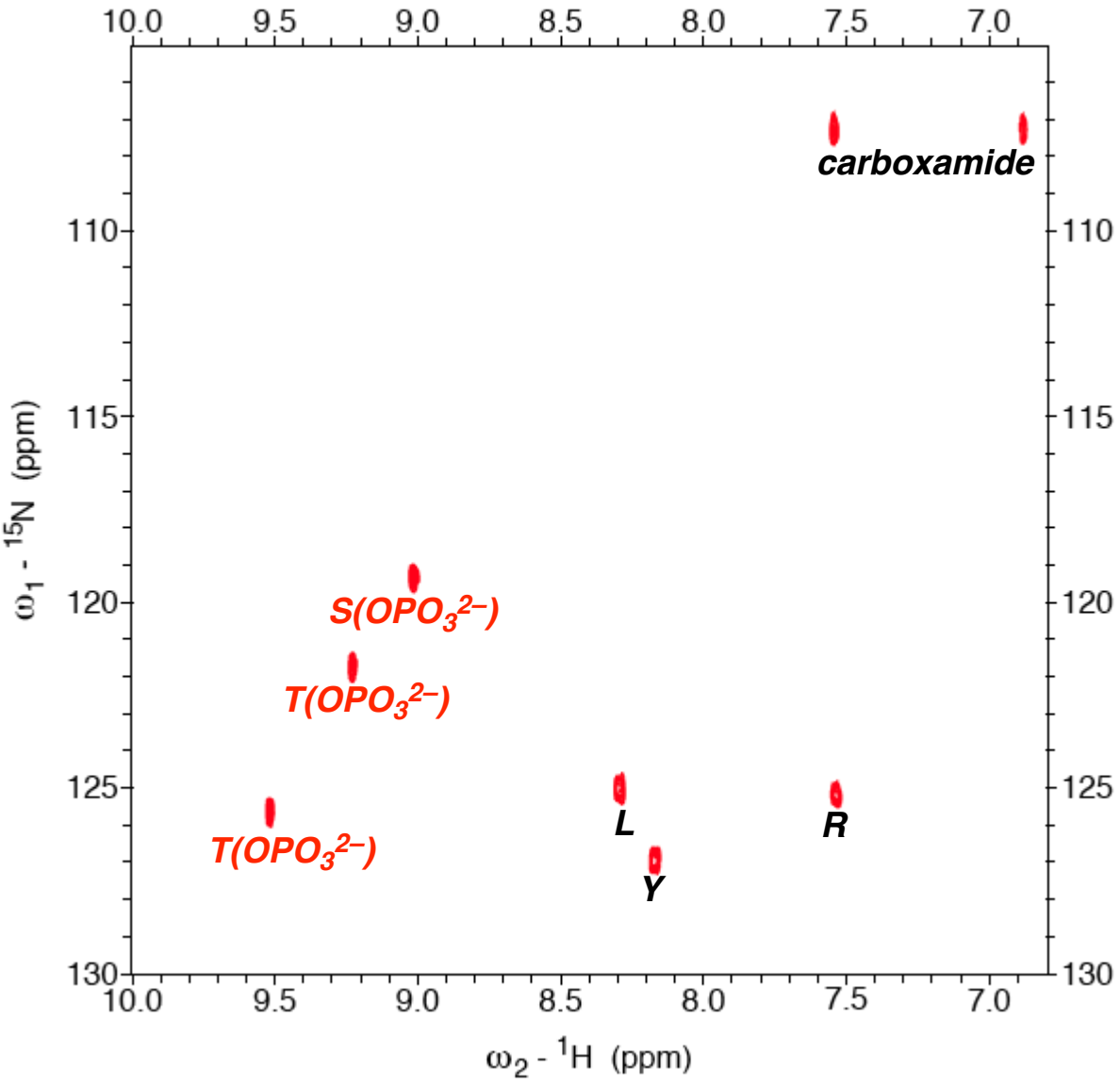

Figure S39. ^{1}H-^{15}N HSQC spectrum of peptide $tau_{211–219}(OPO_3^{2–})$ at pH 7.9 at 298 K in 5 mM phosphate buffer containing 25 mM NaCl.

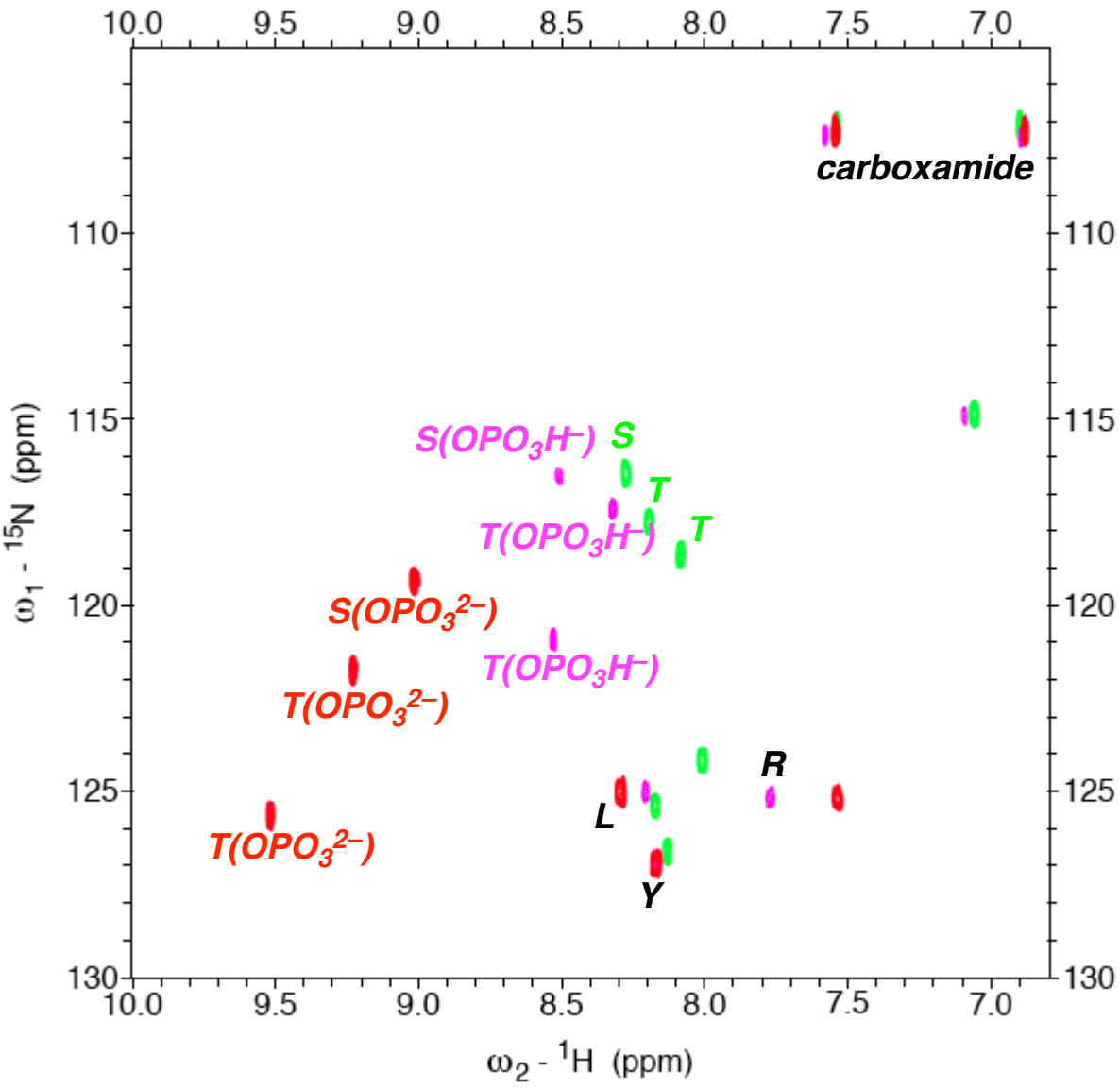

Figure S40. ^{1}H-^{15}N HSQC spectra of peptides $tau_{211–219}$ at pH 4.0 (green), $tau_{211–219}(OPO_3^{2–})$ (red) (pH 7.9), and $tau_{211–219}(OPO_3H^{–})$ (magenta) (pH 4.0) at 298 K. Data were collected with 2–3 mM peptide in 5 mM phosphate buffer (pH 4.0 or 7.9) with 25 mM NaCl.

peptide	Thr_N, ppm	Ser_N, ppm	others	pH, Temp
Ac-YRTPSLPTPP-NH_2	117.8, 118.6	116.5	124.2 (Arg), 125.4 (Leu), 126.6 (Tyr), 107.1 (carboxamide)	4.0, 298 K
Ac-YRT(OPO_3H^-)PS(OPO_3H^-)LPT(OPO_3H^-)PP-NH_2	117.4, 120.9	116.6	125.2 (Arg), 125.0 (Leu), 126.9 (Tyr), 107.4 (carboxamide)	4.0, 298 K
Ac-YRT(OPO_3^{2-})PS(OPO_3^{2-})LPT(OPO_3^{2-})PP-NH_2	121.8, 125.7	119.4	125.2 (Arg), 125.1 (Leu), 127.0 (Tyr), 107.4 (carboxamide)	7.9, 298 K

Table S13. Summary of ^{1}H-^{15}N HSQC NMR data for peptides derived from $tau_{211–219}$. Data were collected with 2–3 mM peptide in 5 mM phosphate buffer (pH 4.0 or 7.9) with 25 mM NaCl.

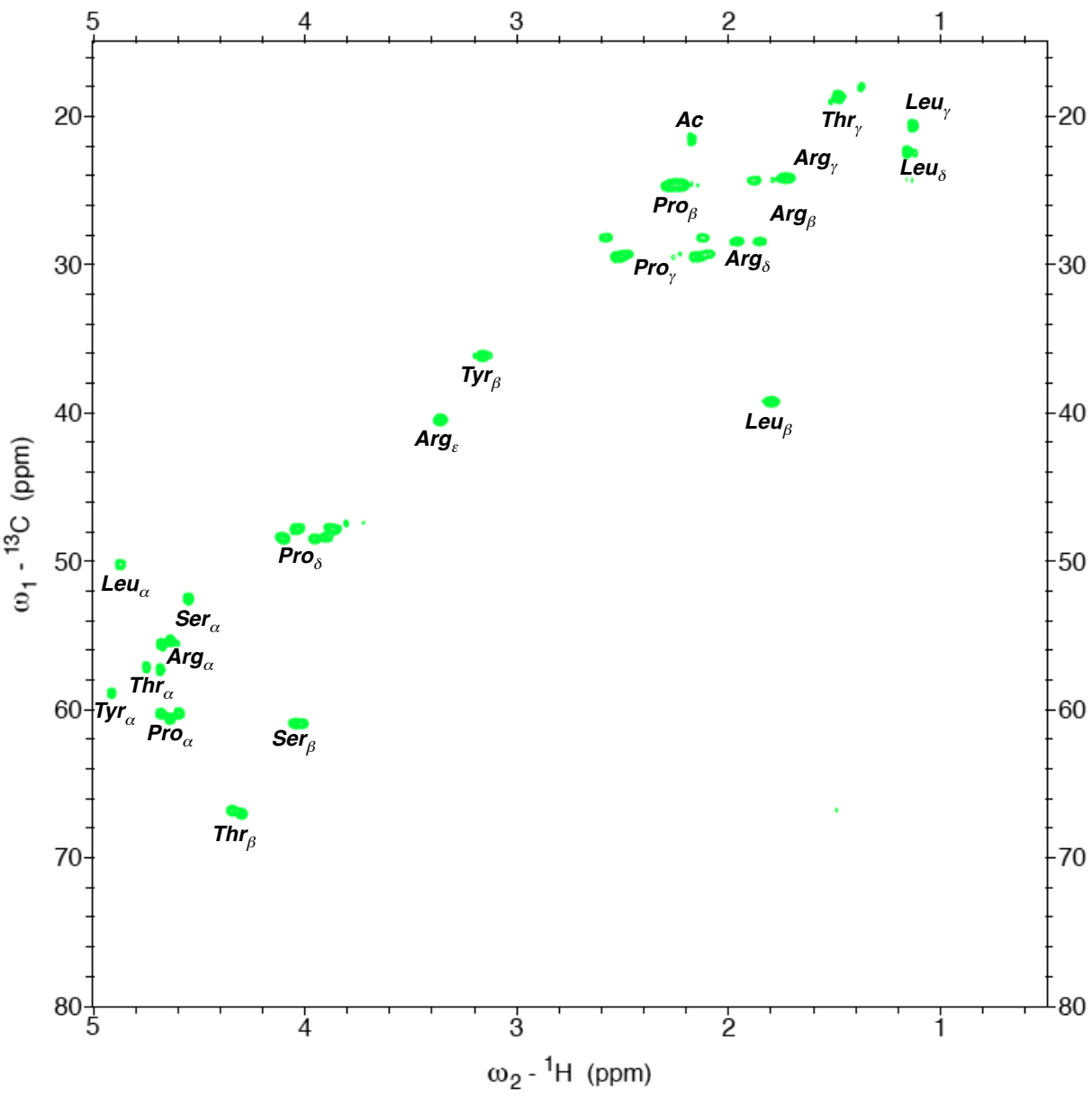

Figure S41. ^{1}H-^{13}C HSQC spectrum of peptide $tau_{211-219}$ at pH 4.0 in 5 mM phosphate buffer with 25 mM NaCl in 100% D_2O at 298 K.

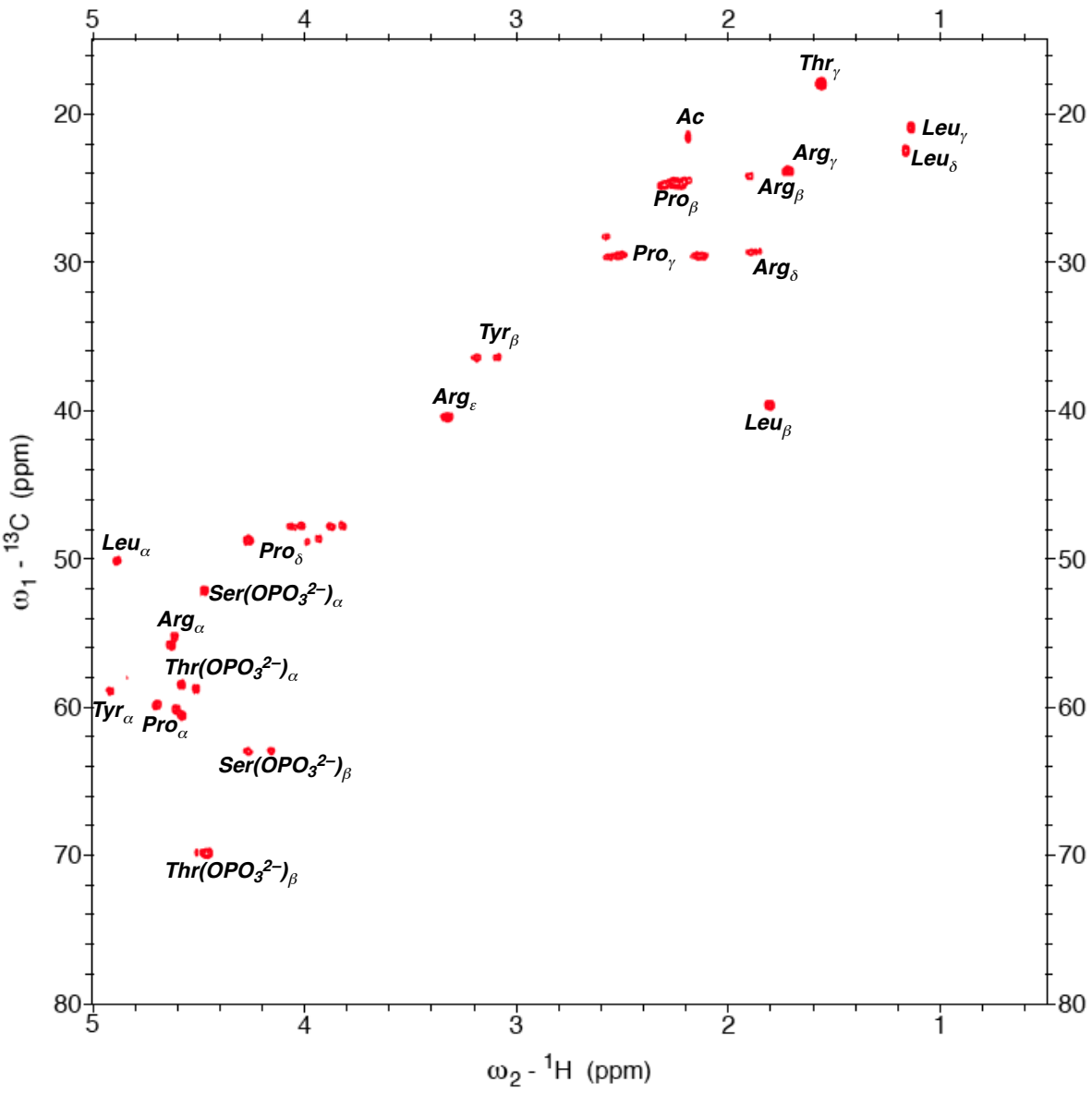

Figure S42. ^{1}H-^{13}C HSQC spectrum of peptide tau$_{211-219}$(OPO$_3^{2-}$) at pH 8.0 in 5 mM phosphate buffer with 25 mM NaCl in 100% D_2O at 298 K.

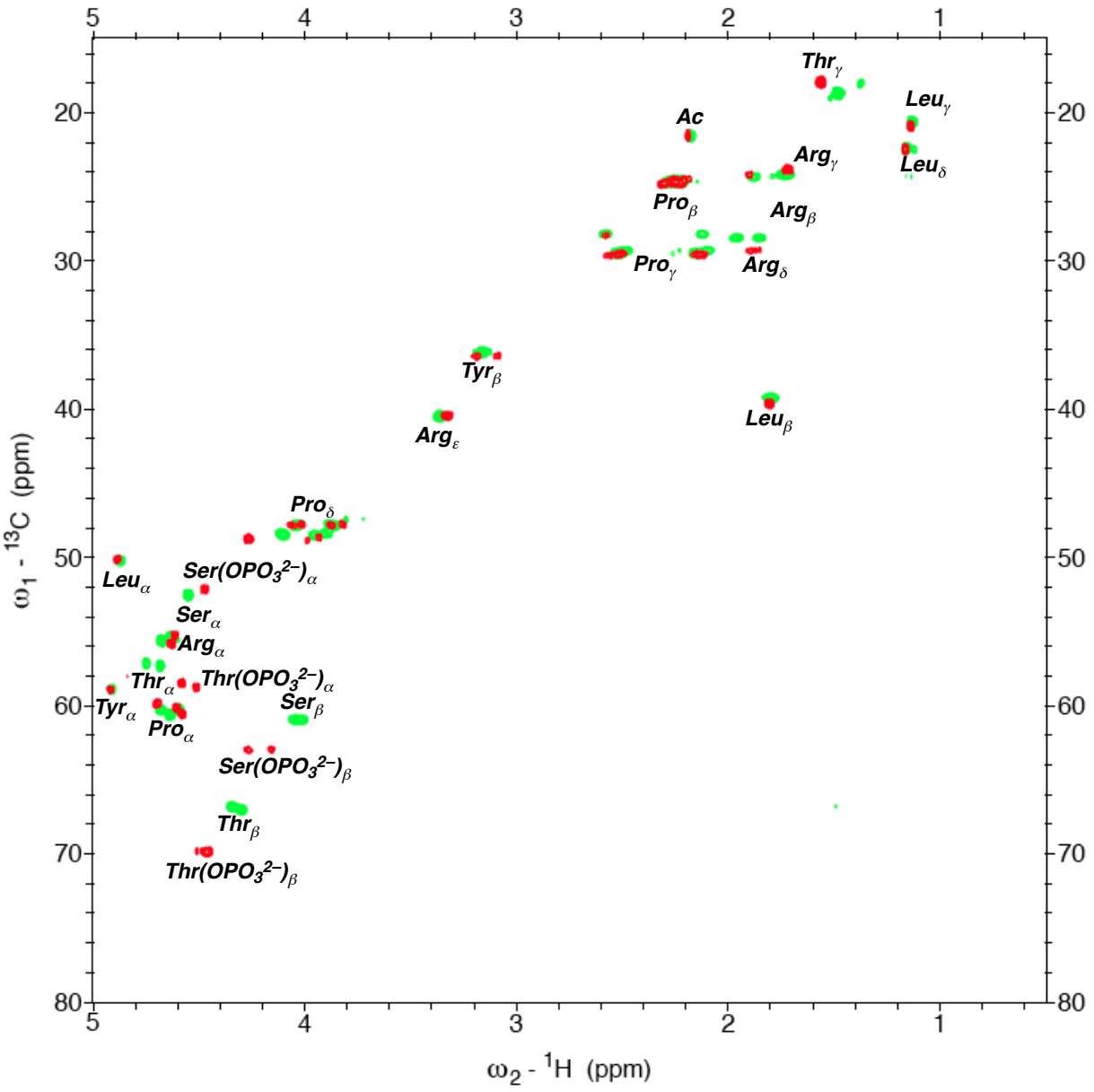

Figure S43. ^{1}H-^{13}C HSQC spectra of peptides tau$_{211–219}$ at pH 4.0 (green) and tau$_{211–219}$(OPO$_3^{2–}$) (red) (pH 8.0) at 298 K. Data were collected with 1 mM peptide in 5 mM phosphate buffer containing 25 mM NaCl.

Ac-YRTPSLPTPP-NH_2		Ac-YRpTPpSLPpTPP-NH_2	
residue	^{13}C δ, ppm	residue	^{13}C δ, ppm
Arg, α	55.4	Arg, α	55.2
Thr, α	57.1, 57.3	pThr, α	58.5, 58.8
Ser, α	52.5	pSer, α	52.2
Leu, α	50.2	Leu, α	50.1
Pro, α	55.6, 60.2, 60.3, 60.6	Pro, α	55.8, 59.8, 60.2, 60.6
Tyr, α	58.9	Tyr, α	58.9
Ser, β	60.9	pSer, β	63.0
Thr, β	66.8, 67.0	pThr, β	69.9, 69.9
Tyr, β	36.2	Tyr, β	36.4
Pro, δ	47.8, 48.4, 48.4	Pro, δ	47.8, 48.8, 48.8
Arg, ε	40.5	Arg, ε	40.4
Pro, γ	29.5, 29.5, 29.5, 29.5	Pro, γ	29.6, 29.6, 29.6, 29.6
Arg, β	n.d.	Arg, β	n.d.
Pro, β	24.6, 24.6, 24.6, 24.6	Pro, β	24.6, 24.6, 24.6, 24.6
Leu, β	39.3	Leu, β	39.6
Leu, γ	20.8	Leu, γ	20.9
Arg, γ	24.2	Arg, γ	23.8
Arg, δ	28.4	Arg, δ	39.6
Leu, δ	22.4	Leu, δ	22.5
Thr, γ	18.7, 18.7	pThr, γ	17.9, 17.9
Ac	21.5	Ac	21.5

Table S14. Summary of ^{1}H-^{13}C NMR data for peptides derived from $tau_{211–219}$. Data were collected with 1 mM peptide in 5 mM phosphate buffer with 25 mM NaCl. pSer or pThr indicates a phosphorylated serine or threonine residue.

Analysis of peptides derived from tau$_{229–238}$

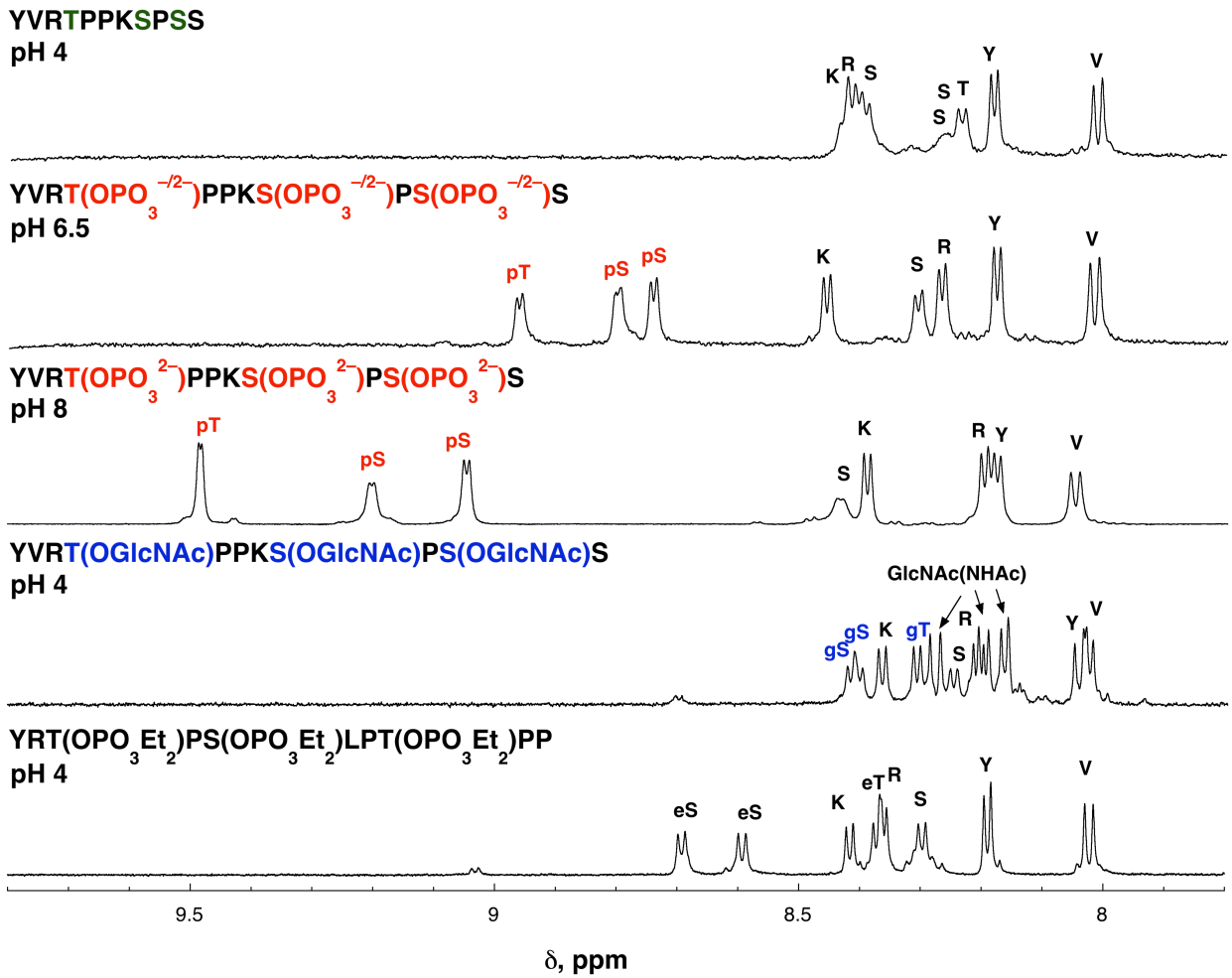

Figure S44. ^{1}H NMR spectra (amide region) of peptides derived from tau$_{229–238}$. Minor peaks in the NMR spectra are due to the presence of cis amide bonds. Peptides were dissolved in 5 mM phosphate buffer (pH 4.0, 6.5, or 8.0) and were internally referenced with TSP. Solutions contained 25 mM NaCl, 100 μM TSP, and 90% H_2O/10% D_2O. pS or pT indicates a phosphorylated serine or threonine residue. eS or eT indicates a diethylphosphorylated (OPO_3Et_2) serine or threonine residue. gS or gT indicates an OGlcNAcylated serine or threonine residue.

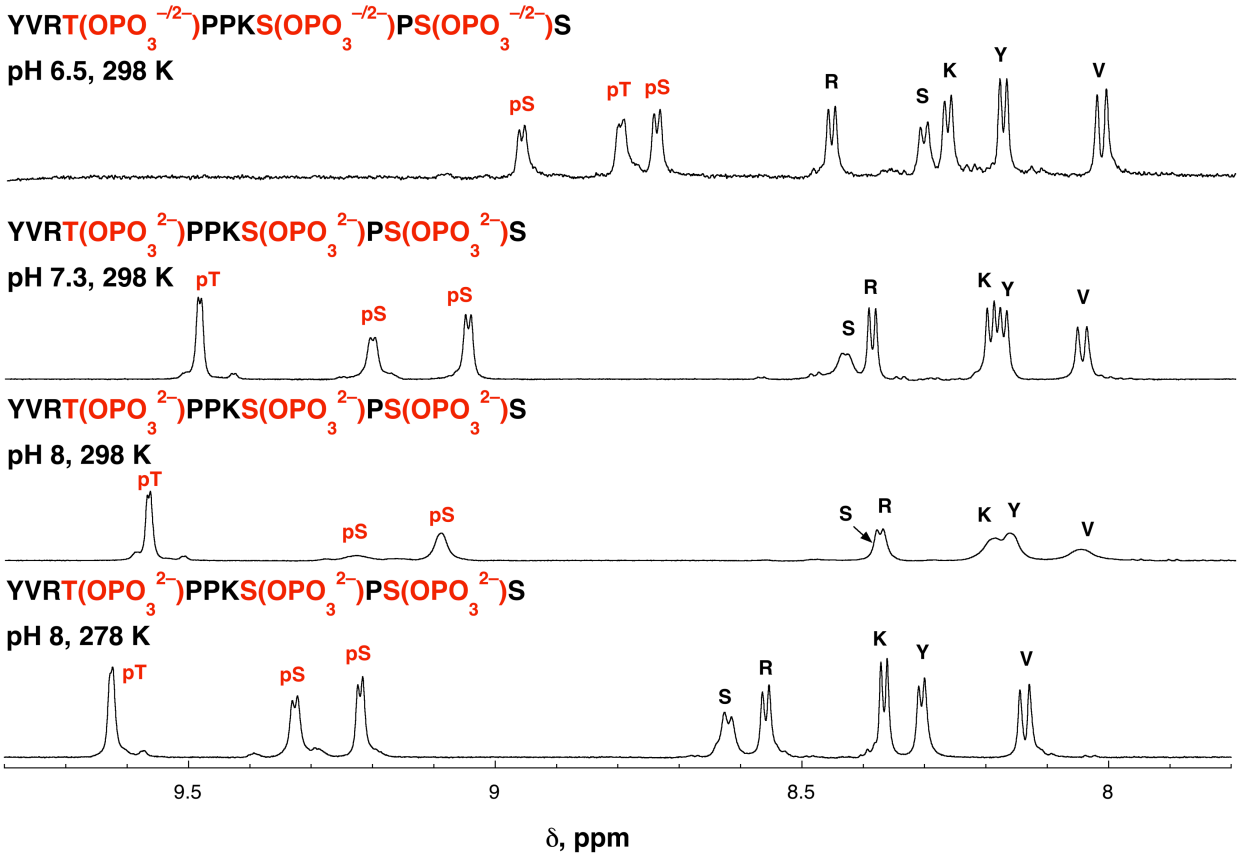

Figure S45. ^{1}H NMR spectra (amide region) of phosphorylated peptide $tau_{229–238}$ at pH 8.0, 7.3, and 6.5 at 298 K or as indicated. Minor peaks in the NMR spectra are due to the presence of cis amide bonds. Peptides were dissolved in 5 mM phosphate buffer and were internally referenced with TSP. Solutions contained 25 mM NaCl, 100 μM TSP, and 90% H_2O/10% D_2O. pS or pT indicates a phosphorylated serine or threonine residue.

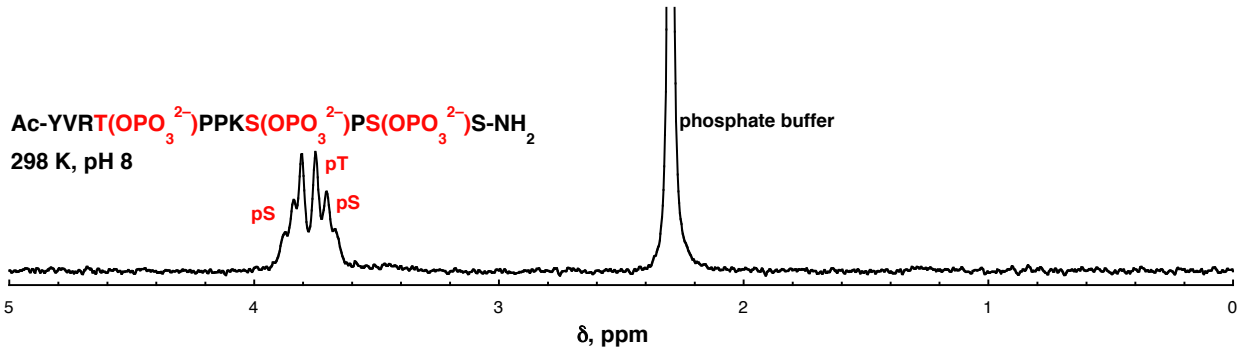

Figure S46. ^{31}P NMR spectrum of phosphorylated peptide $tau_{229–238}$ at pH 8.0 at 298 K in 5 mM phosphate buffer containing 25 mM NaCl. The NMR spectrum was internally referenced with 85% H_3PO_4 (0 ppm) using a capillary filled with H_3PO_4 located in the NMR tube containing the sample.

Full ^{1}H NMR spectra of peptides derived from tau$_{229–238}$ at pH 6.5 or 8, 298 K

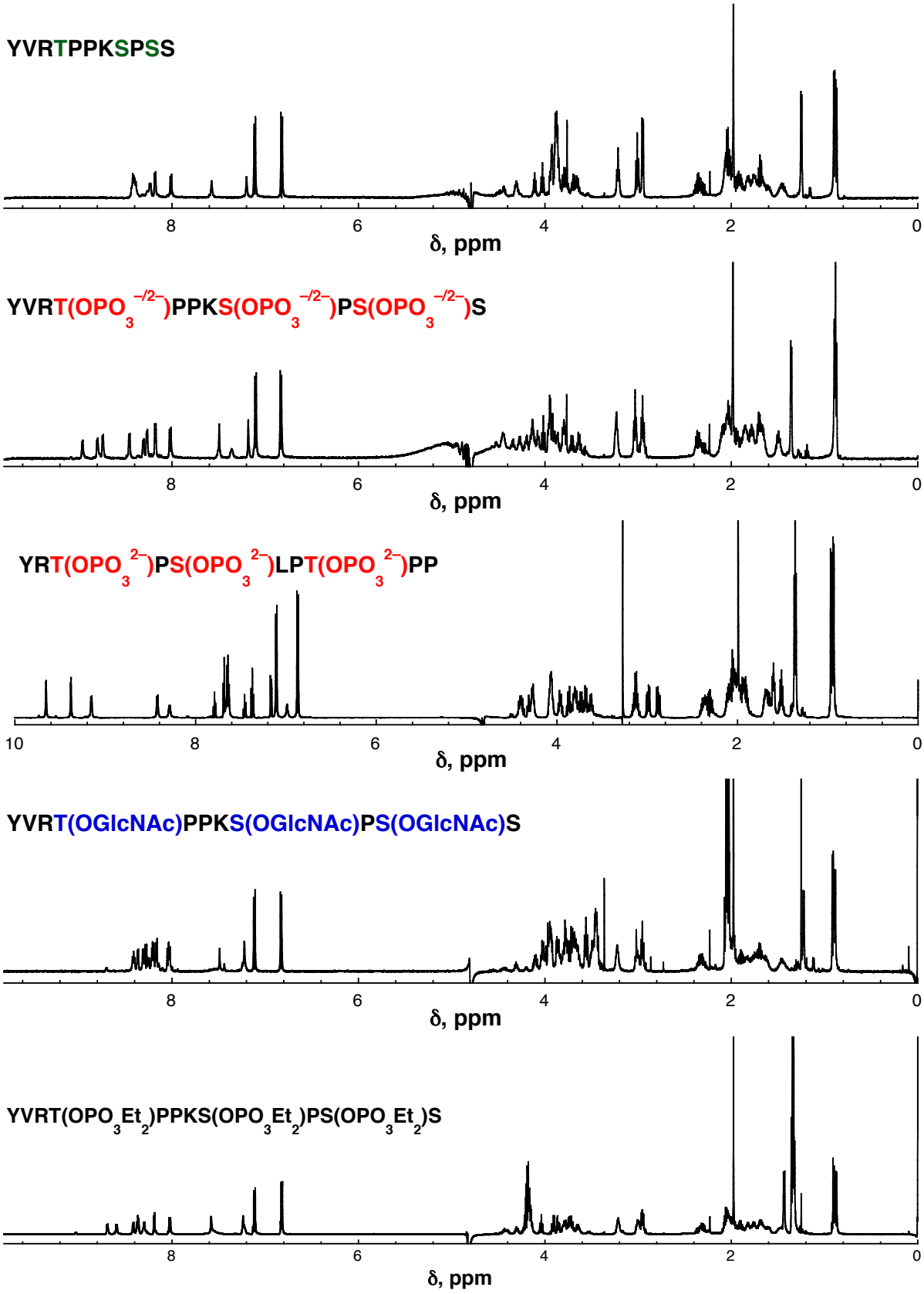

peptide	δ, H^N	$^3J\alpha N$	δ, Hα	δ, Hβ	$^3JH\alpha H\beta$
$tau_{229–238}$ (pH 4.0)					
Y	8.18	6.5	4.52	2.96	
V	8.01	8.6	4.03	1.96	
R	8.39	7.0	4.32	1.84, 1.76	
T	8.23	7.3	4.57	4.12	8.9
K	8.41	n.d.[a]	4.30	1.82, 1.75	
S	8.25	n.d.	4.45	3.94, 3.89	n.d.
S	8.25	n.d.	4.45	3.94, 3.89	n.d.
S	8.40	n.d.	4.48	3.93, 3.88	n.d.
$tau_{229–238}$ (OPO_3H^-) (pH 4.0)					
Y	8.19	6.6	4.50	2.92, 2.92	
V	8.01	8.8	4.00	0.87, 0.87	
R	8.53	6.7	4.32	1.82, 1.77	
pT	8.39	7.1	4.68	4.56	n.d.
K	8.30	7.0	4.27	1.84, 1.76	
S	8.34	6.4	4.42	3.94, 3.90	
pS	8.59	6.4	4.86	4.15, 4.09	n.d.
pS	8.73	6.4	4.57	4.24, 4.15	n.d.
$tau_{229–238}$ ($OPO_3^{-/2-}$) (pH 6.5)					
Y	8.18	6.6	4.52	2.95	
V	8.02	9.0	4.02	1.95	
R	8.26	6.3	4.28	1.85, 1.78	n.d.
pT	8.80	5.0	4.56	4.46	
K	8.45	6.7	4.34	1.84, 1.77	
S	8.30	7.1	4.79	4.44, 3.94	
pS	8.74	5.6	4.85	4.14, 4.07	n.d.
pS	8.96	5.0	4.52	4.20, 4.12	n.d.
$tau_{229–238}$ (OPO_3^{2-}) (pH 8.0)					
Y	8.20	6.5	4.52	2.97, 2.93	
V	8.06	9.1	4.00	1.94	
R	8.18	6.4	4.24	1.85, 1.76	
pT	9.49	3.8	4.37	4.29	n.d.
K	8.39	6.6	4.34	1.81, 1.71	
S	8.44	n.d.	4.43	3.95, 3.91	
pS	9.05	5.5	4.74	4.08, 3.98	n.d.
pS	9.21	5.3	4.46	4.13, 4.07	n.d.
$tau_{229–238}$ (OGlcNAc) (pH 4.0)					
Y	8.17	7.0	4.55	2.96	
V	8.04	8.6	4.49	4.04	
R	8.32	6.8	4.30	1.80, 1.72	
gT	8.02	6.5	4.56	4.10	6.3
K	8.38	7.4	4.32	1.83, 1.77	
S	8.24	6.4	4.42	3.93, 3.87	
gS	8.40	8.0	4.61	4.12, 4.01	6.2
gS	8.42	6.9	4.85	4.02, 3.96	5.9
$tau_{229–238}$ (OPO_3Et_2) (pH 4.0)					
Y	8.18	6.7	4.54	2.96	
V	8.02	8.3	4.05	1.97	
R	8.36	4.7	4.31	1.83, 1.76	
eT	8.37	5.9	4.86	4.66	6.5
K	8.42	6.8	4.30	1.80, 1.75	
S	8.30	7.1	4.46	3.92, 3.86	
eS	8.59	7.4	5.01	4.42, 4.23	4.8
eS	8.69	7.0	4.71	4.44, 4.41	5.0

Table S15. Summary of ^{1}H NMR data for peptides derived from $tau_{229–238}$. Data were collected with 100–200 μM peptide in 5 mM phosphate buffer containing 25 mM NaCl. pS or pT indicates a phosphorylated serine or threonine residue. eS or eT indicates a diethylphosphorylated (OPO_3Et_2) serine or threonine residue. gS or gT indicates an OGlcNAcylated serine or threonine residue. [a] n.d. = not determined due to spectral overlap.

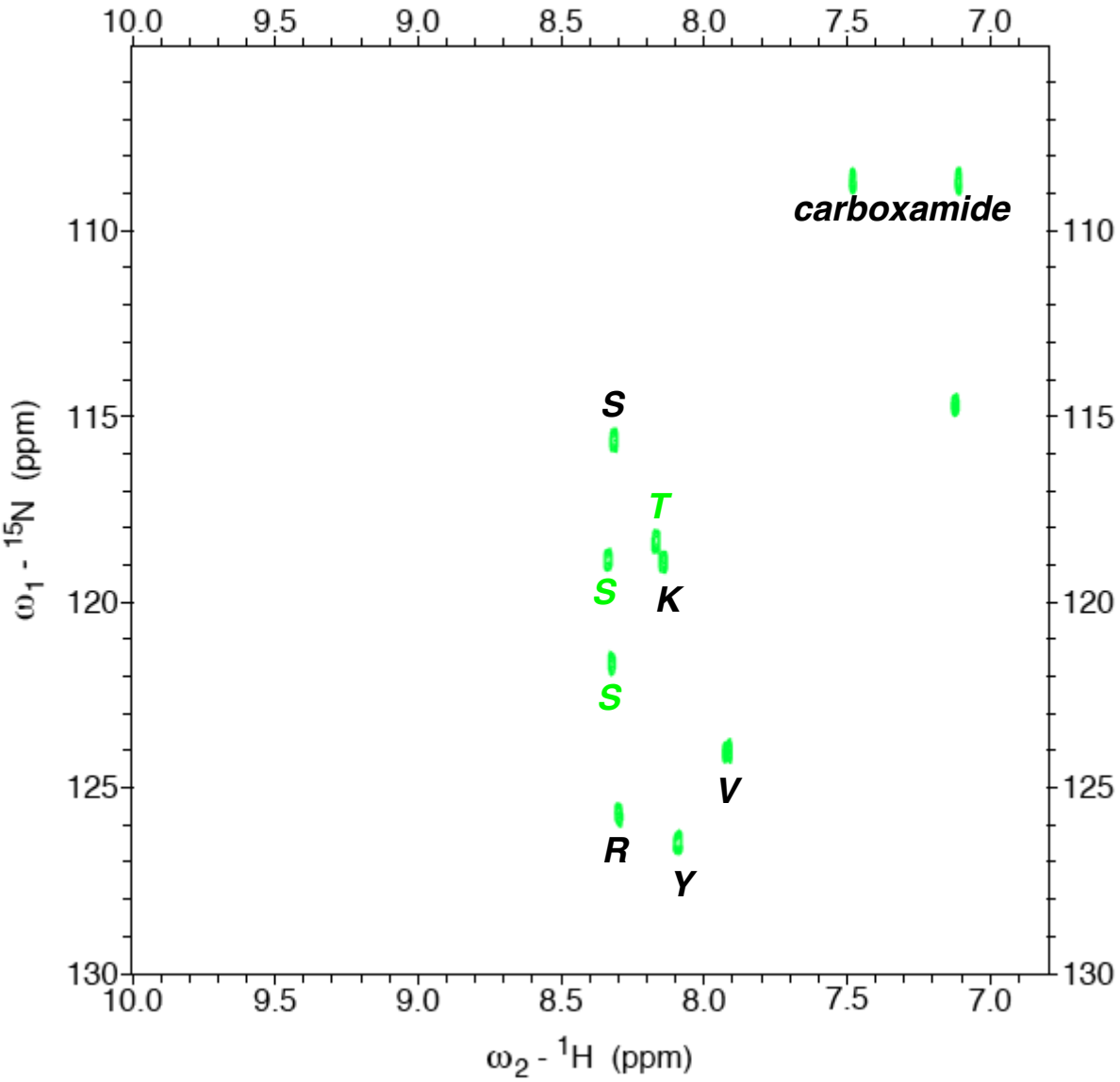

Figure S47. ^{1}H-^{15}N HSQC spectrum of peptide tau$_{229–238}$ at pH 4.0 at 298 K in 5 mM phosphate buffer containing 25 mM NaCl.

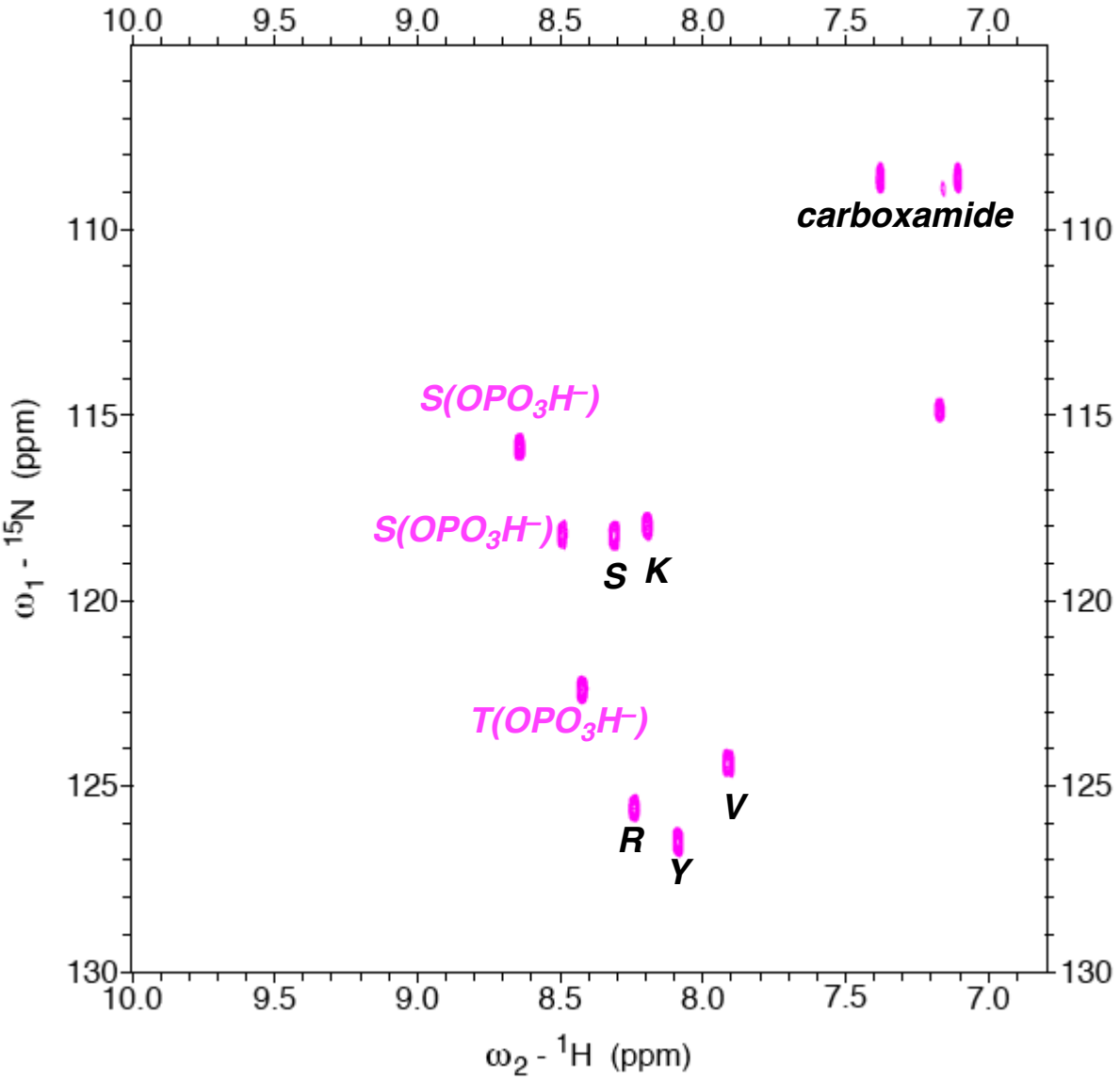

Figure S48. ^{1}H-^{15}N HSQC spectrum of peptide $tau_{229–238}(OPO_3H^-)$ at pH 4.0 at 298 K in 5 mM phosphate buffer containing 25 mM NaCl.

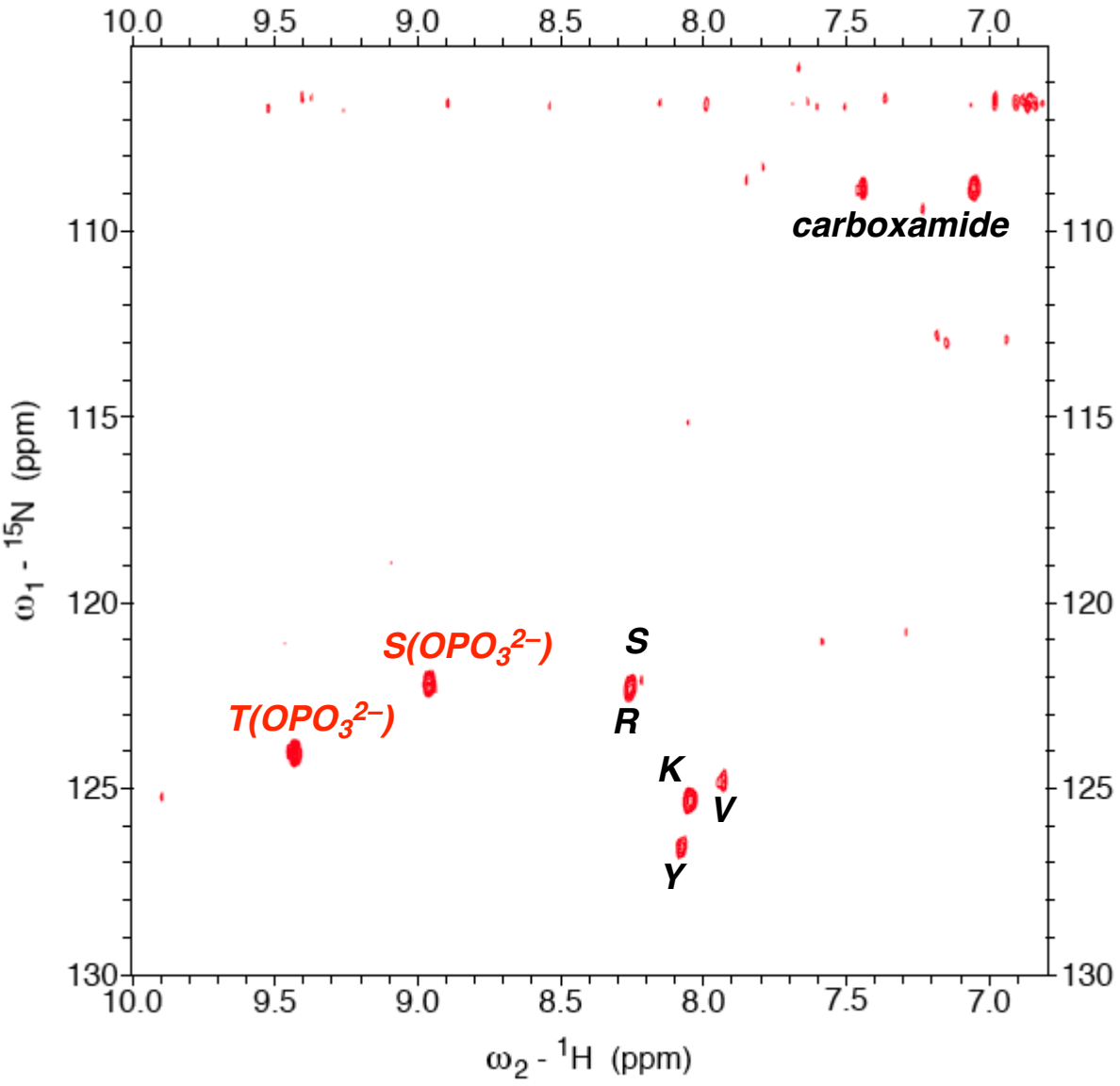

Figure S49. ^{1}H-^{15}N HSQC spectrum of peptide $tau_{229–238}(OPO_3^{2–})$ at pH 8.0 at 298 K in 5 mM phosphate buffer containing 25 mM NaCl. The missing resonance contour for $S(OPO_3^{2–})$ could not be determined because of rapid amide exchange at pH 8.0.

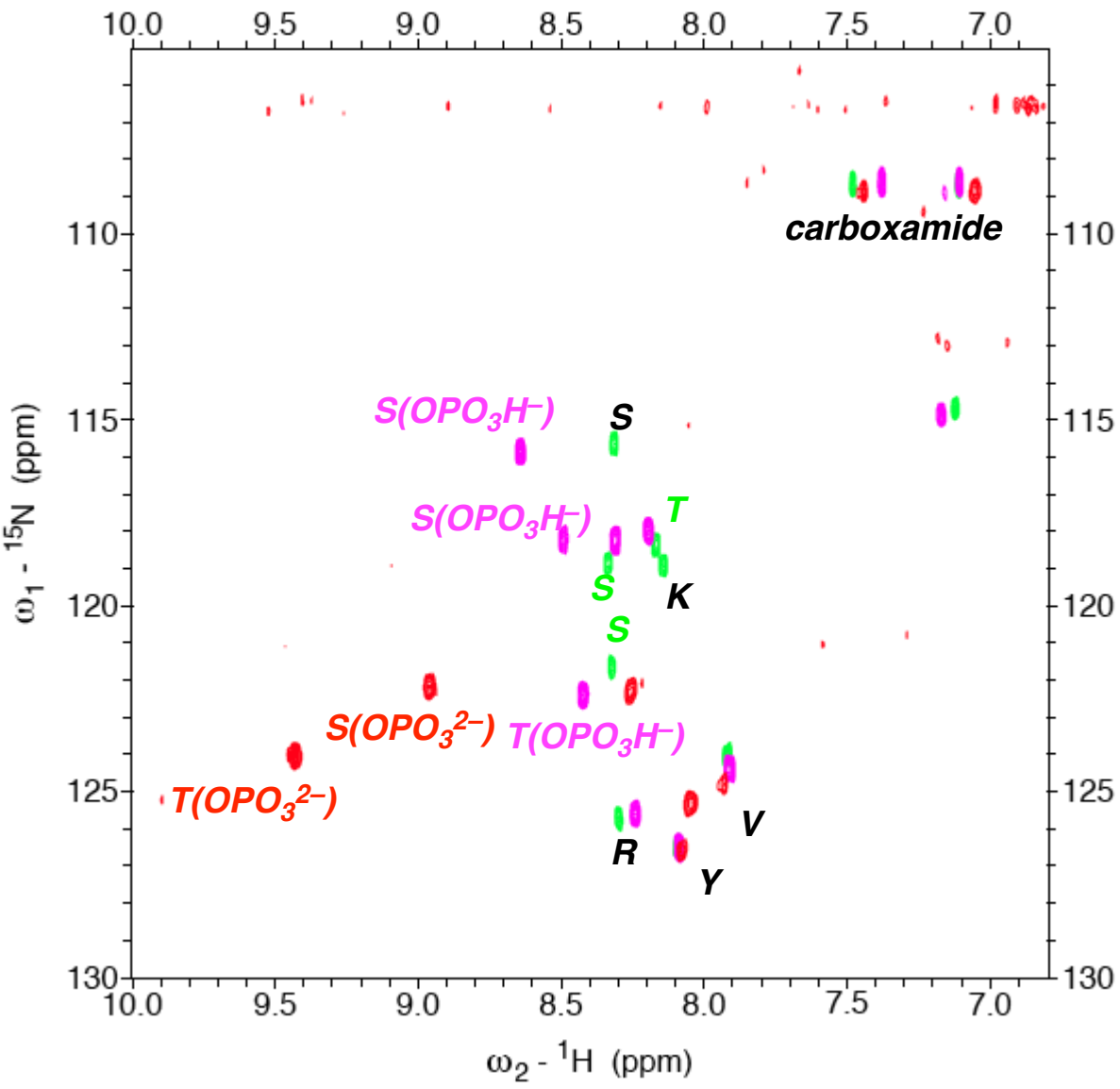

Figure S50. ^{1}H-^{15}N HSQC spectra of peptides $tau_{229–238}$ at pH 4.0 (green), $tau_{229–238}(OPO_3^{2–})$ (red) (pH 8.0), and $tau_{229–238}(OPO_3H^{–})$ (magenta) (pH 4.0) at 298 K. Data were collected with 2–3 mM peptide in 5 mM phosphate buffer (pH 4.0 or 8) with 25 mM NaCl.

peptide	Thr_N, ppm	Ser_N, ppm	others	pH, temp
Ac-YVRTPPKSPSS-NH_2	118.4	115.6,118.9, 121.7	118.9 (Lys), 124.1 (Val), 125.7 (Arg), 126.5 (Tyr), 107.1 (carboxamide)	4.0, 298 K
Ac-YVRT(OPO_3H^-)PPKS(OPO_3H^-)PS(OPO_3H^-)S-NH_2	122.4	115.9 (pS), 118.2 (pS), 118.3 (S)	118.0 (Lys), 124.4 (Val), 125.6 (Arg), 126.5 (Tyr), 107.1 (carboxamide)	4.0, 298 K
Ac-YVRT(OPO_3^{2-})PPKS(OPO_3^{2-})PS(OPO_3^{2-})S-NH_2	124.0	122.2 (pS)	122.3 (Lys), 124.8 (Val), 125.3 (Arg), 126.6 (Tyr), 108.9 (carboxamide)	8.0, 298 K

Table S16. Summary of ^{1}H-^{15}N HSQC NMR data for peptides derived from $tau_{229–238}$. Data were collected with 2–3 mM peptide in 5 mM phosphate buffer (pH 4.0 or 8) with 25 mM NaCl. pS indicates a phosphorylated serine residue.

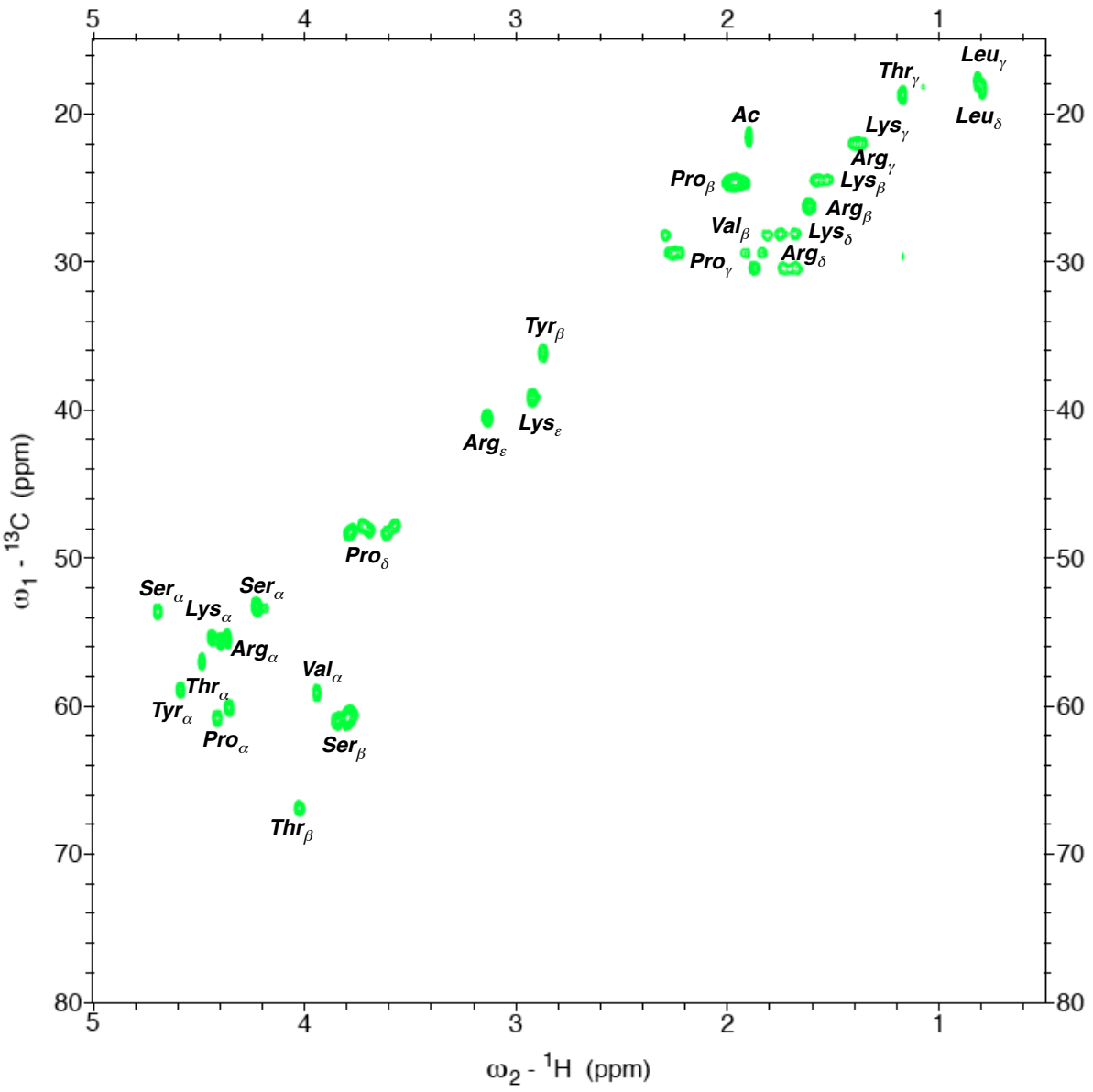

Figure S51. ^{1}H-^{13}C HSQC spectrum of peptide tau$_{229–238}$ at pH 4.0 at 298 K in 5 mM phosphate buffer with 25 mM NaCl in 100% D_2O at 298 K.

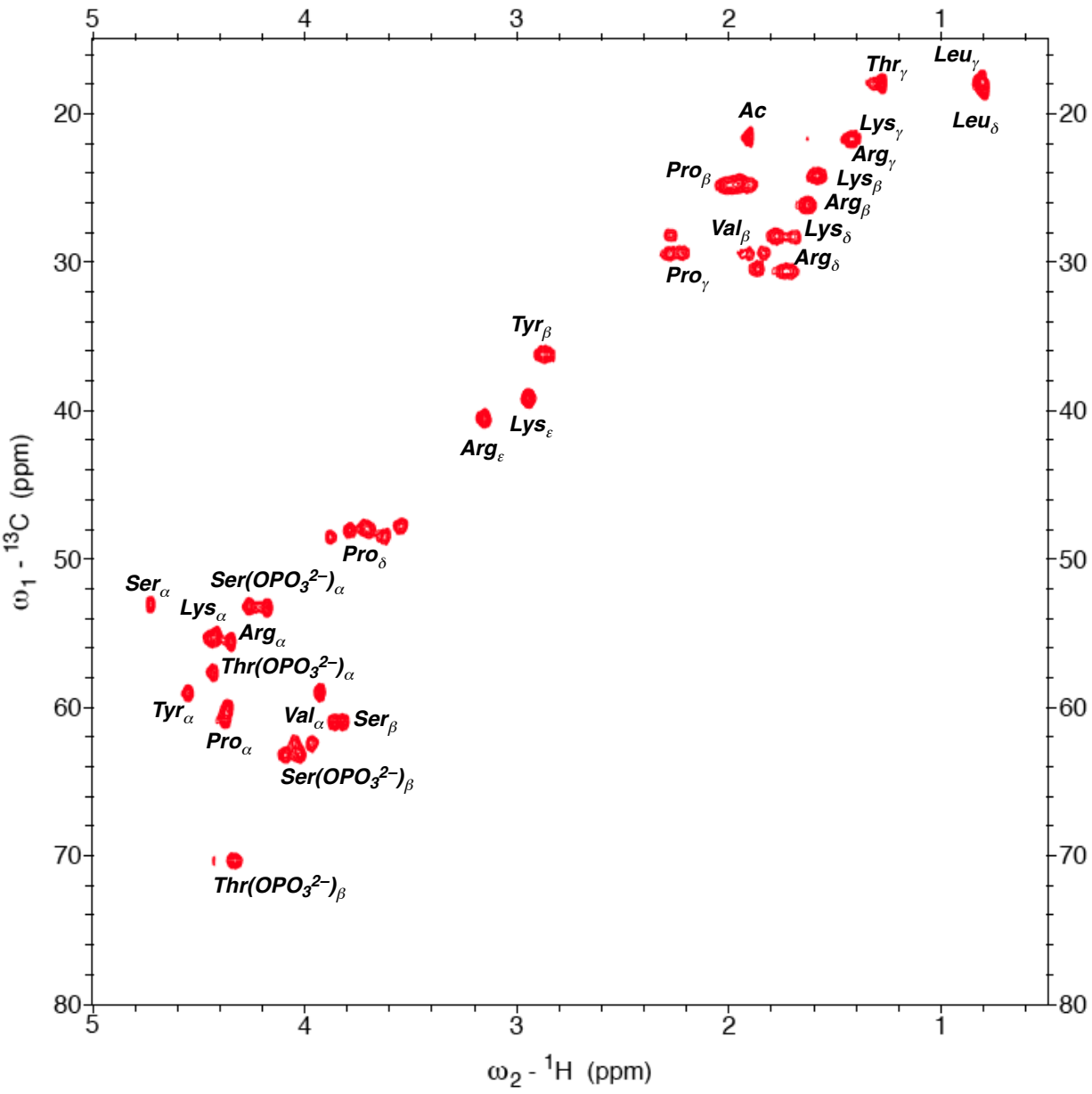

Figure S52. ^{1}H-^{13}C HSQC spectrum of peptide tau$_{229–238}$(OPO_3^{2-}) at pH 8.0 at 298 K in 5 mM phosphate buffer with 25 mM NaCl in 100% D_2O at 298 K.

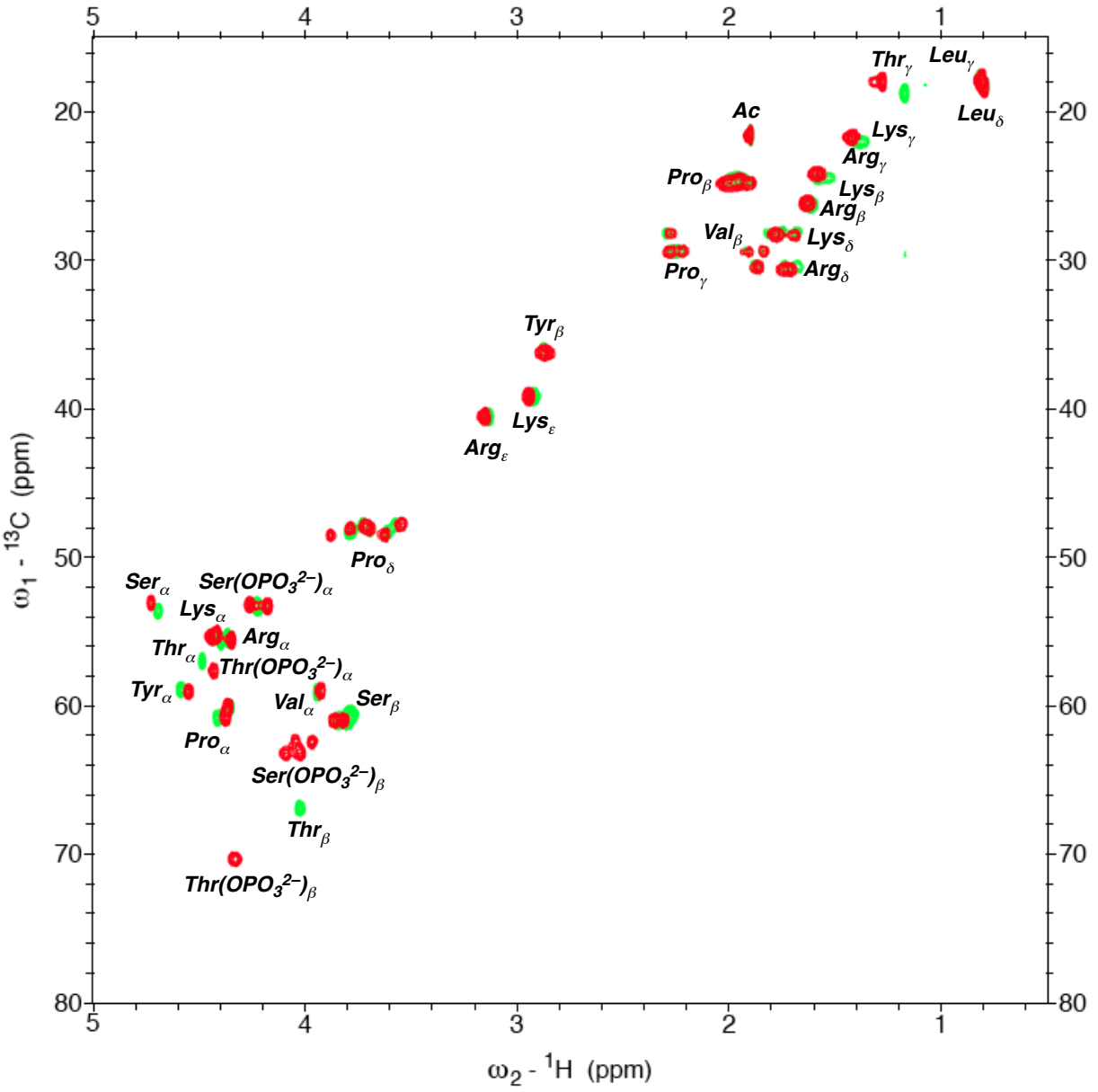

Figure S53. ^{1}H-^{13}C HSQC spectra of peptides tau$_{229–238}$ at pH 4.0 (green) and tau$_{229–238}$(OPO$_3^{2–}$) (red) (pH 8.0) at 298 K. Data were collected with 2 mM peptide in 5 mM phosphate buffer containing 25 mM NaCl.

Ac-YVRTPPKSPSS-NH_2		Ac-YVRpTPPKpSPpSS-NH_2	
residue	^{13}C δ, ppm	residue	^{13}C δ, ppm
Lys, α	55.4	Lys, α	55.6
Thr, α	57.0	pThr, α	57.7
Ser, α	53.6, 53.6	pSer, α	53.1, [a]n.d.
Ser, α	53.3	Ser, α	55.3
Val, α	59.1	Val, α	59.0
Pro, α	60.1, 60.8, 60.8	Pro, α	60.1, 60.8, 60.8
Tyr, α	59.0	Tyr, α	59.0
Arg, α	55.4	Arg, α	53.2
Ser, β	60.7	pSer, β	62.5, 63.2
Ser, β	61.0, 61.0	Ser, β	61.0
Thr, β	66.9	pThr, β	70.4
Val, β	29.4	Val, β	29.4
Tyr, β	36.2	Tyr, β	36.2
Lys, β	24.5	Lys, β	24.6
Arg, β	24.5	Arg, β	24.6
Pro, β	24.6, 24.6, 24.6	Pro, β	24.6, 24.6, 24.6
Pro, δ	47.8, 48.2, 48.2	Pro, δ	48.1, 48.1, 48.5
Lys, δ	26.2	Lys, δ	26.2
Arg, δ	30.4	Arg, δ	30.5
Lys, ε	39.2	Lys, ε	39.2
Arg, ε	40.6	Arg, ε	40.5
Pro, γ	28.1, 29.4, 29.4	Pro, γ	28.2, 29.5, 29.5
Lys, γ	22.0	Lys, γ	21.6
Arg, γ	24.5	Arg, γ	24.1
Val, γ	17.8, 18.3	Val, γ	17.7, 18.3
Thr, γ	18.8	pThr, γ	18.0
Ac	21.5	Ac	21.6

Table S17. Summary of ^{1}H-^{13}C NMR data for peptides derived from $tau_{229–238}$. Data were collected with 2 mM peptide in 5 mM phosphate buffer containing 25 mM NaCl. pSer or pThr indicates a phosphorylated serine or threonine residue. [a] n.d. = not determined due to spectral overlap with residual water peak.

Analysis of peptides derived from $tau_{211–238}$
Ac-RTPSLPTPPTREPKKVAVVRTPPKSPSS-NH_2

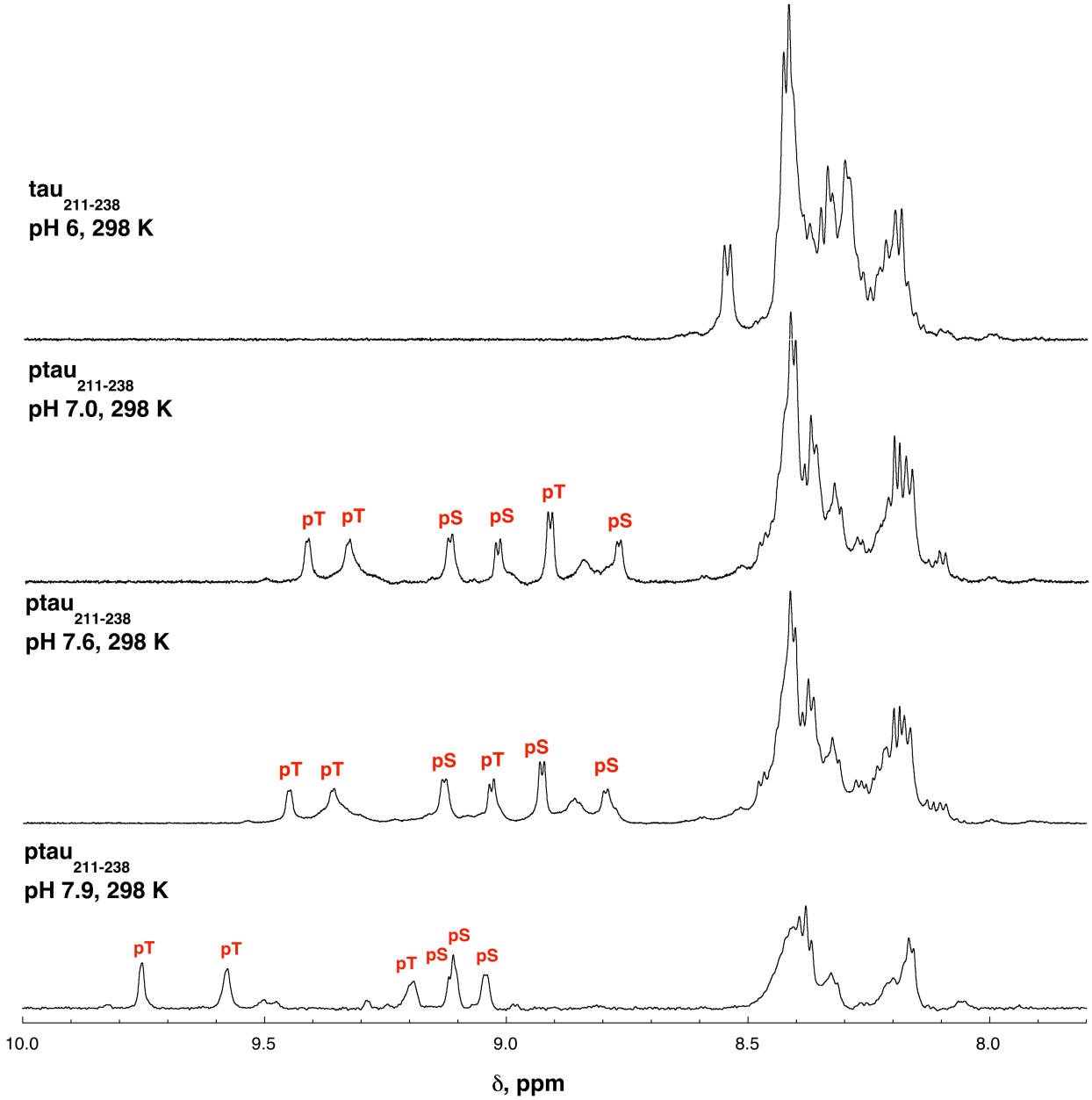

Figure S54. ^{1}H NMR spectra (amide region) of peptides derived from $tau_{211–238}$. Minor peaks in the NMR spectra are due to the presence of cis amide bonds. Peptides were dissolved in 5 mM phosphate buffer (pH 6.0, 7.0, 7.6, or 7.9) and were internally referenced with TSP. Solutions contained 25 mM NaCl, 100 μM TSP, and 90% H_2O/10% D_2O. pS or pT indicates a phosphorylated serine or threonine residue.

Full ^{1}H NMR spectra of peptides derived from tau$_{211–238}$ at 298 K

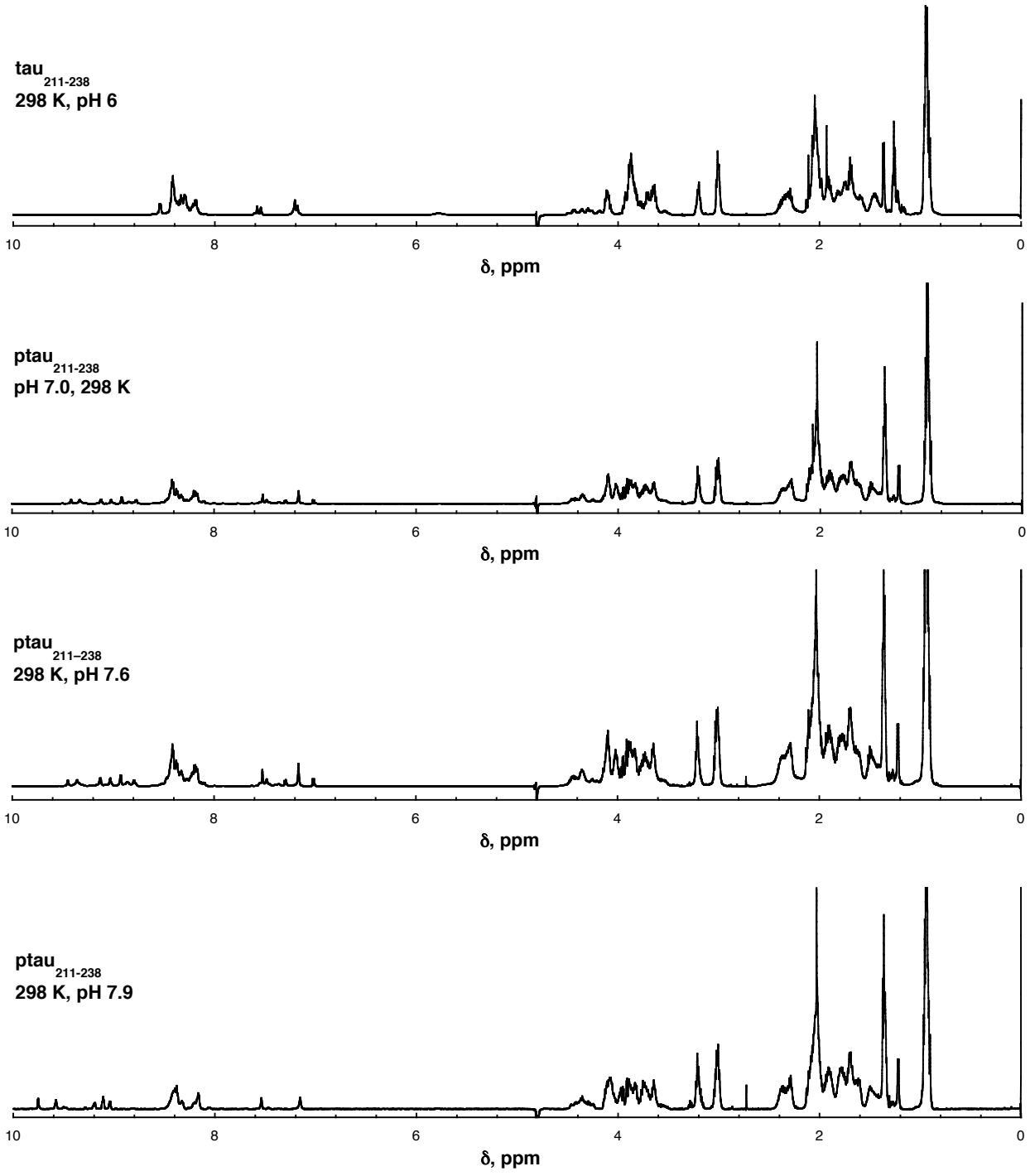

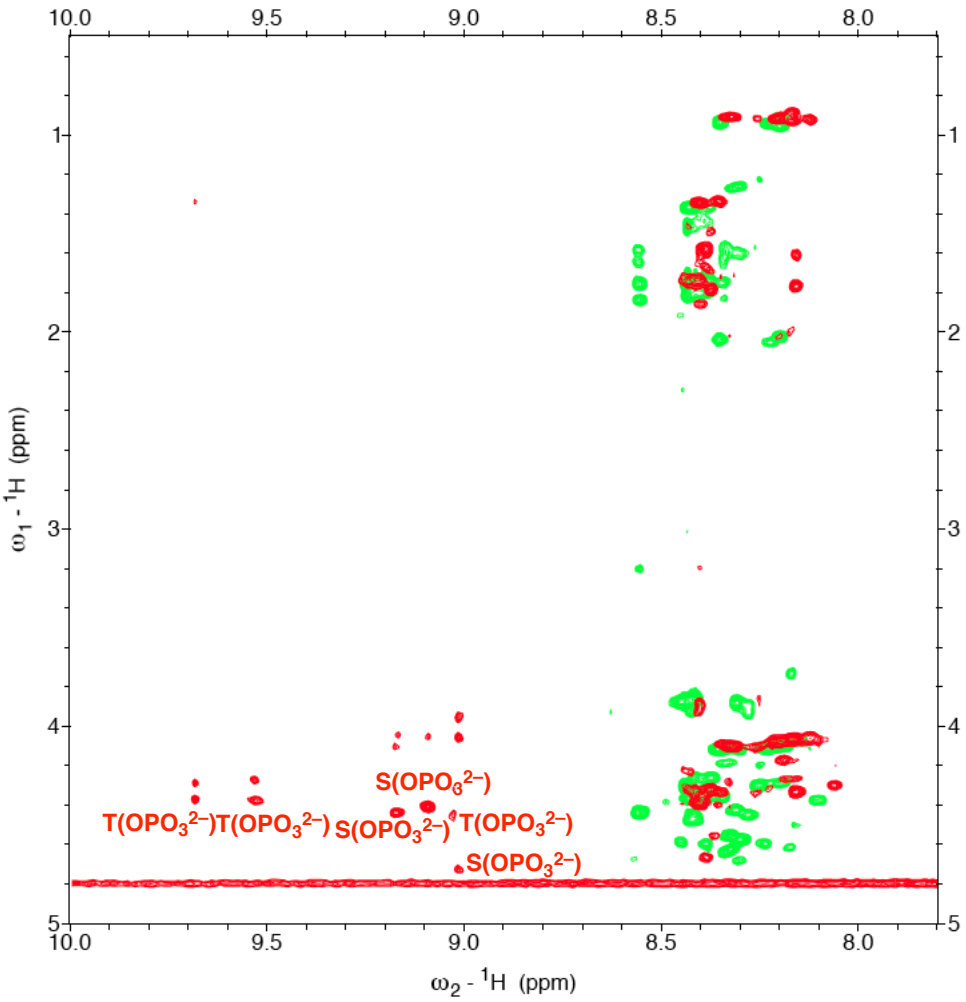

Figure S55. TOCSY spectra (amide region) of peptides $tau_{211–238}$ (green) at pH 6.0 and $tau_{211–238}(OPO_3^{2–})$ (red) at pH 7.9 at 298 K. Minor peaks in the spectrum are due to the presence of cis amide bonds.

peptide	δ, H^N	$^3J_{\alpha N}$	δ, Hα	δ, Hβ
$tau_{211-238}$ (pH 6)				
E	8.57	n.d.	4.66	1.65, 1.55
K	8.56	n.d.	4.30	1.80, 1.68
K	8.56	n.d.	4.30	1.80, 1.68
K	8.56	n.d.	4.30	1.80, 1.68
S	8.45	n.d.	4.58	3.88, 3.88
R	8.44	n.d.	4.42	1.82, 1.73
R	8.44	n.d.	4.42	1.82, 1.73
S	8.42	n.d.	4.47	3.87, 3.87
T	8.40	n.d.	4.58	4.34
R	8.39	n.d.	4.42	1.82, 1.73
V	8.35	n.d.	4.12	2.04
T	8.33	n.d.	4.56	4.42
S	8.31	n.d.	4.43	3.88, 3.88
T	8.30	n.d.	4.56	4.42
A	8.30	n.d.	4.52	1.25
S	8.28	n.d.	4.45	3.90, 3.93
V	8.22	n.d.	4.11	2.05
V	8.20	n.d.	4.09	2.02
T	8.20	n.d.	4.25	4.14
L	8.14	n.d.	4.38	2.01
$tau_{211-238}$ (OPO_3^{2-}) (pH 7.9)				
pT	9.76	3.1[b]	4.38	4.31
pT	9.59	3.7[b]	4.39	4.29
pS	9.22	5.3	4.47	4.08, 4.13
pT	9.21	4.7[b]	4.47	4.35
pS	9.15	5.5	4.43	3.99, 4.10
pS	9.07	5.3	4.75	3.98, 4.08
K	8.43	n.d.	4.32	1.79, 1.72
K	8.43	n.d.	4.32	1.79, 1.72
K	8.43	n.d.	4.32	1.79, 1.72
R	8.36	n.d.	4.41	1.89, 1.77
R	8.36	n.d.	4.41	1.89, 1.77
R	8.36	n.d.	4.41	1.89, 1.77
T	8.26	n.d.	4.57	4.35
S	8.25	n.d.	4.35	3.94, 3.88
V	8.19	n.d.	4.07	2.05
V	8.19	n.d.	4.07	2.03
L	8.18	n.d.	4.36	1.66
V	8.14	n.d.	4.06	2.04
A	n.d.	n.d.	4.13	0.94
E	n.d.	n.d.	n.d.	n.d.

Table S18. Summary of ^{1}H NMR data for peptides derived from $tau_{211-238}$. Data were collected with 200-500 μM peptide in 5 mM phosphate buffer containing 25 mM NaCl. pS or pT indicates a phosphorylated serine or threonine residue. [a] n.d. indicates not determined due to spectral overlap or peak broadening. [b] Data were obtained at pH 7.0 at 298 K.

Analysis of peptides derived from $tau_{234–251}$

Ac-KSPSSAKSRLQTAPVPMP-NH_2, Ac-KpSPSSAKSRLQTAPVPMP-NH_2, and Ac-KpSPpSSAKSRLQTAPVPMP-NH_2,

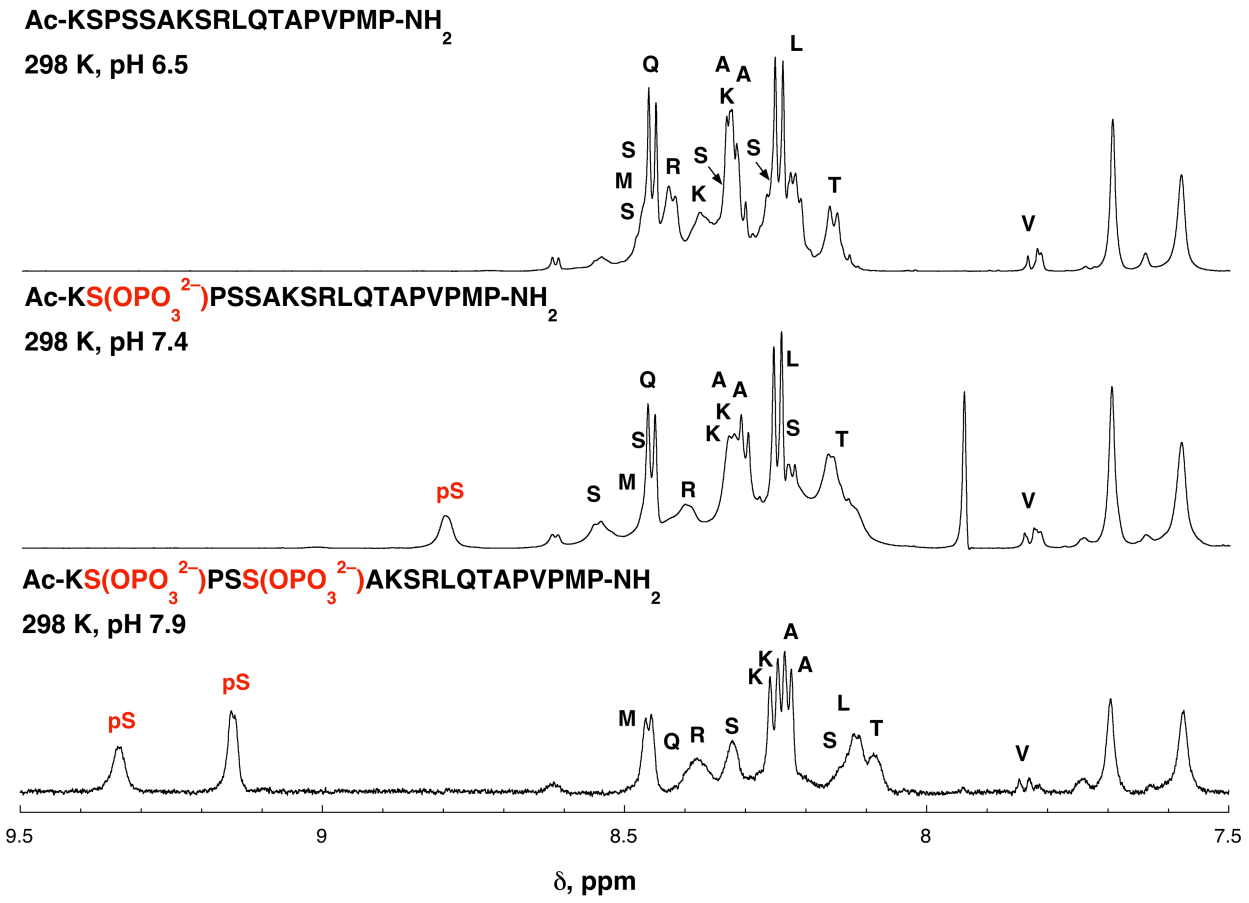

Figure S56. ^{1}H NMR spectra (amide region) of peptides derived from $tau_{234–251}$. Minor peaks in the NMR spectra are due to the presence of cis amide bonds. Peptides were dissolved in 5 mM phosphate buffer (pH 4.0, 7.2, or 7.9) and were internally referenced with TSP. Solutions contained 25 mM NaCl, 100 μM TSP, and 90% H_2O/10% D_2O. pS indicates a phosphorylated serine residue.

Full ^{1}H NMR spectra of peptides derived from tau$_{234–251}$ at pH 6.5, 7.4, or 7.9

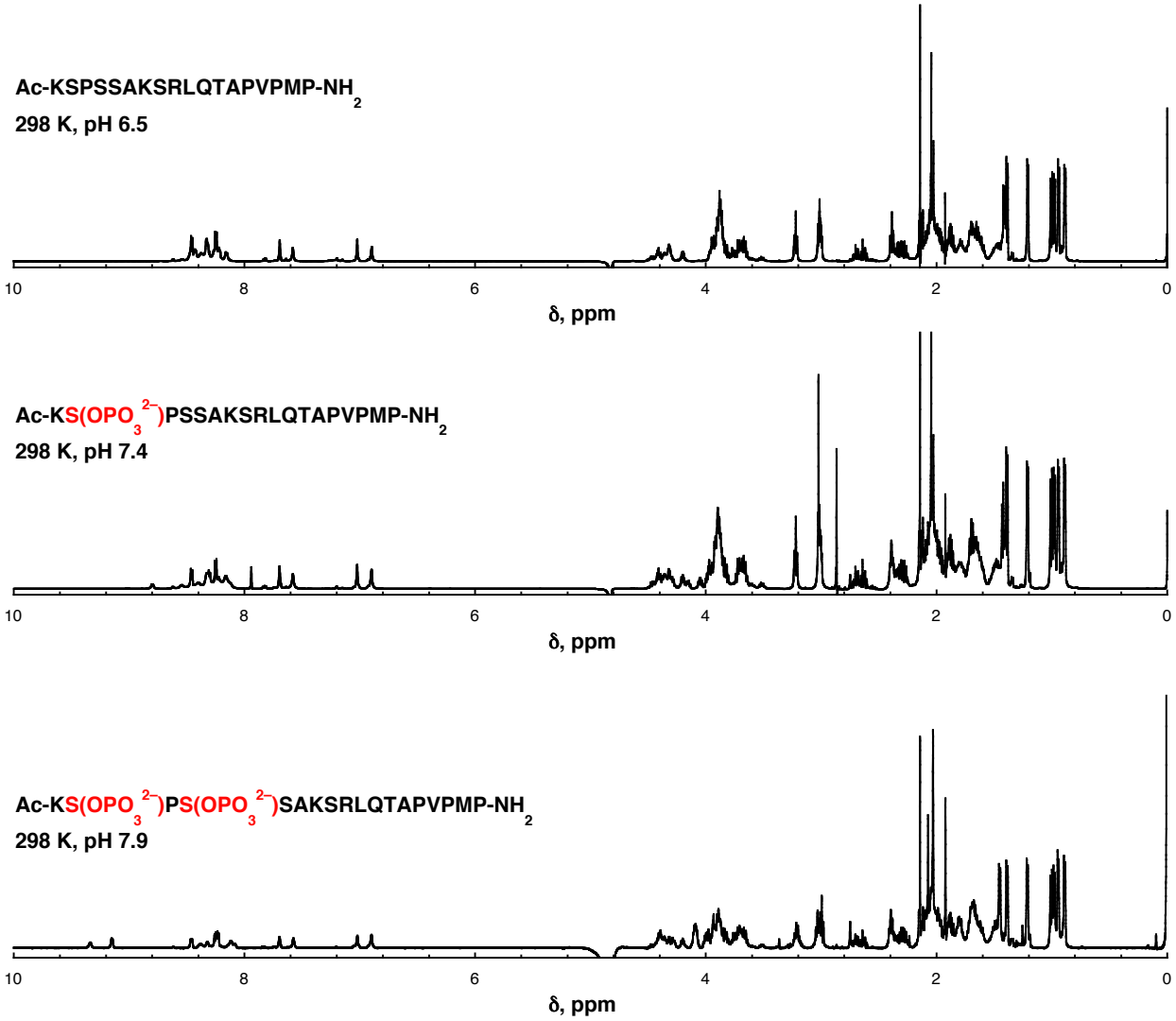

peptide	δ, H^N	$^3J\alpha N$	δ, Hα	δ, Hβ
$tau_{234–251}$ (pH 6)				
K	8.33	n.d.	4.32	1.82, 1.72
S	8.48	n.d.	4.38	3.89, 3.89
S	8.52	n.d.	4.47	3.86, 3.94
S	8.26	n.d.	4.41	3.89, 3.89
A	8.23	n.d.	4.35	1.63
K	8.27	n.d.	4.31	1.89, 1.78
S	8.46	n.d.	4.47	3.94, 3.89
R	8.39	n.d.	4.35	1.90, 1.79
L	8.26	n.d.	4.41	2.10
Q	8.43	n.d.	4.42	2.13, 2.02
T	8.17	7.7	4.32	4.20
A	8.23	n.d.	4.35	1.63
V	7.84	n.d.	4.25	1.98
M	8.46	n.d.	4.47	2.11, 1.97
$tau_{234–251}$(pS235) (pH 7.4)				
K	8.30	n.d.	n.d.	1.88, 1.81
pS	8.80	n.d.	n.d.	4.16, 4.05
S	8.55	n.d.	4.38	3.99, 3.91
S	n.d	n.d.	n.d	n.d
A	8.23	n.d.	4.34	1.64
K	8.22	n.d.	4.40	1.88, 1.81
S	8.19	n.d.	4.41	3.91, 3.91
R	8.31	n.d.	4.34	1.90, 1.80
L	8.25	n.d.	4.41	2.08
Q	8.41	n.d.	4.41	2.14, 2.01
T	8.16	n.d.	4.33	4.19
A	8.23	n.d.	4.34	1.64
V	7.84	n.d.	4.24	1.97
M	8.47	n.d.	4.37	2.10, 1.97
$tau_{234–251}$(pS235/pS237) (pH 7.9)				
K	8.10	n.d.	4.30	1.90, 1.83
pS	9.34	n.d.	4.40	4.10, 4.10
S	8.39	n.d.	4.41	3.94, 3.94
pS	9.15	n.d.	4.74	4.10, 4.00
A	8.23	n.d.	4.39	1.47
K	8.24	n.d.	4.40	1.80, 1.70
S	8.19	n.d.	4.30	3.95, 3.89
R	8.24	n.d.	4.36	1.91, 1.79
L	8.26	n.d.	4.40	2.08
Q	8.37	n.d.	4.44	2.14, 2.02
T	8.14	n.d.	4.33	4.21
A	8.23	n.d.	4.39	1.47
V	7.84	n.d.	4.24	0.92
M	8.46	n.d.	4.38	2.11, 1.99

Table S19. Summary of ^{1}H NMR data for peptides derived from $tau_{234–251}$. Data were collected with 2 mM peptide in 5 mM phosphate buffer containing 25 mM NaCl. pS indicates a phosphorylated serine residue. [a] n.d. indicates not determined due to spectral overlap.

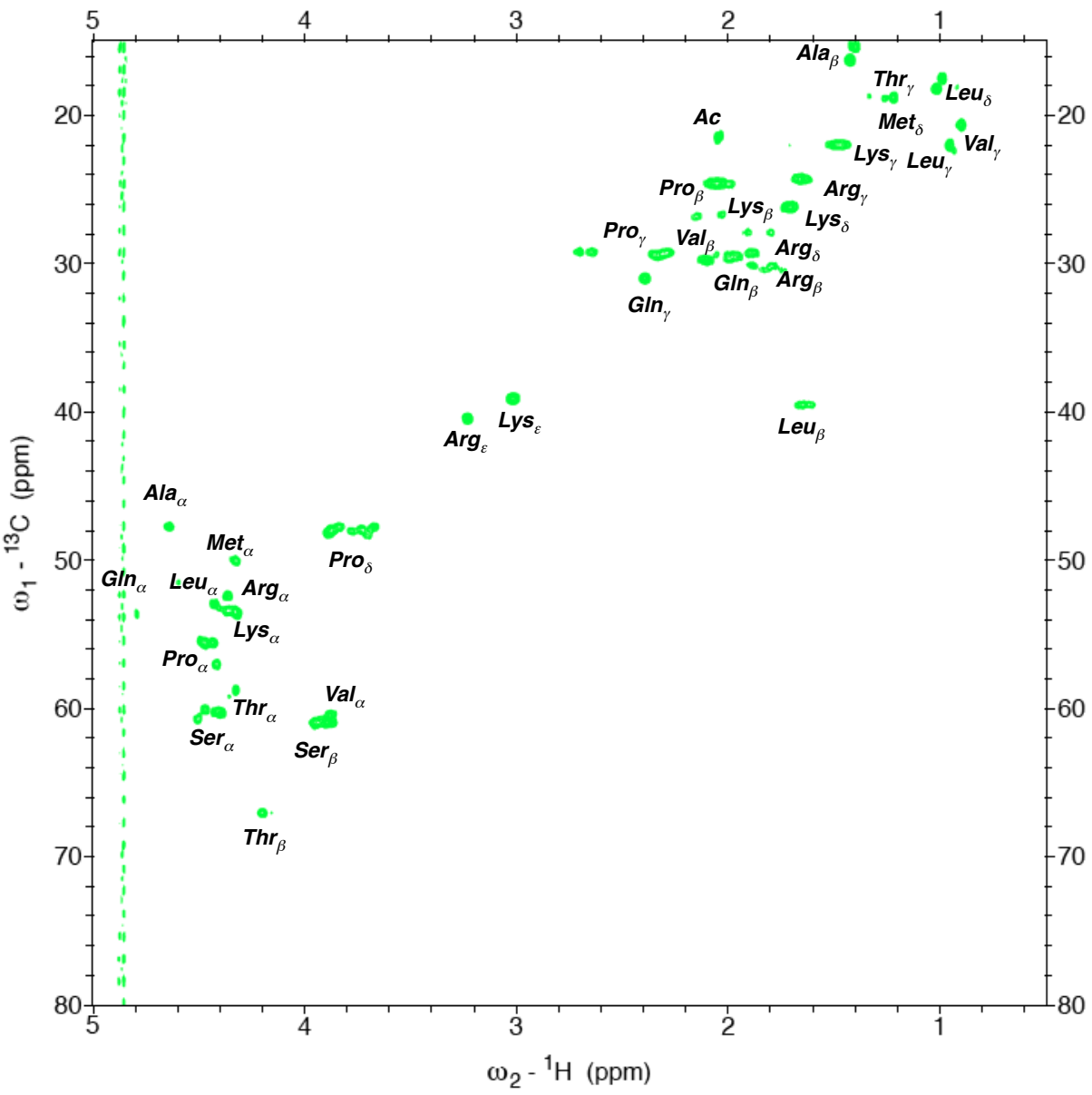

Figure S57. ^{1}H-^{13}C HSQC spectrum of peptide $tau_{234–251}$ at pH 4.0 at 298 K in 5 mM phosphate buffer with 25 mM NaCl in 100% D_2O at 298 K.

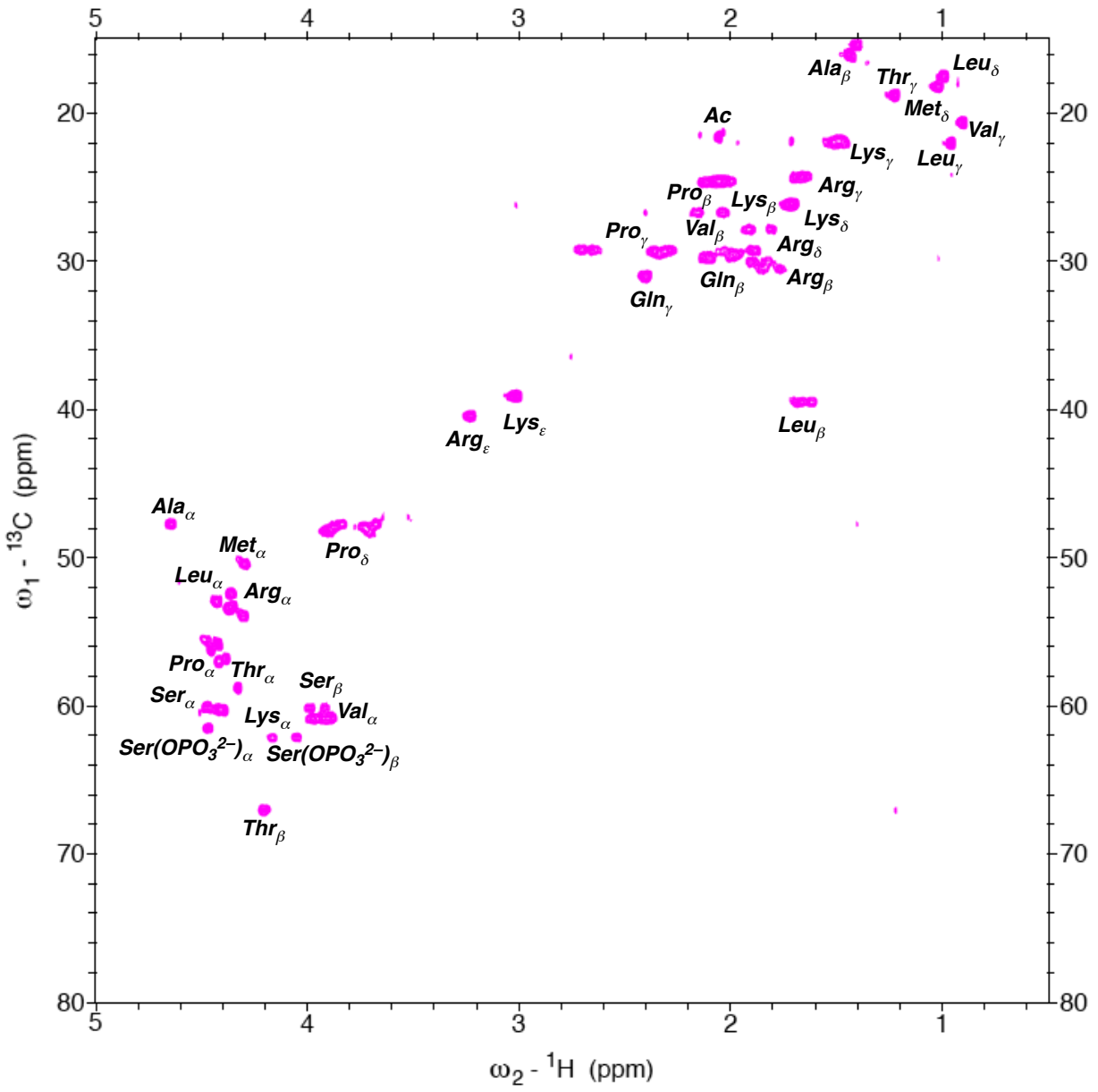

Figure S58. ^{1}H-^{13}C HSQC spectrum of peptide tau$_{234–251}$(pS235) at pH 8.0 at 298 K in 5 mM phosphate buffer with 25 mM NaCl in 100% D_2O at 298 K. pS indicates a phosphorylated serine residue.

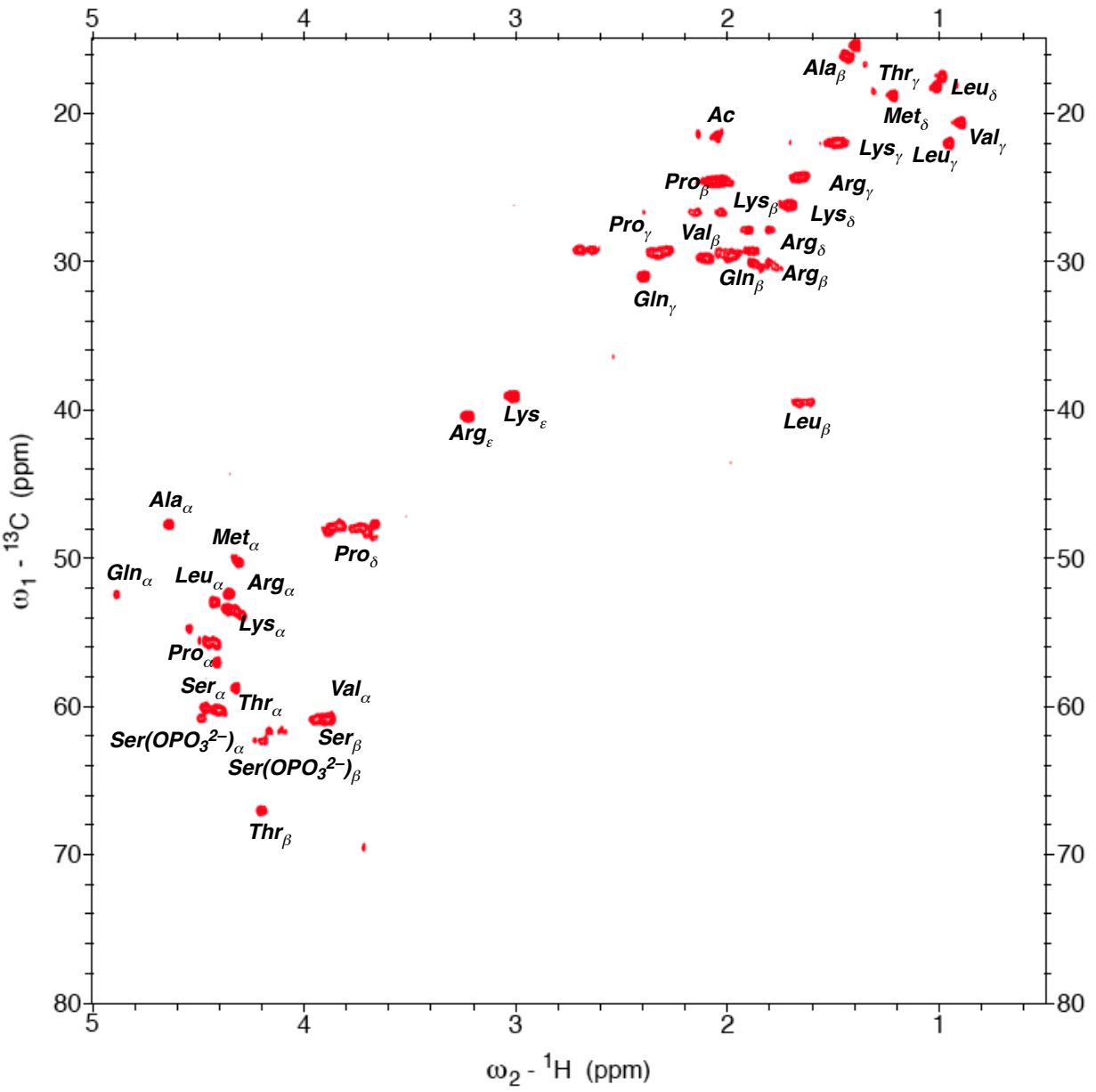

Figure S59. ^{1}H-^{13}C HSQC spectrum of peptide tau$_{234–251}$(pS235/pS237) at pH 8.0 at 298 K in 5 mM phosphate buffer with 25 mM NaCl in 100% D_2O at 298 K. pS indicates a phosphorylated serine residue.

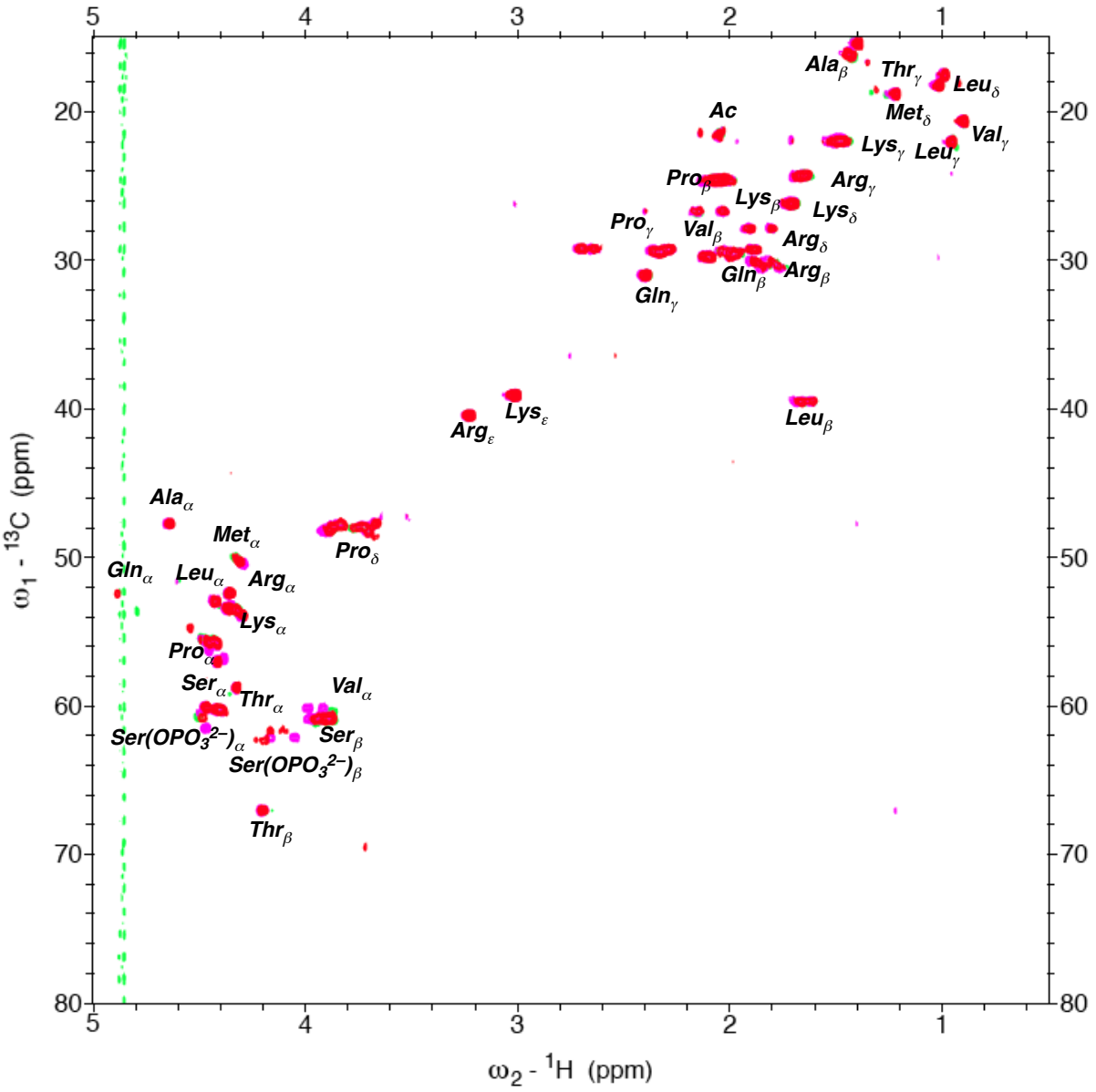

Figure S60. ^{1}H-^{13}C HSQC spectra of peptides tau$_{229–238}$ at pH 4.0 (green), tau$_{234–251}$(pS235) at pH 8.0 (magenta), and tau$_{234–251}$(pS235/pS237) (red) at pH 8.0. Data were collected at 298 K with 2 mM peptide in 5 mM phosphate buffer containing 25 mM NaCl.

KSPSSAKSRLQTAPVPMP residue	^{13}C δ, ppm	KpSPSSAKSRLQTAPVPMP residue	^{13}C δ, ppm	KpSPpSSAKSRLQTAPVPMP	^{13}C δ, ppm
Lys, α	53.5, 53.4	Lys, α	53.8, 53.4	Lys, α	53.7, 53.4
Ser, α	60.7, 60.3, 60.1	Ser, α	60.4, 60.2, 60.1	Ser, α	60.8, 60.1
Ser, α	60.1	pSer, α	60.5	pSer, α	60.3, 60.3
Pro, α	57.0, 55.6, 55.6, 55.6	Pro, α	56.9, 56.1, 55.8, 55.5	Pro, α	57.0, 55.7, 55.7, 55.7
Ala, α	47.7	Ala, α	47.7	Ala, α	47.7
Arg, α	52.4	Arg, α	52.4	Arg, α	52.4
Leu, α	53.0	Leu, α	52.9	Leu, α	53.0
Gln, α	53.6	Gln, α	n.d.	Gln, α	52.4
Thr, α	58.8	Thr, α	58.9	Thr, α	58.8
Val, α	60.2	Val, α	60.2	Val, α	60.3
Met, α	50.0	Met, α	50.4	Met, α	50.3
Lys, β	26.8	Lys, β	26.8	Lys, β	26.8
Ser, β	60.9, 60.9, 60.9	Ser, β	60.9, 60.9, 60.1	Ser, β	60.9, 60.9
Ser, β	60.9	pSer, β	62.2	pSer, β	62.3, 61.7
Pro, β	24.6, 24.6, 24.6, 24.6	Pro, β	24.6, 24.6, 24.6, 24.6	Pro, β	24.6, 24.6, 24.6, 24.6
Ala, β	16.3, 15.4	Ala, β	16.3, 15.4	Ala, β	16.3, 15.4
Arg, β	29.6	Arg, β	29.6	Arg, β	29.6
Leu, β	39.5	Leu, β	39.5	Leu, β	39.5
Gln, β	29.8	Gln, β	29.8	Gln, β	29.8
Thr, β	67.0	Thr, β	67.0	Thr, β	67.0
Val, β	29.4	Val, β	29.4	Val, β	29.4
Met, β	29.3	Met, β	29.3	Met, β	29.3
Lys, γ	22.0	Lys, γ	22.0	Lys, γ	22.0
Pro, γ	29.2	Pro, γ	29.2	Pro, γ	29.2
Arg, γ	24.3	Arg, γ	24.3	Arg, γ	24.3
Leu, γ	22.0	Leu, γ	22.0	Leu, γ	22.0
Gln, γ	31.0	Gln, γ	31.0	Gln, γ	31.0
Thr, γ	18.8	Thr, γ	18.8	Thr, γ	18.8
Val, γ	20.6	Val, γ	20.6	Val, γ	20.6

Pro, δ	47.7, 47.7, 48.8, 48.8	Pro, δ	47.7, 47.7, 48.8, 48.8	Pro, δ	47.7, 47.7, 48.8, 48.8
Leu, δ	17.5	Leu, δ	17.5	Leu, δ	17.5
Met, δ	18.2	Met, δ	18.2	Met, δ	18.2
Arg, δ	29.3	Arg, δ	29.3	Arg, δ	29.3
Arg, ε	40.5	Arg, ε	40.5	Arg, ε	40.5
Lys, ε	39.1	Lys, ε	39.1	Lys, ε	39.1
NHAc	14.2	NHAc	14.2	NHAc	14.2

Table S20. Summary of ^{1}H-^{13}C NMR data for peptides derived from $tau_{234–251}$. Data were collected with 2 mM peptide in 5 mM phosphate buffer containing 25 mM NaCl. pSer indicates a phosphorylated serine residue. [a] n.d. indicates not determined due to spectral overlap with residual water peak.

^{1}H NMR spectra of model peptides Ac-K*Tx*PP-NH$_2$

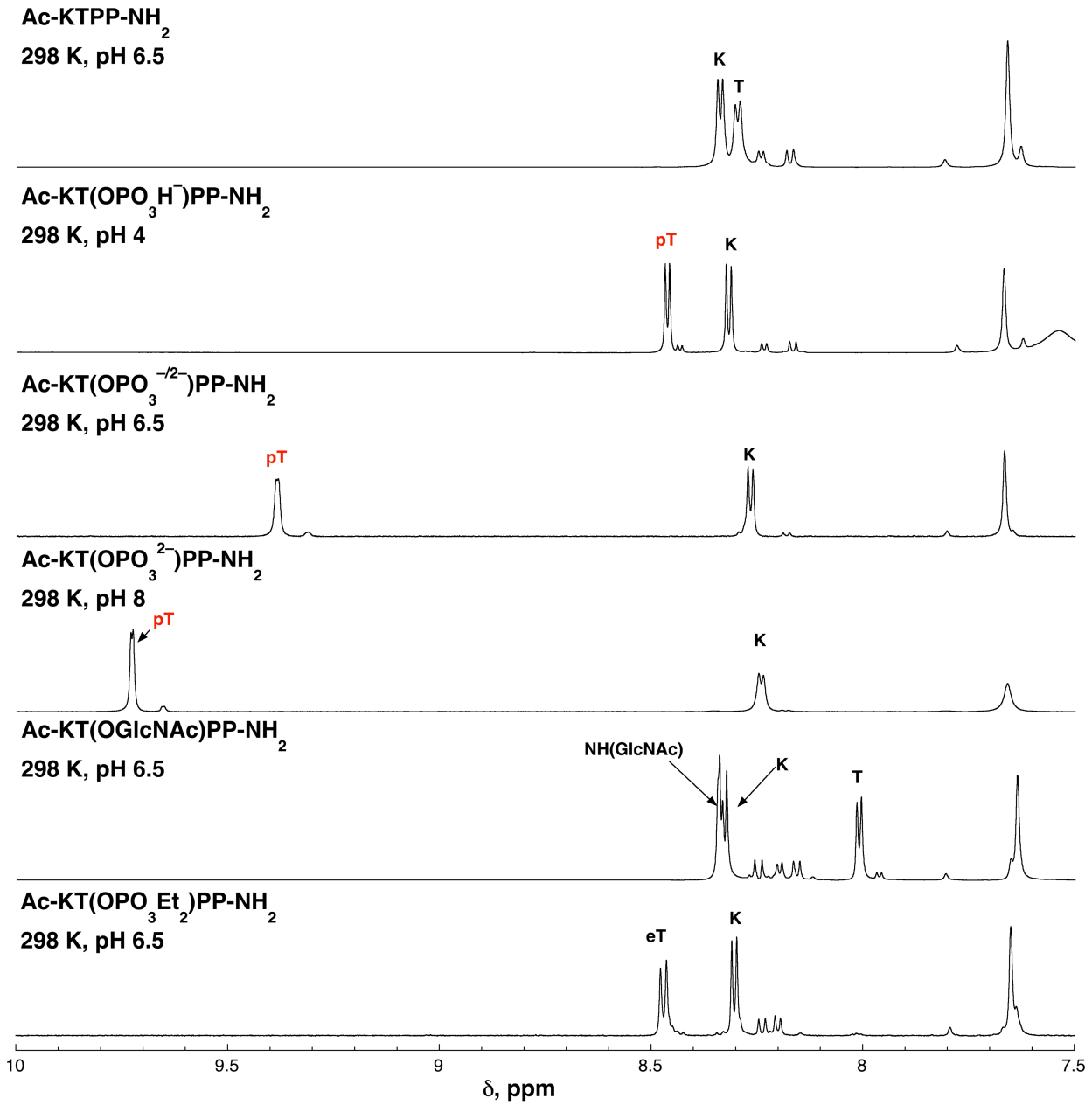

Figure S61. ^{1}H NMR spectra (amide region) of Ac-K*Tx*PP-NH$_2$ peptides at 298 K. Minor peaks in the NMR spectra are due to the presence of cis amide bonds. Peptides were dissolved in 5 mM phosphate buffer (pH 4.0, 6.5, or 8.0) and were internally referenced with TSP. Solutions contained 25 mM NaCl, 100 μM TSP, and 90% H_2O/10% D_2O.

pH-dependent NMR spectra of peptide Ac-KpTPP-NH_2

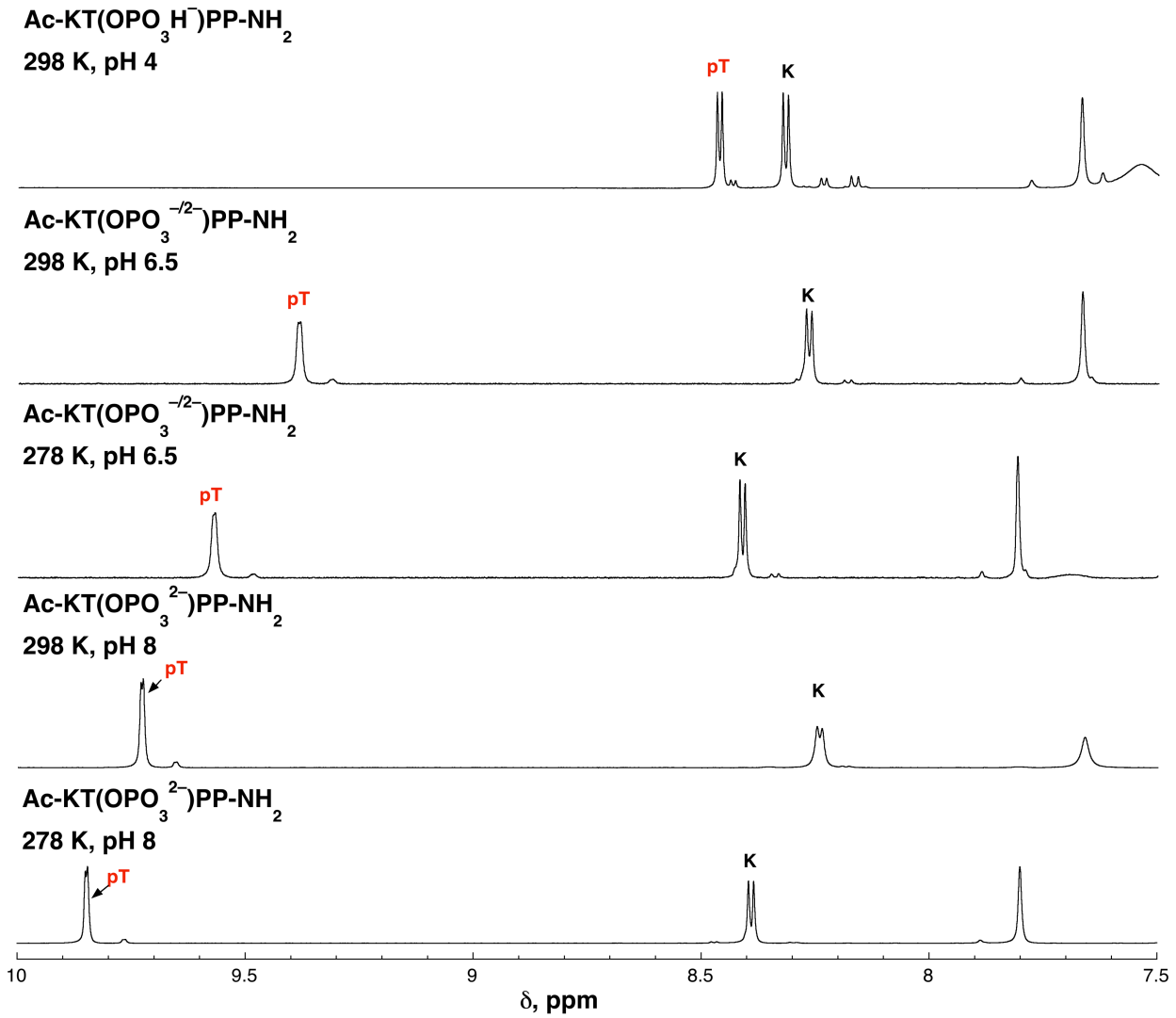

Figure S62. ^{1}H NMR spectra (amide region) of Ac-KpTPP-NH_2 peptides. Minor peaks in the NMR spectra are due to the presence of cis amide bonds. Peptides were dissolved in 5 mM phosphate buffer (pH 4.0, 6.5, or 8.0) and were internally referenced with TSP. Solutions contained 25 mM NaCl, 100 μM TSP, and 90% H_2O/10% D_2O.

Full ^{1}H NMR spectra of Ac-K*Tx*PP-NH$_2$ peptides

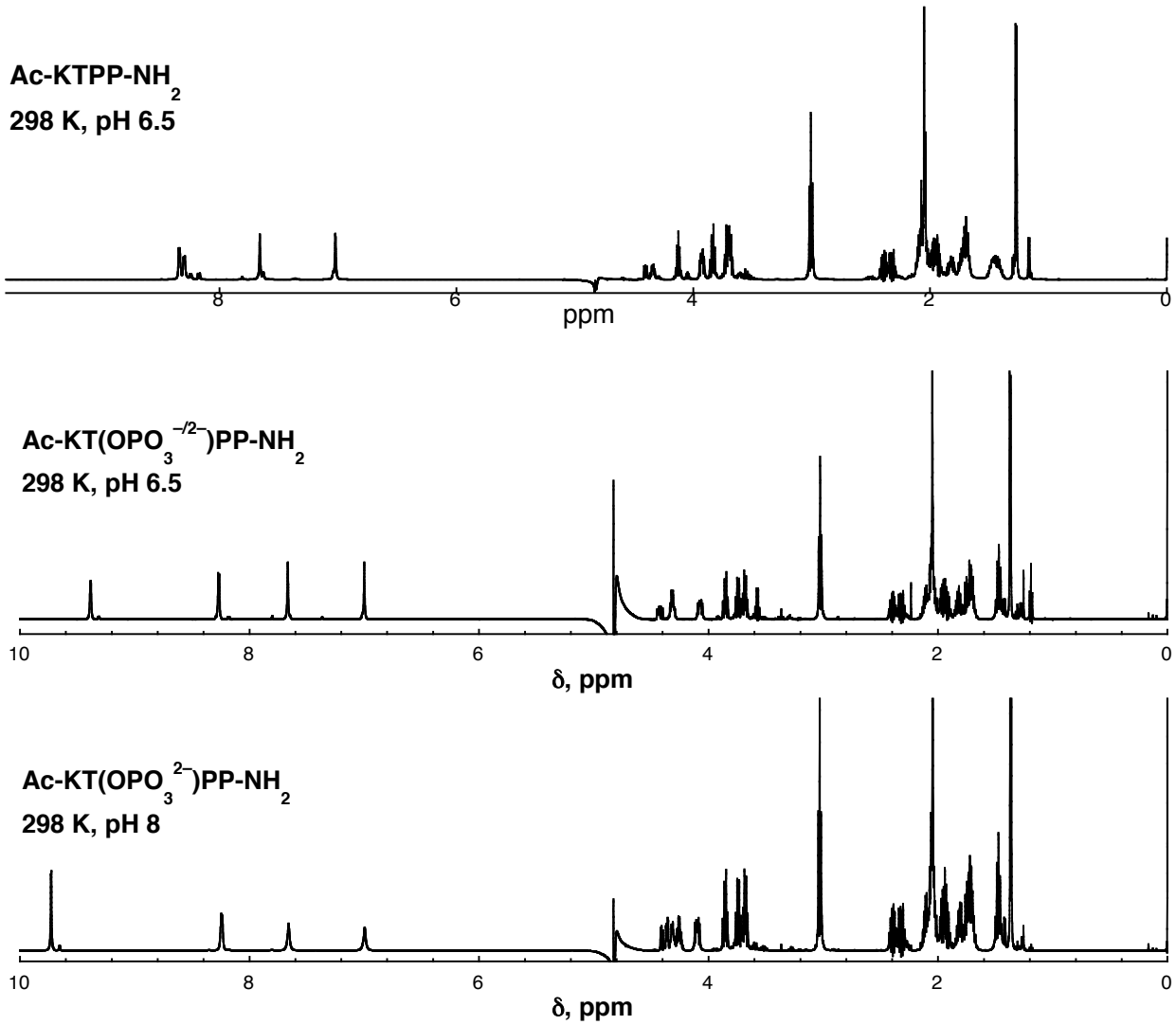

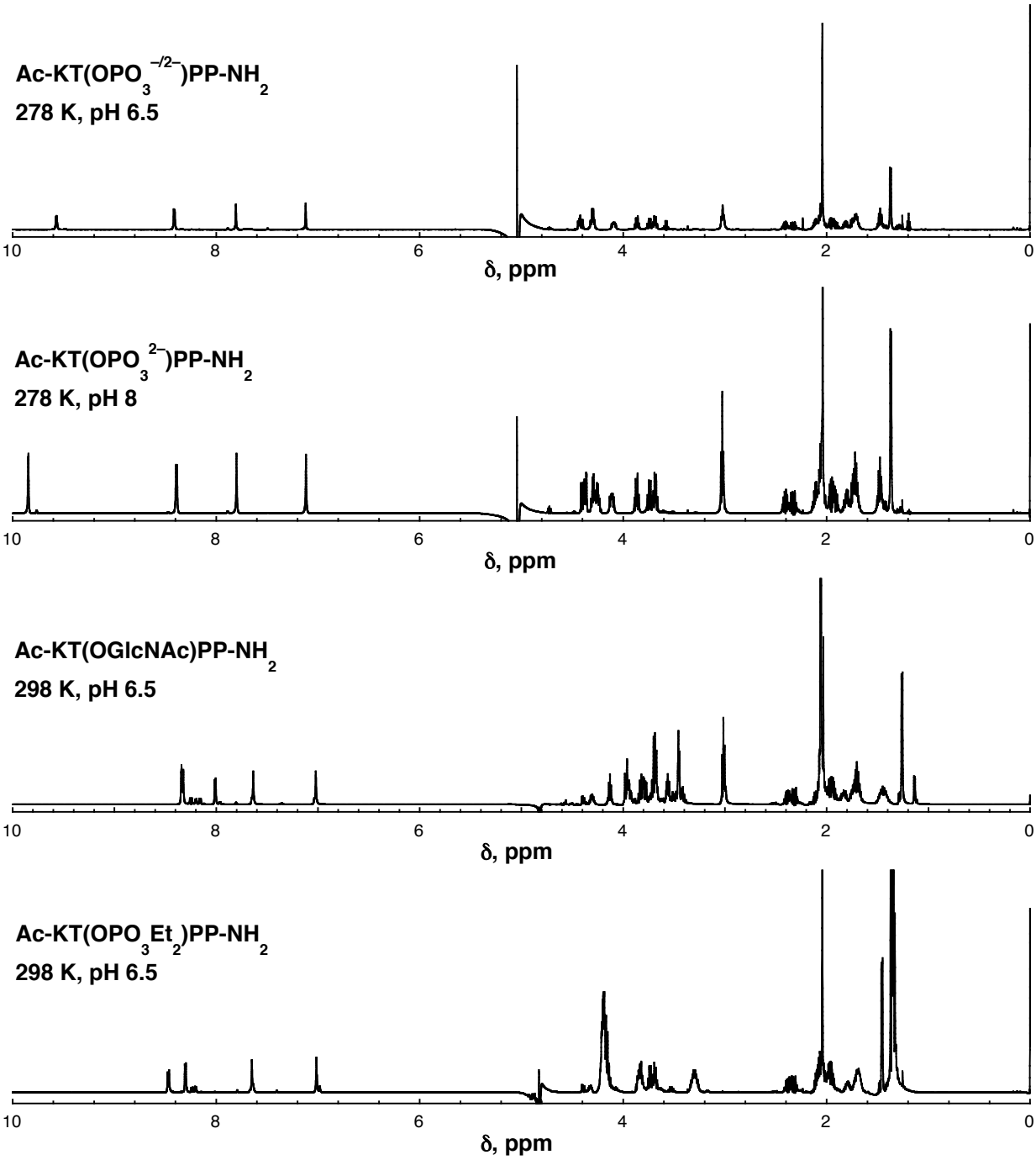
Ac-KT(OPO3 −/2−)PP-NH2
278 K, pH 6.5
10
8
6
4
2
0
δ, ppm
Ac-KT(OPO3 2−)PP-NH2
278 K, pH 8
10
8
6
4
2
0
δ, ppm
Ac-KT(OGlcNAc)PP-NH2
298 K, pH 6.5
10
8
6
4
2
0
δ, ppm
Ac-KT(OPO3Et2)PP-NH2
298 K, pH 6.5
10
8
6
4
2
0
δ, ppm

Due to the unusually slow exchange of the amide protons at pH 8.0 for the peptide Ac-KT(OPO_3^{2-})PP-NH_2, ^{1}H NMR experiments were conducted with increased salt (NaCl) concentrations to identify whether lysine electrostatic interactions were the basis of slow exchange. A very modest upfield shift of the Thr and Lys amide proton was observed with increased NaCl. The rest of the protons throughout the peptide remained essentially unperturbed. The peaks appear to be more resolved at higher salt concentrations. Strikingly, the Thr amide proton at 1 M NaCl concentration at pH 8.0 was still observed to be in slow exchange. These observations are consistent with a dynamic hydrogen bond between the phosphate and Thr backbone amide ordering the peptide and reducing backbone amide exchange rates, potentially via n→π* interactions stabilizing structure. These data are not consistent with a lysine-phosphate electrostatic interaction driving the structure. Notably, experiments were conducted in 5 mM phosphate buffer.

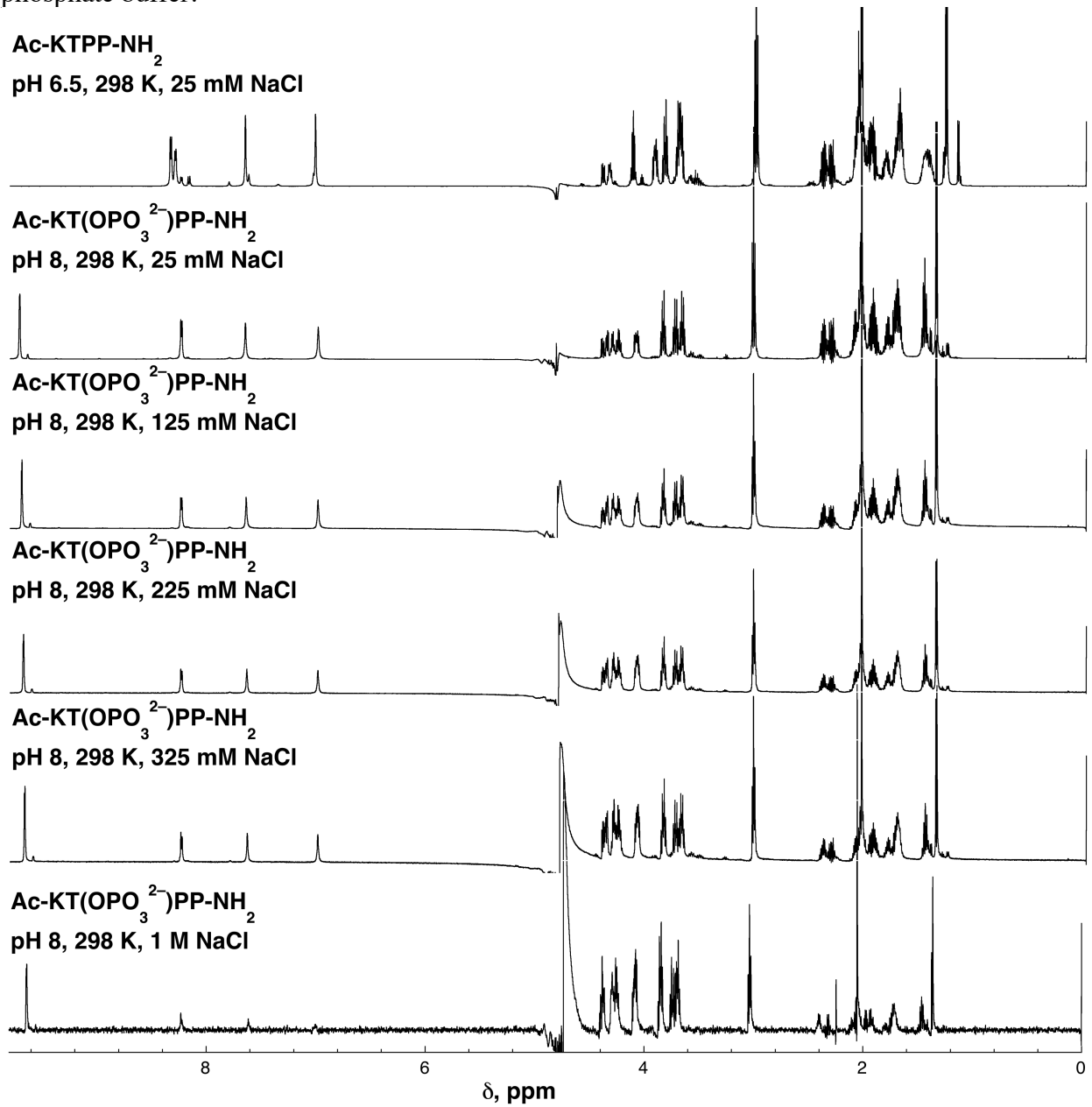

Figure S63. Full ^{1}H NMR spectra of peptide Ac-KT(OPO_3^{2-})PP-NH_2 in 5 mM phosphate buffer containing 25 mM, 125 mM, 225 mM, 325 mM, or 1 M NaCl.

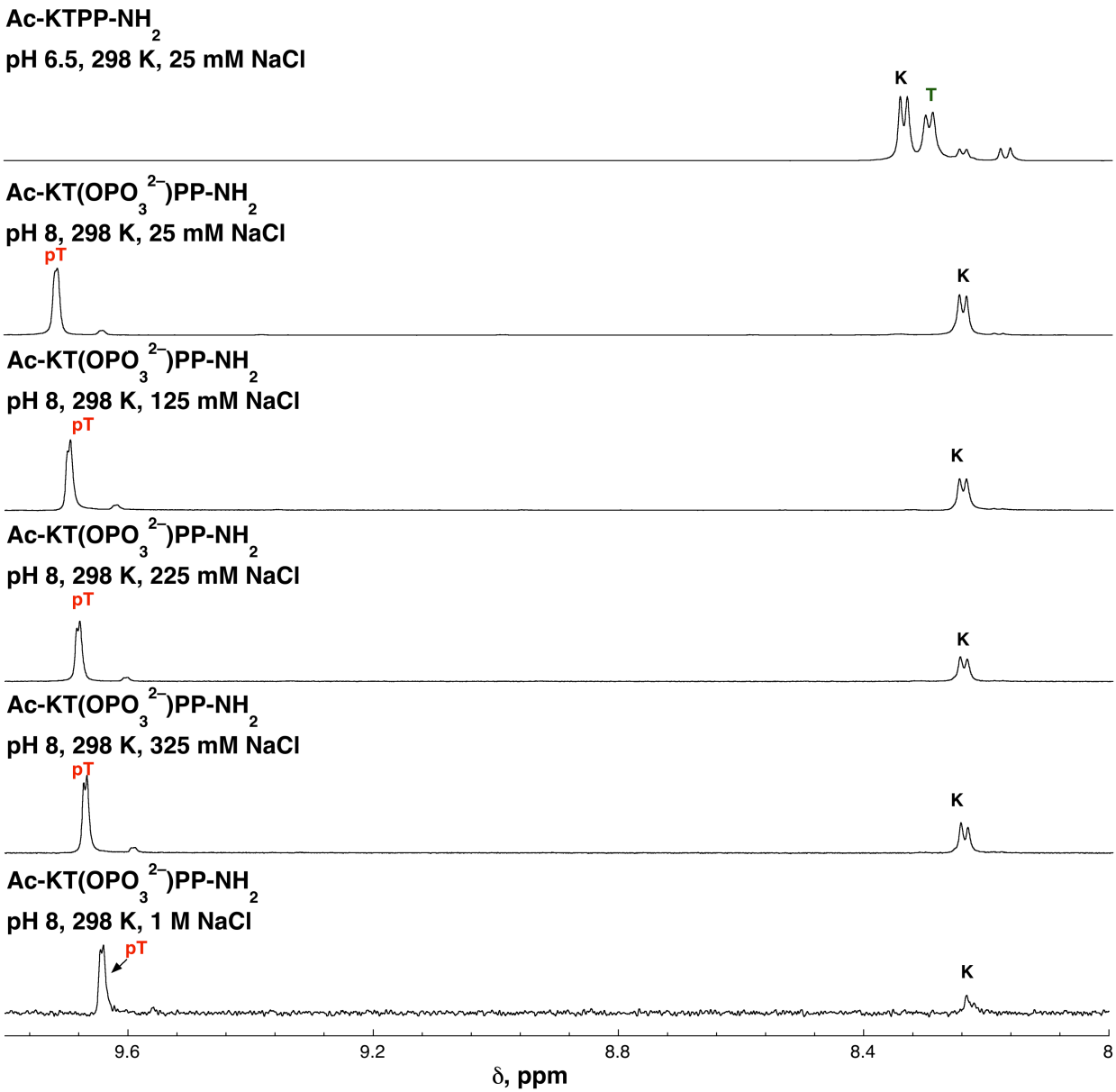

Figure S64. ^{1}H NMR spectra (amide region) of peptide Ac-KT(OPO_3^{2-})PP-NH_2 in 5 mM phosphate buffer containing 25 mM, 125 mM, 225 mM, 325 mM, or 1 M NaCl at pH 8.0.

^{1}H NMR spectra of Ac-KT(OPO_3^{2-})PP-NH_2 at higher temperatures

To examine the possibility of hydrogen bonding between the backbone amide and the side-chain phosphate, ^{1}H NMR experiments were conducted at elevated temperatures. As expected, with increasing temperature the Thr amides exhibited faster exchange rates, and at 338 K no amide resonances were observed. Temperature-dependent NMR experiments at 323 and 338 K were conducted on an AV 400 MHz instrument equipped with a BBO probe. 1–D spectra were collected with a watergate pulse sequence with 65536 acquisition data points and a relaxation delay of 3 s.

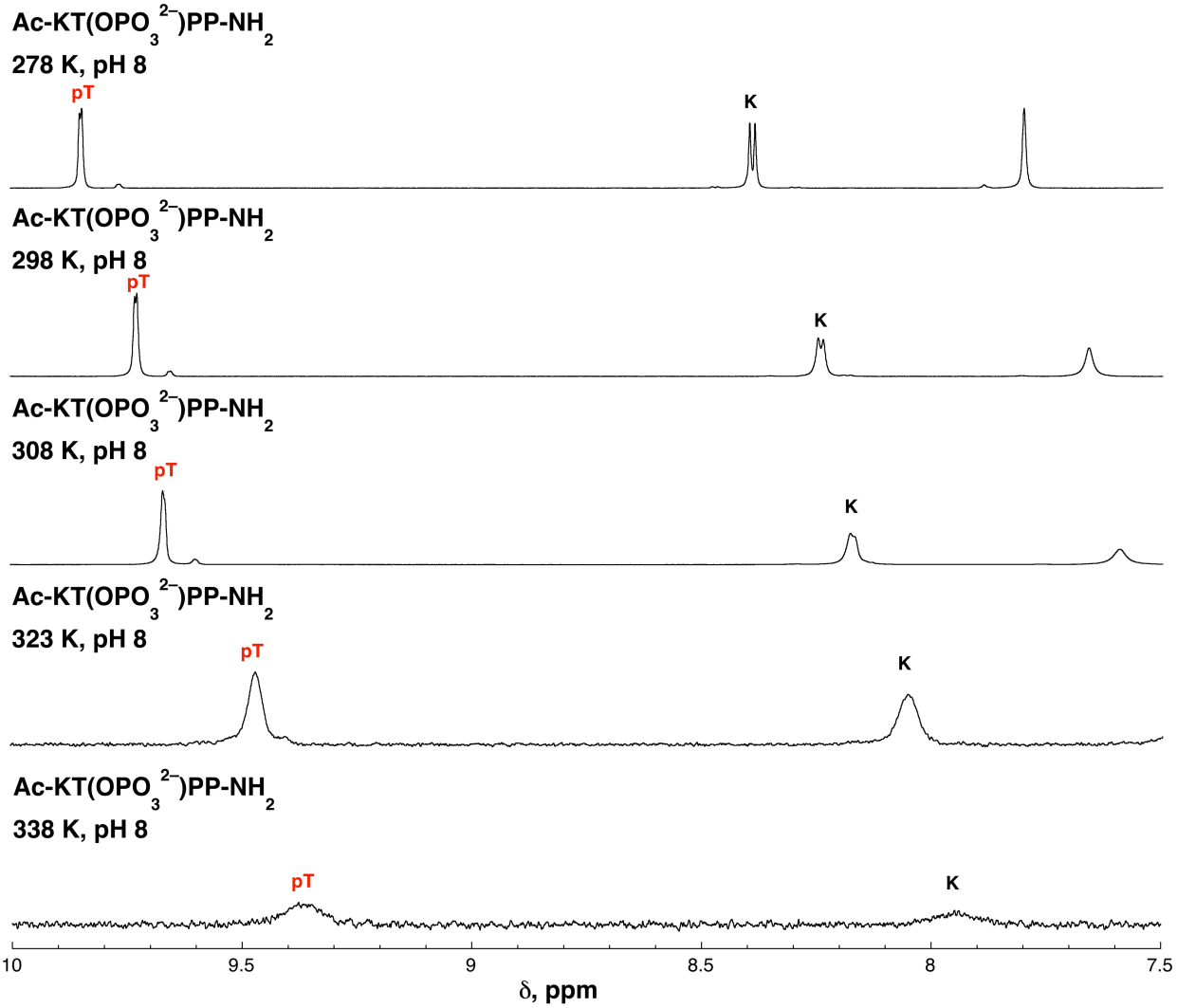

Figure S65. ^{1}H NMR spectra (amide region) of peptide Ac-KT(OPO_3^{2-})PP-NH_2 in 5 mM phosphate buffer containing 25 mM NaCl at 278, 298, 308, 323, and 338 K.

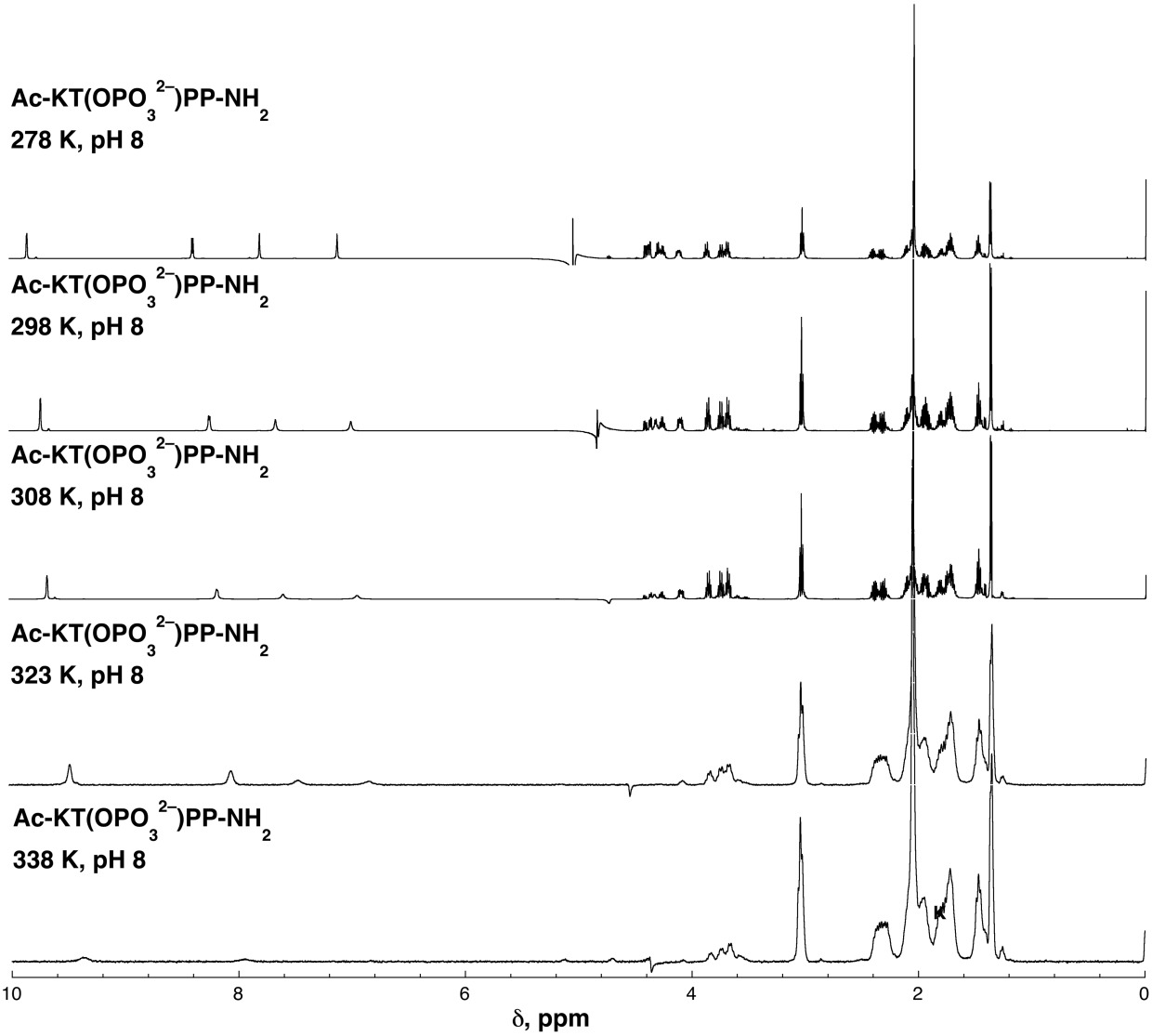

Figure S66. Full ^{1}H NMR spectra of peptide Ac-KT(OPO_3^{2-})PP-NH_2 in 5 mM phosphate buffer containing 25 mM NaCl at 278, 298, 308, 323, and 338 K.

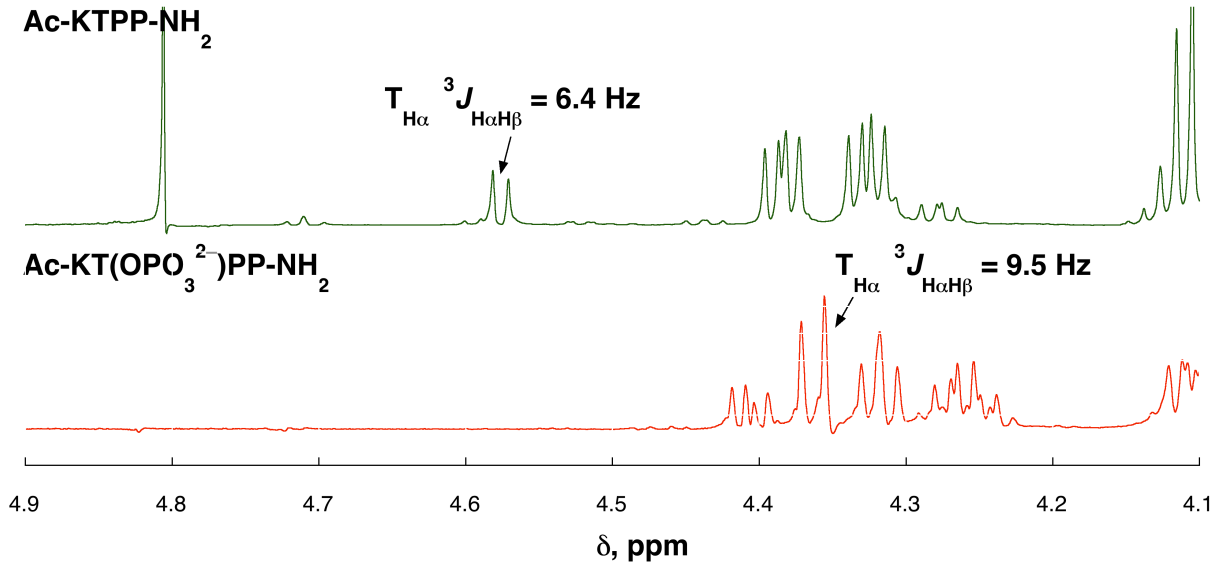

Figure S67. ^{1}H NMR spectra (Hα region) of peptides Ac-KTPP-NH_2 and Ac-KT(OPO_3^{2-})PP-NH_2 at pH 8.0 in 100% D_2O (eliminating HN-Hα coupling due to amide H-D exchange) showing the coupling between Thr Hα and Hβ protons.

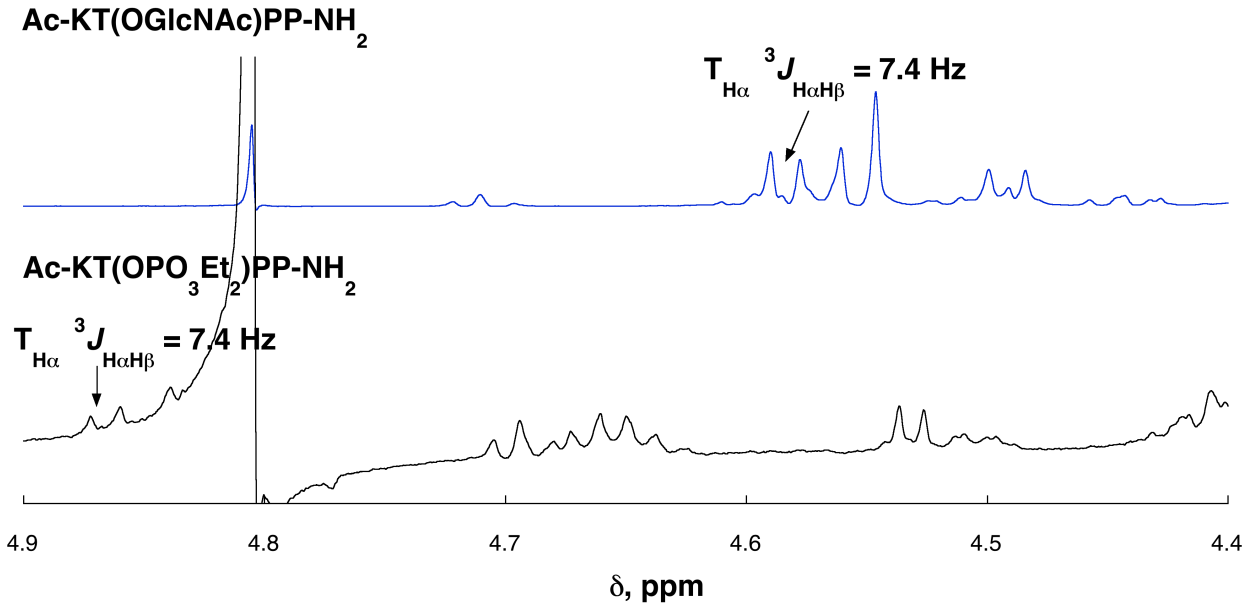

Figure S68. ^{1}H NMR spectra of peptides Ac-KT(OGlcNAc)PP-NH_2 and Ac-KT(OPO_3Et_2)PP-NH_2 at pH 6.5 in 100% D_2O showing the coupling between Thr Hα and Hβ protons.

Summary of NMR data for peptides Ac-K*Tx*PP-NH_2

peptide	δ, H^N	$^3J_{\alpha N}$	δ, Hα	δ, Cα	δ, C_{co}	others
Ac-KTPP-NH_2	**pH 4.0**	**298 K**				
Lys	8.32	6.8	4.33	n.d.	n.d.	2.99, 1.81, 1.71, 1.43
Thr	8.28	7.3	4.58	n.d.	n.d.	4.11, 1.25
Pro3	n.a.	n.a.	4.38	n.d.	n.d.	3.82, 3.67, 2.32, 2.30, 2.05, 1.93
Pro4	n.a.[a]	n.a.	n.d.[b]	n.d.	n.d.	3.91, 3.70, 2.38, 2.07, 2.02, 1.92
Ac-						2.03
Ac-KTPP-NH_2	**pH 6.5**	**298 K**		**δ, Cα[c]**	**δ, C_{co}[c]**	
Lys	8.34	6.8	4.34	53.5	174.2	3.00, 1.82, 1.73, 1.44
Thr	8.30	7.2	4.59	57.1	169.5	4.12, 1.28
Pro3	n.a.	n.a.	4.40	60.2	176.7	3.84, 3.69, 2.31, 2.07, 1.95
Pro4	n.a.	n.a.	4.72	58.9	n.d.	3.92, 3.71, 2.39, 2.09, 2.03, 1.91
Ac-					174.3	2.05
Ac-KTPP-NH_2	**pH 6.5**	**278 K**				
Lys	8.49	6.9	4.33	n.d.	n.d.	3.00, 1.82, 1.72, 1.45
Thr	8.48	6.8	4.58	n.d.	n.d.	4.11, 1.28
Pro3	n.a.	n.a.	4.38	n.d.	n.d.	3.85, 3.69, 2.35, 2.32, 2.06, 1.96
Pro4	n.a.	n.a.	4.74	n.d.	n.d.	3.95, 3.71, 2.40, 2.09, 1.93
Ac-					n.d.	2.04

peptide	δ, H^N	$^3J_{\alpha N}$	δ, Hα	others
Ac-KT(OGlcNAc)PP-NH_2	**pH 6.5**	**298 K**		
Lys	8.34	7.0	4.31	3.01, 1.83, 1.73, 1.45
Thr	8.01	6.4	4.59	4.13, 1.26
Pro3	n.a.	n.a.	4.40	3.82, 3.68, 2.32, 2.06, 1.95
Pro4	n.a.	n.a.	4.72	3.95, 3.69, 2.39, 2.08, 2.04, 1.94
Ac-				2.03
Ac-KT(OPO_3Et_2)PP-NH_2	**pH 4.0**	**298 K**		
Lys	8.30	7.0	4.32	3.16, 1.80, 1.72, 1.36
Thr	8.47	8.4	4.88	4.67, 1.45
Pro3	n.a.	n.a.	4.40	3.84, 3.69, 2.32, 2.07, 1.96
Pro4	n.a.[a]	n.a.	4.64	3.86, 3.74, 2.39, 2.10, 2.04, 1.96
Ac-				2.04

Table S21. Summary of ^{1}H NMR data for peptides Ac-K*Tx*PP-NH_2. [a] n.a. = not applicable. [b] n.d. = not determined. [c] Data obtained at pH 8.0.

peptide	δ, H^N	$^3J_{\alpha N}$	δ, H_α	δ, C_α	δ, C_{co}	others
Ac-KT(OPO_3H^-)PP-NH_2	**pH 4.0 298 K**					
Lys	8.31	7.0	4.31	n.d.	n.d.	3.00, 1.83, 1.74, 1.68, 1.45
Thr	8.46	6.1	4.63	n.d.	n.d.	4.45, 1.37
Pro3	n.a.	n.a.	4.41	n.d.	n.d.	3.82, 3.67, 2.31, 2.05, 1.95
Pro4	n.a.	n.a.	n.d.	n.d.	n.d.	3.99, 3.73, 2.38, 2.10, 2.02, 1.90
Ac-						2.04
Ac-KT($OPO_3^{-/2-}$)PP-NH_2	**pH 6.5 298 K**					
Lys	8.27	7.0	4.32	n.d.	n.d.	3.03, 1.82, 1.75, 1.53
Thr	9.39	3.1	4.44	n.d.	n.d.	4.31, 1.37
Pro3	n.a.	n.a.	4.41	n.d.	n.d.	3.85, 3.68, 2.32, 2.06, 1.95
Pro4	n.a.	n.a.	n.d.	n.d.	n.d.	4.08, 3.73, 2.41, 2.11, 2.04, 1.93
Ac-						2.05
Ac-KT(OPO_3^{2-})PP-NH_2	**pH 8.0 298 K**					
Lys	8.24	6.8	4.32	53.6	173.8	3.03, 1.81, 1.75, 1.47
Thr	9.73	3.5	4.36	57.1	169.7	4.26, 1.37
Pro3	n.a.	n.a.	4.40	60.2	176.9	3.85, 3.68, 2.32, 2.06, 1.95
Pro4	n.a.	n.a.	4.70	59.0	n.d.	4.11, 3.75, 2.40, 2.11, 2.05, 1.93
Ac-					174.3	2.05
Ac-KT($OPO_3^{-/2-}$)PP-NH_2	**pH 6.5 278 K**					
Lys	8.41	6.9	4.14	n.d.	n.d.	2.86, 1.65, 1.58, 1.31
Thr	9.57	3.1	4.27	n.d.	n.d.	4.14, 1.22
Pro3	n.a.	n.a.	4.42	n.d.	n.d.	3.87, 3.70, 2.34, 2.07, 1.96
Pro4	n.a.	n.a.	4.74	n.d.	n.d.	4.11, 3.74, 2.42, 2.03, 1.92
Ac-						2.04
Ac-KT(OPO_3^{2-})PP-NH_2	**pH 8.0 278 K**					
Lys	8.39	6.8	4.13	n.d.	n.d.	2.86, 1.70, 1.57, 1.31
Thr	9.85	3.5	4.20	n.d.	n.d.	4.09, 1.21
Pro3	n.a.	n.a.	4.40	n.d.	n.d.	3.85, 3.67, 2.32, 2.06, 1.95
Pro4	n.a.	n.a.	4.74	n.d.	n.d.	4.12, 3.74, 2.41, 2.11, 2.05, 1.90
Ac-	n.a.	n.a.		n.d.	n.d.	2.04

Table S22. Summary of ^{1}H NMR data for peptides Ac-K*Tx*PP-NH_2. [a] n.a. = not applicable. [b] n.d. = not determined due to overlap with water peak.

peptide	δ, H^N Thr	$^3J_{\alpha N}$, Thr	δ, $H\alpha$ Thr	δ,$H\beta$ Thr	δ, H^N Lys	$^3J_{\alpha N}$, Lys	δ, $H\alpha$ Lys	δ, Lys_{others}	pH
KTPP	8.28	7.3	4.58	4.11	8.32	6.8	4.33	2.99, 1.81, 1.71, 1.43	4.0
KT(OPO_3H^-)PP	8.46	6.1	4.63	4.45	8.31	7.0	4.31	3.00, 1.83, 1.74, 1.68, 1.45	4.0
KT(OPO_3^{2-})PP	9.73	3.5	4.27	4.14	8.24	6.8	4.32	3.03, 1.81, 1.75, 1.47	8.0
KT(OPO_3^{2-})PP[a]	9.85	3.5	4.20	4.09	8.39	6.8	4.13	2.86, 1.70, 1.57, 1.31	8.0
KT(OGlcNAc)PP	8.01	6.4	4.59	4.13	8.34	7.0	4.31	3.01, 1.83, 1.73, 1.45	6.5
KT(OPO_3Et_2)PP	8.47	8.4	4.88	4.67	8.30	7.0	4.32	3.16, 1.80, 1.72, 1.36	4.0

Table S23. Summary of ^{1}H NMR data for peptides Ac-K*Tx*PP-NH_2 at 298 K. [a] NMR at 278 K.

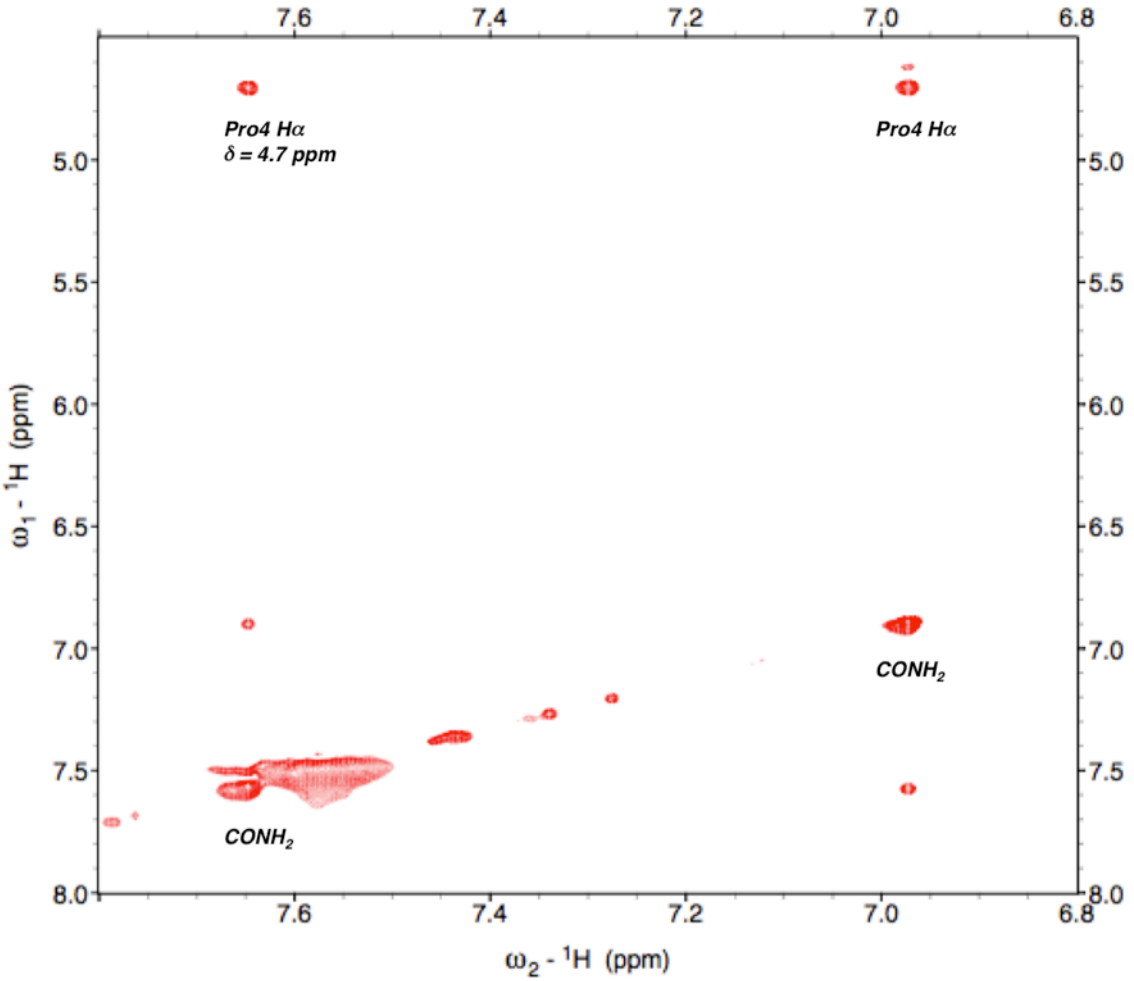

Figure S69. Partial ROESY spectrum of peptide Ac-KT(OPO_3^{2-})PP-NH_2 at pH 8.0 in 5 mM phosphate buffer containing 25 mM NaCl at 298 K. These data were used to assign the proline residues via the expected Cα(i) → HN(i+1) ROEs with the C-terminal carboxamide.

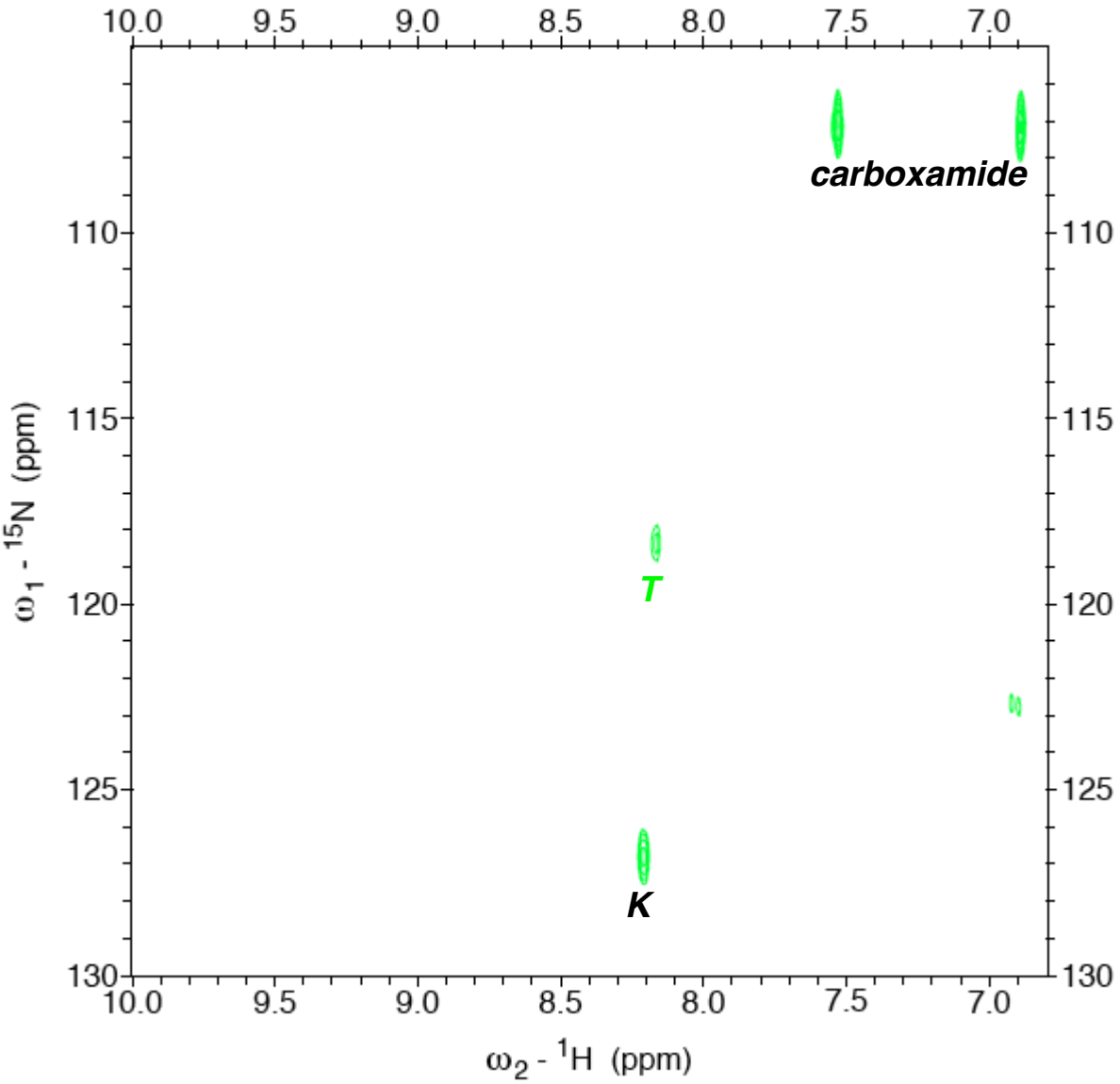

Figure S70. ^{1}H-^{15}N HSQC spectrum of peptide Ac-KTPP-NH_2 at pH 6.5 in 5 mM phosphate buffer containing 25 mM NaCl at 298 K.

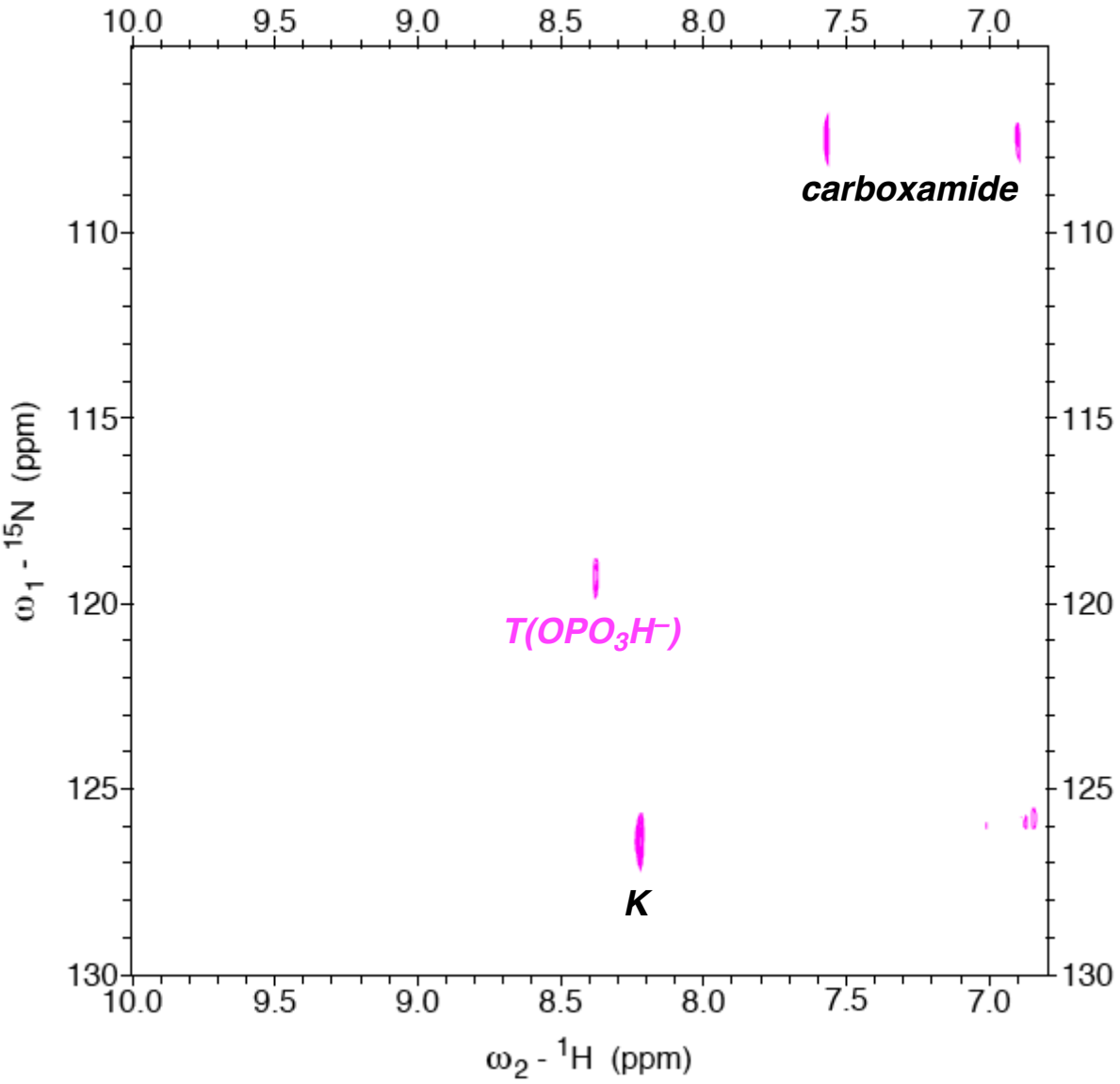

Figure S71. ^{1}H-^{15}N HSQC spectrum of peptide Ac-KT(OPO_3H^-)NH_2 at pH 4.0 in 5 mM phosphate buffer containing 25 mM NaCl at 298 K.

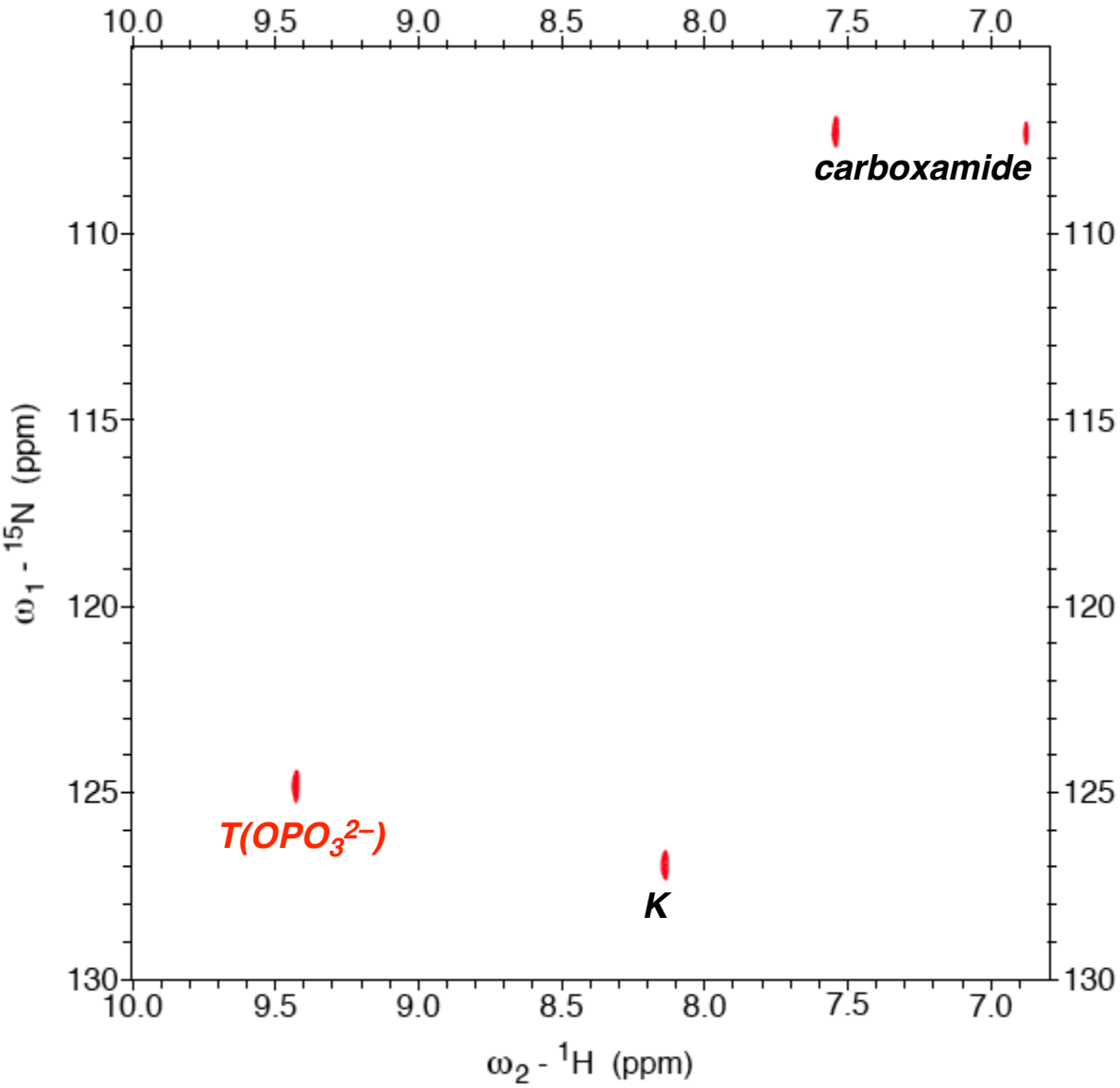

Figure S72. ^{1}H-^{15}N HSQC spectrum of peptide Ac-KT(OPO_3^{2-})NH_2 at pH 7.2 in 5 mM phosphate buffer containing 25 mM NaCl at 298 K.

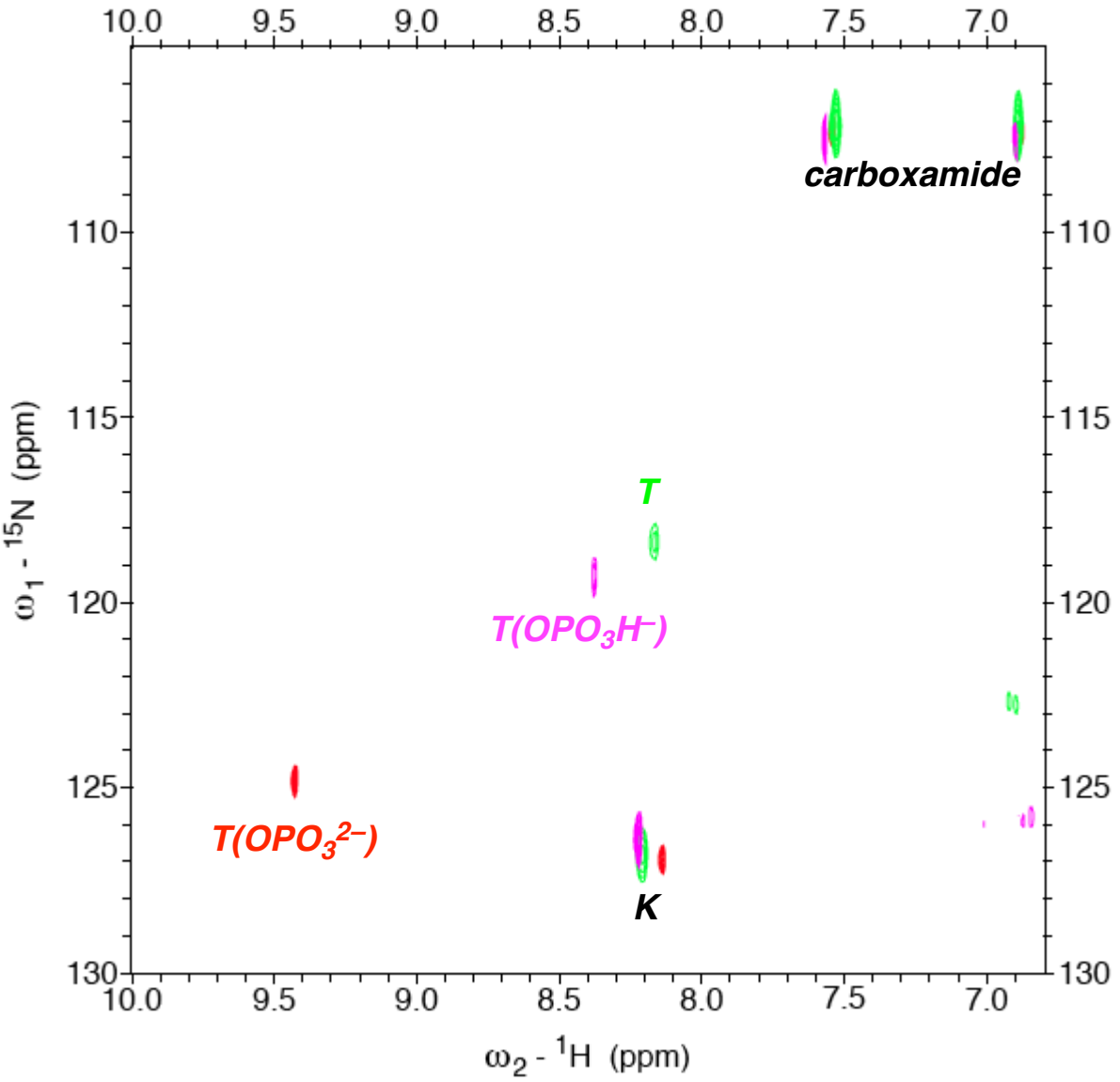

Figure S73. ^{1}H-^{15}N HSQC spectra of peptides Ac-KTPP-NH_2 at pH 6.5 (green), Ac-KT(OPO_3^{2-})PP-NH_2 (red), and Ac-KT(OPO_3H^-)NH_2 (magenta) at 298 K. Data were collected with 1-2 mM peptide in 5 mM phosphate buffer (pH 4.0, 6.5, or 7.2) with 25 mM NaCl.

peptide	Thr_N, ppm	Lys_N, ppm	carboxamide, ppm	pH, temp (K)
Ac-KTPP-NH_2	118.3	126.8	107.2	6.5, 298 K
Ac-KT(OPO_3H^-)PP-NH_2	119.4	126.6	107.4	4.0, 298 K
Ac-KT(OPO_3^{2-})PP-NH_2	124.8	127.1	107.4	7.2, 298 K

Table S24. Summary of ^{1}H-^{15}N HSQC NMR data for peptides Ac-K*Tx*PP-NH_2 at 298 K.

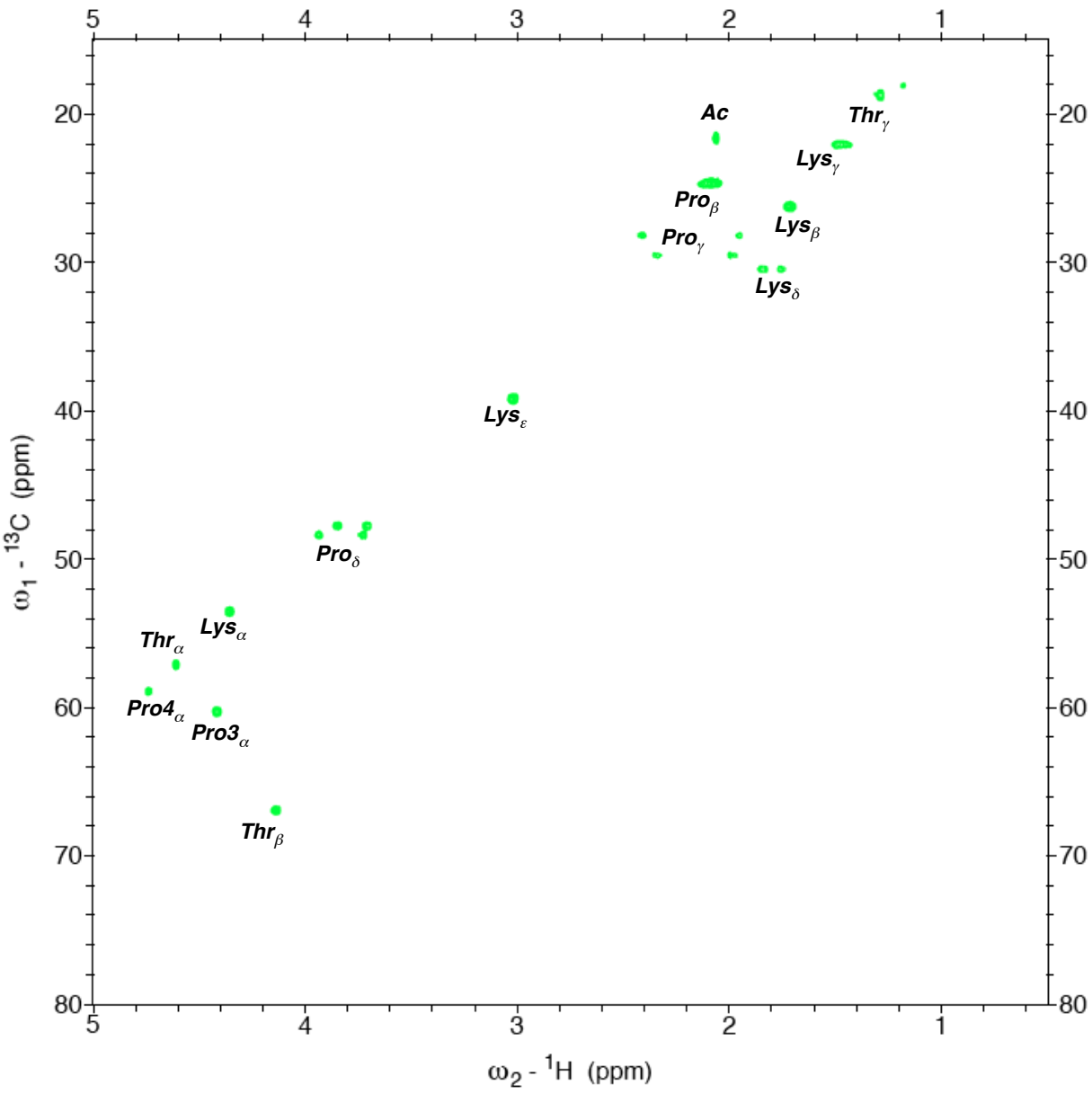

Figure S74. ^{1}H-^{13}C HSQC spectrum of peptide Ac-KTPP-NH_2 at pH 4.0 in 5 mM phosphate buffer with 25 mM NaCl in 100% D_2O at 298 K.

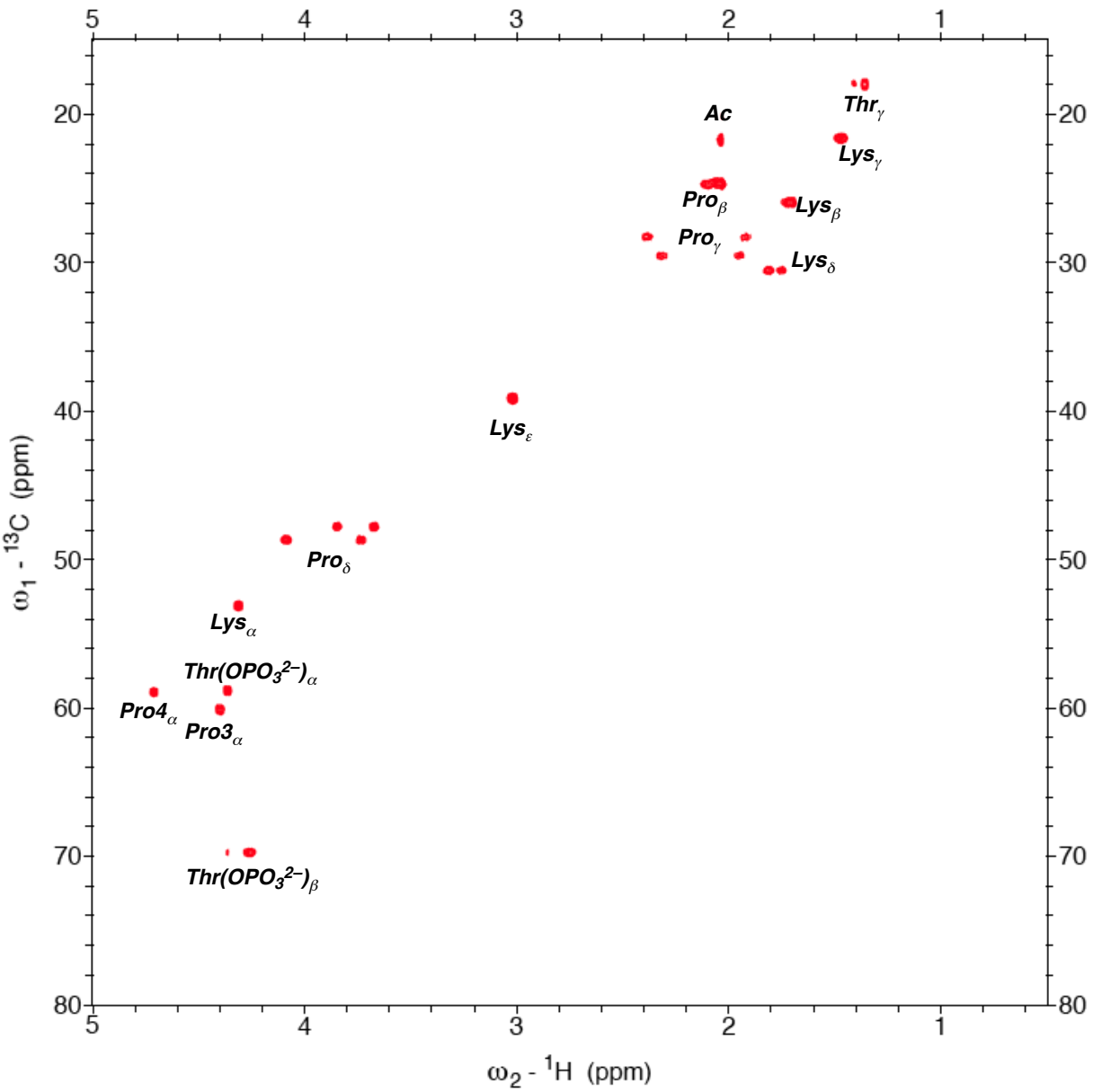

Figure S75. ^{1}H-^{13}C HSQC spectrum of peptide Ac-KT(OPO$_3^{2-}$)PP-NH$_2$ at pH 8.0 in 5 mM phosphate buffer with 25 mM NaCl in 100% D$_2$O at 298 K.

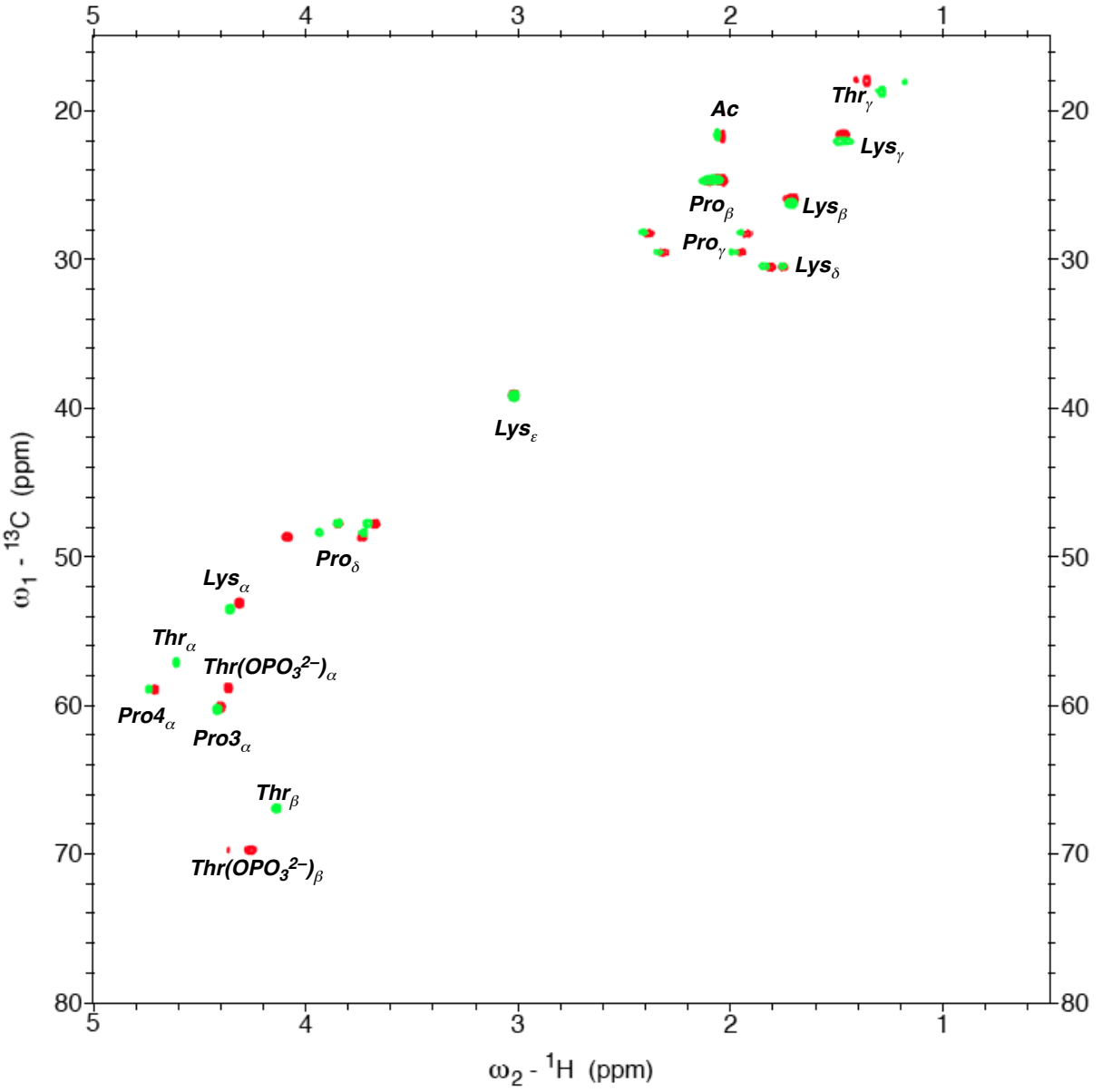

Figure S76. ^{1}H-^{13}C HSQC spectra of peptides Ac-KT(OPO$_3^{2-}$)PP-NH$_2$ (red) at pH 8.0 and Ac-KTPP-NH$_2$ (green) at pH 4.0 in 5 mM phosphate buffer with 25 mM NaCl in 100% D$_2$O at 298 K.

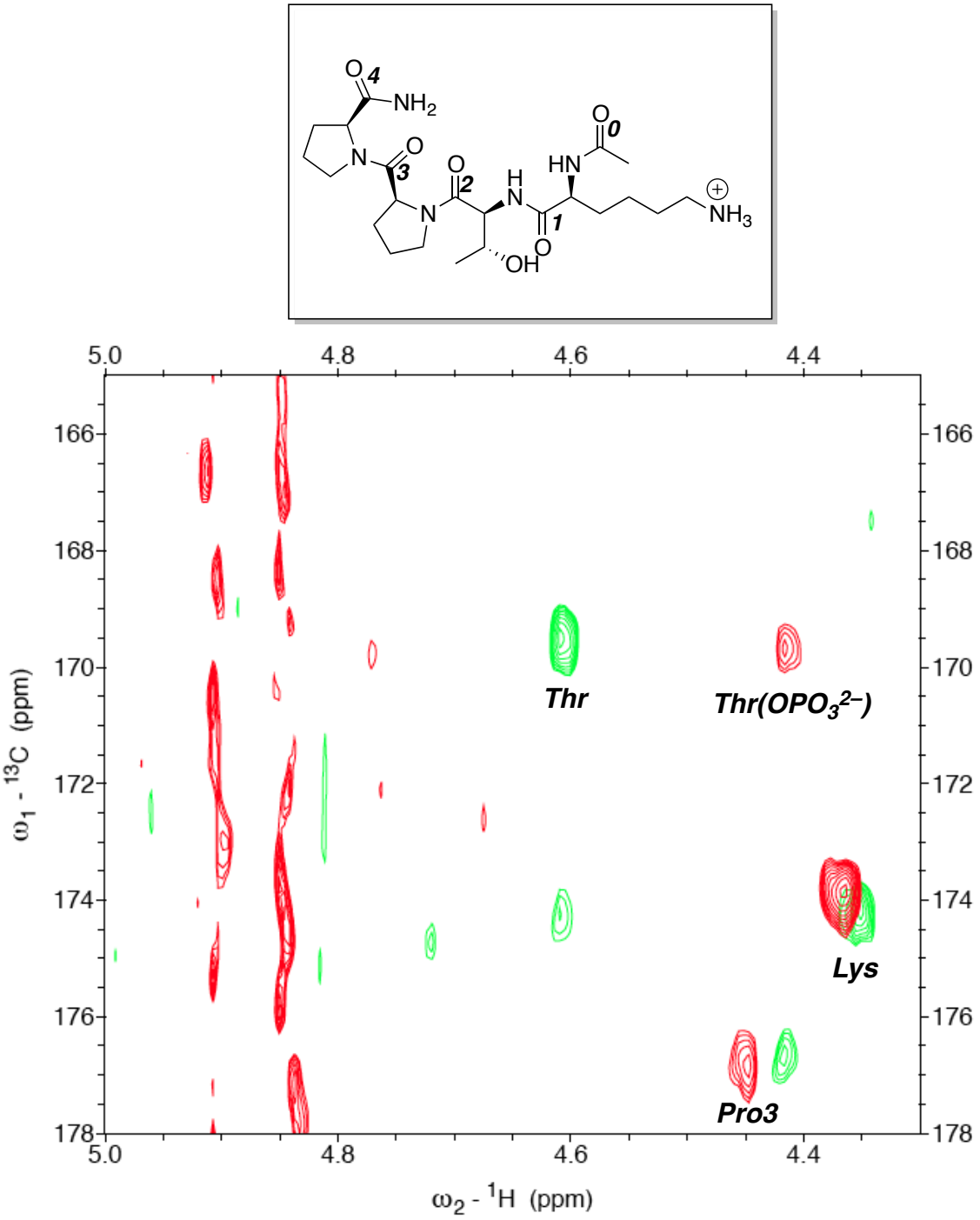

Figure S77. ^{1}H-^{13}C HMBC spectra of peptides Ac-KTPP-NH_2 (green) and Ac-KT(OPO_3^{2-})PP-NH_2 (red) at pH 8.0 in 5 mM phosphate buffer with 25 mM NaCl in 100% D_2O at 298 K. The Pro4 (**4**) carbonyl carbon chemical shift could not be determined due to spectral overlap of Hα with residual water.

Ac-KTPP-NH_2 residue	^{13}C δ, ppm	Ac-KT(OPO_3^{2-})PP-NH_2 residue	^{13}C δ, ppm
Lys, α	53.5	Lys, α	53.1
Thr, α	57.1	pThr, α	58.8
Pro3, α	58.9	Pro3, α	58.9
Pro4, α	60.2	Pro4, α	60.1
Thr, β	66.9	pThr, β	69.8
Pro3, δ	47.8	Pro3, δ	47.8
Pro4, δ	48.4	Pro4, δ	48.7
Lys, ε	39.2	Lys, ε	39.2
Pro3, γ	28.2	Pro3, γ	28.2
Pro4, γ	29.6	Pro4, γ	29.6
Lys, β	30.4	Lys, β	30.5
NHAc	21.6	NHAc	21.6
Pro3, Pro4, β	24.6	Pro3, Pro4, β	24.7
Lys, γ	22.1	Lys, γ	21.6
Lys, δ	26.3	Lys, δ	25.9
Thr, γ	18.7	pThr, γ	18.0
Lys, CO	174.2	Lys, CO	173.8
Thr, CO	169.5	pThr, CO	169.7
Pro3, CO	176.7	Pro3, CO	176.9
Pro4, CO	n.d.	Pro4, CO	n.d.
Ac, CO	174.3	Ac, CO	174.3

Table S25. Summary of ^{13}C NMR data from ^{1}H-^{13}C HSQC and HMBC experiments at 298 K. The spectra were recorded at pH 8.0 in 5 mM phosphate buffer with 25 mM NaCl in 100% D_2O at 298 K. pThr indicates a phosphorylated threonine residue.

Ac-KTPP-NH_2 residue	^{13}C δ, ppm	Ac-KT(OPO_3^{2-})PP-NH_2 residue	^{13}C δ, ppm
Lys, α	53.2	Lys, α	52.8
Thr, α	57.0	pThr, α	58.5
Pro3, α	58.6	Pro3, α	58.7
Pro4, α	59.9	Pro4, α	59.8
Thr, β	66.6	pThr, β	69.4
Pro3, δ	47.6	Pro3, δ	47.5
Pro4, δ	48.1	Pro4, δ	48.4
Lys, ε	38.8	Lys, ε	38.8
Pro3, γ	27.9	Pro3, γ	28.0
Pro4, γ	29.2	Pro4, γ	29.3
Lys, β	30.1	Lys, β	30.1
Pro3, β	21.2	Pro3, β	21.3
Pro4, β	24.4	Pro4, β	24.5
Lys, γ	21.8	Lys, γ	21.4
Lys, δ	25.9	Lys, δ	25.7
Thr, γ	18.4	pThr, γ	17.7

Table S26. Summary of ^{13}C NMR data from ^{1}H-^{13}C HSQC experiments at 278 K. The spectra were recorded at pH 8.0 in 5 mM phosphate buffer with 25 mM NaCl in 100% D_2O at 278 K. pThr indicates a phosphorylated threonine residue.

^{31}P NMR spectra of peptide Ac-KpTPP-NH$_2$

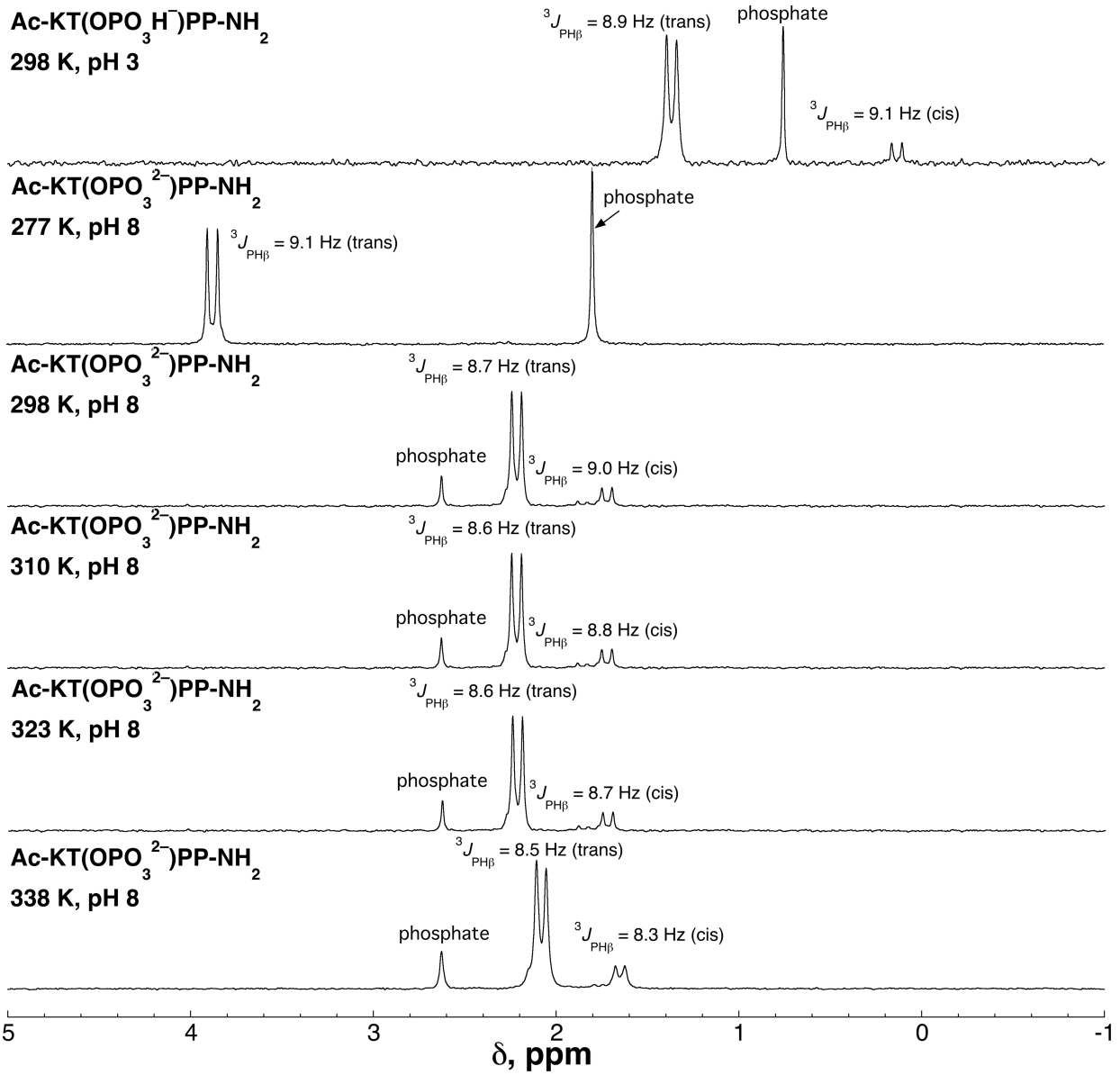

Figure S78. ^{31}P NMR spectra of peptide Ac-KT(OPO$_3$H$^-$)PP-NH$_2$ at pH 3.0 in 5 mM acetate buffer containing 50 μM phosphate and 250 μM NaCl and at pH 8.0 in 5 mM phosphate buffer containing 25 mM NaCl. The NMR spectra were internally referenced with 85% H_3PO_4 (0 ppm) using a capillary filled with H_3PO_4 located in the NMR tube containing the sample.

peptide	δ, P_{trans}	δ, P_{cis}	$^3J_{PH_\beta}$ trans	$^3J_{PH_\beta}$ cis	pH	Temp, K
Ac-KT(OPO_3H^-)PP-NH_2	1.37	0.14	8.9	9.1	3.0	298
Ac-KT(OPO_3^{2-})PP-NH_2	4.75	n.d.	9.1	n.d.	8.0	277
Ac-KT(OPO_3^{2-})PP-NH_2	2.22	1.72	8.7	9.0	8.0	298
Ac-KT(OPO_3^{2-})PP-NH_2	2.21	1.72	8.6	8.8	8.0	310
Ac-KT(OPO_3^{2-})PP-NH_2	2.22	1.72	8.6	8.7	8.0	323
Ac-KT(OPO_3^{2-})PP-NH_2	2.08	1.65	8.5	8.3	8.0	338

Table S27. Summary of ^{31}P NMR data for peptide Ac-KpTPP-NH_2 at pH 3.0 (298 K) and pH 8.0 (277, 298, 310, 323, and 338 K). n.d. = not determined.

^{1}H NMR spectra of Ac-K*Sx*PP-NH_2 peptides

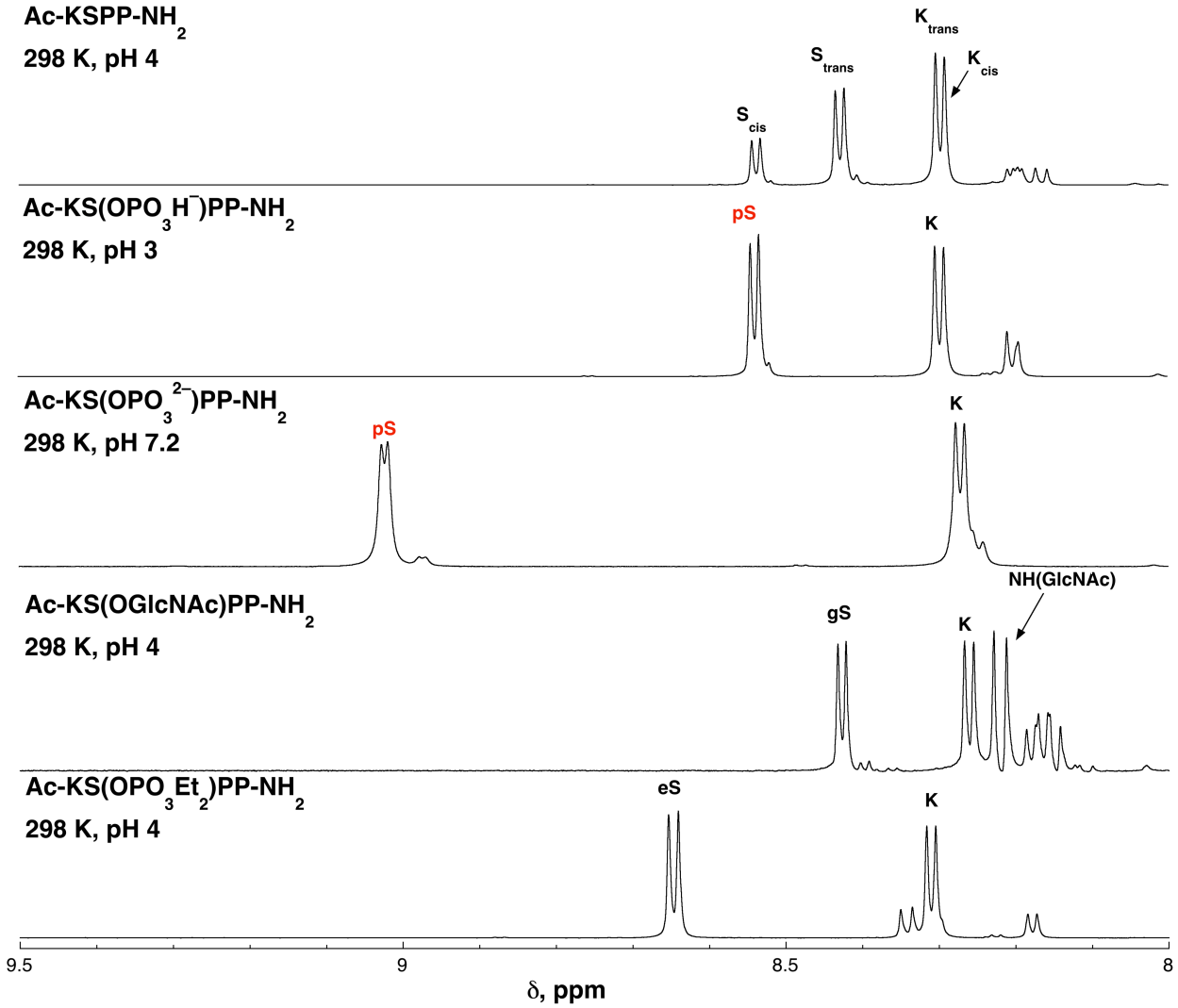

Figure S79. ^{1}H NMR spectra (amide region) of peptides Ac-K*Sx*PP-NH_2 at 298 K. Minor peaks in the NMR spectra are due to the presence of cis amide bonds. Peptides were dissolved in buffer containing 5 mM phosphate buffer (pH 3.0, 4.0, or 7.2) and were internally referenced with TSP. Solutions contained 25 mM NaCl, 100 μM TSP, and 90% H_2O/10% D_2O.

pH-dependent NMR of peptide Ac-KpSPP-NH_2

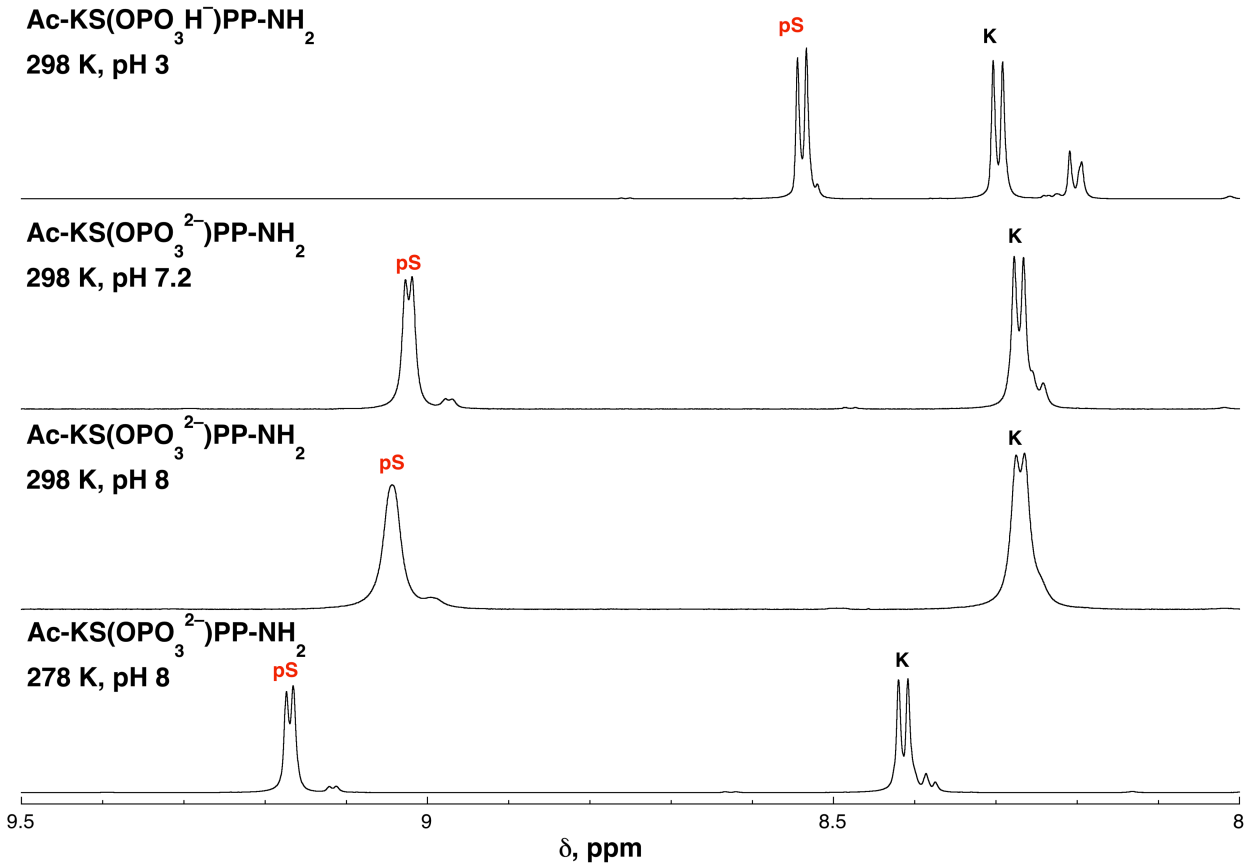

Figure S80. ^{1}H NMR spectra (amide region) of Ac-KpSPP-NH_2. Minor peaks in the NMR spectra are due to the presence of cis amide bonds. Peptides were dissolved in 5 mM phosphate buffer (pH 3.0, 7.2, or 8.0) and were internally referenced with TSP. Solutions contained 25 mM NaCl, 100 μM TSP, and 90% H_2O/10% D_2O.

Full ^{1}H NMR spectra for Ac-K*Sx*PP-NH$_2$ peptides

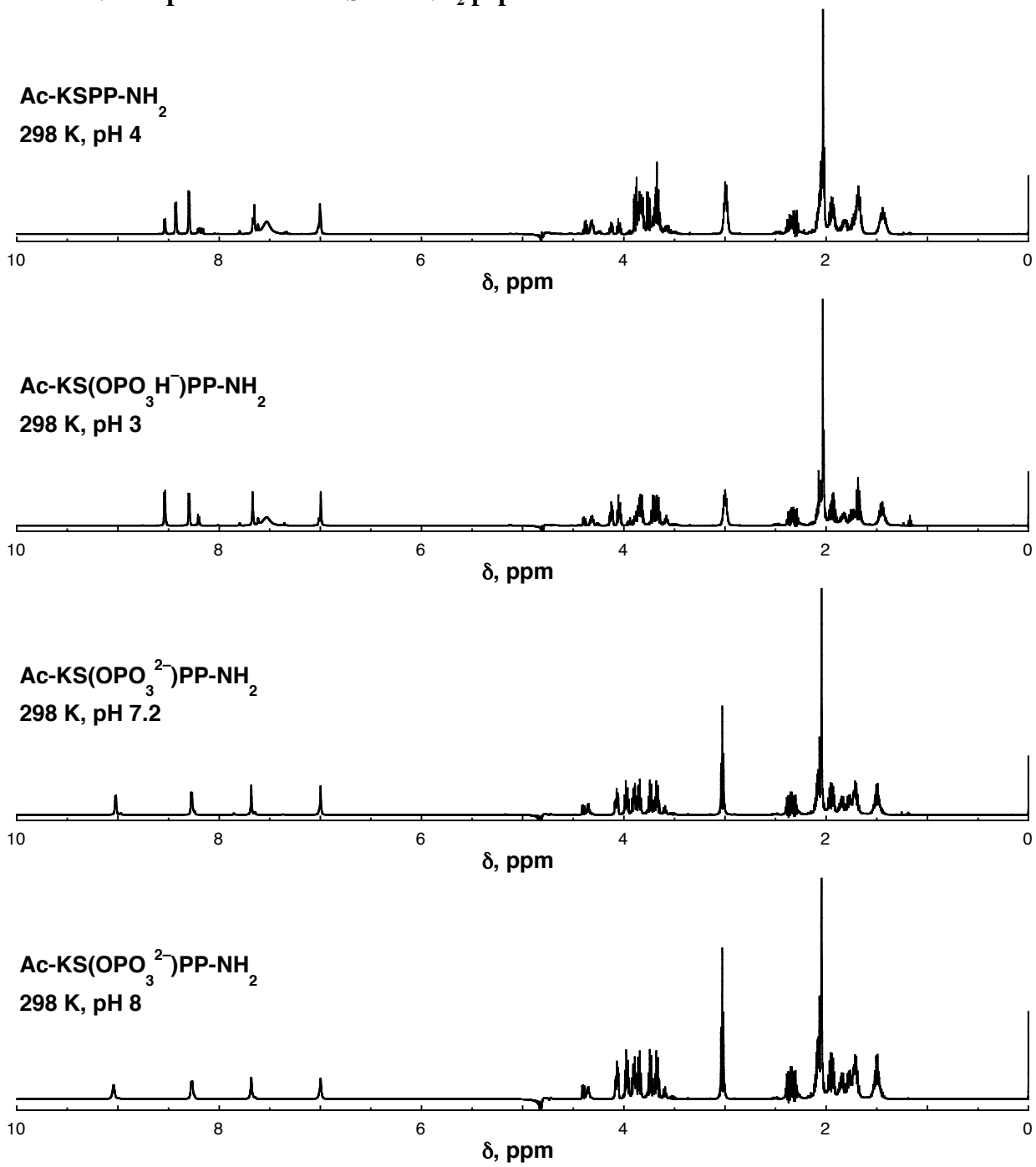

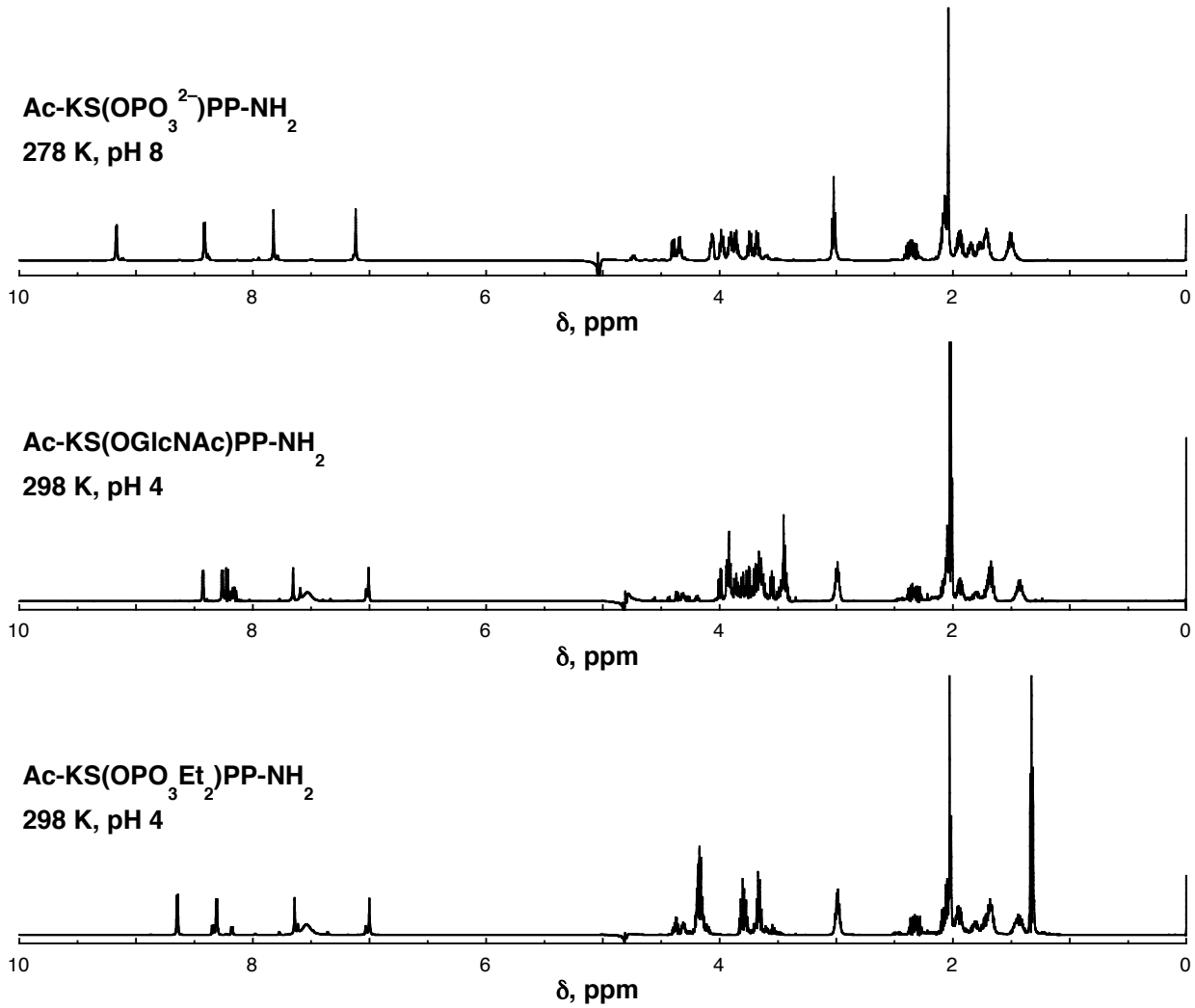
Ac-KS(OPO3 2−)PP-NH2
278 K, pH 8
10
8
6
4
2
0
δ, ppm
Ac-KS(OGlcNAc)PP-NH2
298 K, pH 4
10
8
6
4
2
0
δ, ppm
Ac-KS(OPO3Et2)PP-NH2
298 K, pH 4
10
8
6
4
2
0
δ, ppm

Summary of NMR data for peptides Ac-K*Sx*PP-NH_2

peptide	δ, H^N Ser	$^3J_{\alpha N}$, Ser	δ, Hα Ser	δ, Hβ Ser	δ, H^N Lys	$^3J_{\alpha N}$, Lys	δ, Hα Lys	δ, Lys (others)	pH
KSPP	8.42	6.8	4.75	3.89, 3.76	8.29	7.0	4.32	2.99, 1.82, 1.72, 1.44	4.0
KS(OPO_3H^-)PP	8.54	6.5	4.85	4.12, 4.05	8.30	7.0	4.32	3.00, 1.83, 1.74, 1.43	3.0
KS(OPO_3^{2-})PP	9.02	5.5	4.74	4.07, 3.97	8.27	7.1	4.35	3.03, 1.85, 1.77, 1.50	7.2
KS(OPO_3^{2-})PP	9.05	n.d.	4.73	4.07, 3.97	8.27	7.1	4.35	3.03, 1.85, 1.77, 1.50	8.0
KS(OPO_3^{2-})PP[a]	9.17	5.0	4.64	3.96, 3.88	8.42	6.9	4.24	2.92, 1.75, 1.67, 1.41	8.0
KS(OGlcNAc)PP	8.43	6.4	4.78	4.00, 3.92	8.26	7.2	4.32	2.99, 1.81, 1.69, 1.43	4.0
KS(OPO_3Et_2)PP	8.64	7.6	4.99	4.39, 4.19	8.30	7.1	4.31	2.99, 1.81, 1.72, 1.44	4.0

Table S28. Summary of ^{1}H NMR data for peptides Ac-K*Sx*PP-NH_2. The data were collected at 298 K in 5 mM phosphate buffer containing 25 mM NaCl. [a] NMR data were collected at 278 K.

peptide				
Ac-KSPP-NH_2, pH 4.0, 298K	**δ, Hα**	**δ, Hβ**	**δ, Hγ**	**δ, Hδ**
Pro3	4.38	2.05, 1.93	2.31, 2.05	3.82, 3.67
Pro4	n.d.	2.05, 1.93	2.37, 2.05	3.89, 3.76
Ac-KS(OPO_3H^-)PP-NH_2, pH 3.0, 298 K				
Pro3	4.39	2.05, 1.94	2.31, 2.05	3.83, 3.66
Pro4	4.72	2.03, 1.93	2.37, 2.08	3.86, 3.70
Ac-KS(OPO_3^{2-})PP-NH_2, pH 7.0.2, 298 K				
Pro3	4.40	2.06, 1.96	2.32, 2.06	3.83, 3.67
Pro4	4.73	2.08, 1.94	2.37, 2.08	3.90, 3.73
Ac-KS(OPO_3^{2-})PP-NH_2, pH 8.0, 298 K				
Pro3	4.40	2.06, 1.96	2.32, 2.06	3.85, 3.67
Pro4	4.73	2.08, 1.94	2.38, 2.08	3.90, 3.73
Ac-KS(OPO_3^{2-})PP-NH_2, pH 8.0, 278 K				
Pro3	4.40	2.06, 1.95	2.32, 2.06	3.86, 3.68
Pro4	4.75	2.08, 1.93	2.38, 2.08	3.90, 3.74
Ac-KS(OGlcNAc)PP-NH_2, pH 4.0, 298 K				
Pro3	4.37	2.04, 1.94	2.30, 2.04	3.81, 3.66
Pro4	4.78	2.05, 1.94	2.38, 2.05	3.87, 3.64
Ac-KS(OPO_3Et_2)PP-NH_2, pH 4.0, 298 K				
Pro3	4.37	2.05, 1.94	2.30, 2.05	3.81, 3.67
Pro4	n.d.[a]	2.03, 1.95	2.35, 2.07	3.78, 3.66

Table S29. ^{1}H NMR data for proline protons of peptides Ac-K*Sx*PP-NH_2. The peptides were dissolved in 5 mM phosphate buffer buffer containing 25 mM NaCl. [a] n.d. indicates not determined because the peak is in water peak.

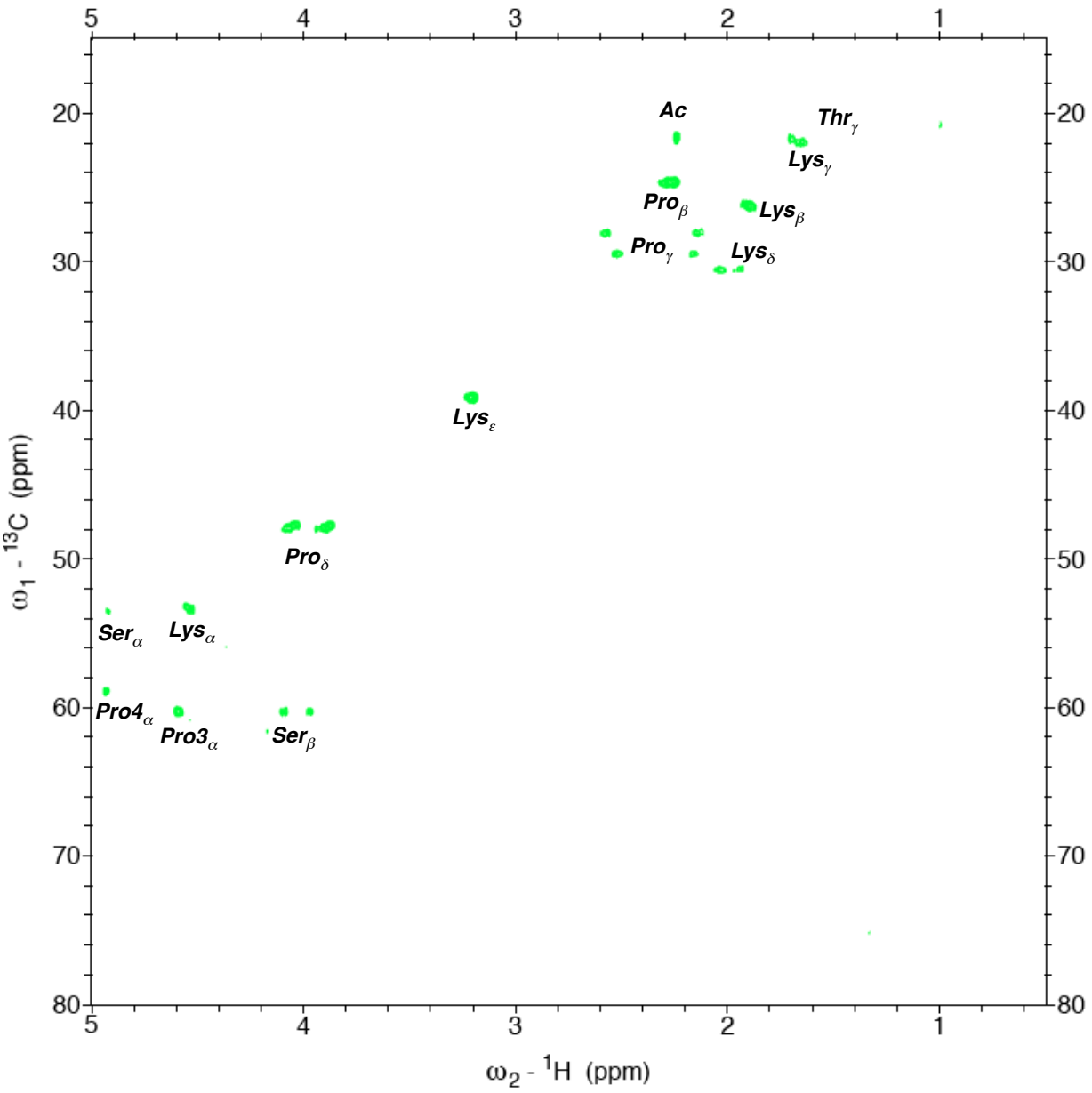

Figure S81. ^{1}H-^{13}C HSQC spectrum of peptide Ac-KSPP-NH_2 at pH 4.0 in 5 mM phosphate buffer with 25 mM NaCl in 100% D_2O at 298 K.

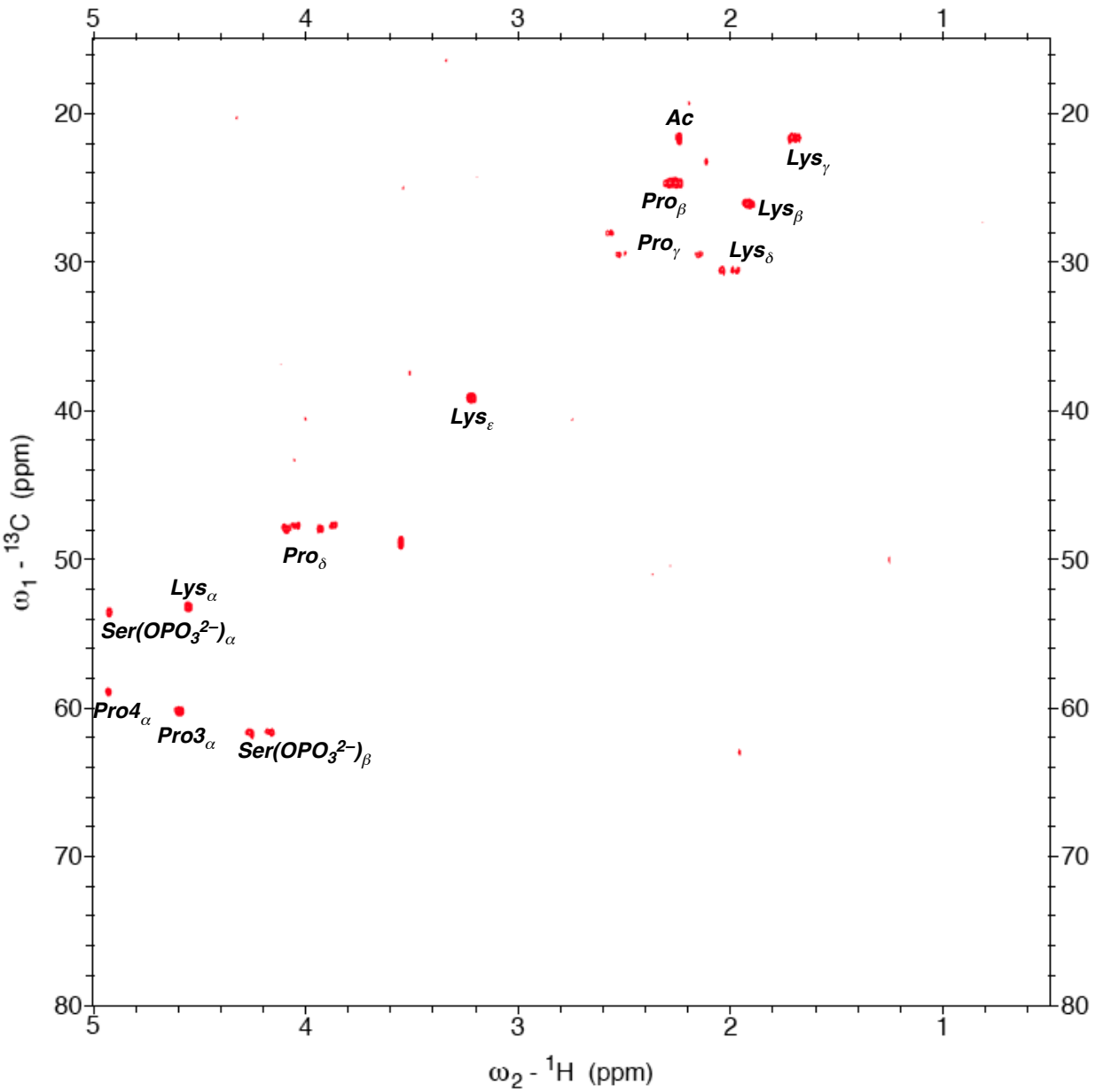

Figure S82. ^{1}H-^{13}C HSQC spectrum of peptide Ac-KS(OPO$_3^{2-}$)PP-NH$_2$ at pH 8.0 in 5 mM phosphate buffer with 25 mM NaCl in 100% D$_2$O at 298 K.

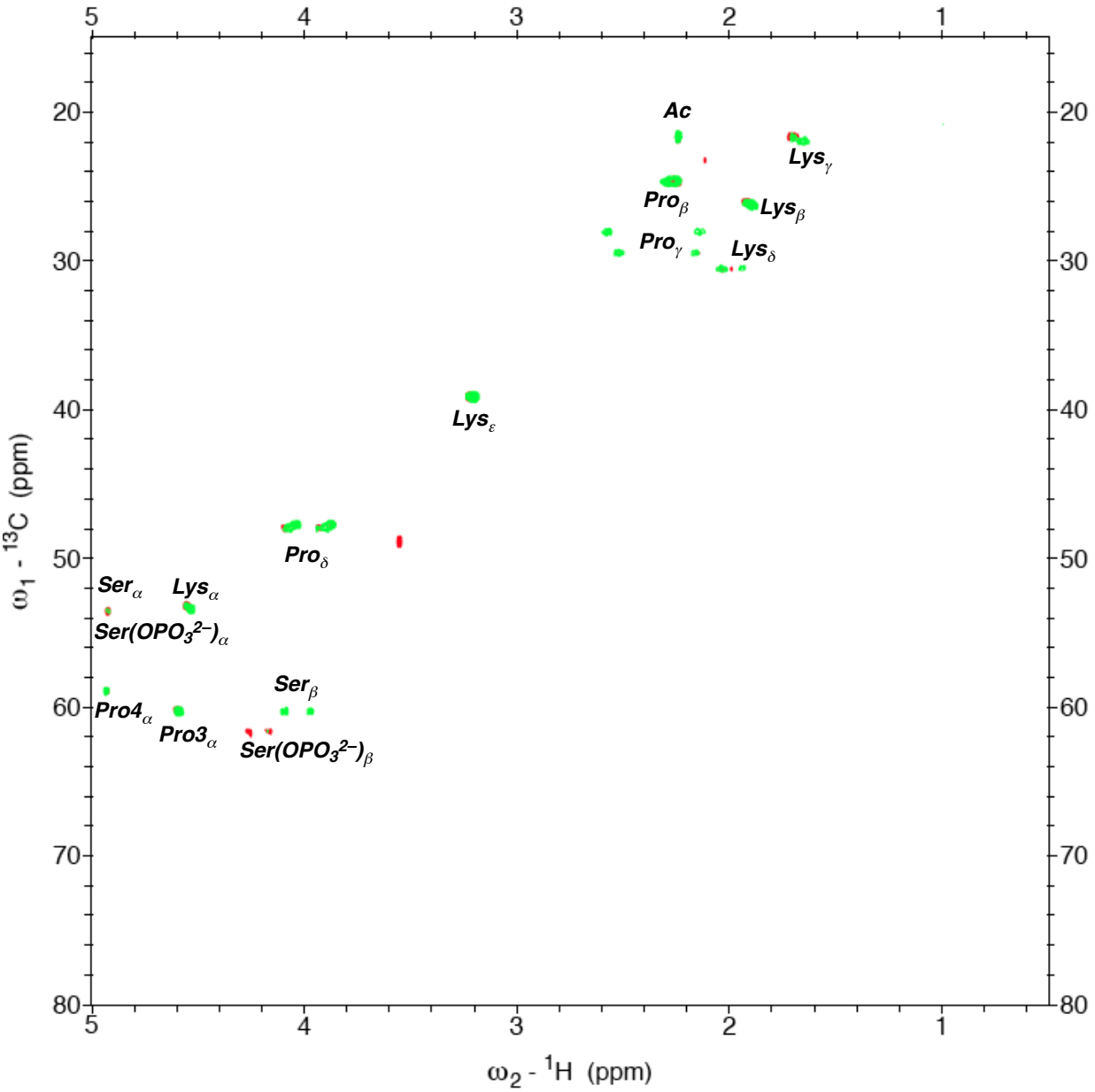

Figure S83. ^{1}H-^{13}C HSQC spectra of peptides Ac-KS(OPO_3^{2-})PP-NH_2 (red) at pH 8.0 and Ac-KSPP-NH_2 (green) at pH 4.0 in 5 mM phosphate buffer with 25 mM NaCl in 100% D_2O at 298 K.

Ac-KSPP-NH_2		Ac-KS(OPO_3^{2-})PP-NH_2	
residue	^{13}C δ, ppm	residue	^{13}C δ, ppm
Lys, α	53.4	Lys, α	53.2
Ser, α	53.6	pSer, α	53.6
Pro3, α	60.3	Pro3, α	60.2
Pro4, α	58.9	Pro4, α	58.9
Ser, β	60.2	pSer, β	61.6
Pro3, δ	47.7	Pro3, δ	47.7
Pro4, δ	47.9	Pro4, δ	48.0
Lys, ε	39.2	Lys, ε	39.1
Pro3, γ	28.0	Pro3, γ	28.0
Pro4, γ	29.5	Pro4, γ	29.5
Lys, β	26.2	Lys, β	26.0
Pro3, β	21.6	Pro3, β	21.6
Pro4, β	24.6	Pro4, β	24.7
Lys, γ	21.7	Lys, γ	21.6
NHAc	23.2	NHAc	23.2
Lys, δ	30.6	Lys, δ	30.6

Table S30. Summary of ^{13}C NMR data from ^{1}H-^{13}C HSQC experiments. The data were collected at pH 4.0 or pH 8.0 in 5 mM phosphate buffer with 25 mM NaCl in D_2O at 298 K. pSer indicates a phosphorylated serine residue.

^{1}H NMR spectra of Ac-GPP*Tx*PPGY-NH$_2$ peptides

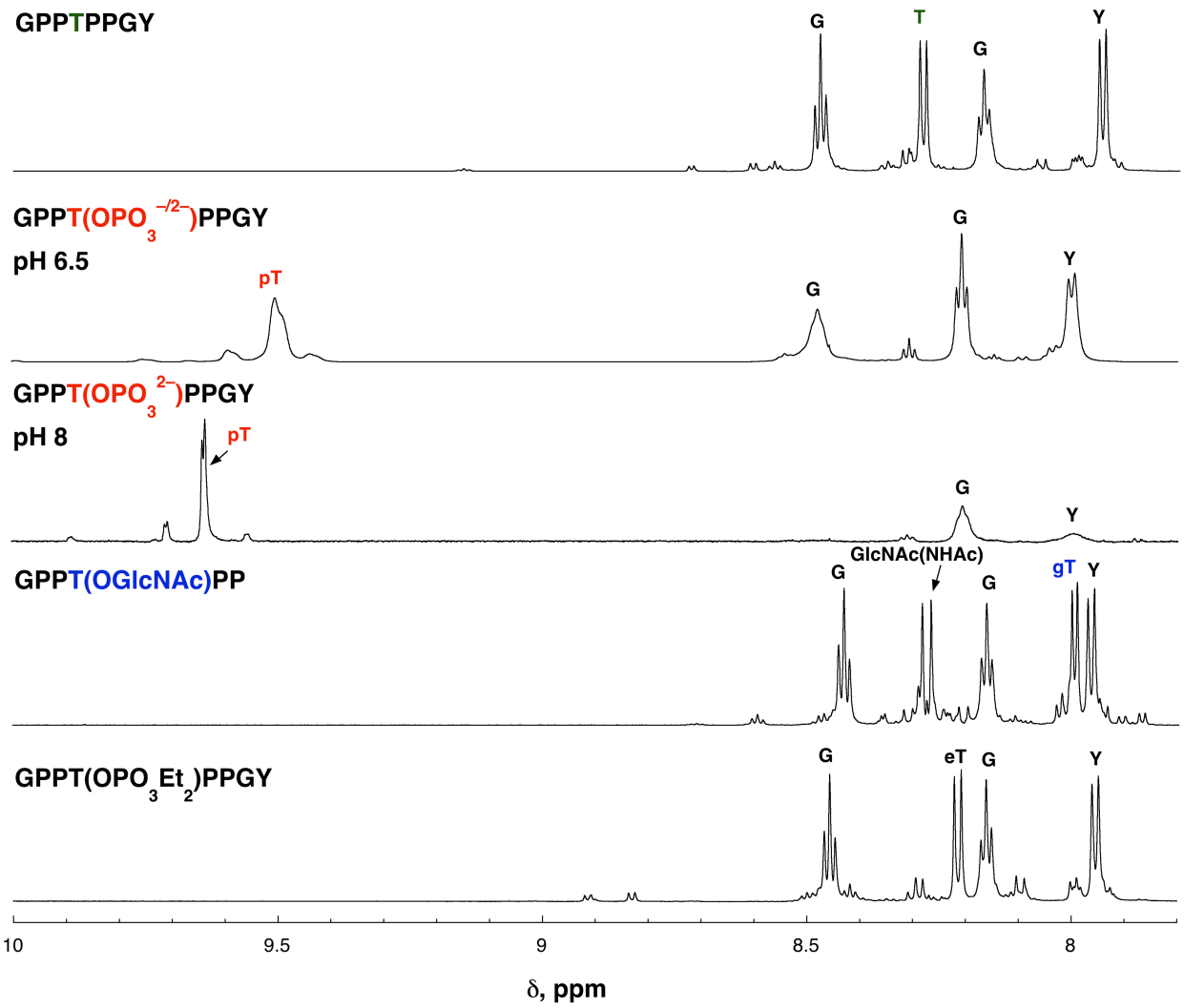

Figure S84. ^{1}H NMR spectra (amide region) of peptides Ac-GPP*Tx*PPGY-NH$_2$ at 298 K. The peptide samples were dissolved in 5 mM phosphate buffer with 25 mM NaCl and 100 μM TSP. NMR experiments were conducted at pH 4.0 unless otherwise specified.

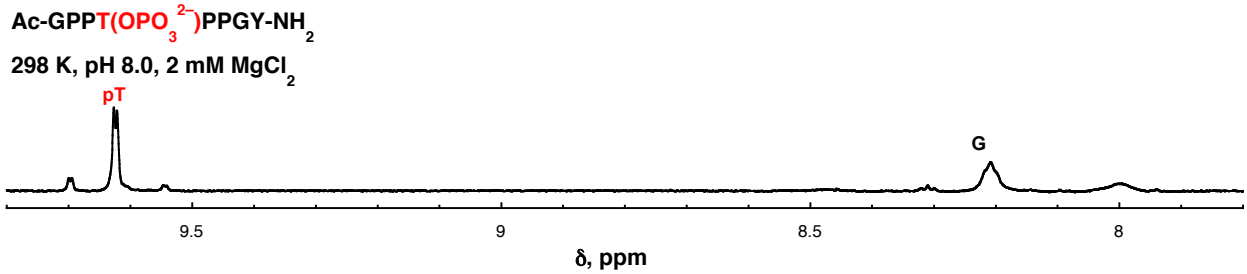

Figure S85. ^{1}H NMR spectrum (amide region) of Ac-GPPT(OPO$_3^{2-}$)PPGY-NH$_2$ in the presence of 2 mM MgCl$_2$ at 298 K. The NMR spectrum is identical to the spectrum obtained in the absence of MgCl$_2$.

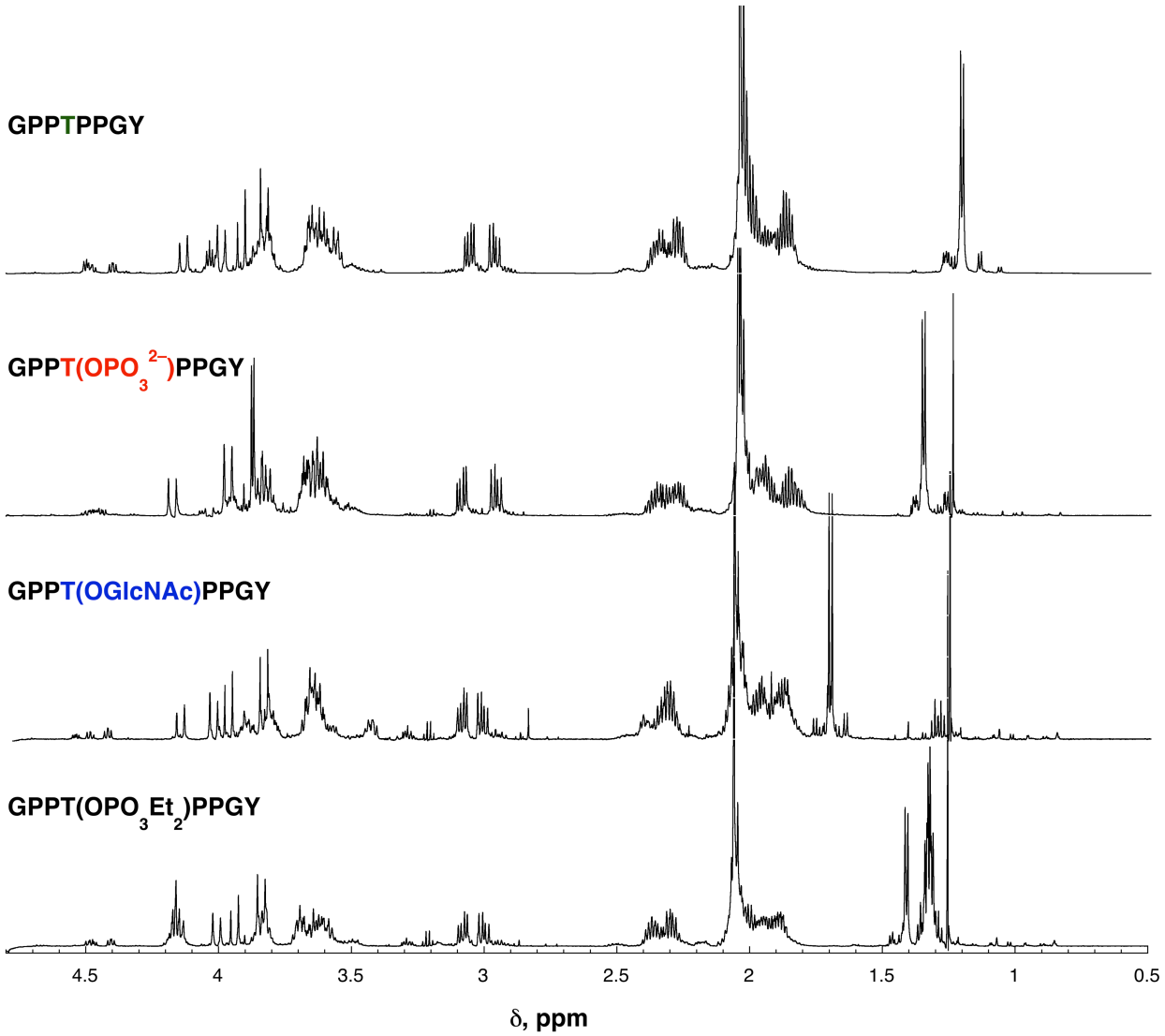

Figure S86. ^{1}H NMR spectra (aliphatic region) of Ac-GPP*Tx*PPGY-NH_2 peptides at 298 K in D_2O. The peptides were dissolved in 5 mM phosphate buffer pH 8.0 with 25 mM NaCl and 100 μM TSP.

The modification on threonine produces structural effects which are evident on the diastereotopic β, γ, and δ protons of proline. In the case of the phosphorylated peptide, the diastereotopic proline δ protons are observed to be more dispersed (ΔH_δ = 0.10 ppm) compared to the unmodified peptide (ΔH_δ = 0.07 ppm) and OGlcNAc and diethylphosphoryl (OPO_3Et_2) peptides (ΔH_δ = 0.06 ppm). The more sterically demanding diethylphosphorated and O-GlcNAcylated peptides showed less dispersion of the δ protons compared to the phosphorylated peptide. This effect can also also be seen on proline H_β and H_γ protons.

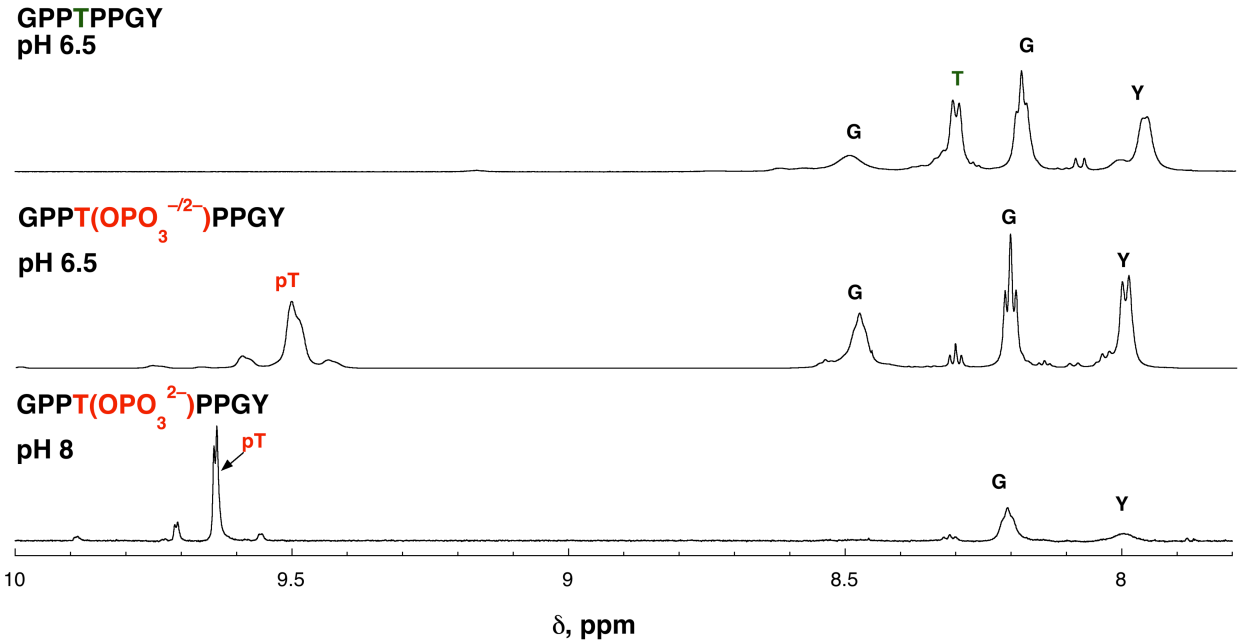

Figure S87. ^{1}H NMR spectra (amide region) of peptides Ac-GPPTPPGY-NH_2 at pH 6.5 and 8. The peptides were dissolved in 5 mM phosphate buffer (pH 8.0 or 6.5) containing 25 mM NaCl and 100 μM TSP.

As noted previously for all phosphorylated tau peptides as well as the model peptides Ac-KpTPP-NH_2 and Ac-KpSPP-NH_2, the amide protons of phosphorylated residues were observed to be more downfield and better resolved at pH 8.0 compared to pH 6.5. This downfield shift and better resolved peaks for the amide protons for the phosphorylated residues at pH 8.0 are general for all the peptides analyzed in this study with the lone exception of $tau_{196–209}$, which showed amides in relatively faster exchange (peak broadening and reduced magnitude, as expected for disordered peptides), but nonetheless more downfield than the nonphosphorylated versions.

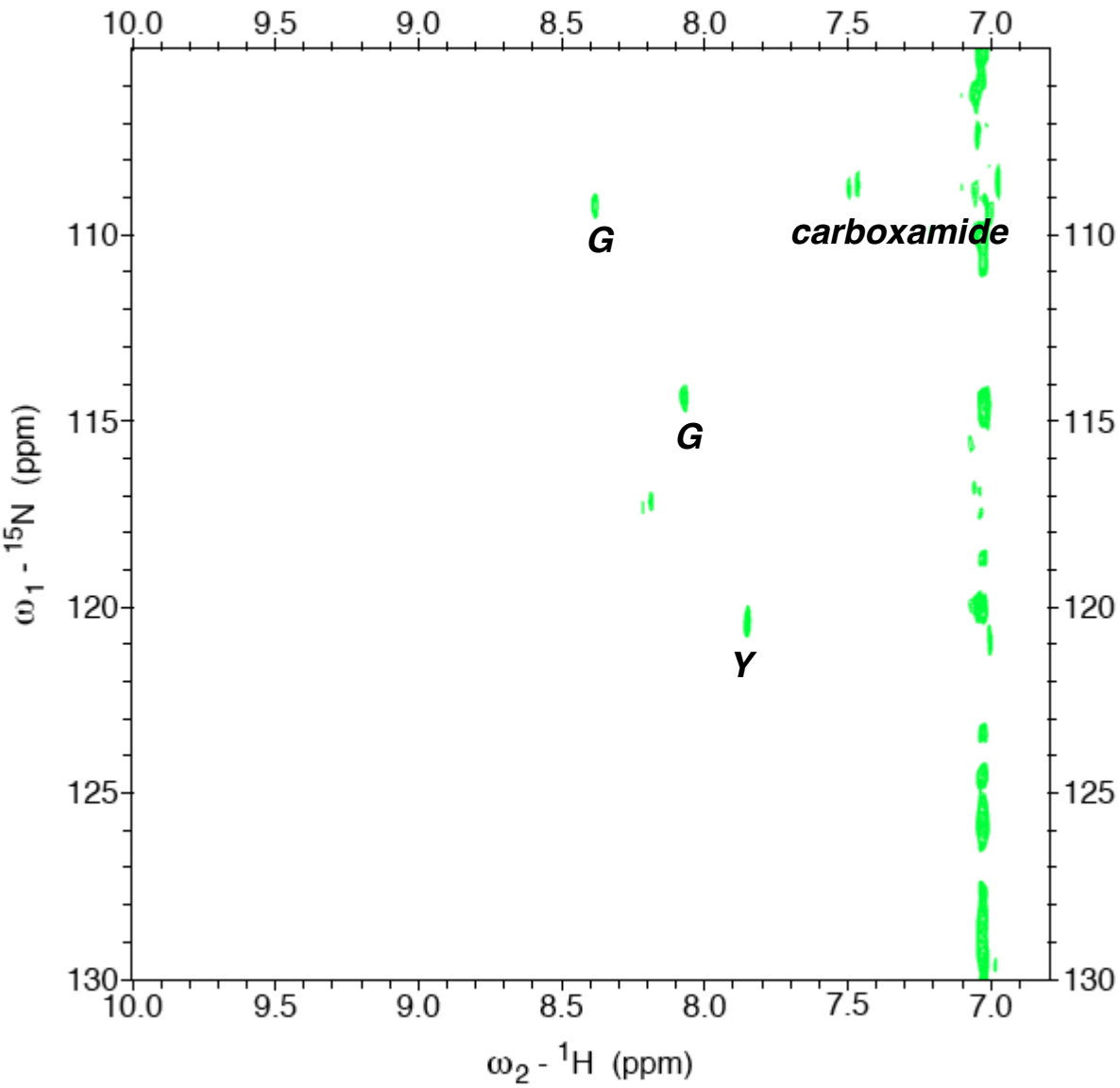

Figure S88. ^{1}H-^{15}N HSQC spectrum of peptide Ac-GPPTPPGY-NH_2 at pH 4.0 in 5 mM phosphate buffer containing 25 mM NaCl at 298 K.

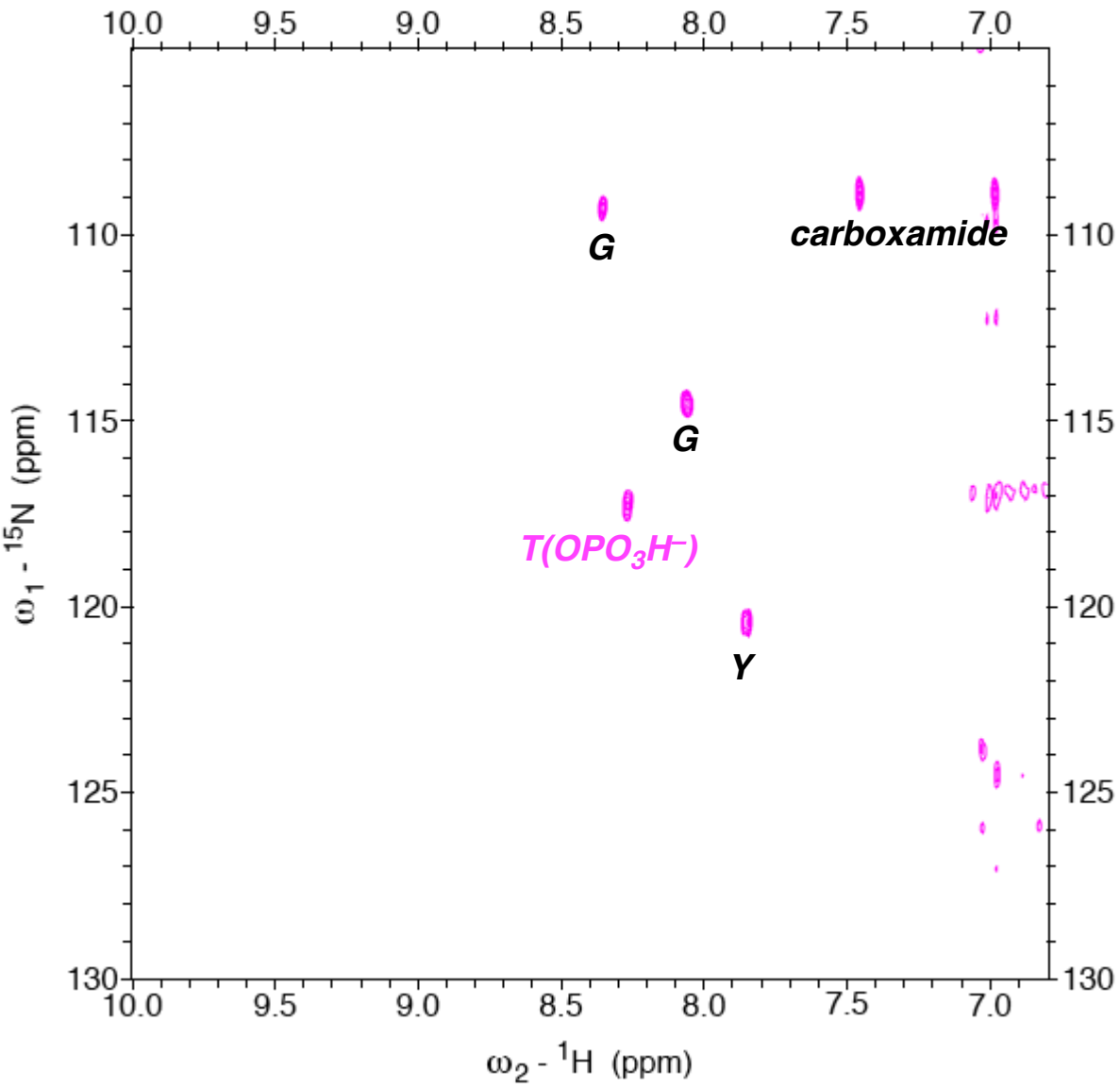

Figure S89. ^{1}H-^{15}N HSQC spectrum of peptide Ac-GPPT(OPO_3H^-)PPGY-NH_2 at pH 4.0 in 5 mM phosphate buffer containing 25 mM NaCl at 298 K.

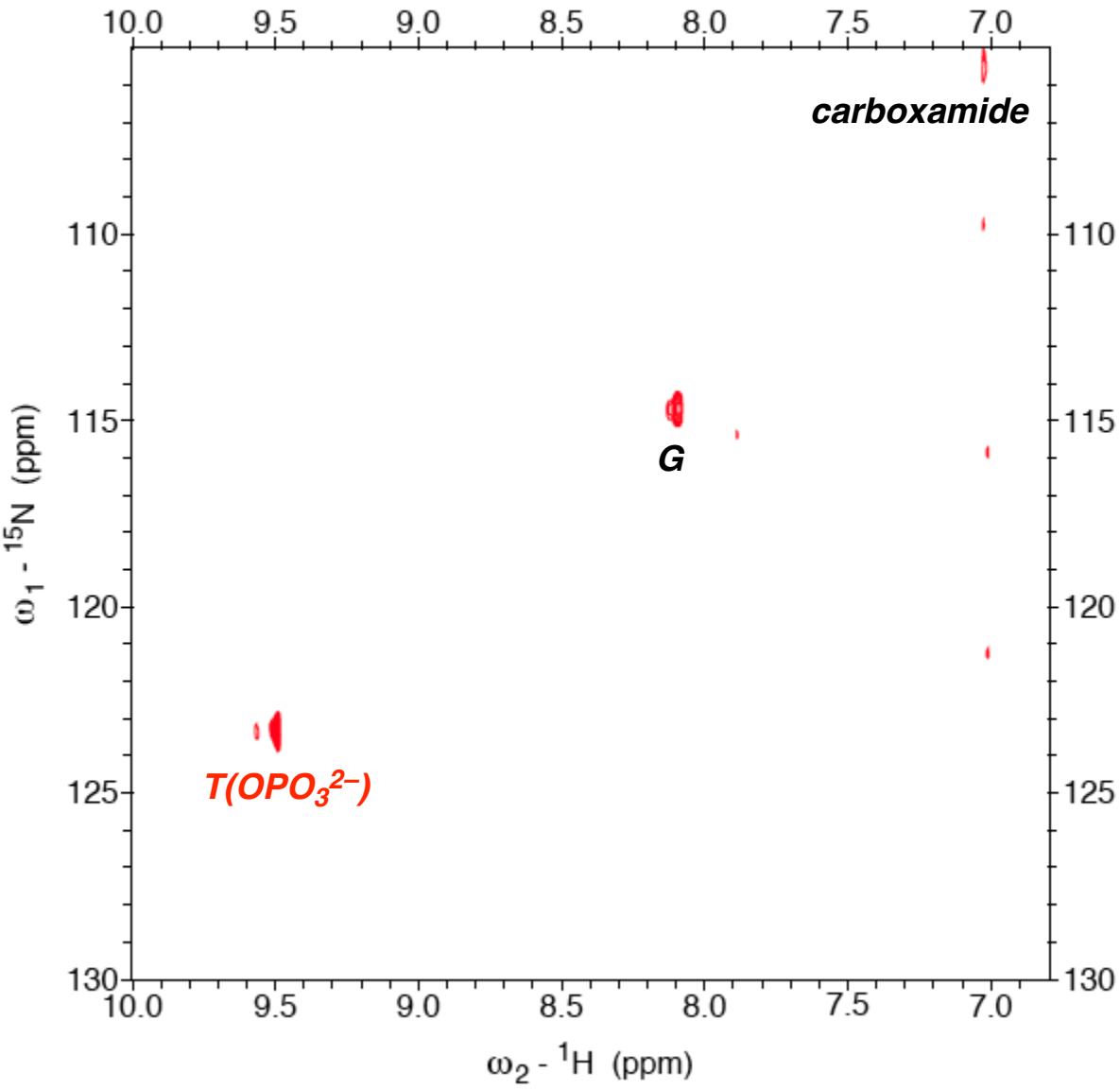

Figure S90. ^{1}H-^{15}N HSQC spectrum of peptide Ac-GPPT(OPO_3^{2-})PPGY-NH_2 at pH 8.0 in 5 mM phosphate buffer containing 25 mM NaCl at 298 K.

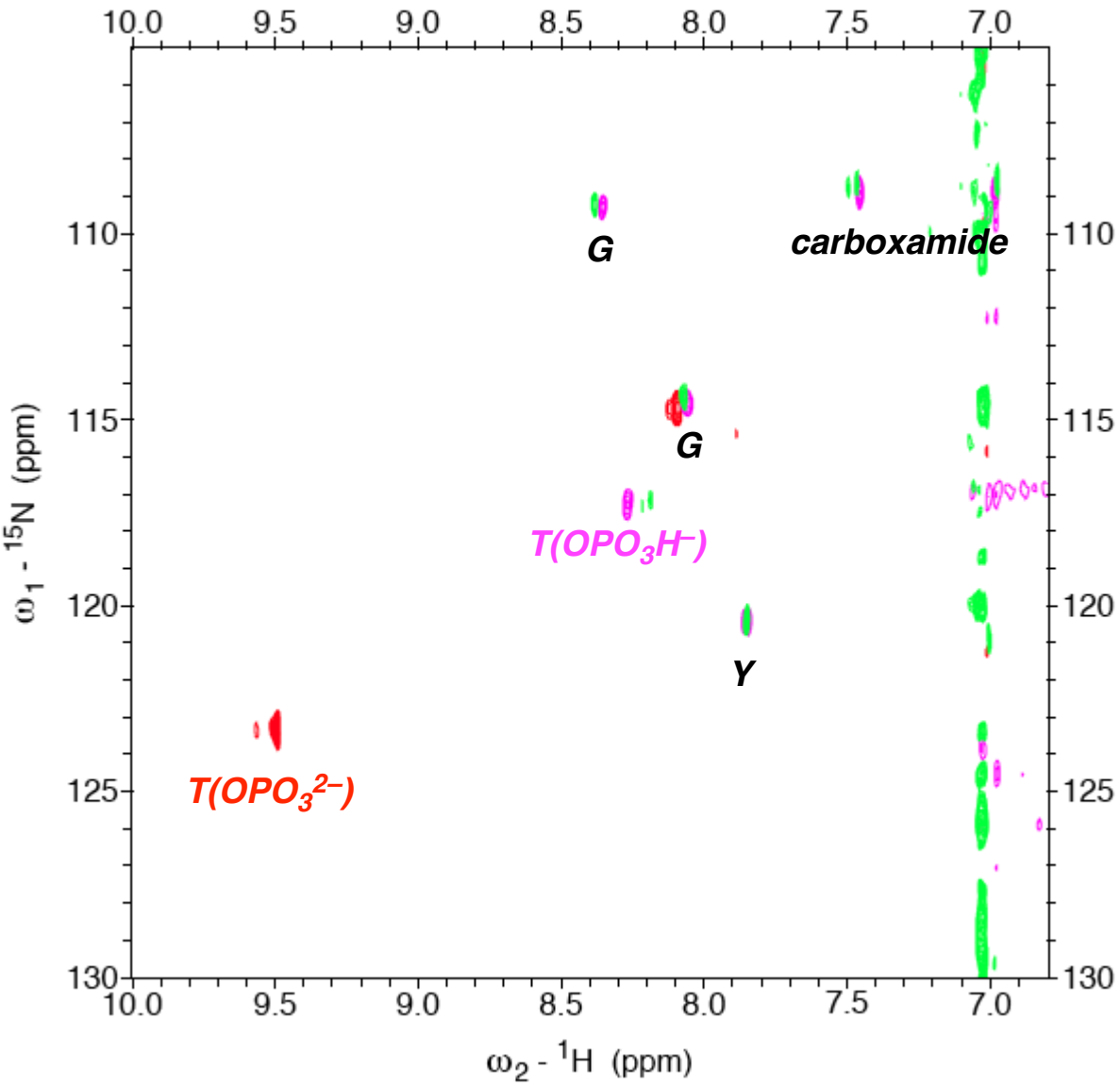

Figure S91. ^{1}H-^{15}N HSQC spectra of peptides Ac-GPPTPPGY-NH_2 at pH 4.0 (green), Ac-GPPT(OPO_3^{2-})PPGY-NH_2 (red) (pH 8.0), and Ac-GPPT(OPO_3H^-)PPGY-NH_2 (magenta) (pH 4.0) at 298 K. Data were collected with 1–2 mM peptide in 5 mM phosphate buffer (pH 4.0 or 8.0) with 25 mM NaCl.

peptide	δ, H^N Thr	$^3J_{\alpha N}$, Thr	δ, H_α Thr	δ, H_β Thr	δ, H^N Gly	δ, H^N Tyr	$^3J_{\alpha N}$, Tyr	pH
GPPTPPGY	8.29	7.3	4.51	4.05	8.49, 8.18	7.95	7.3	4.0
GPPT(OPO_3H^-)PPGY	8.40	6.5	4.63	4.47	8.48, 8.17	7.97	7.5	4.0
GPPT($OPO_3^{-/2-}$)PPGY	9.50	n.d.[a]	4.42	4.30	8.46, 8.20	7.99	n.d.	6.5
GPPT(OPO_3^{2-})PPGY	9.64	3.5	4.33	4.25	8.21, n.d.	7.99	n.d.	8.0
GPPT(OPO_3Et_2)PPGY	8.22	7.9	4.65	n.d.	8.47, 8.18	7.97	7.3	6.5
GPPT(OPO_3Et_2)PPGY	8.22	n.d.	4.65	4.65	8.47, 8.17	7.97	n.d.	7.5
GPPT(OGlcNAc)PPGY	8.01	n.d.	4.51	4.07	8.45, 8.18	7.98	n.d.	7.5
GPPT(OGlcNAc)PPGY	8.01	5.9	4.51	4.07	8.45, 8.18	7.98	7.2	6.5

Table S31. Summary of ^{1}H NMR data for peptides Ac-GPP*Tx*PPGY-NH_2. Data were collected with 100–200 μM peptide at 298 K in 5 mM phosphate buffer (pH 4.0, 6.5, 7.5, or 8.0) with 25 mM NaCl. [a] n.d. = not determined due to rapid amide exchange.

peptide	Thr_N, ppm	Gly_N, ppm	Tyr_N, ppm	carboxamide, ppm	pH, temp
Ac-GPPTPPGY-NH_2	117.2	109.2, 114.4	120.4	108.7	4.0, 298 K
Ac-GPPT(OPO_3H^-)PPGY-NH_2	117.3	109.3, 114.6	120.5	108.9	4.0, 298 K
Ac-GPPT(OPO_3^{2-})PPGY-NH_2	123.4	n.d., 114.7	n.d.	105.5	8.0, 298 K

Table S32. Summary of ^{1}H-^{15}N HSQC NMR data for peptides Ac-GPP*Tx*PPGY-NH_2. Data were collected with 2–3 mM peptide at 298 K in 5 mM phosphate buffer (pH 4.0 or 8.0) with 25 mM NaCl. [a] n.d. = not determined due to rapid amide exchange.

^{1}H NMR spectra of Ac-GPK*Tx*PPGY-NH_2 peptides

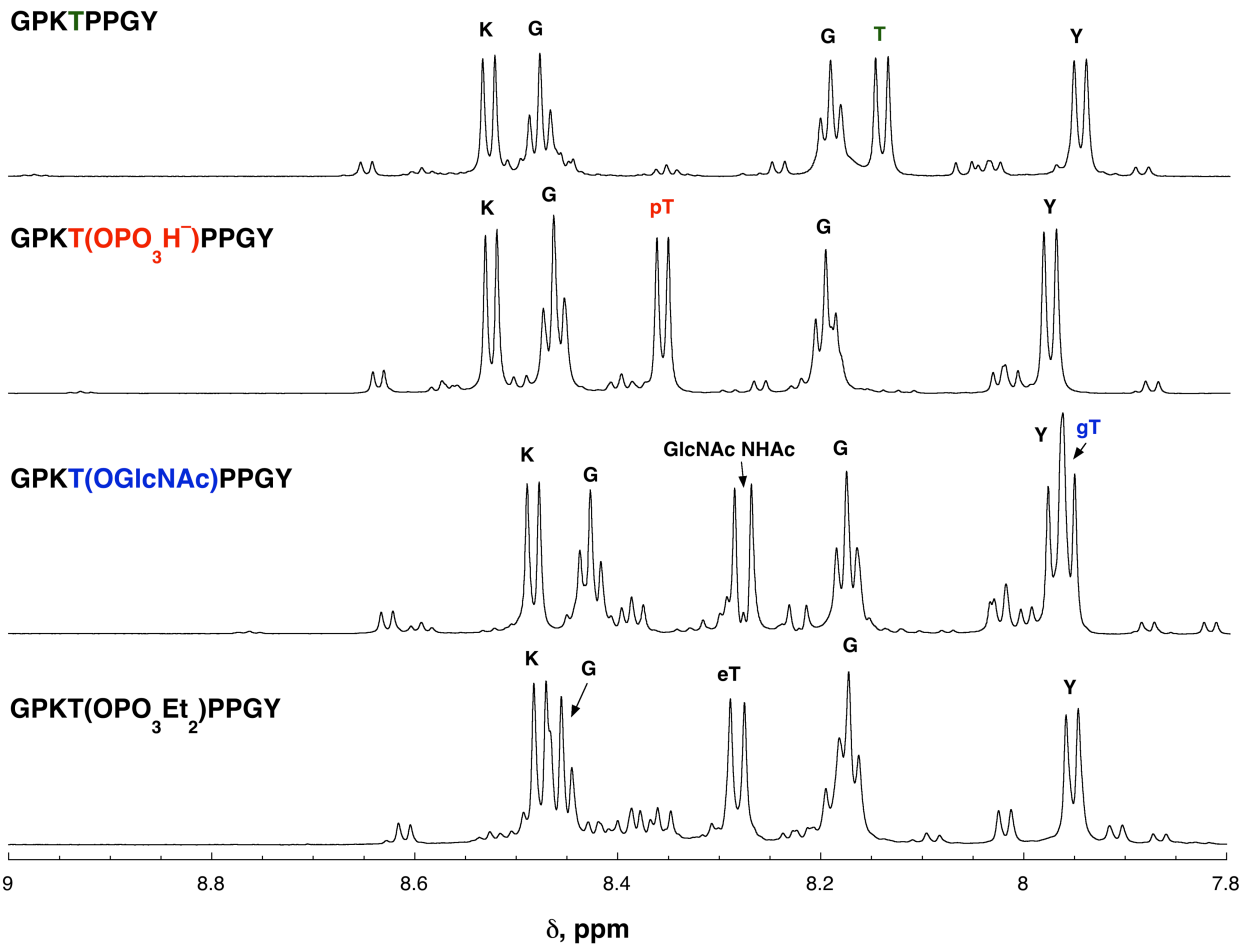

Figure S92. ^{1}H NMR spectra (amide region) of peptides Ac-GPK*Tx*PPGY-NH_2 at 298 K. The peptide samples were dissolved in 5 mM phosphate buffer buffer pH 4.0 with 25 mM NaCl and 100 μM TSP.

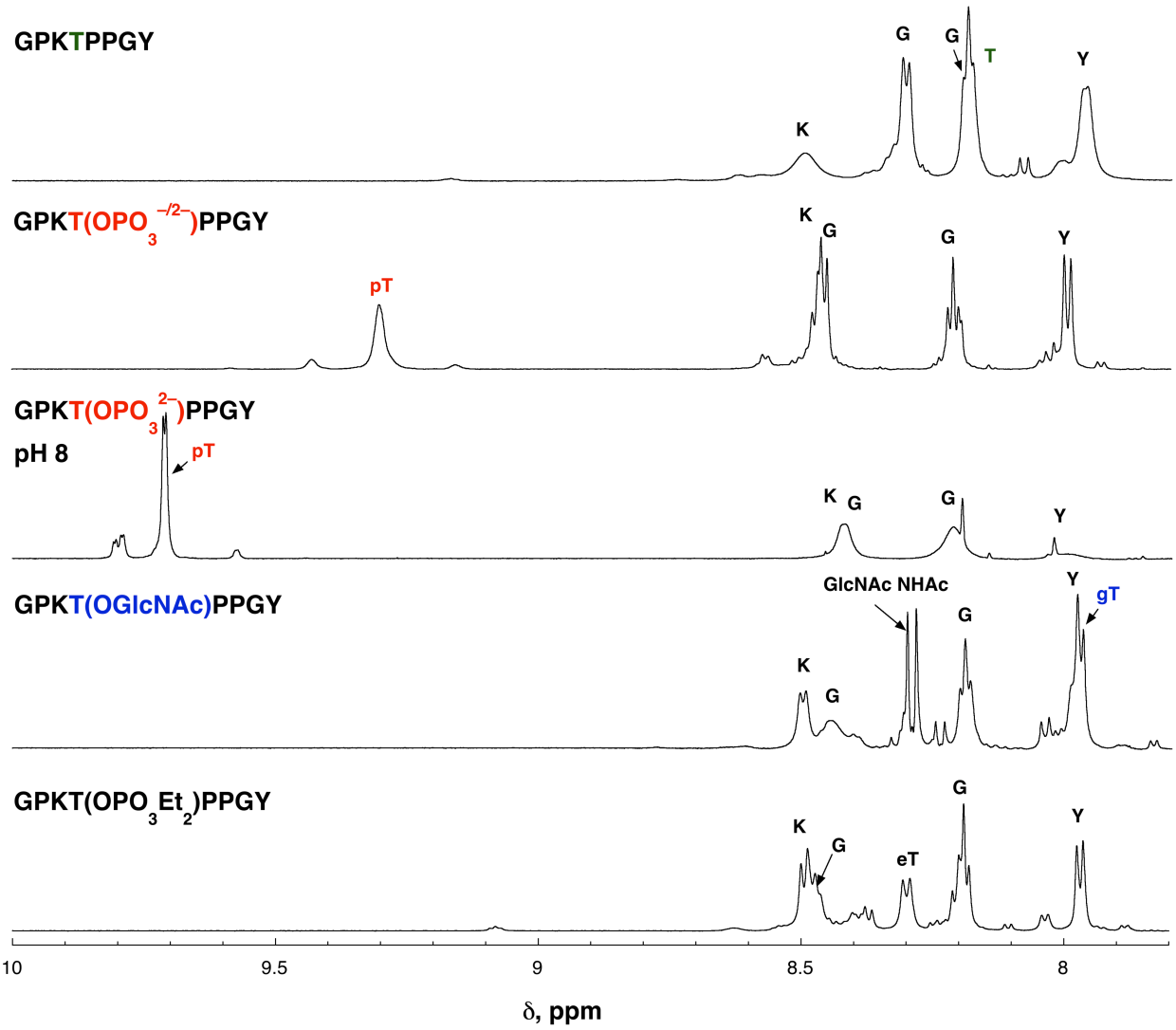

Figure S93. ^{1}H NMR spectra (amide region) of peptides Ac-GPK*Tx*PPGY-NH_2 at 298 K. The peptide samples were dissolved in 5 mM phosphate buffer with 25 mM NaCl and 100 μM TSP (pH 6.5 unless otherwise indicated).

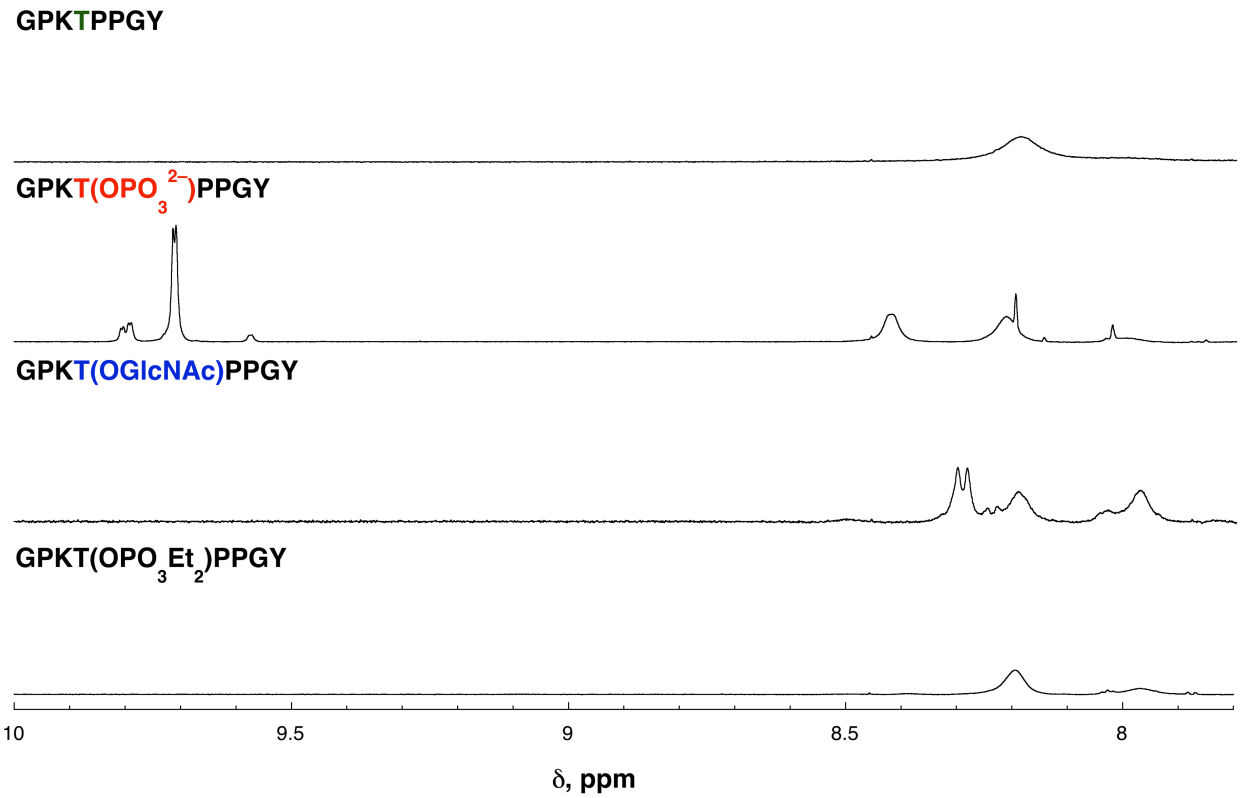

Figure S94. ^{1}H NMR spectra (amide region) of peptides Ac-GPK*Tx*PPGY-NH_2 at pH 8.0 (298 K). The peptide samples were dissolved in 5 mM phosphate buffer pH 8.0 with 25 mM NaCl and 100 μM TSP.

All peptides in Ac-GPK*Tx*PPGY-NH_2 series were analyzed at pH 8.0 to examine amide exchange. All peptides except the phosphorylated peptide Ac-GPKT(OPO_3^{2-})PPGY-NH_2 showed rapid amide exchange with water at pH 8.0.

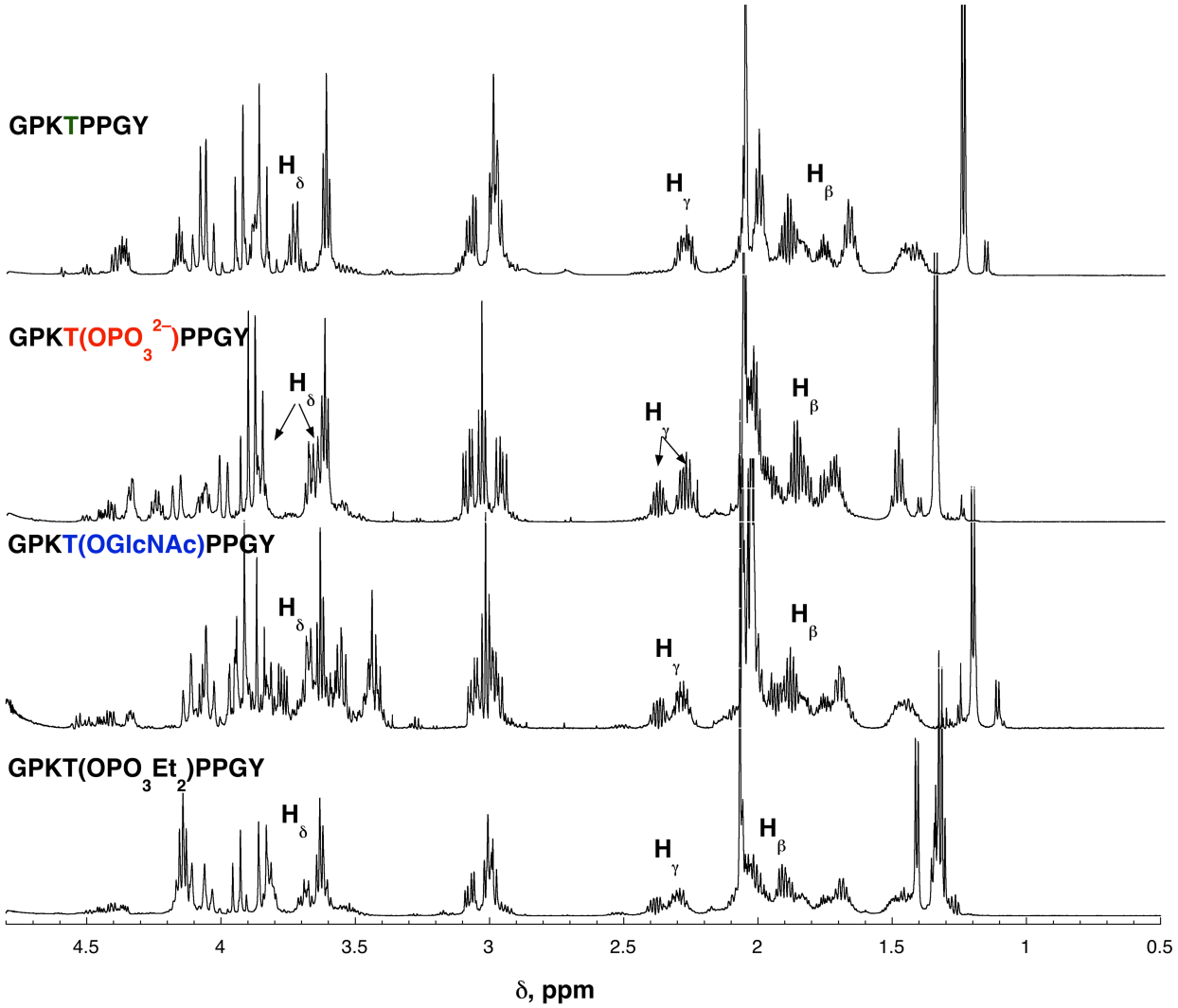

Figure S95. ^{1}H NMR spectra (aliphatic region) of peptides Ac-GPK*Tx*PPGY-NH_2 at pH 8.0 at 298 K. The peptide samples were dissolved in 5 mM phosphate buffer pH 8.0 with 25 mM NaCl and 100 μM TSP.

The effect of threonine side chain modification was propagated through the length of the peptide, as is evident from chemical shift differences in the Hβ, Hγ, and Hδ protons of proline. The phosphorylated peptide notably showed greater dispersion of the diastereotopic Hδ protons than any of the other peptides.

Summary of NMR data for peptides Ac-GPK*Tx*PPGY-NH_2

peptide	δ, H^N Thr	δ, Hα Thr	δ, Hβ, Hγ Thr	δ, H^N Lys	δ, Hα Lys	δ, Lys (others)	δ, H^N Tyr	δ, Hα Tyr	δ, Hβ Tyr	δ, H^N Gly	pH
GPKTPPGY	8.14	4.52	4.05, 1.20	8.52	4.37	3.00, 1.84, 1.75, 1.68	7.94	4.48	3.06, 2.97	8.48, 8.19	4.0
GPKT(OPO_3H^-)PPGY	8.35	4.63	4.45, 1.34	8.52	4.30	3.00, 1.84, 1.78, 1.69, 1.47	7.97	4.50	3.08, 2.95	8.46, 8.20	3.0
GPKT($OPO_3^{-/2-}$)PPGY	9.32	4.31	4.23, 1.35	8.46	4.33	3.03, 1.84, 1.77, 1.48	8.00	4.51	3.09, 2.97	8.48, 8.22	6.5
GPKT(OPO_3^{2-})PPGY	9.72	4.34	4.24, 1.35	8.43	4.34	3.04, 1.83, 1.74, 1.49	7.97	4.39	3.08, 2.93	n.d., 8.20	8.0
GPKT(OPO_3Et_2)PPGY	8.28	4.59	n.d., 1.39	8.47	4.34	2.99, 1.82, 1.74, 1.67, 1.43	7.95	4.47	3.05, 2.98	8.46, 8.17	4.0
GPKT(OPO_3Et_2)PPGY	8.29	4.60	4.60, 1.40	8.50	4.36	3.01, 1.84, 1.75, 1.45	7.97	4.49	3.07, 3.00	8.48, 8.19	6.5
GPKT(OGlcNAc)PPGY	7.96	4.53	4.06, 1.19	8.49	4.33	3.01, 1.82, 1.75, 1.46	7.97	4.48	3.05, 2.97	8.43, 8.18	4.0
GPKT(OGlcNAc)PPGY	7.98	4.55	4.07, 1.21	8.50	4.34	3.02, 1.84, 1.76, 1,46	7.99	4.49	3.06, 2.98	8.45, 8.19	6.5

Table S33. Summary of ^{1}H NMR data of peptides Ac-GPK*Tx*PPGY-NH_2 at 298 K. n.d. indicates not determined due to spectral overlap or fast amide exchange.

peptide	δ, H^N Thr	$^3J_{\alpha N}$, Thr	δ, Hα Thr	δ, Hβ Thr	δ, H^N Lys	$^3J_{\alpha N}$, Lys	δ, Hα Lys	δ, H^N Tyr	$^3J_{\alpha N}$, Tyr	δ, Hα Tyr	pH
Ac-GPKTPPGY-NH_2	8.14	7.4	4.52	4.05	8.52	7.2	4.37	7.94	7.2	4.48	4.0
Ac-GPKT(OPO_3H^-)PPGY-NH_2	8.35	6.7	4.63	4.45	8.52	6.8	4.30	7.97	7.4	4.50	3.0
Ac-GPKT($OPO_3^{-/2-}$)PPGY-NH_2	9.32	n.d.	4.31	4.23	8.46	6.8	4.33	8.00	7.4	4.51	6.5
Ac-GPKT(OPO_3^{2-})PPGY-NH_2	9.72	3.5	4.34	4.24	8.43	n.d.	4.34	7.97	n.d.	4.39	8.0
Ac-GPKT(OPO_3Et_2)PPGY-NH_2	8.28	8.3	4.59	n.d.	8.47	7.3	4.34	7.95	7.2	4.47	4.0
Ac-GPKT(OPO_3Et_2)PPGY-NH_2	8.29	8.3	4.60	4.60	8.50	7.3	4.36	7.97	7.3	4.49	6.5
Ac-GPKT(OGlcNAc)PPGY-NH_2	7.96	6.7	4.53	4.06	8.49	7.1	4.33	7.97	7.2	4.48	4.0
Ac-GPKT(OGlcNAc)PPGY-NH_2	7.98	6.5	4.55	4.07	8.50	6.8	4.34	7.99	n.d.	4.49	6.5

Table S34. ^{1}H NMR data ($^3J_{\alpha N}$ values and key proton chemical shifts) for peptides Ac-GPK*Tx*PPGY-NH_2 at 298 K. n.d. = not determined due to spectral overlap or fast amide exchange.

Analysis of steric vs stereoelectronic effects in Ac-TY*Prox*N-NH_2 and Ac-TA*Prox*N-NH_2 peptides

To understand the conformational effects of phosphorylation via model peptides used to quantify steric and stereoelectronic effects of substituents[2], the peptides Ac-TY*Prox*N-NH_2 were synthesized (*Prox* = 4-substituted prolines). Peptides were post-synthetically modified via proline editing to introduce 4*R*-phosphate, 4*S*-phosphate, 4*R*-diethylphosphate, and 4*S*-diethylphosphate on 4-hydroxyproline. To eliminate the effects on structure due to potential interactions with the hydrophobic tyrosine residue, the peptides Ac-TA*Prox*N-NH_2 were also synthesized and post-synthetically modified to generate peptides with modified prolines with 4*R*-phosphate, 4*S*-phosphate, 4*R*-diethylphosphate, and 4*S*-diethylphosphate substitutions. All peptides thus synthesized were analyzed via ^{1}H NMR spectroscopy for their conformational effects based upon steric and stereoelectronic effects.[2] The phosphorylated peptides were also analyzed as a function of pH to interrogate the effects as a function of phosphate protonation state. The data from ref. 2 on Ac-TY*Prox*N-NH_2 peptides and Ac-TA*Prox*N-NH_2 peptides, other than pH-dependent Ac-TA*Prox*N-NH_2 phosphorylated hydroxyprolines, which were not reported, indicate a smaller magnitude of stereoelectronic effect for diethylphosphates than observed in hydroxyprolines or phosphorylated hydroxyprolines. This result is in contrast to the expectation that the hydroxyproline diethylphosphates should be the most electron-withdrawing, and thus have the largest stereoelectronic effects. Indeed, the diethylphosphorylated serine and threonine residues had the most downfield-shift Hβ chemical shifts of all peptides examined, consistent with the expected greater electron-withdrawing effect of the diethylphosphates. These data support the concept that the diethylphosphate functions significantly sterically, with the steric effect at least partially counterbalancing the stereoelectronic effect in these peptides, as was also seen in the larger $^3J_{\alpha N}$ for serine and threonine diethylphosphates (Table 1).

pH-dependent NMR data on Ac-TA*Prox*N-NH_2 phosphorylated hydroxyprolines (below) were consistent with data on Ac-TY*Prox*N-NH_2 phosphorylated hydroxyprolines (ref. 2), indicating that the stereoelectronic effects of phosphorylation, whether as a monoanionic phosphate or a dianionic phosphate, are relatively similar to those of a hydroxy group. Thus, the structural effects observed due to phosphorylation are not likely to be due to a change in the stereoelectronic effect of a hydroxyl group versus a phosphate.

The diastereotopic β-protons of proline (Hβ) are more dispersed in the 4*R* configuration relative to 4*S* configuration. A characteristic splitting pattern is observed for the two diastereotopic β-protons (Hβ). A reversal in the splitting pattern based upon the 4*R* or 4*S* configuration on the Cγ of proline indicated reversal in ring pucker preferences. Similar observations based upon sterics and stereoelectronics were described recently on a large series of 4-substituted prolines in Ac-TY*Prox*N-NH_2 and Ac-TA*Prox*N-NH_2 peptide context.[2]

pH-dependent ^{1}H NMR analysis for peptides Ac-TAP(4*R*-$OPO_3^{-/2-}$)N-NH_2 and Ac-TAP(4*S*-$OPO_3^{-/2-}$)N-NH_2

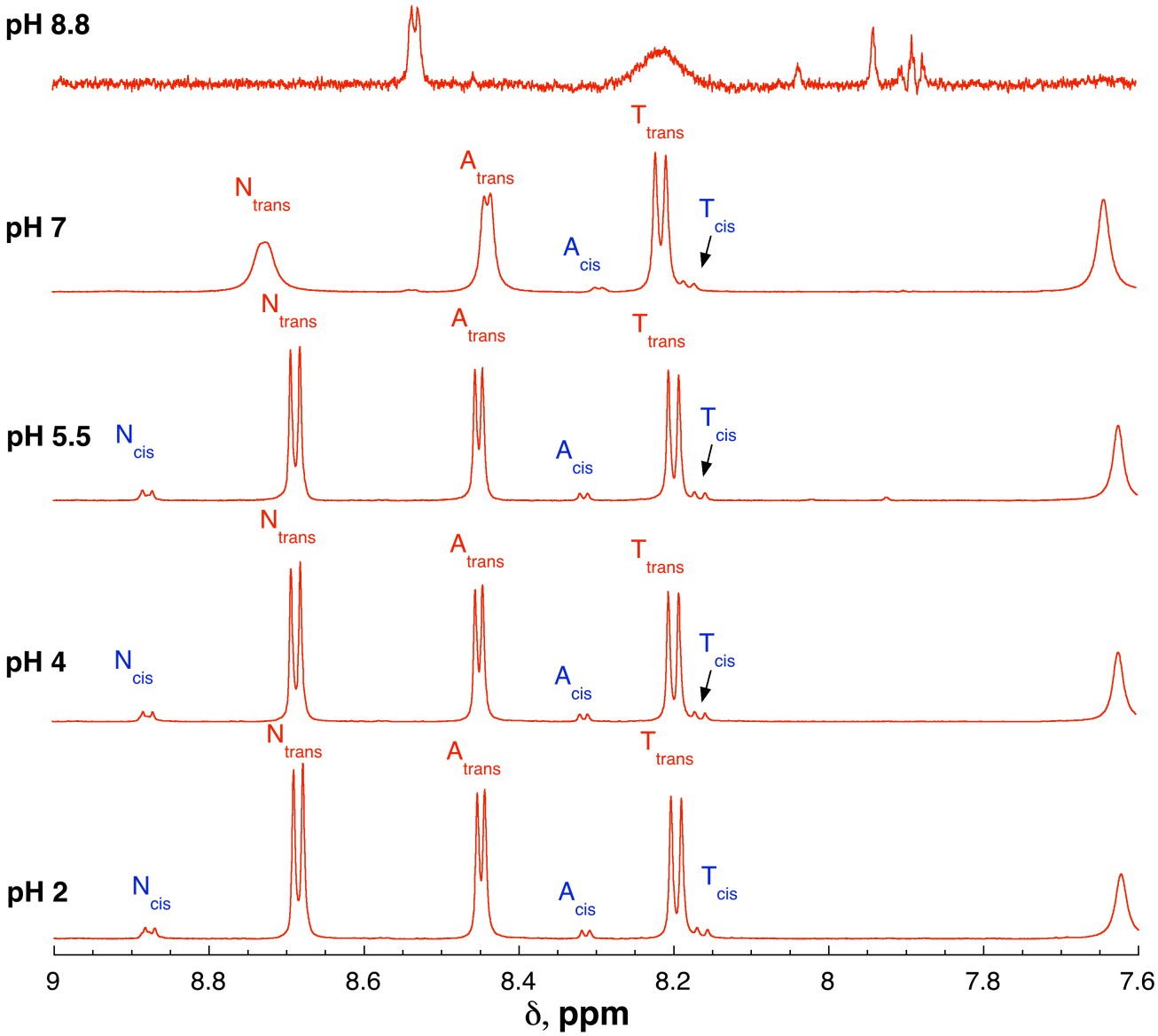

Figure S96. pH-dependent ^{1}H NMR spectra (amide region) of peptide Ac-TAP(4*R*-$OPO_3^{-/2-}$)N-NH_2.

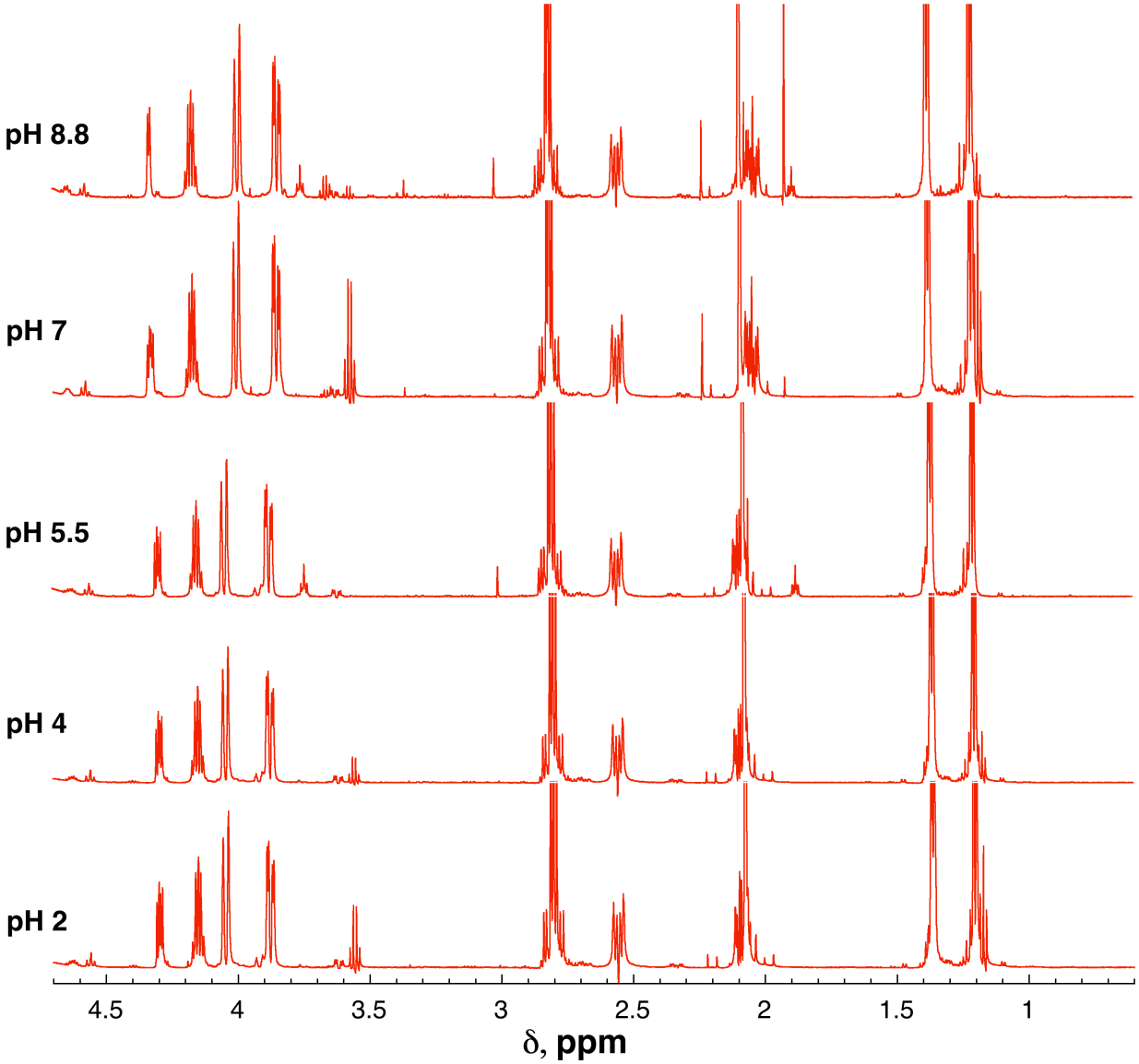

Figure S97. pH-dependent ^{1}H NMR spectra (aliphatic region) of peptide Ac-TAP(4*R*-$OPO_3^{-/2-}$)N-NH_2.

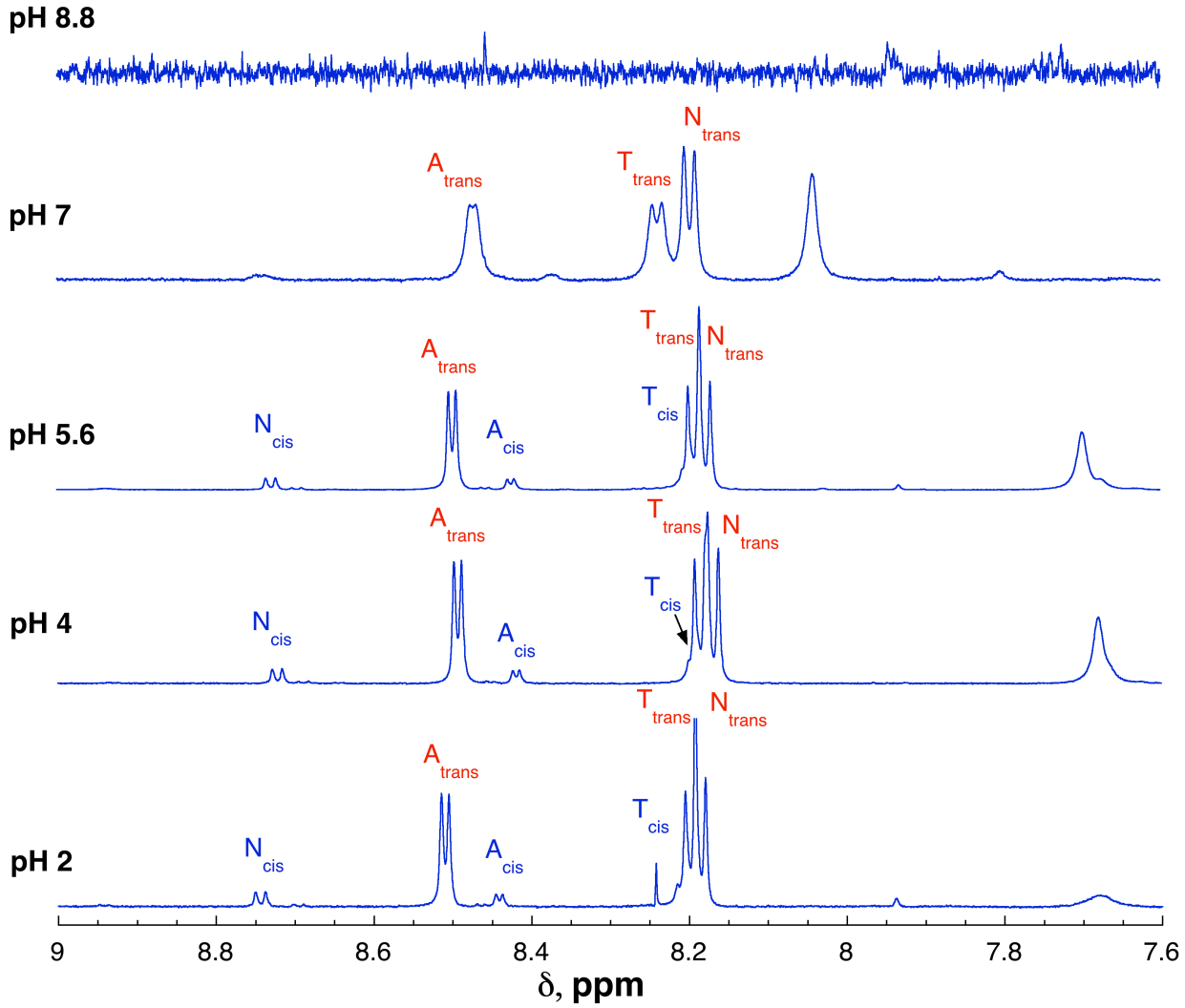

Figure S98. pH-dependent ^{1}H NMR spectra (amide region) of peptide Ac-TAP(4*S*-$OPO_3^{-/2-}$)N-NH_2.

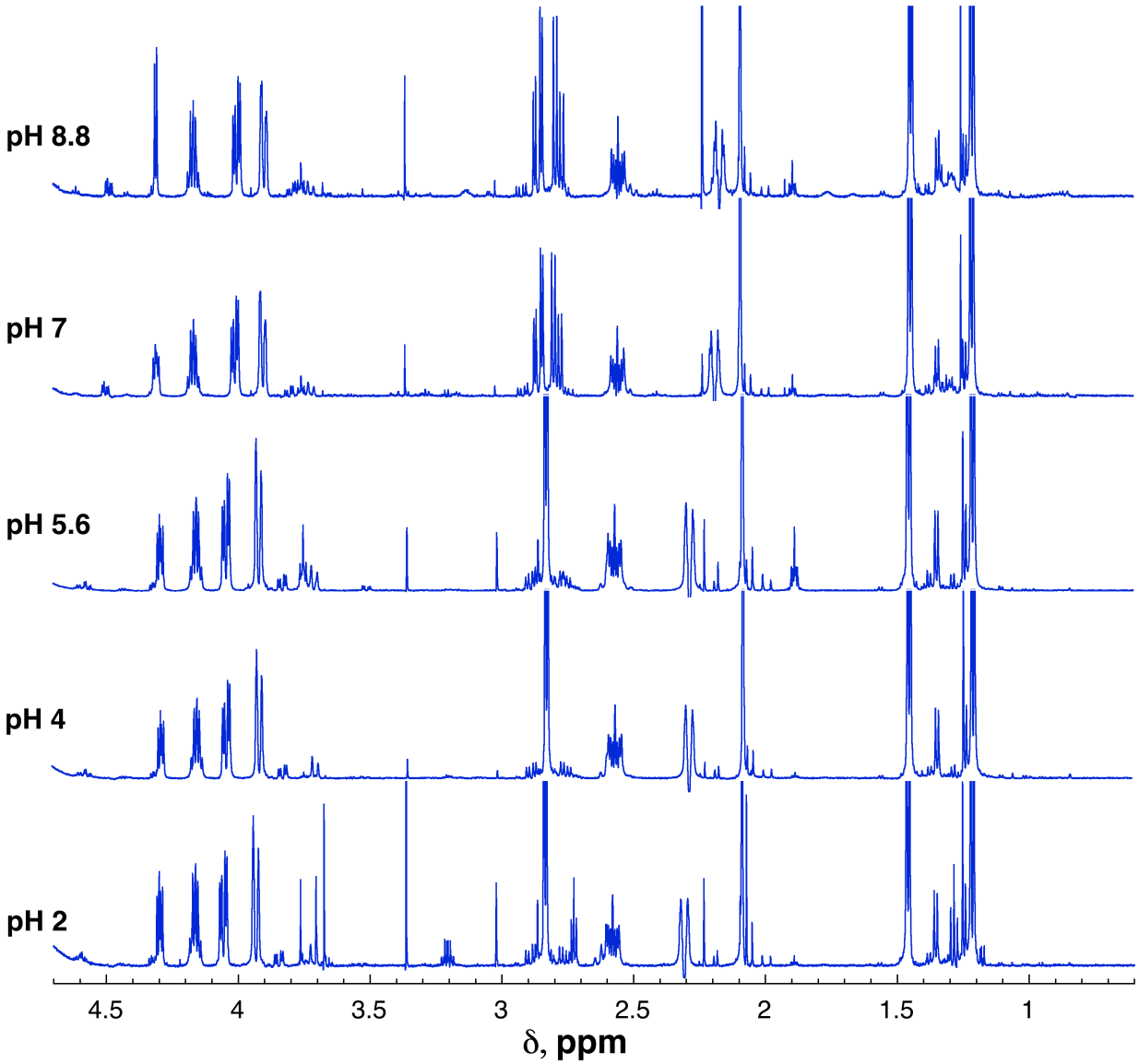

Figure S99. pH-dependent ^{1}H NMR spectra (aliphatic region) of peptide Ac-TAP(4*S*-$OPO_3^{-/2-}$)N-NH_2.

Ac-TAP(4-X)N-NH_2 X =	$K_{trans/cis}$	$\Delta G_{trans/cis}$, kcal mol^{-1}	$\Delta\Delta G_{trans/cis}$, kcal mol^{-1}	$^3J_{\alpha N}$ Ala_{cis}	$^3J_{\alpha N}$ Ala_{trans}	δ, H^N Ala_{cis}	δ, H^N Ala_{trans}	δ, H^N Asn_{trans}	pH
4*R*-OPO_3H^-	21.1	–1.80	-0.40	6.1	5.7	8.31	8.44	8.68	2.0
4*S*-OPO_3H^-	8.2	–1.25	0.15	5.0	5.6	8.44	8.51	8.18	2.0
4*R*-OPO_3H^-	18.2	–1.72	-0.32	5.9	5.7	8.32	8.45	8.69	4.0
4*S*-OPO_3H^-	8.5	–1.27	0.13	4.8	6.0	8.42	8.49	8.17	4.0
4*R*-$OPO_3^{-/2-}$	21.0	–1.80	-0.40	6.1	5.7	8.31	8.45	8.68	5.6
4*S*-$OPO_3^{-/2-}$	8.6	–1.27	0.13	4.9	5.6	8.42	8.49	8.17	5.6
4*R*-$OPO_3^{-/2-}$	18.5	–1.73	-0.33	n.a.[b]	4.9	8.53	8.43	8.73	7.0
4*S*-$OPO_3^{-/2-}$	8.9	–1.29	0.11	n.a.	n.a.	8.37	8.47	8.19	7.0
4*R*-OPO_3^{2-}	n.d.[a]	n.d.	n.d.	n.a.	n.a.	n.a.	n.a.	n.a.	8.8
4*S*-OPO_3^{2-}	7.5	–1.19	0.21	n.a.	n.a.	n.a.	n.a.	n.a.	8.8

Table S35. Summary of pH-dependent ^{1}H NMR data of peptides Ac-TAP(4*S*-$OPO_3^{-/2-}$)N-NH_2 and Ac-TAP(4*S*-$OPO_3^{-/2-}$)N-NH_2. [a] n.d. = not determined due to spectral overlap. [b] n.a. = not applicable.

Summary of serine and threonine NMR chemical shift data across all peptides as a function of residue and post-translational modification

peptide	ThrOPO$_3^{2-}$	ThrOPO$_3^{-/2-}$	ThrOPO$_3$H$^-$	SerOPO$_3^{2-}$	SerOPO$_3^{-/2-}$	SerOPO$_3$H$^-$	Thr	Ser	ThrOGlcNAc	SerOGlcNAc	ThrOPO$_3$Et$_2$	SerOPO$_3$Et$_2$
tau$_{174-183}$	9.73	9.08	8.45				8.29		7.97		8.42	
tau$_{174-183}$	9.68	8.96	8.38				8.22		7.96		8.28	
tau$_{196-209}$	9.67	8.50		8.78	8.49		8.07	8.23	8.19	8.28	8.43	8.48
tau$_{196-209}$				8.69	8.45			8.18		8.18		8.36
tau$_{211-219}$	9.66	8.62	8.58	9.17	8.62	8.58	8.34	8.41	8.03	8.15	8.29	8.48
tau$_{211-219}$	9.39	8.42	8.40				8.21		7.93		8.19	
tau$_{229-238}$	9.49	8.80	8.38	9.21	8.96	8.75	8.23	8.40	8.02	8.42	8.37	8.69
tau$_{229-238}$				9.05	8.74	8.59		8.25		8.40		8.59
KTPP	9.73	9.39	8.46				8.30		8.01		8.47	
KSPP				9.05		8.54		8.42		8.43		8.64
GPPTPPGY	9.64	9.50	8.40				8.29		8.01		8.22	
GPKTPPGY	9.72	9.32	8.35				8.14		7.98		8.29	
mean	9.63	8.95	8.43	8.99	8.65	8.62	8.23	8.32	8.01	8.31	8.33	8.54
standard dev	0.12	0.40	0.07	0.21	0.21		0.09	0.11	0.07	0.12	0.10	0.12

Table S36. Summary of serine and threonine amide NMR chemical shift data for all peptides.

peptide	ThrOPO$_3^{2-}$	ThrOPO$_3^{-/2-}$	ThrOPO$_3$H$^-$	SerOPO$_3^{2-}$	SerOPO$_3^{-/2-}$	SerOPO$_3$H$^-$	Thr	Ser	ThrOGlcNAc	SerOGlcNAc	ThrOPO$_3$Et$_2$	SerOPO$_3$Et$_2$
tau$_{174-183}$	4.39	4.55	4.67				4.59		4.58		4.87	
tau$_{174-183}$	4.37	4.51	4.64				4.58		4.58		4.87	
tau$_{196-209}$		4.53			4.90		4.63	4.45	4.70	4.59	4.91	5.04
tau$_{196-209}$					4.69			4.43		4.57		4.99
tau$_{211-219}$	4.41	4.68	4.65	4.42	4.53	4.42	4.55	4.44	4.53	4.54	4.82	4.62
tau$_{211-219}$	4.30	4.53	4.53				4.48		4.34		4.74	
tau$_{229-238}$	4.37	4.56	4.67	4.74	4.85	4.86	4.57	4.48	4.56	4.85	4.86	5.01
tau$_{229-238}$				4.46	4.52	4.57		4.45		4.61		4.71
KTPP	4.27	4.44	4.63				4.58		4.59		4.88	
KSPP				4.73		4.85		4.75		4.78		4.99
GPPTPPGY	4.33	4.42	4.63				4.51		4.51		4.65	
GPKTPPGY	4.34	4.31	4.63				4.52		4.55		4.60	
mean	4.35	4.50	4.63	4.59	4.70	4.68	4.56	4.50	4.55	4.66	4.80	4.89
standard dev	0.05	0.10	0.10	0.17	0.18		0.05	0.12	0.09	0.13	0.11	0.18

Table S37. Summary of serine and threonine Hα NMR chemical shift data for all peptides.

peptide	ThrOPO$_3^{2-}$	ThrOPO$_3^{-/2-}$	ThrOPO$_3$H$^-$	SerOPO$_3^{2-}$	SerOPO$_3^{-/2-}$	SerOPO$_3$H$^-$	Thr	Ser	ThrOGlcNAc	SerOGlcNAc	ThrOPO$_3$Et$_2$	SerOPO$_3$Et$_2$
tau$_{174-183}$	4.26	4.37	4.48				4.11		4.13		4.66	
tau$_{174-183}$	4.26	4.38	4.47				4.13		4.10		4.66	
tau$_{196-209}$					4.22		4.19	3.85	4.27	3.72		4.40
tau$_{196-209}$					4.11			3.79		3.57		4.24
tau$_{196-209}$					4.22			3.88		3.64		4.39
tau$_{196-209}$					4.10			3.87		3.55		4.26
tau$_{211-219}$	4.30	4.53	4.42	4.09	4.14	4.11	4.15	3.85	4.11	3.54	4.70	4.35
tau$_{211-219}$	4.28	4.53	4.11	3.97		4.11	4.11		4.06	3.43	4.47	
tau$_{229-238}$	4.29	4.46	4.57	4.13	4.20	4.24	4.12	3.94	4.10	4.12	4.66	4.44
tau$_{229-238}$				4.07	4.12	4.15		3.89		4.01		4.41
tau$_{229-238}$				4.08	4.14	4.15		3.93		4.02		4.42
tau$_{229-238}$				3.98	4.07	4.10		3.88		3.96		4.23
KTPP	4.26	4.31	4.45				4.12		4.13		4.67	
KSPP				4.07		4.12		3.89		4.00		4.39
KSPP				3.97		4.05		3.76		3.92		4.19
GPPTPPGY	4.25	4.30	4.47				4.05		4.07		4.65	
GPKTPPGY	4.24	4.23	4.45				4.05		4.07		4.60	
mean	4.27	4.39	4.43	4.05	4.15	4.13	4.11	3.87	4.12	3.79	4.63	4.34
standard dev	0.02	0.11	0.14	0.06	0.05	0.05	0.04	0.05	0.06	0.24	0.07	0.09

Table S38. Summary of serine and threonine Hβ NMR chemical shift data for all peptides.

peptide	$ThrOPO_3^{2-}$	$ThrOPO_3^{-/2-}$	$ThrOPO_3H^-$	$SerOPO_3^{2-}$	$SerOPO_3^{-/2-}$	$SerOPO_3H^-$	Thr	Ser	ThrOGlcNAc
$tau_{174-183}$	125.1		118.5				118.2		118.8
$tau_{174-183}$	125.6		119.0				118.3		118.8
$tau_{196-209}$									
$tau_{196-209}$									
$tau_{211-219}$	121.8		117.4	119.4		116.6	117.8	116.5	
$tau_{211-219}$	125.7		120.9				118.6		
$tau_{229-238}$	124.0		122.4	122.2		118.2	118.4	115.6	
$tau_{229-238}$						115.9		118.9	
								121.7	
KTPP	124.8		119.4				118.3		
KSPP									
GPPTPPGY	123.4		117.3				117.2		
GPKTPPGY									
mean	124.3		119.3	120.8		116.9	118.1	118.2	118.8
standard dev	1.4		1.8	2.0		1.2	0.5	2.7	0.0

Table S39. Summary of serine and threonine ^{15}N NMR chemical shift data for all peptides.

δ, Ser/Thr	^{13}C Thrα	^{13}C Thrβ	^{13}C Thrγ	^{13}C ThrC=O	^{13}C Serα	^{13}C Serβ	^{13}C Thrα	^{13}C Thrβ	^{13}C Thrγ	^{13}C ThrC=O	^{13}C Serα	^{13}C Serβ
peptide	$ThrOPO_3^{2-}$	$ThrOPO_3^{2-}$	$ThrOPO_3^{2-}$	$ThrOPO_3^{2-}$	$SerOPO_3^{2-}$	$SerOPO_3^{2-}$	Thr	Thr	Thr	Thr	Ser	Ser
$tau_{174-183}$	58.1	70.0	17.8	169.7			57.0	66.9	18.7	169.6		
$tau_{174-183}$	58.4	70.0	17.8	169.7			57.0	66.9	18.7	169.6		
$tau_{196-209}$												
$tau_{196-209}$												
$tau_{211-219}$	58.8	69.9	17.9		52.2	63.0	57.1	66.8	18.7		52.5	60.9
$tau_{211-219}$	58.5	69.9	17.9				57.3	67.0	18.7			
$tau_{229-238}$	57.7	70.4	18.0		53.1	63.2	57.0	66.9	18.8		53.6	60.7
$tau_{229-238}$						62.5					53.6	61.0
KTPP	58.8	69.8	18.0	169.7			57.1	66.9	18.7	169.5		
KSPP					53.6	61.6					53.6	60.2
GPPTPPGY												
GPKTPPGY												
mean	58.4	70.0	17.9	169.7	53.0	62.6	57.1	66.9	18.7	169.6	53.3	60.7
standard dev	0.4	0.2	0.1	0.0	0.7	0.7	0.1	0.1	0.0	0.1	0.6	0.4

Table S40. Summary of serine and threonine ^{13}C NMR chemical shift data for all peptides.

References

1. Thomas, K. M.; Naduthambi, D.; Tririya, G.; Zondlo, N. J. *Org. Lett.* **2005**, *7*, 2397–2400.
2. Pandey, A. K.; Naduthambi, D.; Thomas, K. M.; Zondlo, N. J. *J. Am. Chem. Soc.* **2013**, *135*, 4333–4363.
3. Waddell, W. J. *J. Lab. Clin. Med* **1956**, *48*, 311–314.
4. Arsequell, G.; Kripper, L.; Dwek, R. A.; Wong, S.Y.C. *J. Chem. Soc., Chem. Commun.* **1994**, *20*, 2283–2284.
5. Bielska, A. A.; Zondlo, N. J. *Biochemistry* **2006**, *45*, 5527–5537.
6. Vuister, G. W.; Delaglio, F.; Bax, A. *J. Am. Chem. Soc.* **1992**, *114*, 9674–9675.
7. Schmidt, J. M. *J. Biomol. NMR* **2007**, *37*, 287–301.
8. Lankhorst, P. P.; Haasnoot, C. A. G.; Erkelens, C.; Altona, C. *J. Biomol. Struct. Dynam.* **1984**, *1*, 1387–1405.